Applied Ecology and Environmental Research

International Scientific Journal

7th Hungarian Conference on Biometrics and Biomathematics

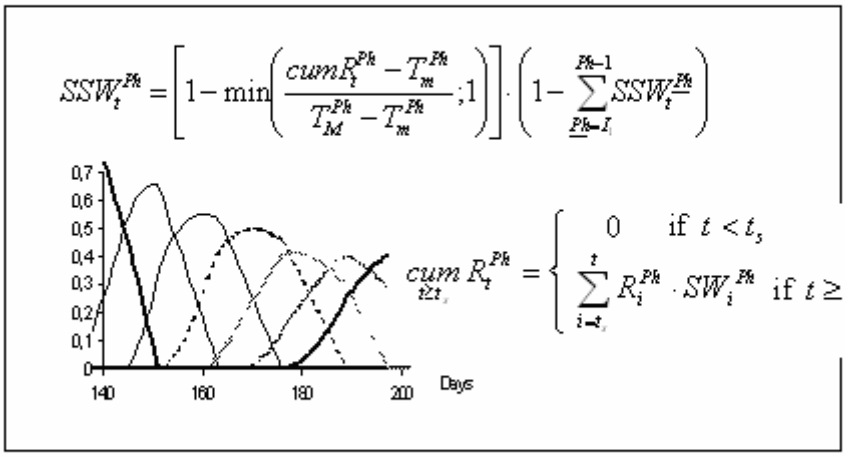

Biomathematical Thematic Issue of AEER

VOLUME 4 * NUMBER 2 * 2006

http://www.ecology.kee.hu
ISSN 1589 1623

ANALYSING ASSOCIATIONS AMONG MORE THAN TWO SPECIES

Z. BOTTA-DUKÁT

Institute of Ecology and Botany, Hungarian Academy of Sciences
Alkotmány u. 2-4, Vácrátót, H-2163 Hungary
(phone: +36-28-360-122; fax: +36-28-360-110)

e-mail: bdz@botanika.hu

(Received 10th Sep 2005, accepted 10th Oct 2006)

Abstract: Although the existence of higher order associations has been proved, interspecific association is generally treated as a pair-wise phenomenon. Its possible reason is that although pair-wise association is only an imperfect description of the relationships among species, its methods are simple and well known. Unfortunately, the complexity of vegetation can not be described by such simplex methods. This paper shows two methods which enable detailed analysis of higher-order associations: Juhász-Nagy's information theory functions and the log-linear contingency table analysis. From mathematical point of view, the two methods are closely related (both methods measure the non-randomness in the multi-way contingency tables). On the other hand, their theoretical backgrounds are different. The log-linear contingency table analysis was developed by statisticians to solve general statistical problems, while Juhász-Nagy's approach was developed by a biologist to solve biological problems.
The aim of this paper is to show how these two approaches decompose the total association, to point at the similarities and differences between the two approaches, and by this way to facilitate the analysis of higher order associations.
Keywords*: associatum, diversity of species combinations, pattern analysis, 3rd-order association*

Introduction

Positive and negative associations among species are very common phenomena in plant communities. Association measures the departure of frequency of species combinations from the random expectation [32]. The association among species may arise from biological interactions or different responses of species to abiotic factors [10], and on the other hand, it influences the possible interactions among species [8, 9], i.e. species can interact only where they co-occur.

In case studies, interspecific association is generally treated as a pair-wise phenomenon. Showing the structure of a community as a plexus graph or table of the significant pair-wise associations has a long tradition [1, 14, 35, 49, 53]. In addition, the matrix of pair-wise associations is often used in multivariate methods (e.g. PCA and related ordination methods [36, 43]).

However, there may be higher-order associations among species, i.e. the presence/absence of other species can affect association between a particular pair of species [11]. The following example with an artificial data set was developed by M. Kertész (personal communication):

	plots							
species	1	2	3	4	5	6	7	8
A	1	1	1	1	0	0	0	0
B	1	1	0	0	1	1	0	0
C	0	0	1	1	1	1	0	0

<1>

http://www.ecology.uni-corvinus.hu ● ISSN 1589 1623

In this data set all pair-wise associations are zero, but any species pair determines the presence/absence of the third species, i.e. the third species occurs only in the plots where one of the other two species occurs, thus the number of species can be only 2 or 0. Disregarding higher order associations may yield underestimation of association among species or a confused network of pair-wise associations (*Fig. 1*).

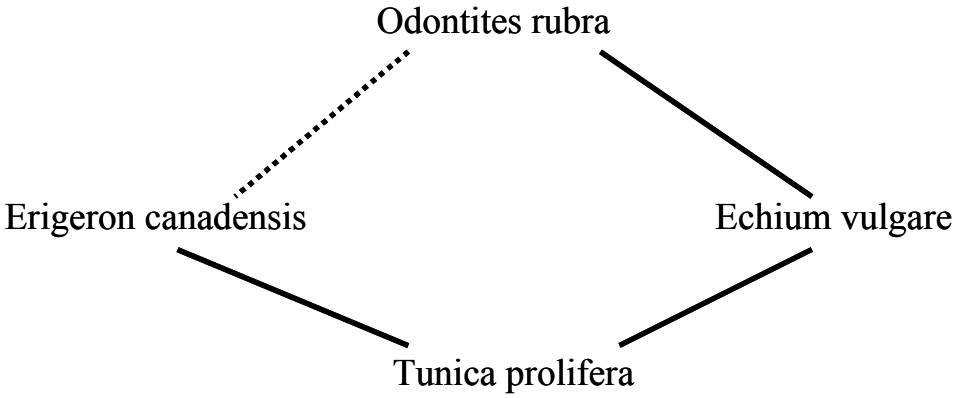

a)

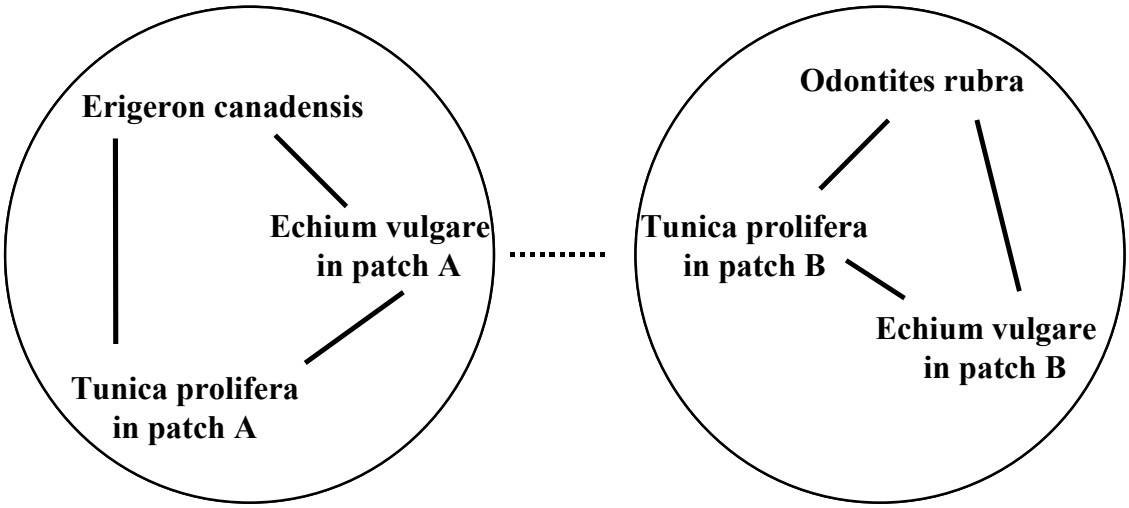

b)

Figure 1. *Illogical graf structure in the 19-year-old stage of primary succession on dumps of a strip coal-mine (after [2]). Pairwise associations were analysed by the standard chi-squrare procedure at 5.8 m^2 (at the area of maximum associatum). Positive associations were ploted by solid lines, negative association by dashed line. (a.) Erigeron canadensis and Odontites rubra associated negatively directly, while through Tunica prolifera and Echium vulgare they are associated positively. It seems to be paradoxical. The explanation of this paradox (Bartha S. pers. comm.), that there are three patch type (A, B, C) in the area. Erigeron lives only in A, Odontites lives only in B, Tunica and Echium live both in A and B, neither of them lives in C. It means that there are negative associations between two triplets and positive within them (b)*

http://www.ecology.uni-corvinus.hu ● ISSN 1589 1623

In spite of its importance, only few attempts have been made to measure these higher-order associations. This paper considers two approaches which seem to be suitable to describe the associations among species (incl. higher order associations) in detail.

The log-linear contingency table analysis was developed for describing and testing relations among categorical variables at 1960's [5, 6, 12, 33]. It was showed in detail in many books alone [19] or as a special case of GLM [15, 34]. Statistical handbooks [48, 54] also deal with it and it is implemented by the generally used statistical programs. Fienberg [18] presented the theory and some possible biological application, and it is used by other field of biology [21]. Its application to two-dimensional contingency tables in the vegetation science (incl. describing spatial pattern of plant communities) was discussed by Feoli et collegues [17] and Orlóci [37] in detail. In spite of this fact, I found only one example [11] to use it for describing associations among more than two species, and even there only one (i.e. test of total independence hypothesis) of the numerous possibilities of this method was used. Its reason may be that biological meaning of these possibilities has not been clear yet. By other words, statistical terms are not connected to the biological terms [28, 29, 30]. Without this connection, neither mathematical method can be used in biology.

The generally used systems of biological terms are not complex enough to describe the many possible relations among species (e.g. in the community with 10 species, there are 1024 possible species combinations and the number of possible relations are even higher, because there may be associations among species combinations). Juhász-Nagy recognised this problem in the 1960's, and developed a model family on the „coexistentional structures in coenology" [23, 24, 25, 26, 27, 31]. In this model family he considered the possible types of associations and the relationships among them from biological point of view. Beyond this theoretical foundation, he proposed information theory functions to measure the different types of associations. Due to the theoretical framework, his functions are more than ad hoc indices; they are theoretically well established, their biological meaning and the relationships among them are clear. In spite of its benefits, the approach did not become widespread.

Previously I showed that from mathematical point of view these two approaches are closely related [7]. In that paper I concentrated on the three main functions of Juhász-Nagy's family (i.e. local distinctiveness, diversity of species combinations and associatum), and did not consider the partitioning the overall association of community. This paper concentrates this topic and it aims to compare how the overall association (associatum) is partitioned in these two approaches and to show similarities and differences between them.

I supposed that the readers are familiar with basics of information theory and log-linear contingency table analysis. Therefore, their terminology is used here without any detailed explanation. However, the most important information was summarised and further literatures were listed in Appendices.

Partitioning of the associatum

In the previous paper [7] I showed that the measure of associatum (the overall association in the community) in Juhász-Nagy's approach equals the half of G(A,B,...,S) statistic. In this section I compare how the associatum can be partitioned in the two

http://www.ecology.uni-corvinus.hu ● ISSN 1589 1623

approaches. I do not follow the logic of either approach, I rather try to list the possible questions/problems and consider how the two approaches answer these questions.

For simplicity, I shall restrict my consideration to a community of three species (A, B, C). Let us introduce some notations. Let f_{ijk} (i = 0, 1; j = 0, 1; k = 0, 1) denote cell of three-way contingency table, e.g. f_{110} is the frequency of plots where species A and B are present and species C is absent. Let be $f_{\bullet jk} = \sum_i f_{ijk}$, $f_{i\bullet k} = \sum_j f_{ijk}$, $f_{ij\bullet} = \sum_k f_{ijk}$, $f_{i\bullet\bullet} = \sum_j \sum_k f_{ijk}$, $f_{\bullet j\bullet} = \sum_i \sum_k f_{ijk}$, $f_{\bullet\bullet k} = \sum_i \sum_j f_{ijk}$, and $f_{\bullet\bullet\bullet} = \sum_i \sum_j \sum_k f_{ijk}$.

Pair-wise association between species

The association between species A and species B is measured by G(A,B)-G(AB) in the log-linear contingency table analysis, and by nI(A,B) in Juhász-Nagy's approach. It can be showed that in the two-way contingency table G(A,B)=2nI(A,B) [7]. However, it is only the special case of the general relationship: G(A,B)-G(AB)=2nI(A,B) (i.e. in the two-way contingency table G(AB)=0).

Homogeneity of pair-wise associations

Let us consider again the example in <1>. It was mentioned above that in this community the pair-wise association between species A and B is zero. When we calculate pair-wise association, we suppose that the association between species is homogeneous, i.e. if the community is divided into parts based on the occurence other species, it is the same in the two parts. Let us divide this community into two parts based on the occurrence of species C:

	plots							
species	1	2	7	8	5	6	3	4
A	1	1	0	0	0	0	1	1
B	1	1	0	0	1	1	0	0
C	0	0	0	0	1	1	1	1

<2>

and calculate association between A and B in the two parts of the table separately. In Juhász-Nagy's approach, the two associations are $f_{\bullet\bullet 1} I(\mathrm{A,B|C}=0) = 4$ bit* and $f_{\bullet\bullet 0} I(\mathrm{A,B|C}=1) = 4$ bit, respectively. $nI(\mathrm{A,B|C}) = f_{\bullet\bullet 0} I(\mathrm{A,B|C}=0) + f_{\bullet\bullet 1} I(\mathrm{A,B|C}=1)$ is called association between A and B conditional to C or shortly, conditional association between A and B. (It should be mentioned that Juhász-Nagy [23] used partial association instead of conditional association. Because the partial association is used with different meaning in the log-linear contingency table analysis, I propose using conditional association to avoid confusion.) Conditional association between two species is higher than the association between them if the association is not homogeneous; i.e. it is not the same in the two parts of the community.

* Calculation of entropy and information in binary tables is easier with binary logarithm than natural logarithm. The values calculated by different logarithms differ only in units (viz. bit and nit, respectively).

http://www.ecology.uni-corvinus.hu ● ISSN 1589 1623

On the other hand, conditional association may be lower than pair-wise association if both species A and B are strongly associated to C. For example, in the following table:

	plots							
species	1	2	3	4	5	6	7	8
A	1	1	1	1	0	0	0	0
B	1	1	1	1	0	0	0	0
C	1	1	1	1	0	0	0	0

<3>

$f_{\bullet\bullet 0} I(\mathrm{A},\mathrm{B}|\mathrm{C}=0) = f_{\bullet\bullet 1} I(\mathrm{A},\mathrm{B}|\mathrm{C}=1) = nI(\mathrm{A},\mathrm{B}|\mathrm{C}) = 0$ bit, while $nI(\mathrm{A},\mathrm{B}) = 8$ bit.

Association of species to the community

The association of species C to the community is called complete association of C [27]. Its complementary is the subassociatum of the species C, which is the associatum of the community if species C is disregarded. The sum of complete association and subassociatum of species C equals the associatum.

The complete association of species C can be calculated by another way, by multiple association between C and [A,B]. Multiple association is a generalisation of pair-wise association. The three-way contingency table can be reduced to two-way table by joining two species. For example, we join species A and B and create a new four-state variable [A,B]. Its states are 11 (both species are present), 10 (species A is present, species B is absent), 01 (species A is absent, species B is present) and 00 (both species are absent):

		[A,B]				
		11	10	01	00	Σ
C	1	f_{111}	f_{101}	f_{011}	f_{001}	$f_{..1}$
	0	f_{110}	f_{100}	f_{010}	f_{000}	$f_{..0}$
	Σ	$f_{11.}$	$f_{10.}$	$f_{01.}$	$f_{00.}$	$f_{...}$

<4>

The multiple association between C and [A,B] (the complete association of C) is measured by the information content of this new two-way table [22]:

$$nI(\mathrm{C},[\mathrm{A},\mathrm{B}]) = nH(\mathrm{C}) + nH([\mathrm{A},\mathrm{B}]) - nH(\mathrm{C},[\mathrm{A},\mathrm{B}]) \quad \text{(Eq. 1)}$$

where:

$$nH(\mathrm{A}) = n\ln n - \sum_k f_{\bullet\bullet k} \ln f_{\bullet\bullet k} \quad \text{(Eq. 2)}$$

$$nH([\mathrm{A},\mathrm{B}]) = nH(\mathrm{A},\mathrm{B}) = n\ln n - \sum_i \sum_j f_{ij\bullet} \ln f_{ij\bullet} \quad \text{(Eq. 3)}$$

$$nH(\mathrm{C},[\mathrm{A},\mathrm{B}]) = nH(\mathrm{A},\mathrm{B},\mathrm{C}) = n\ln n - \sum_i \sum_j \sum_k f_{ijk} \ln f_{ijk} \quad \text{(Eq. 4)}$$

Based on (1), (2), (3), and (4):

$$nI(\mathrm{C},[\mathrm{A},\mathrm{B}]) = n\ln n + \sum_i \sum_j \sum_k f_{ijk} \ln \frac{f_{ijk}}{f_{ij\bullet} f_{\bullet\bullet k}} = \sum_i \sum_j \sum_k f_{ijk} \ln \frac{f_{ijk}}{\left(f_{ij\bullet} f_{\bullet\bullet k}\right)/n} \quad \text{(Eq. 5)}$$

Since $(f_{ij.} f_{..k})/n$ is the expected value of the model (AB, C),

$$2nI(\mathrm{C},[\mathrm{A},\mathrm{B}]) = G(\mathrm{AB},\mathrm{C}) \quad \text{(Eq. 6)}$$

http://www.ecology.uni-corvinus.hu ● ISSN 1589 1623

Third-order interaction

First, the meaning of third-order interaction has to be clarified. Let us consider the following three examples:

	plots							
species	1	2	3	4	5	6	7	8
A	1	1	1	1	0	0	0	0
B	1	1	1	1	0	0	0	0
C	1	1	1	1	0	0	0	0

<5>

	plots							
species	1	2	3	4	5	6	7	8
A	1	1	1	0	0	0	0	0
B	0	0	0	1	1	1	0	0
C	1	1	1	1	1	1	0	0

<6>

	plots							
species	1	2	3	4	5	6	7	8
A	1	1	1	1	0	0	0	0
B	1	1	0	0	1	1	0	0
C	0	0	1	1	1	1	0	0

<7>

In table <5>, all pair-wise associations are positive, and the table can be described completely by any two of them, i.e. expected values in all of the model AB,AC, the model AB,BC, or the model AC,BC equal the observed values. Thus, the third pair-wise association does not have additional information; it can be regarded as redundant.

In table <6>, the association between species A and B is negative, while species C is associated positively to both other species. Thus the third pair-wise association have additional information, it is not redundant. The association between A and C conditional to B is higher than their pair-wise association, because the occurrence of species B prevents the manifestation of the positive association between A and C, while in the absence of species B, the positive association is stronger than in the whole community. In spite of this effect, the table can be described completely by the three pair-wise associations, i.e. expected values of model AB,AC,BC equal to the observed values.

In table <7>, all the pair-wise associations are zero, but any two species determine the occurrence of the third. The table can not be described completely by the three pair-wise associations, i.e. expected values of model AB,AC,BC considerably differ from the observed values.

In the terminology of log-linear contingency table analysis, there is third-order interaction only in the third case. Its measure is G(AB,AC,BC)–G(ABC) (in the case of three species G(ABC)=0).

In Juhász-Nagy's approach, third-order interaction means that the sum of pair-wise associations differs from the associatum. Its measure is the third-order interassociatum: the difference between the sum of pair-wise associations and the associatum (Juhász-Nagy 1967a):

$$nI([\mathrm{A};\mathrm{B};\mathrm{C}]) = nI(\mathrm{A},\mathrm{B}) + nI(\mathrm{A},\mathrm{C}) + nI(\mathrm{B},\mathrm{C}) - nI([\mathrm{A},\mathrm{B},\mathrm{C}]) \qquad \text{(Eq. 7)}$$

http://www.ecology.uni-corvinus.hu ● ISSN 1589 1623

Generally, the k-order interassociatum is obtained by the subtraction of overall association (k-2) times from the sum of (k-1)-way associations [26, 27]. It should be noted that -2nI([A;B;C]) equals 'RCD-interaction' in Kullback [33], and in the case of three species:

(Eq. 8)

$$nI([A;B;C]) = nI(A,B|C) - nI(A,B) = nI(A,C|B) - nI(A,C) = nI(B,C|A) - nI(B,C)$$

In table <5>, the interassociatum is positive; it indicates the redundancy among the pair-wise associations, i.e. we try to describe the fact that the three species form coalition by three pair-wise associations. On the other hand, in table <6> and <7> the interassociatum is negative. It indicates that the pair-wise associations are not homogeneous.

This different definition of third order interaction in the two approaches has historical reasons. Expected values in the model AB,AC,BC can not be calculated without iterative procedure. Although this iterative procedure was developed in 1940 [13, cit. 18], it became widely used much later: for example, Kullback [33] did not mention this procedure. Instead, he applied an inappropriate method to calculate expected values [18]. Later, this iterative procedure became widely used, and RCD-interaction was not applied by statisticians [19].

Juhász-Nagy began developing his models in the early 1960's and he applied the information statistical methods of that time (e.g. he used Kullback's [33] book). Later, he concentrated on the biological meaning of the models, rather than their refinement from mathematical point of view.

Kullback's [33] RCD interaction (it is analogous to the interassociatum) were strongly criticised [18], because it can lead to negative values for G-statistic. From mathematical point of view, the negative value is a mistake. However, in the analysis of associations among species it has meaning. Another possible drawback of interassociatum is that in a species-rich community there may be positive interassociatum among some species, while negative among others and zero in the whole community. This problem can be avoided if interassociatum is calculated not only in the whole community, but also in the sub-communities.

Comparison of the two approaches

Above I considered five topics. Two of them (pair-wise association, complete association of species) can be treated in both approaches and the result is the same (except the multiplication by two). Homogeneity of associations and the corresponding conditional association are very important in ecology. Although it is not part of the standard methodology, conditional associations can be calculated from the G-statistics, due to the additive relations between the information theory functions. The third-order interaction is defined and measured differently in the two approaches. The third-order interaction of log-linear contingency table analysis is a subset of third-order interaction of Juhász-Nagy's approach. I think *G*(AB,AC,BC) /or it analogues in the case of more species/ should be incorporated into Juhász-Nagy's methodological framework, because the distinction of two types of third-order interactions may be useful.

In this paper I concentrate on the associations among species, therefore many functions from Juhász-Nagy's model (e.g. dissociatum) are not considered here. However, it should be mentioned that in Juhász-Nagy's approach not only the

http://www.ecology.uni-corvinus.hu ● ISSN 1589 1623

dependencies among species (i.e. association), but also their independence can be measured. In the log-linear contingency table analysis, this aspect is neglected.

An example for analysing higher-order associations

Above, the meaning or properties of the functions are illustrated only with sporadic examples. Here I will analyse associations in an artificial community in detail. The community consists of three species: species A is a tree, species B is a tussock forming grass, and species C is an annual herb. There are only two assembly rules in this community: (1) Species C lives in the gaps among the tussocks of species B. (2) Both species B and C occur in the shadow of species A, however the tussocks of species B and the gaps among the tussocks become smaller here. In this simple case, the structure of the community seems to be clear by looking at the maps of species (*Fig. 2*). It is expected that there are significant negative association between species A and B, and the other associations are non-significant. However, it will be showed that the situation is more complex.

a) Species A

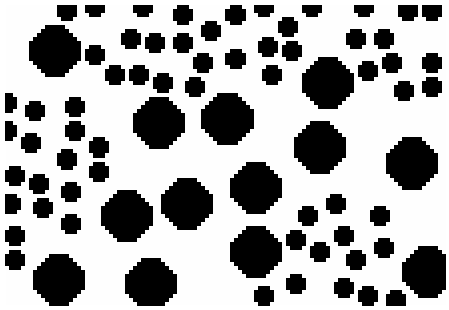

b) Species B

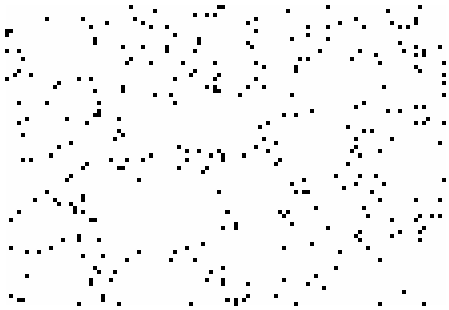

c) Species C

Figure 2. *Distribution map of the species in the artificial dataset*

http://www.ecology.uni-corvinus.hu ● ISSN 1589 1623

The size of distribution map is 22x15 m; its resolution is 20x20 cm. Nine different plot sizes were used between 0.04 and 16 m^2. From Juhász-Nagy's functions the associatum, the pair-wise and conditional associations, the complete association of species, and the interassociatum were calculated. Beyond these functions, G(AB,AC,BC) statistic was used because it can not be calculated from Juhász-Nagy's functions. To determine their significance, observed functions were compared to functions calculated from random references produced by random shift method [4, 38]. One thousand random references were used. The sign of pair-wise associations were determined according to Bartha and Kertész [4], i.e. the association is positive if $(a+d)>(a_0+d_0)$, while it is negative if $(a+d)<(a_0+d_0)$, where a and d are observed values in the 2x2 contingency table, a_0 and d_0 are their average in the random cases.

As it is expected, there is a significant negative association between species B and C at a wide range of scales (*Fig. 3c.*).

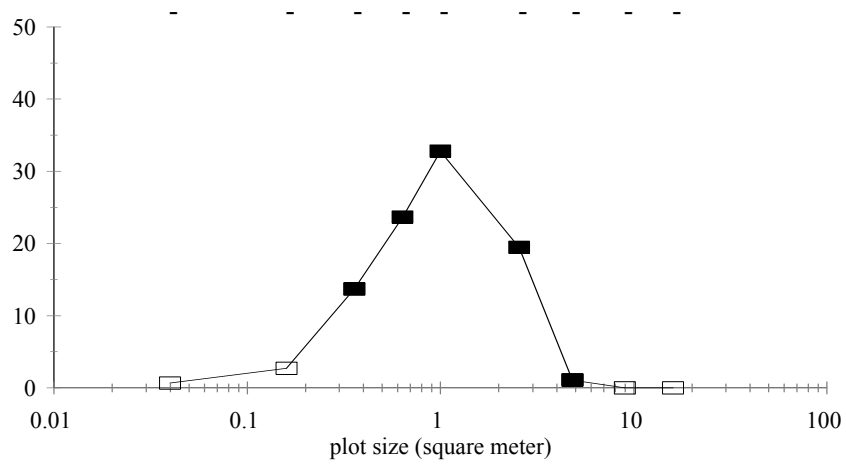

a) association between species A and B

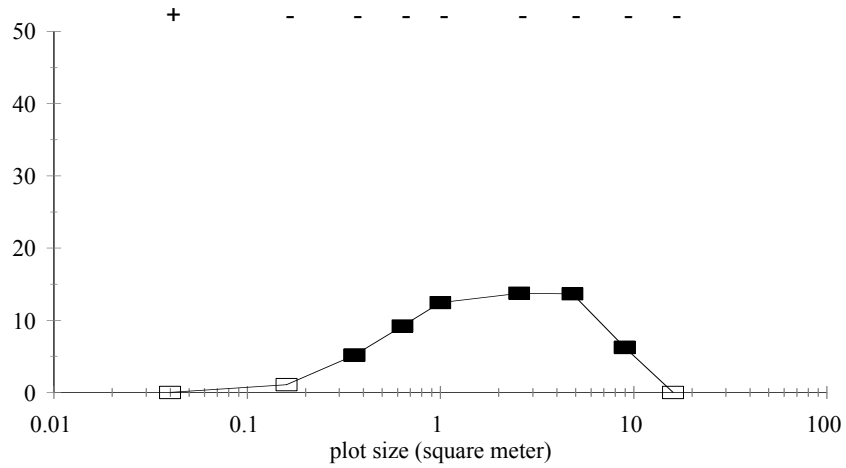

b) association between species A and C

http://www.ecology.uni-corvinus.hu ● ISSN 1589 1623

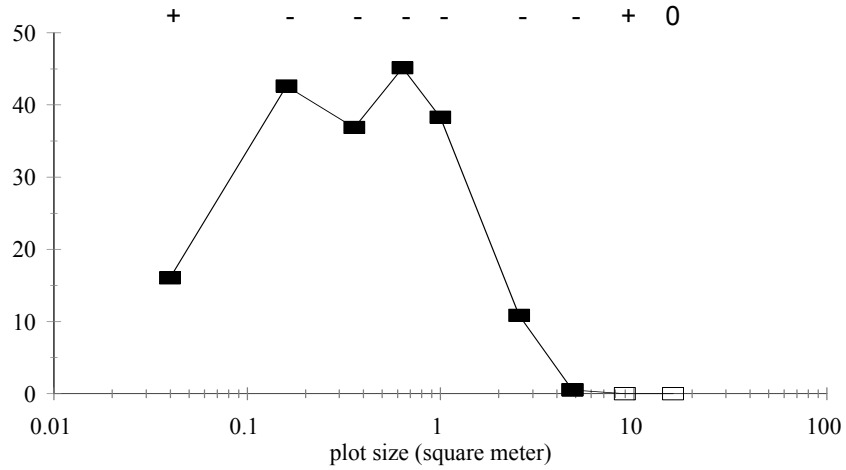

c) association between species B and C

Figure 3. *Pairwise associations as a function of scale. Filled squares mark field data significantly different from random, empty squares field data not different from random. Direction of association are indicated at the top of figure by + or -.*

However, this association is significantly positive at 0.04 m^2. This pattern of signs is inconsistent with the pattern expected by Greig-Smith [20], and Kershaw and Looney [32], i.e. association is negative at fine scale that changes to positive at coarse scale. On the other hand, it is in line with results of Bartha and Kertész [4] who suggested that at fine scale the positive association is the consequence of high proportion of empty cells. Indeed, the detailed analysis of signs (*Fig. 4*) shows that at the smallest plot size the sign of the association is determined by the difference between the observed and expected number of empty cells (d-d_0). Thus, this positive association does not mean that at this scale the two species coexist more frequently than expected, but it means that the frequency of empty plots is higher than expected.

The other two pair-wise associations also have significant negative values at a broad range of scales (*Fig. 3a,b*). These relations can not be predicted without detailed analysis, by looking at the distribution map only. Both negative associations are the consequence of the effect of species A to the spatial pattern of species B (i.e. size and density of tussocks). Due to the smaller tussocks and smaller gaps in the presence of species A, the frequency of both species B and C is smaller here than expected.

Because of the relationships between pair-wise associations (Eq. 8), I consider in detail the homogeneity of association between species B and C only. It is selected because it is the highest from the three pair-wise associations at broad range of plot sizes (*Fig. 3*). At intermediate plot sizes, conditional association between species A and B is considerable higher than pair-wise association between them (*Fig. 5*). It suggests that the association between the two species is inhomogeneous. In the case of three species, the difference between the conditional and pair-wise association equals the interassociatum (cf. Eq. 8), which is significantly lower than the random expectation from 0.16 m^2 to 4.84 m^2 plot size (*Fig. 6*). It means that in this range the association between species B and C is inhomogeneous. The association between the two species is considerably lower and the maximum area of the association is smaller in the presence of species A than in its absence (*Fig. 7*). It is the consequence of smaller gaps and tussocks.

http://www.ecology.uni-corvinus.hu ● ISSN 1589 1623

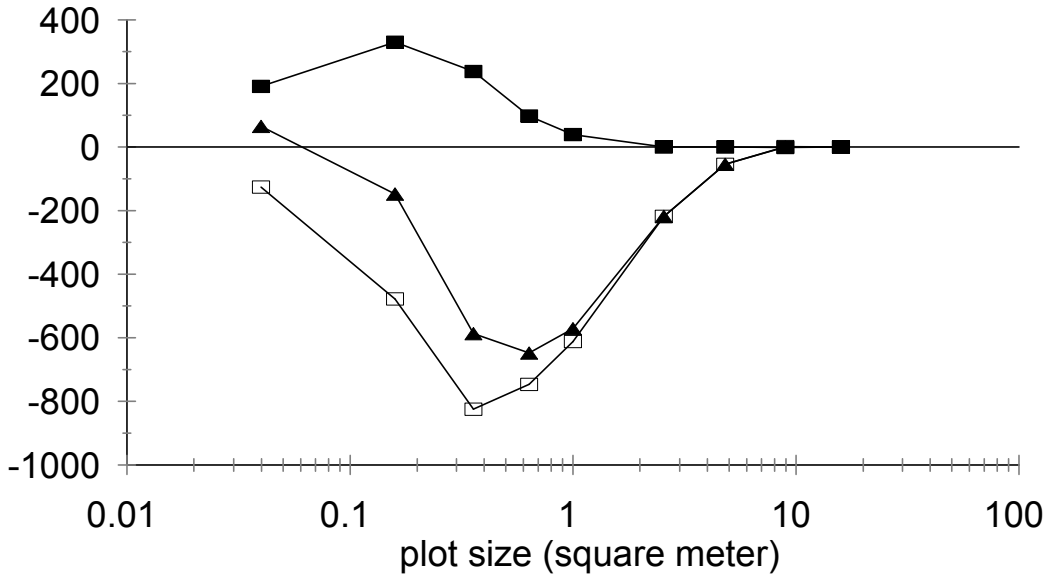

Figure 4. *Factors of sign of assoctiation between species A and B. Empty square: a-a_0, filled square: d-d_0, filled triangle: (a+d)-(a_0+d_0).*

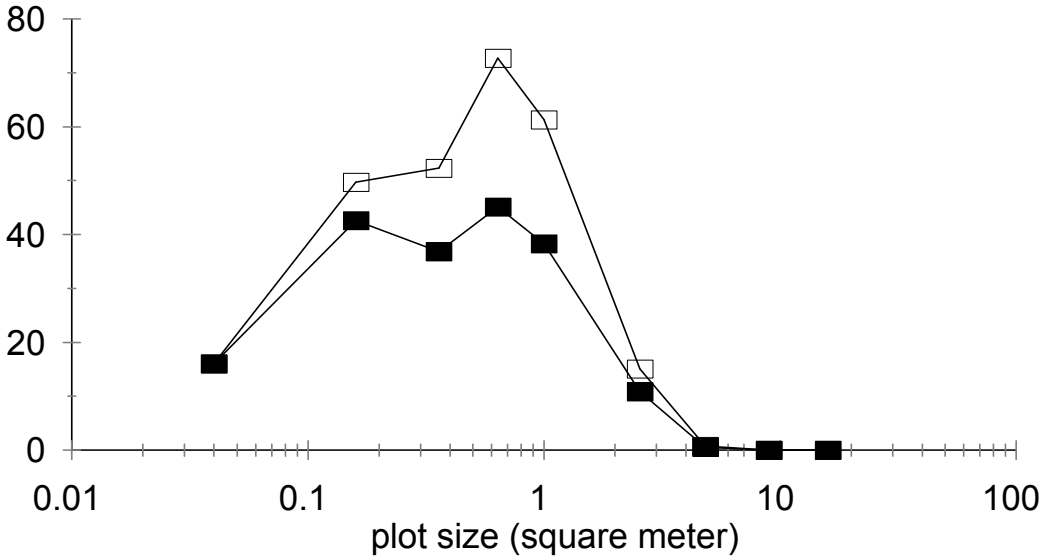

Figure 5. *Pairwise (filled square) and conditional (empty square) association between species B and C.*

G(AB,AC,BC) is significantly higher than expected in random situation between 0.16 and 1 m^2 plot size (*Fig. 8*). It indicates that at this range the structure of the community can not be described sufficiently by pair-wise associations.

http://www.ecology.uni-corvinus.hu ● ISSN 1589 1623

At small and intermediate plot sizes species B has the highest complete association (*Fig. 9*). The explanation may be that on one hand, the pattern of species B is affected by species A, on the other hand, species B affects the pattern of species C. Thus, pattern of this species is strongly related to the pattern of the other two species, while the pattern of species A and C are not related directly, only through species B.

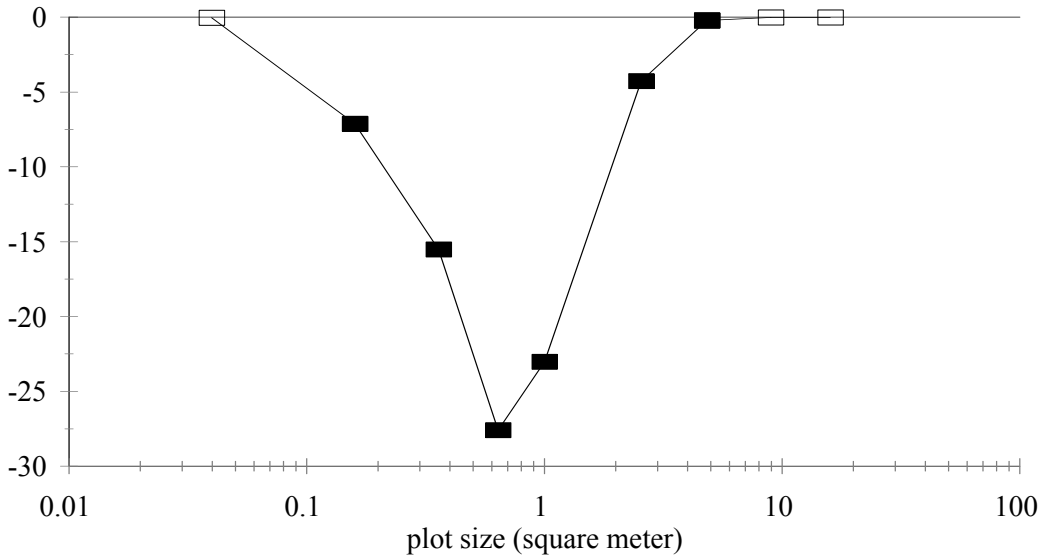

Figure 6. *Interassociatum as a function of scale. Filled squares mark field data significantly different from random, empty squares field data not different from random.*

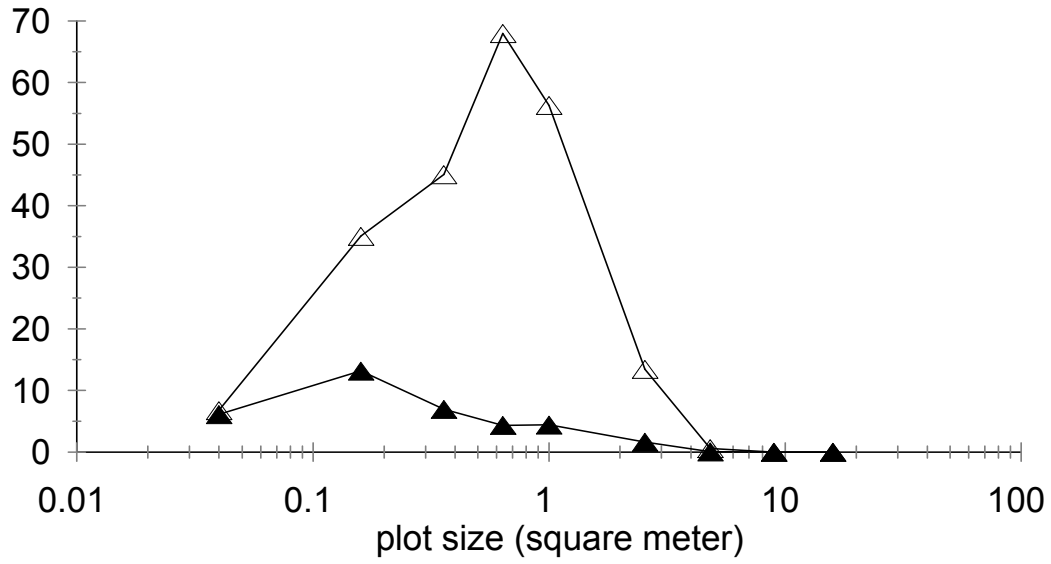

Figure 7. *Association between species B and C in the shadow of species A (filled triangle) and in the light (empty triangle).*

http://www.ecology.uni-corvinus.hu ● ISSN 1589 1623

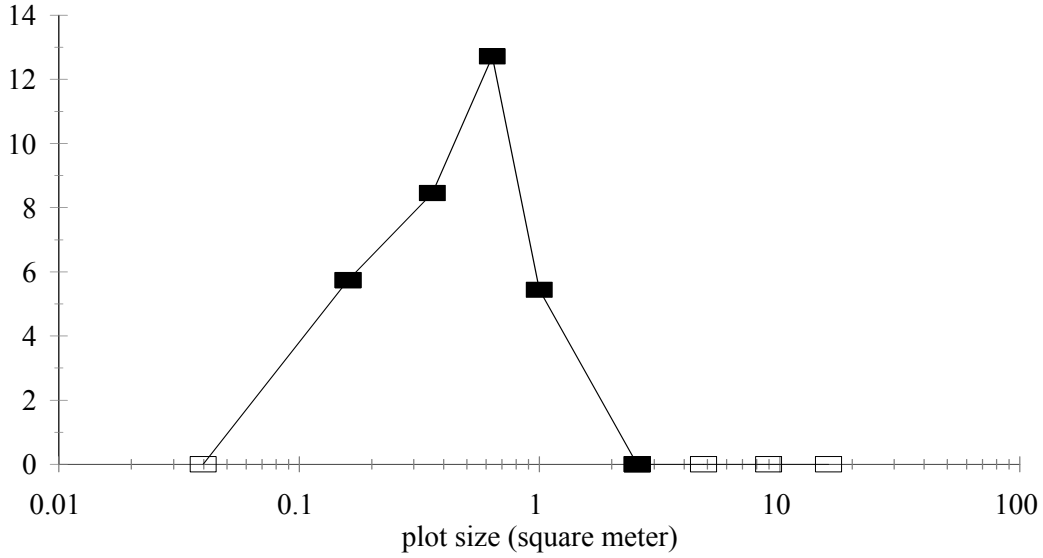

Figure 8. *G(AB, AC, BC)-statistic as a function of scale. Filled squares mark field data significantly different from random, empty squares field data not different from random, filled triangles: upper and lower bound of 95% confidence interval.*

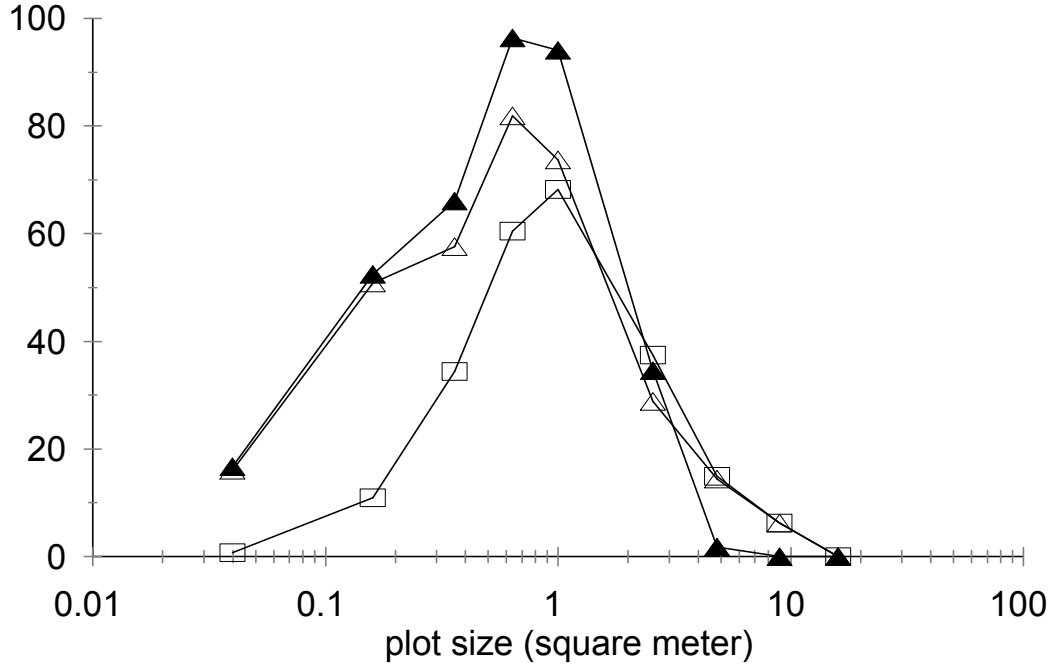

Figure 9. *Complete association of species A (empty square), B (filled triangle), and C (empty triangle).*

Even in this simple example, including only three species and two rules, associations among species can not be understood only by looking at distribution map or by calculating only pair-wise associations. It should be emphasised that in real communities the pattern is much more complex (there are more species and more rules) and they cannot be understood without detailed analyses.

http://www.ecology.uni-corvinus.hu ● ISSN 1589 1623

Conclusion

Although, the existence of higher order associations is theoretically justified [10], only few attempts have been made to reveal them. In case studies, association is generally treated as a pair-wise phenomenon. The possible reason is that although pair-wise association is only an imperfect description of the relationships among species, its methods are simple and well known.

Unfortunately, the complexity of vegetation can not be described by such simple methods. It is well known that vegetation is not in equilibrium [39, 40], homogeneity and stationarity criteria do not hold [9, 52], and several mechanisms (e.g. competition, propagule limitation, etc.) are acting together. However, the consequence of these facts, i.e. the complexity of vegetation, has not been generally acknowledged yet. I think the analysis of more complex relationships than the pair-wise associations should not be delayed longer.

The study of this complex relationship is impossible without solid methodological basis. The aim of both approaches, considered in this paper, are the establishment of such methodological basis. The main difference between them is that the log-linear contingency table analysis was developed by statisticians to solve general statistical problems. It can be used in vegetation science if these general statistical problems are translated into the special problems of vegetation science. This translation has not been done yet. I know only one application in this field by Dale et collegues [11], and they used only one of the numerous possibilities of this method. One aim of this paper is to begin this translation (I considered the possible relations only in the case of three species), and by this way to help to use log-linear contingency table analysis in vegetation science. However, it should be emphasised that this research field is characterised by special features [7], e.g. the importance of diversity, which can not be handled by the standard statistical methods (including log-linear contingency table analysis).

On the other hand, Juhász-Nagy's approach was developed by a biologist to solve biological problems. Therefore, although both approaches use many difficult terms, in Juhász-Nagy's approach, these terms come from the Central-European phytosociological tradition and field experiences and these terms always have biological meaning. By contrast, in the log-linear contingency table analysis terms come from the analogous statistical methods (e.g. regression analysis) and these terms have only statistical meaning. According to this advantage of Juhász-Nagy's framework, I propose to incorporate additional facilities of log-linear contingency table analysis (eg. calculation of G(AB,AC,BC) by iterative algorithm) into this framework, rather than replace this framework by loglinear contingency table analysis.

Acknowledgements. Many thanks to Sándor Bartha for his valuable comments and suggestions.

REFERENCES

[1] Agnew, A.D.Q. (1961): The ecology of Juncus effusus in North Wales. – Journal of Ecology 49: 83-102.

[2] Bartha, S. (1992): Preliminary scaling for multi-species coalitions in primary sucession. – Abstracta Botanica 16: 31-41.

[3] Bartha, S., Czárán, T., Podani, J. (1998): Exploring plant community dynamics in abstract coenostate spaces. – Abstracta Botanica 22: 49-66.

http://www.ecology.uni-corvinus.hu ● ISSN 1589 1623

[4] Bartha, S., Kertész, M. (1998): The importance of neutral-models in detecting interspecific spatial associations from 'trainsect' data. – Tiscia 31: 85-98.
[5] Birch, M. W. (1963): Maximum likelihood in three-way contingency tables. – J. Roy. Statist. Soc. B. 25: 220-233.
[6] Bishop, Y.M.M. (1969): Full contingency tables, logits and split contingency tables. – Biometrics 25: 383-400.
[7] Botta Dukát, Z. (2005): The relationship between Juhász-Nagy's information theory functions and the log-linear contingency table analysis. – Acta Botanica Hungarica 47: 53-73.
[8] Czárán, T. (1998): Spatiotemporal Models of Population and Community Dynamics. – Chapman and Hall, New York.
[9] Czárán, T., Bartha, S. (1992): Spatiotemporal dynamics models of plant populations and communities. – Trends in Ecology and Evolution 7: 38-42.
[10] Dale, M.R.T. (1999): Spatial pattern analysis in plant ecology. – Cambridge University Press, Cambridge.
[11] Dale, M.R.T., Blundon, D.J., MacIsaac, D.A,. Thomas, A.G. (1991): Multiple species effects and spatial autocorrelation in detecting species associations. – Journal of Vegetation Science 2: 635-642.
[12] Darroch, J.N. (1962): Interactions in multi-factor contingency tables. – J. Roy. Statist. Soc. B. 24: 251-263.
[13] Deming, W.E., Stephan, F.F. (1940): On a least square adjustment of a sampled frequency table when the expected marginal totals are known. – Ann. Math. Statist. 11: 427-444.
[14] de Vries, D.M. (1953): Objective combinations of species. – Acta Botanica Neerlandica 1: 497-499.
[15] Dobson, A.J. (2002): An introduction to generalized linear models. – Chapman and Hall/CRC, Boca Raton. 2nd ed.
[16] Erdei, Zs., Tóthmérész, B. (1993): MULTI-PATTERN 1.00. Program package to analyze and simulate community-wide patterns. – Tiscia 27: 45-48.
[17] Feoli, E., Lagonegro, M., Orlóci, L. (1984): Information analysis of vegetation data. – Dr. W. Junk, The Hague.
[18] Fienberg, S.E. (1970): The analysis of multidimensional contingency tables. – Ecology 51: 419-433.
[19] Gokhale, D.V, Kullback, S. (1978): The Information in Contingency Tables. – Marcel Dekker, Inc., New York.
[20] Greig-Smith, P. (1983): Quantitative Plant Ecology. –University of California Press, Berkeley. 3rd ed.
[21] Herben, T., Liska, J. (1988): The use of multi-way contingency tables for the study of epiphytic lichen distribution. – Coenoses 3: 135-139.
[22] Horváth, A. (1998): INFOTHEM program: new possibilities of spatial series analysis based on information theory methods. – Tiscia 31: 71-84.
[23] Juhász-Nagy, P. (1967a): On association among plant populations I. Multiple and partial association: a new approach. – Acta Biologica Debrecina 5: 43-56
[24] Juhász-Nagy, P. (1967b): On some "Characteristic areas" of plant community stands. – In Rényi, A. (ed.): Proceedings of the Colloquium on Information Theory, organized by the Bolyai Mathematical Society in Debrecen, Hungary.
[25] Juhász-Nagy, P. (1976): Spatial dependence of plant population. Part 1. Equivalence analysis (an outline for a new model). – Acta Botanica Academiae Scientiarum Hungaricae 22: 61-78.
[26] Juhász-Nagy, P. (1980): A cönológia koegzisztenciális szerkezeteinek modellezése. – Doctoral Thesis, Budapest.
[27] Juhász-Nagy, P. (1984): Spatial dependence of plant population. Part 2. A family of new models. – Acta Botanica Hungarica 30: 363-402.

http://www.ecology.uni-corvinus.hu ● ISSN 1589 1623

[28] Juhász-Nagy, P. (1985): Some problems of a conceptual system in biology. Part 1. Creative critical comments on a dictionary. – Abstracta Botanica 9: 33-58. (in Hungarian with English summary)
[29] Juhász-Nagy, P. (1986): Some problems of a conceptual system in biology. Part 2. Speculations on missing concepts. – Abstracta Botanica 10: 35-78. (in Hungarian with English summary)
[30] Juhász-Nagy, P. (1987): Some problems of a conceptual system in biology. Part 3. Importance of conceptual constructions. – Abstracta Botanica 11: 97-116. (in Hungarian with English summary)
[31] Juhász-Nagy, P., Podani, J. (1983): Information theory methods for the study of spatial processes and sucession. – Vegetatio 51: 129-140
[32] Kershaw, K.A., Looney, J.H.H. (1985): Quantitative and Dynamic Plant Ecology. – Edward Arnold, Baltimore. 3rd. ed.
[33] Kullback, S. (1959): Information theory and statistics. – John Wiley and Sons, New York.
[34] Lindsey, J.K. (1997): Applying generalized linear models. – Spinger, New York.
[35] Nuñez, C.I., Aizen, M.A., Ezcurra, C. (1999): Species associations and nurse plant effects in patches of high-Andean vegetation. – Journal of Vegetation Science 10: 357-364.
[36] Orlóci, L. (1978): Multivariate Analysis in Vegetation Research. – Junk, The Hague. 2nd ed.
[37] Orlóci, L. (1991): CONAPACK: program for canonical analysis of classification tables. Ecological Computations Series. Vol. 4. – SPB Acedemic Publishing bv, The Hague.
[38] Palmer, M. W., van der Maarel, E. (1995): Variance in species richness, species association, and niche limitation. – Oikos 73: 203-213.
[39] Pickett, S.T.A. (1980): Non-equilibrium coexistence of plants. – Bulletin of the Torrey Botanical Club 107: 238-248.
[40] Pickett, S.T.A., White, P.S. (eds.) (1985): The ecology of natural disturbance and patch dynamics. – Academic Press, New York.
[41] Pielou, E.C. (1969): An introduction to mathematical ecology. – Johm Wiley and Sons, New York.
[42] Podani, J. (1991): SYN-TAX IV. Computer programs for data analysis in ecology and systematics. – In: Feoli, E., Orlóci, L. (eds.): Computer Assisted Vegetation Analysis. Kluwer, The Neatherlands.
[43] Podani, J. (2000): Introduction to the Exploration of Multivariate Biological Data. – Backhuys Publishers, Leiden.
[44] Rényi, A. (1961): On measure of entropy and information. – In Neyman, J. (ed): Proceedings of the 4th Berkeley Symposium on Mathemathical Statistics and Probability. University of California Press, Berkeley.
[45] Rényi, A. (1987): A Diary on Information Theory. – John Wiley and Sons, Chichester.
[46] Shannon, C.E. (1948): A Mathematical Theory of Communication. – Bell System Technical Journal 27: 379-423, 623-656
[47] Shannon, C.E. and Weaver, W. (1999): The Mathematical Theory of Communication. – University of Illinois Press, Urbana.
[48] Sokal, R.R., Rohlf, F.J. (1981): Biometry. The priciples and practice of statistics in biological research. –Freeman, New York. 2nd eds.
[49] Soro, A., Sundberg, S., Rydin, H. (1999): Species diversity, niche metrics and species associations in harvested and undisturbed bogs. – Journal of Vegetation Science 10: 549-560.
[50] Taneja, I.J. (1989): On Generalized Information Measures and Their Applications. – Advances in Electronics and Electron Physics 76: 327-413.
[51] Taneja, I.J. (2001): Generalized Information Measures and Their Applications. – http://www.mtm.ufsc.br/~taneja/book/book.html
[52] Tilman, D. (1994): Competition and biodiversity in spatially structured habitats. – Ecology 75:2-16.

http://www.ecology.uni-corvinus.hu ● ISSN 1589 1623

[53] Welch, J.R. (1960): Observations on deciduous woodland in the eastern province of Tanganyika. – Journal of Ecology 48:557-573.
[54] Zar, J.H. (1999): Biostatistical Analysis. – Prentice Hall International Inc., New Jersey.

Appendix 1.: Basics of log-linear contingency table analysis

Log-linear contingency table analysis was developed to analyse the relationship among categorical variables (or by other words the structure of multidimensional contingency tables). Here I concentrate on the binary variables (species) and the corresponding binary tables only. Frequencies in the cells of such tables depend on the following effects: grand total of the table, frequency of species and associations among species. One aim of the analysis is to choose the important effects. Sets of effects are called models and each model corresponds to an expected contingency table. These expected contingency tables were calculated by an iterative procedure. The number of possible models is restricted by some constructional rules. For example, if the model contains association between species A and B, it has to contain their frequencies.

It can be tested by G-statistic whether the expected contingency table significantly differs from the observed contingency table or not. Let $G(X)$ denote the G-statistic calculated from the expected contingency table corresponding to model X. If value of $G(X)$ does not exceed the critical value (the expected contingency table does not differ significantly from the observed one), the model X contains all important effects.

Another aim of the analysis may be to measure the importance of the factor(s). The difference of G-statistics can be used for this purpose. The advantage of G-statistic over Pearson's chi-square is that the difference between two Pearson's chi-square statistics does not have chi-square distribution, while $G(X_1)$-$G(X_2)$ has approximately chi-square distribution if (and only if) X_1 contains all effects of X_2. Thus, the importance of effects also has approximately chi-square distribution.

More details can be found for example in [18, 19, 48].

There are not consistent notations of models in the literature. Here I use a simple notations, which similar to that used in the information functions. Some possible models, their notations and effects considered by them are listed below for the case of 3 species (A, B, C):

Models	considered effect
0	number of plots,
A	number of plots, frequency of species A
B	number of plots, frequency of species B
C	number of plots, frequency of species C
AB	number of plots, frequency of species A, frequency of species B, association between species A and B
AB,C	number of plots, frequency of species A, frequency of species B, frequency of species C, association between species A and B
AC	number of plots, frequency of species A, frequency of species C, association between species A and C
AC,B	number of plots, frequency of species A, frequency of species B, frequency of species C, association between species A and C
BC	number of plots, frequency of species B, frequency of species C, association between species B and C

http://www.ecology.uni-corvinus.hu ● ISSN 1589 1623

BC, A	number of plots, frequency of species A, frequency of species B, frequency of species C, association between species B and C
AB, AC	number of plots, frequency of species A, frequency of species B, frequency of species C, association between species A and B, association between species A and C
AB, BC	number of plots, frequency of species A, frequency of species B, frequency of species C, association between species A and B, association between species B and C
AC, BC	number of plots, frequency of species A, frequency of species B, frequency of species C, association between species A and C, association between species B and C
AB, AC, BC	number of plots, frequency of species A, frequency of species B, frequency of species C, association between species A and B, association between species A and C, association between species B and C
ABC	number of plots, frequency of species A, frequency of species B, frequency of species C, association between species A and B, association between species A and C, association between species B and C, third-order interactions among species.

Appendix 2: Entropy and mutual information

Here I consider only the simplest case: two binary variables (species), because it is enough to explain the meaning of terms. Let us assume that we study the spatial association of two species (A and B). During the sampling the presence/absence of species were recorded in *n* plots, and the results of sampling, i.e. the observed data, were summarised in the well-known 2x2 contingency table:

		A		
		1	0	Σ
B	1	*a*	*b*	*a*+*b*
	0	*c*	*d*	*c*+*d*
	Σ	*a*+*c*	*b*+*d*	*n*

Let us assume that we randomly choose one from the *n* plot, but before choosing we try to predict the properties of this plot. The entropies measure the uncertainty of our prediction. The entropy of species A (its symbol is $H(A)$) is the uncertainty of our prediction with respect to occurrence of species A. It is zero if species A is present in or absent from all plots, while it is maximal if species A is present in the half of the plots. The entropy of species B (its symbol is $H(B)$) can be defined by the same way.

The joint entropy of the two species is the uncertainty of our prediction about the species composition of the chosen plot. In this case, there are four possible species combinations: i.e. both species are present, A is present and B is absent, A is absent and B is present, both species are absent. Our uncertainty (the joint entropy of the two species, (its symbol is $H(A,B)$) is zero if the species composition of all plots is the same, while it is maximal if the frequency of all possible species combinations are equal.

Let us assume that we try predicting occurrence of species B when we know that species A is present or absent in the plot. The uncertainty of this prediction is the

http://www.ecology.uni-corvinus.hu ● ISSN 1589 1623

entropy of species B conditional to species A (its symbol is $H(B|A)$). The information about the occurrence of species A can decrease our uncertainty about the occurrence of species B, if the occurrence of two species are not independent. This decrease of the uncertainty is the mutual information of the two species:

$$I(A,B) = H(A) - H(A|B) = H(B) - H(B|A)$$

The mutual information is a symmetric measure. It is zero if the occurrence of two species independent from each other, and positive otherwise. It measures the strength of association between two species. Mutual information can be calculated from the joint entropy and the two entropies:

$$I(A, B) = H(A)+H(B)-H(AB)$$

With some rearrangement of this equation we find that if the occurrence of two species are independent /I(A,B)=0/, their joint entropy equals the sum of their entropies.

Entropies can be estimated by different entropy functions (e.g. Rényi's family of entropy functions, [44]), however Shannon-function is the most commonly used [41].

Further information can be found in the following books and papers: Rényi's [45] book is an excellent introduction to the mathematics of information theory, Shannon's classical work [46, 47] explains well the logic of his entropy function, Kullback [33] treats the statistical aspects of the information theory in detail, Taneja [50, 51] gives a good overview on the properties of Shannon's entropy and the generalized entropy functions, biological applications of information theory were discussed by e.g. Feoli et collegues [17].

Appendix 3: Computer programs

The log-linear contingency table analysis is a standard statistical procedure; therefore, it is part of the widely used statistical programs (e.g. Statistica, SPSS, Statgraphics, etc.). There are some drawbacks of these programs:

- computerised sampling and randomisation have to be done with another program,
- the maximal number of species may be restricted,
- sometimes, the iterative algorithm cannot handle the contingency tables with many empty cells.

These problems should be overcome in the future.

There are many different programs to calculate Juhász-Nagy's functions [3, 16, 22, 42]. They often perform not only the calculations but the computerised sampling and randomisation too. Thus, their use seems to be more convenient than use of general statistical packages. Unfortunately, as I mentioned above, some G-statistics (first of all third-order interactions) can not be calculated from Juhász-Nagy's functions, because they are calculated by the iterative procedure.

http://www.ecology.uni-corvinus.hu ● ISSN 1589 1623

PHYLOGENETIC TREE BUILDING USING A NOVEL COMPRESSION-BASED NON-SYMMETRIC DISSIMILARITY MEASURE

R. BUSA-FEKETE[1] – A. KOCSOR[1]*– CS. BAGYINKA[2]

[1]Research Group on Artificial Intelligence of the Hungarian Academy of Sciences and University of Szeged H-6720 Szeged, Aradi vértanúk tere 1., Hungary (phone: +36-62-524-140; fax: +36-62-425-508)

**Corresponding author e-mail: busarobi.kocsor@inf.u-szeged.hu*

[2]MTA SZBK Institute of Biophysics H-6701 Szeged, POBox. 521., Hungary (phone: +36-62-599-605; fax: +36-62-433-133) e-mail: csaba@nucleus.szbk.u-szeged.hu

(Received 10th Sep 2005, accepted 10th Oct 2006)

Abstract. An approach of building phylogenetic trees is to define a distance function based on amino acid sequences of distinct proteins. The aim of this approach is to determine a weighted tree topology that approximates the entire functional similarity relations between proteins, defined by a distance function. In this case – according to the definition - the similarity relation has a symmetric property. However, the assumption of symmetry is not always appropriate, because non-symmetric similarity relations between proteins might have a biological significance. This notion inspired us to define a novel, compression-based, non-symmetric dissimilarity measure and to modify the ubiquitous *'Unweighted Pair Group Method with Arithmetic Mean'* (UPGMA)-based tree-building algorithm so that the new measure can be applied.

Keywords: *phylogenetic trees, non-symmetric dissimilarity measures, Unweighted Pair Group Method with Arithmetic Mean, compression–based similarity measure, hydrogenase proteins*

Introduction

Over the past decades researchers have studied proteins in order to learn more about their functionality. Now work has moved on to the systematisation of proteins isolated from distinct species that have similar functionality, and this has become one of key question in phylogenetics. This methodology allows us to examine the proteins by comparing their AA (amino acid) sequences. There are several distance functions available in the literature for calculating distance values between aligned AA sequences. The best-known ones are the Jukes-Cantor distance function [8], and the Kimura 2-parameter model [7]. One drawback of these models, however, is that the AA sequences in question first have to be aligned, which might require an algorithm that makes use of dynamic programming [14], [13].

When examining the proteins we should also ask whether a symmetric similarity measure (e.g. a distance function) describes protein relations in the right way. In the real world a similarity relation is not necessarily symmetric, as one of the proteins being compared might contain more information than the other. That is why we decided to

http://www.ecology.uni-corvinus.hu ● ISSN 1589 1623

develop a mathematical model that employs a non-symmetric dissimilarity measure (NSDM) in order to learn how dissimilar these proteins are. This model might have interesting biological applications.

The tree-building algorithms can usually handle only a symmetric measure. One of the methods used is the traditional '*Unweighted Pair Group Method with Arithmetic Mean*' (UPGMA), which is a bottom-up algorithm (agglomerative). Here we extend the UPGMA procedure using the symmetrised NSDM for building phylogenetic tree structures, and we use the original asymmetric dissimilarity measure when we calculate the dissimilarity measures of individual nodes and leaves by UPGMA.

The biological example used in this study is the hydrogenase enzyme group. Hydrogenases (H2ases) catalyze the reversible oxidation of molecular hydrogen and play a central role in microbial energy metabolism. Most of these enzymes are found in *Archaea* and *Bacteria*, but a few are present in *Eucarya* as well. They can be placed into three classes: the [Fe]-H2ases, the [NiFe]-H2ases, and the metal-free H2ases. The vast majority of known H2ases belong to the first two classes, and over 100 of these enzymes have been characterized genetically and/or biochemically. 73 sequences of different [NiFe] hydrogenases from various microorganisms were chosen for our study (tree building and classification of this enzyme family into different classes). The sample set of sequences were taken from [15].

In Section 2, we describe in detail our novel non-symmetric dissimilarity measure and its mathematical background. In Section 3 an extension of the UPGMA algorithm is presented, which calculates the distances between the nodes and leaves using NSDM defined in Section 2. In the next section we test our new method and present the results obtained in the case of the [NiFe] hydrogenase enzyme group. Finally, in Section 5, we summarise our findings and draw some conclusions about the practical usefulness of our measure.

A compression-based novel non-symmetric dissimilarity measure

Before introducing our compression-based non-symmetric dissimilarity measure we would like to clarify the relationship between the concept of distance functions, metrics and non-symmetric dissimilarity measures.

Distance function, metric and non-symmetric dissimilarity measure

Let us assume that there are a given set of objects (in our case protein sequences). Then it is necessary to define what we mean by 'similarity' and 'dissimilarity'. Furthermore, we need to express this value in numerical terms. If we already have a formal definition of 'similarity' or 'dissimilarity', then the other definition could be calculated by carrying out a monotone decreasing transformation of the original definition.

In order to define dissimilarity it is customary to apply a distance function, or a metric. The distance function is a function $f(x,y)$ over a given set Ω that has the following properties:

a) the value of the distance function is 0, if and only if the two elements coincide for any $x, y \in \Omega$;

b) the function is called *symmetric* when $d(x,y) = d(y,x)$ for any $x, y \in \Omega$. Otherwise it is called non-symmetric.

http://www.ecology.uni-corvinus.hu ● ISSN 1589 1623

If a distance function also satisfies the triangle inequality, it will be a metric.

A metric and a distance function usually have symmetric properties, but we have a feeling that the concept of similarity and dissimilarity does not categorically determine a symmetric 'relation' between objects. Hence it is worth defining the non-symmetric versions of the definitions stated above, which we could obtain by abandoning the symmetric property requirement. Henceforth, instead of talking about a 'non-symmetric distance function' and a 'non-symmetric dissimilarity metric' we shall use a more general term, that of 'non-symmetric dissimilarity measure' (NSDM).

Compression based non-symmetric dissimilarity measure

When solving many problems in bioinformatics we may successfully apply an information theoretical similarity measure. The information theoretical distance functions are based on a comparison of how much information objects contain relative to each other [3]. Here we shall introduce a non-symmetric compression-based version of it. But first of all we need to review the concept of the Universal Turing Machine and Kolmogorov-complexity.

The Universal Turing Machine (UTM) is roughly a mathematical model of present-day computers [1], since it is necessary to input a word x, say, and a program M, say, over the same alphabet, Σ, for it to work. Then the UTM simulates the operation of the Turing Machine coded in the program M with the input word x. (In general it is not a problem if we further assume that the alphabet is binary as we can always have an equivalent subset of positive numbers for any set, where the numbers are represented in binary form.)

The language recognised by UTM is a recursively enumerable set, but is not recursive; hence it is not computable 'algorithmically'. This is an important fact in our approach, because the Kolmogorov-complexity of a given word x over an alphabet Σ means the length of the shortest program, so the UTM has to count the word x with an empty input [2]. In other words, the Kolmogorov-complexity of a given word is also not computable algorithmically, so we need to use approximation methods to determine it.

In another approach, the Kolmogorov-complexity means that we give the shortest representation of a word, from which we can restore the original word without loss of information. That is why it seems to be worth approximating the Kolmogorov-complexity with an efficient compressor method in the following way: given a compressor algorithm, we can calculate the length of the sequence after compression, and then assign this value to the word in question. Let *C(x)* denote the length of the sequence we get after compressing a given word x using a given compressor algorithm. Next, let us define the following non-symmetric dissimilarity measure:

Definition: Let n(x,y) be a non-symmetric dissimilarity measure that associates a non-negative real number with any two sequences x,y over Σ defined by:

$$n(x,y) = \frac{C(xy) - C(x)}{C(xy)}, \qquad \text{(Eq. 1)}$$

where xy is the concatenation of words x and y.

http://www.ecology.uni-corvinus.hu ● ISSN 1589 1623

Phylogenetic tree building using a non-symmetric dissimilarity measure

Phylogenetic tree-building methods usually construct a tree with a symmetric distance matrix, whose leaves represent proteins. By distance, we mean that the distance between two proteins in the tree is the sum of the weights of edges that connect the two proteins in a unique way. There are two sorts of phylogenetic tree-building algorithms: the so-called 1-stage methods, which determine the weights of edges during the tree-building process, and the 2-stage methods, whose algorithms first build up a tree, and then they calculate the optimal weighting of edges based on a target function.

The problem of phylogenetic tree-building will still be NP-complete if we consider only a subclass of the original problem set [11] (Maximum Parsimony Principle [10]). So it is necessary to use a heuristic to look for the right tree topology.

In this section we will describe a phylogenetic tree-building method that employs a non-symmetric dissimilarity measure which we defined above. This is a 2-stage method, so it must first look for an appropriate tree topology, and it must then assign optimal weights to edges (between i and j in both directions) of the tree based on the least square procedure.

Least Squares Unweighted Pair Group Method with Arithmetic Mean (LS-UPGMA)

The UPGMA method [9] is a hierarchical agglomerative procedure. It is a bottom-up algorithm, so it first considers all points as subtrees, and then it iteratively joins a pair of subtrees which seem most appropriate for the heuristic used.

It is straightforward to extend the UPGMA method to one which has a non-symmetric dissimilarity measure. The method we developed determines a tree topology using a modified UPGMA, and then it applies a numerical algorithm to optimise the tree weighting. The framework of the procedure can be seen in the following:

1. Algorithm: *Least Square Unweighted Pair Group Method with Arithmetic Mean* (LS-UPGMA):
   Input: D^{nxn} *(non-symmetric) similarity matrix*
   Output: $C^{(2n-1)x(2n-1)}$ *incidence matrix, W optimal weights of edges*
   C: = MUPGMA(D) % seeking a tree topology
   W:= LS(C,D) % determine the optimal edge weighting

The *Modified Unweighted Pair Group Method with Arithmetic Mean (MUPGMA)* differs from the original one as it only determines a tree topology. The edge-weighting task is performed by another algorithm. Furthermore, we must not forget the fact that when choosing and joining sub-trees, the dissimilarity measure used is not symmetric. The algorithm needed for this is given below:

2. Algorithm: (MUPGMA):
Input: D^{nxn} *dissimiliarity matrix*
Output: $C^{(2n-1)x(2n-1)}$ *incidence matrix*
Given a $D=[d_{ij}]$ *(non-symmetric) dissimilarity matrix between n elements. After we consider all the elements as different clusters, and carry out the following steps when it has only one cluster left (n-1 times):*

1. *Find the (i,j) indices so that* $\max(d_{ij}, d_{ji})$ *is minimal for any cluster*
2. *Create a new u cluster joining the i and j cluster*

http://www.ecology.uni-corvinus.hu ● ISSN 1589 1623

3. Determine the u cluster's distance from other clusters in the following way:

$$d_{k,u} = \frac{n_i d_{k,i} + n_j d_{k,j}}{n_i + n_j} \quad \text{(Eq. 2)}$$

$$\text{and } d_{u,k} = \frac{n_i d_{i,k} + n_j d_{j,k}}{n_i + n_j} \quad \text{(Eq. 3)}$$

where n_i and n_j denote the number of elements in cluster i and cluster j

4. Delete clusters i and j

After running the MUPGMA method we get a tree-topology, where each leaf represents a protein. We would like to calculate the optimal weighting of edges so that the mean squared error between the distances of leaves is found by the tree and the dissimilarity measure is given by the D matrix above. Actually, we can express this task as a constrained least squares problem, as we shall now see.

Let us consider the tree which is built up using the MUPGMA method. The path-edge incidence matrix P to this tree could be constructed, whose rows correspond to the paths between the leaves, and whose columns correspond to the edges in a fixed order. The element with row index *(i,j)* and column index *k* in matrix P has the value *1*, if the edge *k* can be found on the path between the points *i* and *j;* otherwise it has the value *0.*

Furthermore, let *v* denote the vector whose distances between the leaves are given by the elements of the matrix D, and let y denote the vector that contains the unknown edge weightings, whose order are determined by columns in the matrix P. Next, we need to minimise the following expression for the optimal weights of edges:

$$y^* = \arg\min_{y \in \mathbb{R}^{2n-1}} \|Py - v\|$$
$$s.t. \quad 0 \le y \quad \text{(Eq. 4)}$$

This algorithm can be expressed in a compact way by the following:

3. Algorithm: Least Square Method for Optimising the Weights of Edges :

Input: D^{nxn} *dissimilarity matrix,* $C^{(2n-1)x(2n-1)}$ *incidence matrix*

Output:, W, the optimised weights of edges

- *Find the path-edge incidence matrix P using the incidence matrix C*
- *Find the* y^* *optima of Eq.4*
- *Generate the W matrix using* y^* *and return*

Based on the above extensions, the LS-UPGMA method is suitable for handling a non-symmetric dissimilarity measure.

Experiments

In the experiments 73 different [NiFe] hydrogenase sequences were used for testing the proposed algorithms, i.e. we built phylogenetic trees using the LS-UPGMA method with a specific non-symmetric dissimilarity measure. But first we will describe the dissimilarity measure used for testing, and then we will apply it to the evaluation domain- After we will discuss the results.

http://www.ecology.uni-corvinus.hu ● ISSN 1589 1623

The dissimilarity measure used for testing

In Section 2 we defined the non-symmetric dissimilarity measure concept. It was mentioned that we need to select a compressor algorithm to fully determine an NSDM. In the literature two types of compressor method are known: the statistical (Huffmann algorithm) one and the factorisation one (PPMZ, Lempel-Ziv algorithm [4], [5]). Roughly speaking, a statistical compressor first measures the frequency of each symbol occurring in the input, and in the output it defines shorter codes for higher frequency symbols. Instead of statistical information factorisation, compressors work with connected substrings of the string to be compressed. These methods try to find the substring factorisation in a quasi-optimal way.

Our main aim here is to furnish a measure which can estimate the relative information content among strings. This seems to be obvious if we want to express a string in terms of the substring of another string. This approach is very similar to ours. That is why we chose the Lempel-Ziv algorithm [4], [5] - a factorisation compressor method - to define a non-symmetric dissimilarity measure.

Evaluation domain and tests

The calculated tree topologies are shown in *Fig. 1* and *Fig. 2* for the large subunit of 73 [NiFe] hydrogenases. Since the phylogenetic trees are derived from a symmetric dissimilarity matrix the topology of the left and right handed trees are the same. Only the weights of the paths between the root and the leaves are different. Other differences between the right and left oriented trees will not be discussed here.

The topology of phylogenetic tree is different from the phylogenetic trees obtained by different methods [12], [6] for hydrogenases but, the main characteristics of the [NiFe] hydrogenase family remain the same. We can also distinguish four different hydrogenase groups. The second group (Group-B) contains almost exclusively membrane bound hydrogen uptake hydrogenases (Hup). According to the classification made by Vignais, this corresponds to Group-1 [6]. The main difference is that membrane-bound Hyn hydrogenases do not belong to this group. In our algorithm these hydrogenases form a separate group (Group-A), together with some membrane bound H_2 evolving hydrogenases which were previously assigned to a different group (Group-4). Since the physiological role of these Hyn hydrogenases are not completely elucidated we assign this Group-A as the group of H_2 evolving hydrogenases. Group-C is a mixed group of Group-2 and Group-3 [12]. It contains almost all HoxH hydrogenases as a separate subgroup, some ferredoxin reducing hydrogenases, all Hup hydrogenases from cyanobacteria and also the sensory hydrogenases. The subgrouping of these types of hydrogenases is not well established. The D Group can, however, be divided unequivocally into 3 separate subgroups. All bifunctional thermophylic hydrogenases, most of the ferredoxin reducing hydrogenases and some of the hydrogen evolving hydrogenases form a separate subgroup.

It is also striking that these groups can not just be recognised by the second division from the root as they were classified previously [6], but the distance from the root is uniform within the groups. This distance is different for right and left handed trees, however. Moreover this tendency can be justified within the subgroups as well (see Group-D). These two criteria make our trees more reliable than any other previously described phylogenetic tree.

http://www.ecology.uni-corvinus.hu ● ISSN 1589 1623

Conclusions and future work

In this paper we presented a new tree-building methodology that is based on NSDM. Then we defined a compression-based NSDM on which we could build a variant of the modified UPGMA method. The optimal weightings for edges of the tree were obtained using the method of least squares. It enabled us to build a weighted directed phylogenetic tree. We applied this to a biological problem, namely that of protein sequences. We performed tests on data for 73 different [NiFe] hydrogenases. It turned out that our dissimilarity measure could provide relevant information for biologists, which could be of advantage in phylogenetic studies. The notion of a non-symmetric dissimilarity measure will also be examined further to learn more about its advantages and limitations in real applications.

http://www.ecology.uni-corvinus.hu ● ISSN 1589 1623

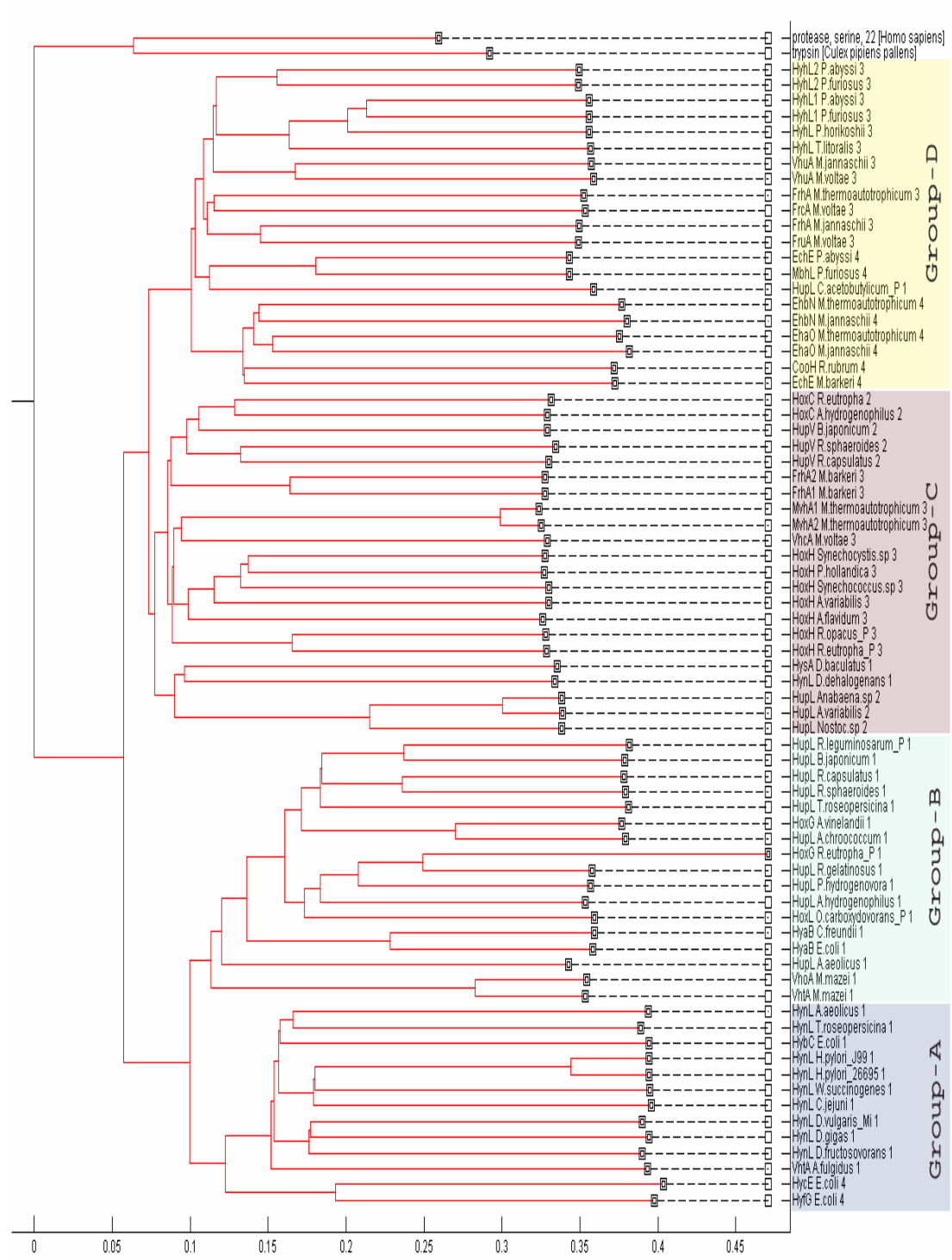

Figure 1. *The left-handed phylogenetic tree of [NiFe]-H2-ases with an outgroup. On the right of the picture there are the names of the hydrogenases with the group number they were previously classified in [9]. The shading indicates our group classification.*

http://www.ecology.uni-corvinus.hu ● ISSN 1589 1623

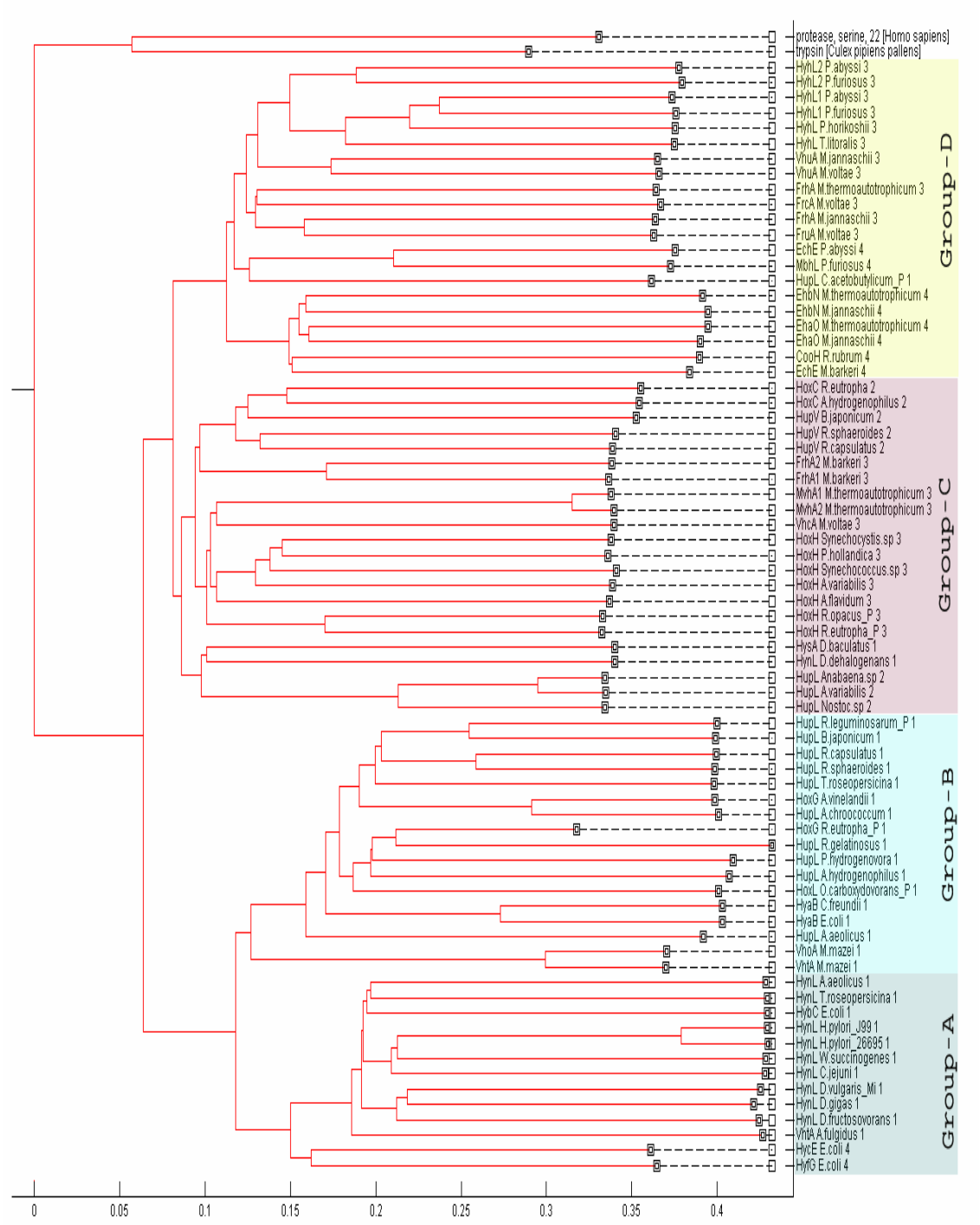

Figure 2. *The right-handed phylogenetic tree of [NiFe]-H2-ases with an outgroup. On the right of the picture there are the names of the hydrogenases with the group number they were previously classified in [9]. The shading indicates our group classification.*

We intend to further examine the algorithm which was presented here to find out whether additional extensions of UPGMA are possible, and also examine other algorithms that use a non-symmetric dissimilarity measure. Another aggregation operator in the first step of MUPGMA could be used as well instead of the current one.

http://www.ecology.uni-corvinus.hu ● ISSN 1589 1623

We would also like to build a number of tree topologies at the same time in order to cover a greater part of the solution space.

REFERENCES

[1] Papadimitriou, C.H. (1994): Computational complexity. - Addison-Wesley Publishing Company, Inc.
[2] Li, M., Vitányi, P. (1993): An Introduction to Kolmogorov Complexity and its Applications. – Springer-Verlag, New York.
[3] Cilibrasi, R., Vitanyi, P. (2004): Clustering by compression. - IEEE Transactions on Infomation Theory, See http://arxiv.org/abs/cs.CV/0312044.
[4] Ziv, J., Lempel, A. (1977): A universal algorithm for sequential data compression. - IEEE Trans. on Inf. Th. IT-23 337-343.
[5] Ziv J., Lempel A. (1978): Compression of individual sequences via variable-rate coding. - IEEE Trans. on Inf. Th. IT-24 530-536.
[6] Vignais, P.M., Billoud, B., Meyer, J. (2001): Classification and phylogeny of hydrogenases. - FEMS Microbiology Reviews 25: 455-501
[7] Kimura, M. (1980): A simple method for estimating evolutionary rate of base substitution through comparative studies of nucleotide sequences. - J Mol Evol 16: 111-120.
[8] Jukes, T.H., Cantor, C. (1969): Mammalian Protein Metabolism, chapter Evolution of protein molecules, pages 21-132. - Academic Press, New York.
[9] Michenerand, C.D., Sokal, R.R. (1957): A quantitative approach to a problem in classification. - Evolution, 11:130-162
[10] Cavalli-Sforza, L.L., Edwards, A.W.F. (1967): Phylogenetic analysis: models and estimation procedures. - Evolution 21: 550-570.
[11] Foulds, L.R., Graham, R.L. (1982): The Steiner problem in phylogeny is NP-complete. - Adv. Appl. Math., 3: 43-49.
[12] Wu, L.F., Mandrand, M. A. (1993): Microbial hydrogenases: Primary structure, classification, signatures and phylogeny. - FEMS Microbiol. Rev. 104: 243-270.
[13] Smith, T.F., Waterman, M. S. (1981): Identification of Common Molecular Subsequences. -, J. Mol. Biol. 147: 195-197.
[14] Needleman, S.B., Wunsch, C.D. (1970): A general method applicable to the search for similarities in the amino acid sequence of two proteins. - J. Mol. Biol. 48: 443-453.
[15] http://wwwabi.snv.jussieu.fr/research/hydrogenases/index.html

http://www.ecology.uni-corvinus.hu ● ISSN 1589 1623

ANALYSING MORTALITY RATES AND DATA OF CHILDHOOD LEUKAEMIA BY TIME SERIES METHODS

M. KIS

University of Debrecen, Department of Economic- and Agroinformatics
H-4032 Debrecen, Böszörményi út 138. Hungary
(phone: +36-52-508-444; fax: +36-52-486-255)

e-mail: kiss@thor.agr.unideb.hu

(Received 10th Sep 2005, accepted 10th Oct 2006)

Abstract. The Hungarian mortality rates were analyzed by autoregressive integrated moving average models and seasonal time series models examined the data of acute childhood lymphoid leukaemia. The mortality data may be analyzed by time series methods such as autoregressive integrated moving average (ARIMA) modelling. This method is demonstrated by two examples: analysis of the mortality rates of cerebrovascular diseases and analysis of the mortality rates of cancer of cervix. The relationships between time series of mortality rates were studied with ARIMA models. Calculations of confidence intervals for autoregressive parameters by tree methods: standard normal distribution as estimation and estimation of the White's theory and the continuous time case estimation. We present a new approach to analyzing the occurrence of acute childhood lymphoid leukaemia. We decompose time series into components. The periodicity of acute childhood lymphoid leukaemia in Hungary was examined using seasonal decomposition time series method. The seasonal components of the dates of diagnosis revealed that a higher percent of the peaks fell within the winter months than in the other seasons. This proves the seasonal occurrence of the childhood leukaemia in Hungary.
Keywords: *time series analysis, autoregressive integrated moving average models, mortality rates, seasonal decomposition time series method, acute childhood lymphoid leukaemia*

Introduction

Time series analysis is a well-known method for many years. Box and Jenkins provided a method for constructing time series models in practice [3]. Their method often referred to as the Box-Jenkins approach and the autoregressive integrated moving average models (ARIMA). This method has been applied in the beginning such fields as industry and economics later in medical research as well as [6, 11, 10].

The method of seasonal time series analysis can be used in various fields of the medicine. With such time series one can detect the periodic trend of the occurrence of a certain disease [8, 7, 2]. Among other diseases, the seasonal periodicity of the childhood lymphoid leukaemia was also analysed using statistical methods [4, 9]. The pathogenesis of the childhood lymphoid leukaemia is still uncertain, but certain environmental effects may provoke the manifestation of latent genes during viral infections, epidemics or pregnancy.

The date of the diagnosis of patients were statistically analysed to determine the role, which the accumulating viral infections and other environmental effects may play during the conception and fatal period on the manifestation of the disease. Because the available data is rather limited and controversial, it seemed logical to make an in-depth analysis of the date of diagnosis of the acute lymphoid leukaemia in Hungarian children.

http://www.ecology.uni-corvinus.hu ● ISSN 1589 1623

Methods

The Hungarian mortality rates were analysed by autoregressive integrated moving average models. The periodicity of acute childhood lymphoid leukaemia in Hungary was examined using seasonal decomposition time series method.

Autoregressive Moving Average Models

The mortality data often change in the form of 'time series'. Data of frequencies of mortality rates are usually collected in fixed intervals for several age groups and sexes of the population. Let the value of the mortality rates z_t, z_{t-1}, z_{t-2}, … in the years t, t-1, t-2, … . For simplicity we assume that the mean value of z_t is zero, otherwise the z_t may be considered as deviations from their mean. Denote a_t, a_{t-1}, a_{t-2}, … a sequence of identically distributed uncorrelated random variables with mean 0 and variance σ_a^2. The a_t are called white noise.

The autoregressive moving average model of order p, q (ARMA(p, q)) can be represent with the following expression [3, 5]:

$$z_t=\phi_1 z_{t-1}+ \ldots +\phi_p z_{t-p}+a_t+\theta_1 a_{t-1}+\ldots+\theta_q a_{t-q}\,. \qquad \text{(Eq. 1)}$$

Where ϕ_1, ϕ_2, … , ϕ_p and θ_1, θ_2, … , θ_q are parameters, p means the p order of autoregressive process and q denotes the q order of moving average process.

The time series that has a constant mean, variance, and covariance structure, which depends only on the difference between two time points, is called stationary. Many time series are not stationary. It has been found that the series of first differences is often stationary. Let w_t the series of first differences, z_t the original time series, than

$$w_t=z_t-z_{t-1}=\nabla z_t\,. \qquad \text{(Eq. 2)}$$

The Box-Jenkins modelling may be used for stationary time series [3, 5]. The dependence structure of a stationary time series z_t is described by the autocorrelation function: ρ_k=correlation(z_t;z_{t+k}); k is called the time lag. This function determines the correlation between z_t and z_{t+k}. To identify an ARIMA model Box and Jenkins have suggested an iterative procedure [3]:

- for provisional model may be chosen by looking at the autocorrelation function and partial autocorrelation function
- parameters of the model are estimated
- the fitted model is checked
- if the model does not fit the data adequately one goes back to the start and chooses an improved model.

Among different models, which represent the data equally well, one chooses the simplest one, the model with fewest parameters [3, 5]. The relation between two time series z_t and y_t can be give by the cross correlation function (ρ_{zy}(k)); ρ_{zy}(k)=correlation(z_t;y_{t+k}); where k=0, ±1, ±2, … . The cross correlation function determines the correlation between the time series as a function of the time lag k [3].

Estimations for Confidence Intervals

For estimation the parameter of first order autoregressive model two methods are well known: apply the standard normal distribution as estimation and the White method [1]. These methods cannot be applied in non-stationary case. Little known for estimation of the parameter of first order autoregressive parameter is the application of

http://www.ecology.uni-corvinus.hu ● ISSN 1589 1623

estimation for continuous time case processes [1]. This method can be applied in each case properly.

Seasonal Time Series

The time series usually consist of three components: the trend, the periodicity and the random effects. The trend is a long-term movement representing the main direction of changes. The periodicity marks cyclic fluctuations within the time series. The irregularity of the peaks and drops form a more-or-less constant pattern around the trend line. Due this stability the length and the amplitude of the seasonal changes is constant or changes very slowly. If the periodic fluctuation pattern is stable, it is called a constant periodic fluctuation. When the pattern changes slowly and regularly over the time, we speak of a changing periodicity. The third component of the time series is the random error causing irregular, unpredictable, non-systematic fluctuations in the data independent from the trend line.

An important part of the time series analysis is the identification and isolation of the time series components. One might ask how these components come together and how can we define the connection between the time series and its components with a mathematical formula. The relationship between the components of a time series can be described either with an additive or a multiplicative model.

Let $y_{i,j}$ (i=1, … , n; j=1, … , m) marks the observed value of the time series. The index *i* stands for the time interval (i.e. a year), the *j* stands for a particular period in the time interval (i.e. a month of the year). By breaking down the time series based on the time intervals and the periods we get a matrix-like table. In the rows of the matrix are the values from the various periods of the same time interval; while in the columns are the values from the same periods over various time intervals.

$$\begin{array}{c} y_{1,1}; y_{1,2}; \ldots; y_{1,m}; \\ y_{2,1}; y_{2,2}; \ldots; y_{2,m}; \\ y_{3;1}; y_{3,2}; \ldots; y_{3,m}; \\ \ldots \\ y_{n,1}; y_{n,2}; \ldots; y_{n,m}. \end{array} \quad \text{(Eq. 3)}$$

Let $d_{i,j}$ (i=1,2, … , n; j=1,2, … , m) mark the trend of the time series, $s_{i,j}$ (i=1,2, … , n; j=1,2, … , m), the periodic fluctuation and $\varepsilon_{i,j}$ (i=1,2, … , n; j=1,2, … , m), the random error. Using these denotations the additive seasonal model can be defined as

$$y_{i,j}=d_{i,j}+s_{i,j}+\varepsilon_{i,j},\ (i=1,2, \ldots, n;\ j=1,2, \ldots, m)\ . \quad \text{(Eq. 4)}$$

the multiplicative model as

$$y_{i,j}=d_{i,j}*s_{i,j}*\varepsilon_{i,j};\ (i=1,2, \ldots, n;\ j=1,2, \ldots, m)\ . \quad \text{(Eq. 5)}$$

The trend of a time series can easily be computed with moving averages or analytic trend calculation. Moving averaging generates the trend as the dynamic average of the time series. Analytic trend calculation approximates the long-term movement in the time series with a simple curve (linear, parabolic or exponential curve) and estimates its parameters. The indices of the periodic fluctuation are called seasonal differences (in the additive model) or seasonal ratios (in the multiplicative model). These indices represent the absolute difference from the average of the time interval using the additive model or the percentile difference using the multiplicative model. Seasonal adjustment is done by subtracting the *j* seasonal difference from the *j* data value of each *i* season (additive model) or by dividing the *j* data value of each *i* season by the *j* seasonal ratio

http://www.ecology.uni-corvinus.hu ● ISSN 1589 1623

(multiplicative model). The seasonally adjusted data reflect only the effect of the trend and the random error.

Results

The SPSS program-package was used for analysing. ARIMA models were identified for some mortality rates. The results are demonstrated two cases from Hungarian mortality rates.

Analysing the Mortality Rates

The mortality rates of cerebrovascular disease over age 65 for male and female were examined**.** The autocorrelation functions decay for both data series. The partial autocorrelation functions have a significance value at k=1 lag. The first order autoregressive model can be acceptable on the basis of autocorrelation and partial autocorrelation functions. So the stochastic equation over age 65 years of male:

$$z_t=0{,}792z_{t-1}+\varepsilon_t\,. \qquad \text{(Eq. 6)}$$

The model over age 65 of female is the following:

$$z_t=0{,}809z_{t-1}+\varepsilon_t\,. \qquad \text{(Eq. 7)}$$

When the fitted model is adequate then the autocorrelation of residuals have χ^2 distribution with (K-p-q) degree of freedom [3]. On the basis of test the selected models were adequate because

$$\chi^2_{male}=1{,}7478;\ \chi^2_{female}=3{,}886;\ \chi^2_{0,05;5}=11{,}07. \qquad \text{(Eq. 8)}$$

The cross correlation function before fitting model and after fitting model were examined. The function has more significance values before fitting model. The cross correlation function for the residuals has one significance values after fitting model. From behaviour of residuals we may be conclude that between examined time series is "synchronisation". In that years when the mortality rates for male increased the mortality rates for female increased as well.

The change in the mortality rates of cancer of cervix between age class 0-64 years and over age class 65 years were examined as well. The stochastic equation for the mortality rates for younger age class:

$$z_t=0{,}576z_{t-1}+\varepsilon_t\,. \qquad \text{(Eq. 9)}$$

for older age class:

$$z_t=0{,}7032z_{t-1}+\varepsilon_t\,. \qquad \text{(Eq. 10)}$$

On the basis of the χ^2 test the selected models were adequate; because

$$\chi^2_{0\text{-}64}=1{,}956;\ \chi^2_{over\ 65}=2{,}304;\ \chi^2_{0,05}=11{,}07\,. \qquad \text{(Eq. 11)}$$

The cross correlation function for residuals has not significance value at k=0 lag on 95% significance level. It may be concluded that there is not "synchronisation" between time series.

The confidence intervals were carried out by three mentioned methods. For the calculations of the confidence limits we used the tables of the known exact distribution of the maximum-likelihood estimator of the damping parameter of an autoregressive process [1]. The confidence intervals for different significance levels for the first order autoregressive parameter of stochastic equation for male of cerebrovascular diseases can be seen in *Table 1*.

http://www.ecology.uni-corvinus.hu ● ISSN 1589 1623

Table 1. *Confidence intervals for different significance levels for the first order autoregressive parameter of stochastic equation for male of cerebrovascular diseases.*

$\phi \approx 0{,}792$ (male)	p=0,1	p=0,05	p=0,01
Normal distribution	(0,5956;0,9884)	(0,5523;1,0317)	(0,4736;1,1104)
White method	(0,5993;0,9847)	(0,5596;1,0244)	(0,4791;1,1105)
Continuous time process	(0,6949;0,9424)	(0,6649;0,9723)	(0,6116;0,9978)

Analysing the Periodicity of Acute Childhood Lymphoid Leukaemia

The databank of the Hungarian Paediatric Oncology Workgroup contains the data of all the patients with lymphoid leukaemia diagnosed between 1988 and 2000. In this time interval a total of 814 children were registered (of which 467 were boys). The patients were 0-18 years old, with a mean age of 6,4 years and a median of 5,4 years. The components of the time series can be identified and isolated using statistical program packages. The analysis of the seasonal periodicity of the acute childhood lymphoid leukaemia was done with the SPSS statistical program package.

The analysis of the periodicity of acute childhood lymphoid leukaemia was performed on the basis of the date of the diagnosis (year + month) of the disease. We analysed three data series. The first data series contained the number of all the patients diagnosed monthly, the second contained the number of those patients younger than the value of the median, the third contained the number those older than the value of the median.

The seasonal components of all patients revealed 9 peaks. 6 of these peaks fell within the winter months, 1 in the autumn period, 1 in the summer months, 1 in the spring months (*Fig. 1*). The seasonal components of the younger age group showed 7 peaks in the winter, 1 in the spring and 1 in the summer months. The seasonal components of the older age group showed 7 peaks in the winter, 1 in the spring, 1 in the autumn and 4 in the summer months.

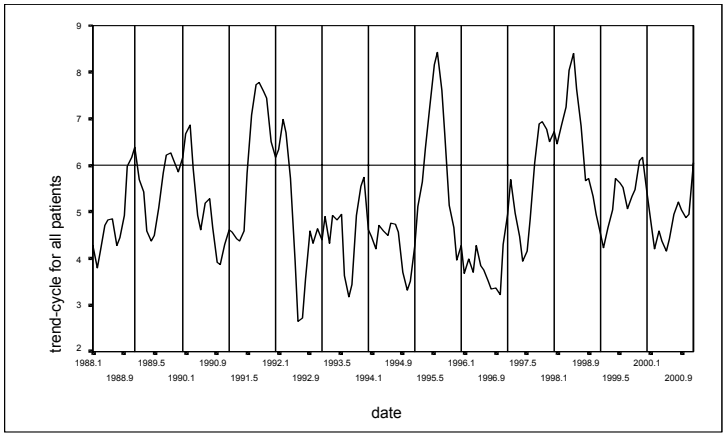

Figure 1. *Seasonal components of all patients of acute lymphoid leukaemia diagnosed monthly in the observed period.*

http://www.ecology.uni-corvinus.hu ● ISSN 1589 1623

Discussion

The Box-Jenkins models may be useful for analysing epidemiological time series. The method described the relationships between time series of mortality rates. It reveals strong synchronised behaviour of cerebrovascular diseases between the sexes. For time series of mortality data for cancer of cervix no such synchronisation is found between subgroups.

From the analysis of the first order autoregressive parameters it may be seen that by applying the normal distribution as estimation and White method the confidence intervals are near equal. For the upper estimations of confidence limits we can get larger than one applying these methods. Applying the continuous time process for the estimation of the confidence intervals they are much smaller and it can be used in each case [1].

Analysis of the seasonality of childhood lymphoid leukaemia in Hungary was performed both on the total number of patients and on the data series divided at the median. A certain periodicity was found in the dates of the diagnosis in patients with leukaemia. Although there was some difference in the patterns of the seasonal components peaks of the three time series, the majority of the peaks fell within the winter months in all three-time series. This was more significant in the group of all the patients and in the younger age group. The results of the analyses proved the seasonal occurrence of the childhood lymphoid leukaemia. Some studies reported similar seasonality [13], while other studies denied any kind such periodicity [12]. Our results prove the seasonal occurrence of the childhood lymphoid leukaemia in Hungary. Due to the controversial nature of the available international data, further studies should be carried out.

REFERENCES

[1] Arato, M., Benczur, A. (1986): Exact distribution of the maximum likelihood estimation for Gaussian-Markovian processes. - In: Tusnady, G., Ziermann, M. (ed.): Time Series Analysis. Technical Publishing House, Budapest.

[2] Barnett, A.G., Dobson, A.J. (2004): Estimating trends and seasonality in coronary heart disease. – Statistics in Medicine 23: 3505-3523.

[3] Box, G.E.R., Jenkins, G.M. (1976): Time Series Analysis, Forecasting and Control. - Holden-Day, San Francisco.

[4] Cohen, P. (1987): The influence on survival of onset of childhood acute leukaemia (ALL). - Chronobiology International 4: 291-297.

[5] Csaki, P. (1984): ARMA processes. - In: Tusnady, G., Ziermann, M., (ed.): Time Series Analysis. Technical Publishing House, Budapest.

[6] Diaz, J., Garcia, R., Lopez, C., Linares, C., Tobias, A., Prieto, L. (2005): Mortality impact of extreme temperatures. - International Journal of Biometerology 49: 179-183.

[7] Fung, K.Y., Luginaah, I., Gorey, K.M., Webster, G. (2005): Air pollution and daily hospital admissions for cardiovascular diseases in Windsor, Ontario. – Canadian Journal of Public Health 96: 29-33.

[8] Gallerani, M., Boari, B., de Toma, D., Salmi, R., Manfredini, R. (2004): Seasonal variation in the occurrence of deep vein thrombosis. - Med Sci Monit 10: 191-196.

[9] Harris, R.E., Harrel, F.E., Patil, K.D., Al-Rashid, R. (1987): The seasonal risk of paediatric/childhood acute lymphocyte leukaemia in the United States. - J Chronic Dis 40: 915-923.

http://www.ecology.uni-corvinus.hu ● ISSN 1589 1623

[10] Pereira, A. (2004): Performance of time series methods in forecasting the demand for red blood cell transfusion. - Transfusion 44: 739-746.
[11] Reichert, T.A., Simonsen, L., Sharma, A., Pardo, S.A., Fedson, D.S., Miller, M.A. (2004): Influenza and the winter increase in mortality in the United States, 1959-1999. - American Journal of Epidemiology 160: 492-502.
[12] Sorenson, H.T., Pedersen, L., Olse, J.H., et al.: Seasonal variation in month of birth and diagnosis of early childhood acute lymphoblastic leukaemia. - J A M A 285: 168-169.
[13] Vienna, N.J., Polan, A.K. (1976): Childhood lymphatic leukaemia prenatal seasonality and possible association with congenital Varicella. - American Journal of Epidemiology 103: 321-332.

http://www.ecology.uni-corvinus.hu ● ISSN 1589 1623

DETERMINATION OF THE PHOSPHATE CONTENT ORIGINALLY ADSORBED ON THE SOIL BY FITTING AN ADSORPTION ISOTHERM MODEL

G. FÜLEKY – L. TOLNER*

Department of Soil Science and Agricultural Chemistry,
University of Agricultural Sciences Gödöllő
H-2103 Gödöllő, Hungary

**e-mail: TolnerLaszlo@mkk.szie.hu*

(Received 10th Sep 2005, accepted 10th Oct 2006)

Abstract. In order to replace the rather complicated physico-chemical method, a mathematical technique related to the binding of phosphate ions was elaborated to determine the labile, and thus plant-available phosphate content of the soil.
The technique is based on the analysis of the quantity of phosphate bound to the soil in the equilibrium state when soil samples are suspended in solutions containing various concentrations of phosphate. The majority of soils contain a certain amount of adsorbed phosphate, so negative adsorption is observed if the analysis is carried out with solutions containing little or no phosphate. The isotherm models generally used to describe adsorption processes do not assume the presence of any material originally bound on the adsorbent surface, so their starting point is a state with a zero quantity of adsorbed material on the adsorbent in a solution with an initial equilibrium concentration of zero. In the case of soil phosphate adsorption, however, different results are obtained, as the soil already contains adsorbed phosphate in its original state. For this reason the isotherm model was modified.
The modified isotherm model was fitted to the measurement data using non-linear regression. The quantity of phosphate originally adsorbed on the soil can be calculated using a model parameter. The phosphate quantity calculated in this way exhibits a close correlation both with the isotopically exchangeable phosphate content, and with the results obtained with the best chemical extraction methods.
Keywords: *soil, phosphate, adsorption, model*

Introduction

Many characteristics of the soil phosphate cycle, such as the maximum adsorbable phosphate quantity, the equilibrium quantity of phosphate, the various binding energies and, of course, the phosphate buffering capacity of the soil, can all be calculated with the help of phosphate adsorption isotherms. In general, the two-term Langmuir isotherm and the Freundlich isotherm models give the best fit to measured data [2, 8, 10]. The quantity of phosphate originally adsorbed on the soil (Q) must be known before either of these isotherms can be fitted [2, 3, 4]. The most accurate way of calculating this is to determine the quantity of isotopically exchangeable phosphate (E) [2, 8, 9], but this calculation is extremely complicated. For this reason, many authors have attempted to find a simpler way of determining the quantity of phosphate originally adsorbed on the soil, for instance by using the quantity of phosphate extractable in $NaHCO_3$ solution (Olsen-P) [1].

The value of Q can also be calculated by extrapolating the adsorption curve to 0 equilibrium concentration [6]. However, the Q value determined in this way is greatly influenced by the model applied [4].

http://www.ecology.uni-corvinus.hu ● ISSN 1589 1623

The Freundlich and Langmuir isotherm models previously applied do not always give a satisfactory fit, so increasingly complicated models with a larger number of parameters have been elaborated, such as the two-term Langmuir isotherm [8, 10], the BET isotherm [11].

Although physico-chemical explanations were given for the parameters, the goodness of fit could really be attributed to the flexibility gained by the increase in the number of parameters. However, the real values of the parameters is to provide information on the properties of the soil. This possibility decreases as the number of parameters increases, as the individual parameters cannot be estimated independently of each other. This problem is particularly obvious in the case of samples from the same soil given different treatments [12]. It could be expected that some of the parameters would be constant characteristics of the soil, while others would vary depending on the treatment. However, experience shows that the parameters of multifactorial models do not meet this criterion.

The theoretical problem involved in the independent estimation of coefficients is further aggravated by the practical problem that the fitting of the models is carried out by means of non-linear regression, i.e. by iteration. Most earlier attempts to "linearise" these models also contained errors [12]. The possibility of using a modified Freundlich isotherm (Eq. 1.) with a constant exponent to solve this problem was also examined:

$$P_{ads} = k * c^{\frac{1}{n}} - Q \qquad \text{(Eq. 1.)}$$

When investigating the adsorption of phosphate on acidic Hawaiian soils, Davis [5] found that the correlation between the phosphate adsorbed on the soil and the concentration of the equilibrium solution could be expressed by a simple radical function. Among the whole root exponents examined (**n** = 1, 2, 3, 4), the best fit was obtained at a value of **n** = 3, i.e. an index of 1/3. This model was confirmed and applied by the present authors in previous work [12]. Barrow [4] found a value of **n** = 2.5 to be the most suitable.

Hartikainen [7] used phosphate solutions with extremely low concentrations (0–0.5 mg*dm^{-3}) to calculate the sorption isotherm. In this narrow range the isotherm could be taken as a straight line to a good approximation, i.e. the value of the root exponent was **n** = 1.

The present paper demonstrates that the problem can also be solved in a less restricted manner using a combination of linear and non-linear regression. These relationship help to determine the originally sorbed phosphate content of soil.

Materials and methods

Phosphate adsorption was examined on three Hungarian soils *(Table 1)*.

As the purpose of this work was determine the quantity of phosphate originally present in the sorbed state by the help of a model, the soils were first treated with phosphate to achieve various levels of originally adsorbed phosphate. In general these treatments involved 0, 10, 20, 40, 80, 160, 320 and 640 mg P/kg soil, achieved by mixing KH_2PO_4 into the soil. The treated samples were then incubated at room temperature at constant moisture content for 18 months.

http://www.ecology.uni-corvinus.hu ● ISSN 1589 1623

Table 1. *The main characteristics of soils*

Soil No.	Soil type	Tex-ture	pH (KCl)	CaCO3 %	OM %	Olsen-P $mg.kg^{-1}$	E $mg.kg^{-1}$
Orosháza	Chernozem, solonetz in the deeper layers	loam	7.1	1.7	3.72	8,2	17,2
Hajdú-böszörmény	Meadow solonetz	clay-loam	5.7	-	7.73	8,8	27,3
Őrbottyán	Calcareous sand	sand	7.4	3.3	1.03	8,1	15,5

The phosphate quantities adsorbed on the soil samples after the preliminary treatments were determined using two methods, including the measurement of isotopically exchangeable phosphate (E) and the quantity of phosphate extractable with $NaHCO_3$ solution (Olsen-P) *(Table 1)*.

Phosphate adsorption analysis was carried out on the treated samples. In general, the initial concentrations used for adsorption were again 0, 10, 20, 40, 80, 160, 320 and 640 mg P/kg soil.

All the regression calculations and figures were carried out using the Windows Excel program. The linear regression was carried out with the worksheet function, while the one-parameter non-linear regression combined with this was carried out with a macro written in Visual Basic.

Results and discussion

The eight levels of originally adsorbed phosphate (Q) achieved on each of the three soils by means of preliminary treatment were determined by fitting adsorption isotherms. The modified Freundlich isotherm (Eq. 1.) model used for the calculations, was linearised using the Eq. 2 equation. For a specific value of **n**, the model is thus converted to the following linear function (Eq. 3.):

$$x = c^{\frac{1}{n}} \qquad \text{(Eq. 2.)}$$

$$P_{ads} = k * x - Q \qquad \text{(Eq. 3.)}$$

where **k** gives the steepness of the slope, and **Q** the intersection, the absolute value of which gives the quantity of adsorbed phosphate associated with 0 equilibrium concentration, i.e. the quantity of phosphate originally adsorbed on the soil sample.

For a given value of n the linear regression clearly reveals the **k**, **Q** parameter pair belonging to the closest fitting model, i.e. that with the minimum value for the sum of squares (**SQ**) between the measured and calculated values.

Using various values of **n**, the sum of squares between measured and calculated values (**SQ**) was calculated using the models evolved with the **k** and **Q** parameters obtained from linear regression. Depending on the **n** values, the values of the sum of squares (**SQ**) could be plotted on a curve containing a minimum. The search for this single-parameter minimum was carried out using a simple technique, involving a macro

http://www.ecology.uni-corvinus.hu ● ISSN 1589 1623

that finds the optimum **n** value with the desired precision using the regression parameters and sums of squares (**SQ**) automatically generated by the Excel program.

The following adsorption curves were fitted to the data of samples adjusted to the eight different levels of originally adsorbed phosphate by means of preliminary treatment on soil from Orosháza *(Fig. 1)*.

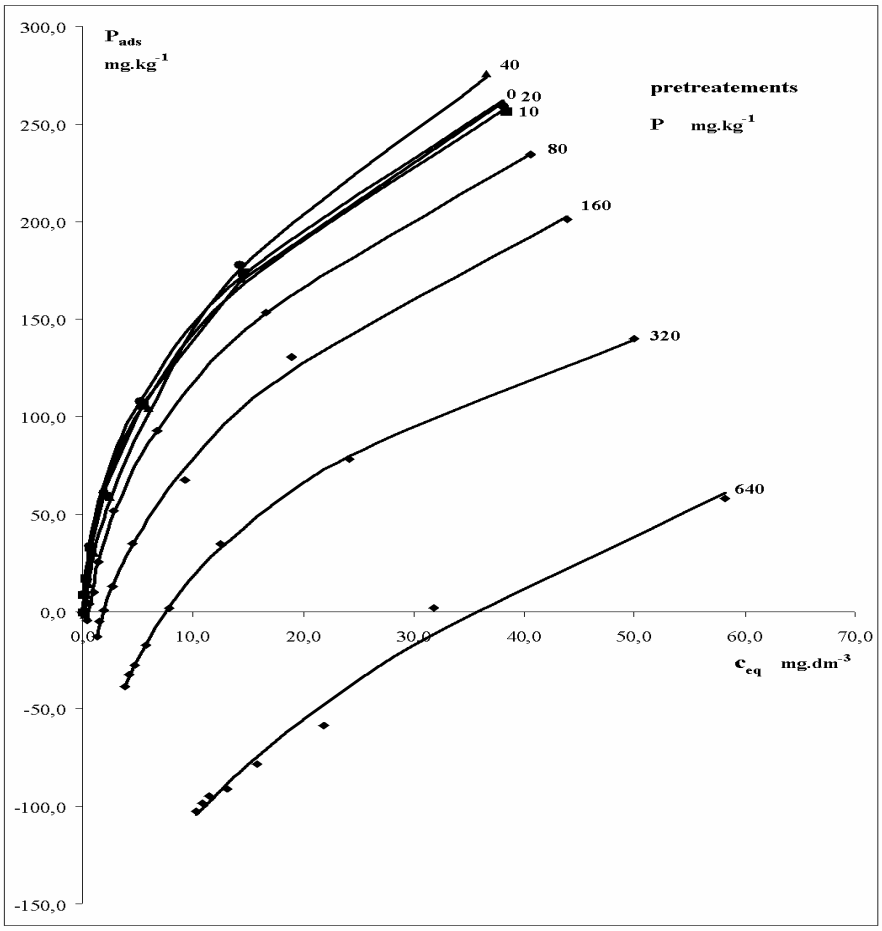

Figure 1. *Adsorption isotherms of the pretreated Orosháza soil.*

The optimum parameters and the corresponding values of the sum of squares (SQ) are presented in *Table 2*.

Table 2. *The parameters of the model on Orosháza soil*

Preliminary treatments mg P/kg soil	n	k	Q	SQ
0	2.53	67.27	20.92	93.25
10	2.50	65.71	23.96	60.80
20	2.61	72.92	32.19	98.99
40	2.19	58.88	28.81	53.69
80	2.79	79.26	64.60	27.01
160	2.69	72.17	91.55	92.64
320	5.07	206.90	308.37	13.05
640	2.22	48.89	243.83	353.45

http://www.ecology.uni-corvinus.hu ● ISSN 1589 1623

The Q values obtained were compared with the E values representing the isotopically exchangeable quantities of adsorbed phosphate. The correlation was linear *(Fig. 2)*.

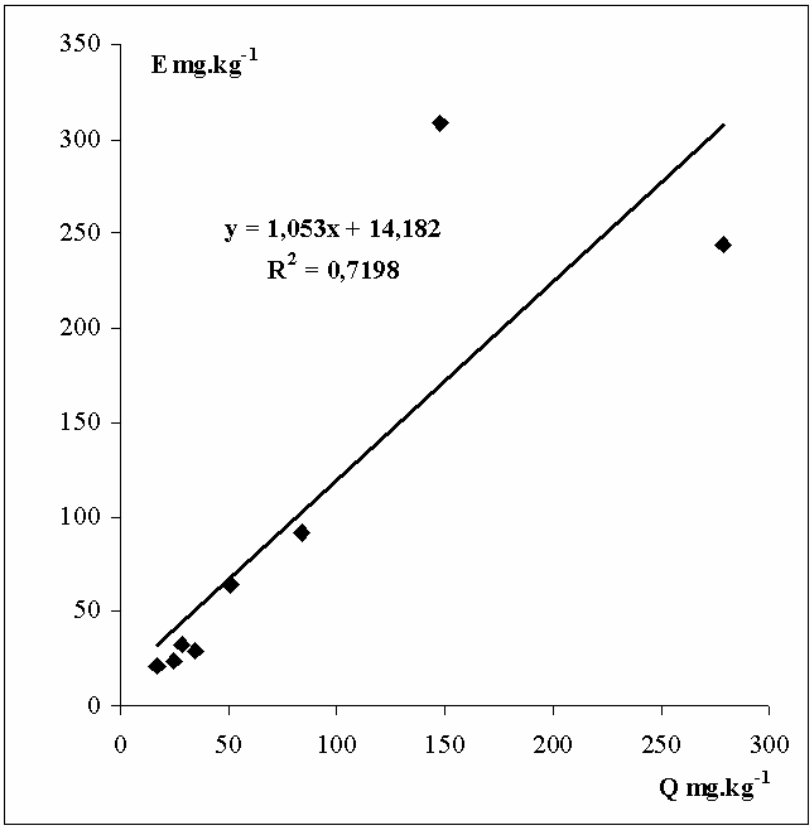

Figure 2. *Correlation of Q and E values of Orosháza soil.*

The linear function between **Q** and **E** values (Eq. 4.):

$$E = a + b * Q \qquad \text{(Eq. 4.)}$$

The parameters of linear function and determination coefficients ($\mathbf{R^2}$) characteristic of the correlation between **Q** and **E** values are presented for all three soils in *Table 3*.

Table 3. *Parameters of linear correlation between **Q** and **E** values*

Soil No.	a	b	R^2
Orosháza	14.97	1.103	0.6419
Hajdúböszörmény	-5.23	0.908	0.7698
Őrbottyán	1745,9	99,117	0,0918

The **Q** values did not increase as unambiguously as the **E** values as the result of preliminary treatment, so the correlation between them was not very close. It can be seen from the **k** and **n** values *(Table 2)* obtained during fitting that these values differed considerably for the same soil in different treatments. The deviations were greatest in cases where there were also anomalies in the **Q** values.

http://www.ecology.uni-corvinus.hu ● ISSN 1589 1623

In order to solve this problem, it was assumed that the **n** values did not differ for different treatments on the same soil, and the Excel worksheets were modified accordingly, the same **n** value being applied for the linearisation of all eight treated samples of each individual soil. The best common **n** value was determined as described above, by iteration using an Excel macro, except that the value of the sum of squares characteristic of the goodness of fit was formed by summing the values obtained for the eight samples. The parameters and determination coefficients ($\mathbf{R^2}$) characterising the correlation between the **Q** and **E** values are given for all three soils in the following table *(Table 4)*.

Table 4. *Parameters of linear correlation between **Q** and **E** values using common **n***

Soil No.	a	b	R^2
Orosháza	3,56	0.950	0.9970
Hajdúböszörmény	14.67	0.943	0.9993
Őrbottyán	-17.16	2.185	0.8959

The Q values obtained in this way exhibited closer correlation with the E values, as is clearly seen for the Orosháza soil on the following figure *(Fig. 3)*.

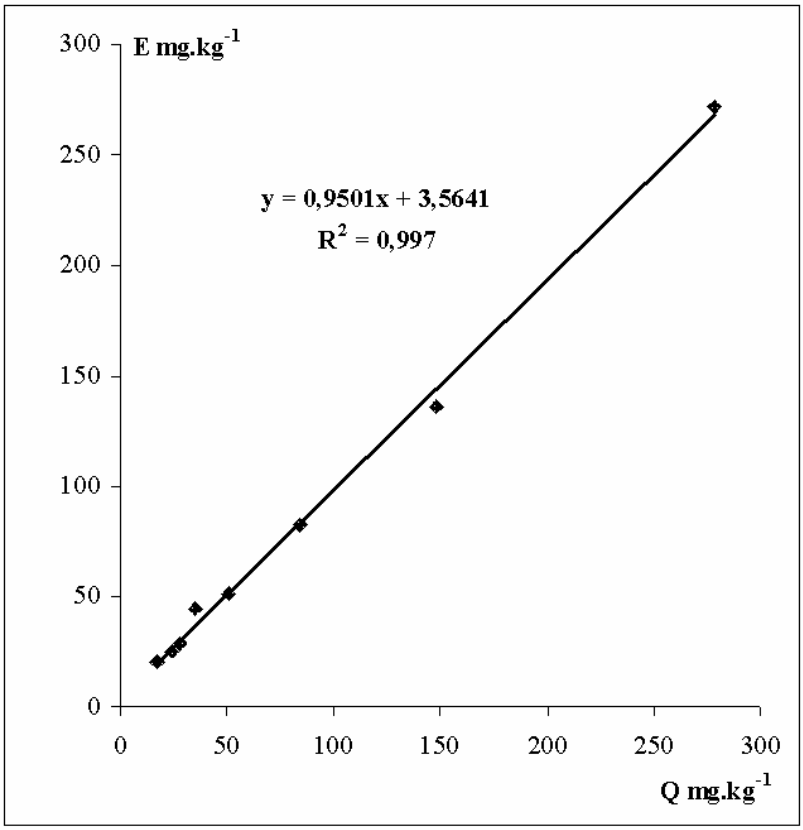

Figure 3. *Correlation of **Q** and **E** values of Orosháza soil using common **n**.*

http://www.ecology.uni-corvinus.hu ● ISSN 1589 1623

Table 5. *The parameters of the model using common* ***n***

Preliminary treatments	Orosháza n=2.53		Hajdúböszörmény n=3.61		Őrbottyán n=4.13	
mg P/kg soil	k	Q	k	Q	k	Q
0	66,96	20,65	79,70	41,50	81,63	47,73
10	66,84	24,93	77,00	44,46	80,26	50,40
20	68,96	28,69	75,06	45,46	77,15	51,80
40	75,97	44,74	76,18	55,30	70,00	52,57
80	66,64	51,66	79,49	77,12	75,12	75,87
160	64,01	82,15	80,00	115,84	68,15	99,94
320	59,69	135,88	82,01	189,30	53,13	131,48
640	66,45	272,05	92,71	347,07	145,67	535,76

The **k** values *(Table 5)* obtained during the calculations were also nearly constant within each soil, indicating that the **k** and **n** parameters of the Freundlich isotherm are constants characteristic of the soil, irrespective of the preliminary treatments, while the **Q** values are clearly indicative of the phosphate amount sorbed on the soil as the result of the preliminary treatments.

REFERENCES

[1] Assimakoupoulos et al. (1986): The effect of previous P aditions on sorption indices of calcareous soils determined with commonly employed methods. – Z. Pflanzenernaehr. Bodenk. 149: 548-560.
[2] Bache, B.W., Williams, E.G. (1971): A phosphate sorption index for soils. – J. Soil Sci. 22: 289-301.
[3] Barrow, N.J. (1974): Effect of previous additions of phosphate on phosphate adsorption by soils. – Soil Sci. 118: 82-89.
[4] Barrow, N.J. (1978): The description of phosphate adsorption curves. – J. Soil Sci. 29: 447-462.
[5] Davis, L.E. (1935): Sorption of phosphates by non-calcareous Hawaian soils. – Soil Sci. 40:129-158.
[6] Fitter, A.H., Sutton, C.D. (1975): The use of the Freundlich isotherm for soil phosphate sorption data. – J. Soil Sci. 26: 241-246.
[7] Hartikainen, H. (1991): Potential mobility of accumlated phosphorus in soil as estimated by the indices of Q/I plots and by extractant. – Soil Sci. 152: 204-209.
[8] Holford, I.C.R., Wedderburn, N.W.M., Mattingly, G.E.G. (1974): A Langmuir two surface equation as a model for phosphete adsorption by soils. – J. Soil Sci. 25: 242-255.
[9] Ryden, J.C. et al. (1977): Mechanism of phosphate sorption by soils and hidrous ferric exide gel. – J. Soil Sci. 28: 72-92
[10] Syers, J.K. et al. (1973): Phosphate sorption by soils evaluated by the Langmuir adsorption equation. – Soil Sci. Soc. Amer. Proc. 37: 358-363.
[11] Taylor, R.W., and Ellis B.G. (1978): A mechanism of phosphate adsorption on soil and anion axchange resin surfaces. – Soil Sci. Amer. J. 42: 432.
[12] Tolner, L., Füleky, Gy. (1995): Determination of the originally adsorbed soil phosphorus by modified Freundlich isotherm. – Commun. Soil Sci. Plant Anal. 26: 1213-1231.

http://www.ecology.uni-corvinus.hu ● ISSN 1589 1623

MODELLING NET PHOTOSYNTHETIC RATE OF TEMPERATE DRY GRASSLAND SPECIES AND WINTER WHEAT AT ELEVATED AIR CO_2 CONCENTRATION

N. HARNOS[1]* - Z. NAGY[2] - J. BALOGH[2] - Z. TUBA[2]

[1]*Agricultural Research Institute of the Hungarian Academy of Sciences*
P.O.Box 19. H-2462, Martonvásár, Hungary
(phone: +36-22-569-508)

[2]*Department of Botany and Plant Physiology, Fac. Agric. Env. Sci., St. István University*
Páter K. u. 1., H-2103, Gödöllő, Hungary
(phone: +36-28-522-075)

**e-mail: noemi@mail.mgki.hu*

(Received 10th Sep 2005, accepted 10th Oct 2006)

Abstract. A number of C_3 temperate dry grassland species and winter wheat plants were grown in open top chambers either at 365 μmol mol^{-1} (AC) or at 700 μmol mol^{-1} (EC) air CO_2 concentrations. Gas exchange measurements were made at several air CO_2 concentrations. When measured at higher CO_2 concentrations, net photosynthetic rate was higher in plants grown at EC than at AC. The widely accepted Farquhar net photosynthesis model was parameterized and tested using several observed data. After parameterization the test results corresponded satisfactorily with observed values under several environmental conditions.
Keywords: *temperate grasses, winter wheat, photosynthesis, modelling*

Introduction

Many authors use simulation models, in addition to experimental work, to describe plant development and plant production responses to several environmental factors such as higher temperature, drought stress and elevated air CO_2 concentrations (EC). Simulation models describing carbon balance of leaves, whole plants, and ecosystems use a biochemical model of the net photosynthetic rate (P_N). The most popular model is the biochemical model of Farquhar *et al.* (1980), Farquhar and Caemmerer (1982), and their modified versions [9, 4]. In general, the parameterization of a simulation model is not an easy task. Most plants respond to their environment in different ways. As a result, parameter values may differ depending on the plant species and possibly even the plant variety being used. Simulation models are important for describing the effects of EC on photosynthesis. They allow P_N to be predicted without having to carry out measurements.

Abbreviations: AC = ambient [CO_2]; [CO_2] = air CO_2 concentration; C_i = partial pressure of CO_2 in the intercellular space; EC = elevated [CO_2]; M = average deviation; OTC = open top chamber; P_N = net photosynthetic rate; r^2 = determination coefficient.

http://www.ecology.uni-corvinus.hu ● ISSN 1589 1623

Materials and methods

Plants and CO_2 fumigation

The experiments were carried out in perspex open top chambers (OTC) (130 cm in diameter and 100 cm in height) at the Global Climate Change and Plant Research Station in Gödöllő, Hungary. The climate of the region is temperate-continental with hot, dry summers. The annual mean temperature is 11 °C and the annual precipitation is 500 mm. [CO_2] was kept at the present-day concentration, AC (365 μmol mol^{-1}) for the control and at 700 μmol mol^{-1} for the EC treatment. The plants were occasionally irrigated as needed and weed control was carried out mechanically.

Winter wheat

Seeds of winter wheat (Triticum aestivum L.) were sown in OTC in two different years with two cultivars (cv. Emma in the first and cv. Martonvásári 15, MV-15) in the second experiment) [5, 11]. The seed spacing was 13.0×1.5 cm. The soil was a light moderately calcareous sandy soil. N,P and K fertilisers were applied at rates of 10, 5 and 5 g m-2 (100, 50, and 50 kg ha-1), respectively before sowing.

Grassland

The studied vegetation was a xeric temperate loess steppe situated on the edge of the Hungarian Great Plain [8]. The parent rock was sandy loess or loess with thick humus and a nutrient-rich A horizon. The original grassland was made up of more than 90 species. Monoliths (size: 50x50x30 cm in depth) were removed from the grassland and transplanted into the open top chambers with four monoliths to a chamber. The soil in the chambers was removed and replaced by soil from the profiles the monoliths had been collected from. Four weeks after transplantation the grass was cut. Following a two-month adaptation period, the monoliths in the EC chambers were gradually exposed, over a 4-week period, to 700 μmol mol^{-1} [CO_2]. The species studied during the 3-year exposure to EC and AC were the monocot *Festuca rupicola* Heuff. and the dicot *Filipendula vulgaris* Mönch. *F. rupicola*, the dominant species of the grassland, has sclerenchymatous erect leaves with a waxy surface, while *F. vulgaris* has soft, large incised leaves. Both species are perennial and have C_3 photosynthesis.

Measurements

The C_i dependence of light-saturated P_N (P_N/C_i curves) was measured in the flag leaves of winter wheat at the beginning of flowering and on the grassland species *F. rupicola* and *F. vulgaris* two and 36 months after the beginning of exposition. Measurements were made using an *LCA2*-type IRGA system (*ADC*, Hoddesdon, UK), operated in differential mode and a *Parkinson LC-N* leaf chamber with an airflow of 5 cm^3 s^{-1}. [CO_2] values of 30, 100, 200, 330, 540, 730 and 900 μmol mol^{-1} were produced using a gas diluter (*GD 600*, *ADC*, Hoddesdon, UK). The photosynthetically active radiation (PAR) and the leaf surface temperature were kept constant at 1 000±100 μmol m^{-2} s^{-1} and 20.5±1.5 °C for winter wheat cv. Emma, 800±100 μmol m^{-2} s^{-1} and 20±1 °C for winter wheat cv. MV-15 and 1 200 μmol m^{-2} s^{-1} and 23±1.5 °C for grassland.

http://www.ecology.uni-corvinus.hu ● ISSN 1589 1623

Farquhar model

The gas exchange measurements were used to set the parameters and validate the biochemical model described by Farquhar *et al.* (1980) and Farquhar and Caemmerer (1982), and the modified version elaborated by Sharkey (1985) and Harley and Sharkey (1991) (referred to as the Farquhar model in this work).

P_N can be expressed by the Farquhar model (for detailed description, see Appendix):

$$P_N = V_c - 0.5V_o - R_{day} = V_c(1 - \frac{0.5O_i}{\tau \cdot C_i}) - R_{day}, \quad \text{(Eq. 1)}$$

where the rate of carboxylation, V_c, is assumed to be limited by one of three factors: the activation state and kinetic properties of Rubisco, the regeneration of RuBP in the Calvin cycle, or the rate of phosphate release during triose phosphate utilization (starch and sucrose production). The micrometeorological variables included temperature, irradiance and [CO_2], which were measured and calculated with the IRGA equipment. Determination coefficients (r^2) were calculated to compare and analyze the relationship between observed and simulated P_N, and average deviation (M) to calculate the difference between observed and simulated P_N.

Results

The parameterization of the Farquhar model was performed on winter wheat cv. Emma, using P_N measurements on flag leaves at seven different air CO_2 concentrations at the beginning of flowering for plants grown at AC or EC. After parameterization, the Farquhar model gave a good estimation of the P_N of winter wheat cv. Emma in both treatments (*Fig. 1 A*). The determination coefficients and average deviation between observed and simulated net photosynthetic rates were $r^2 = 0.9$, M=0.98 for plants grown at AC and $r^2 = 0.98$, M=0.34 for plants grown at EC. The simulation results were not affected by irradiation because of the light saturated conditions. In both treatments P_N was limited by the rate of phosphate release during triose phosphate utilization at higher [CO_2]. The CO_2 saturation concentration and the saturated P_N were smaller for AC plants than at EC.

To validate the model the data set from the other experiment was used. Using the same parameter values as in the first experiment the model simulated P_N accurately, as shown by the r^2 and M values in *Fig. 1 B*.

http://www.ecology.uni-corvinus.hu ● ISSN 1589 1623

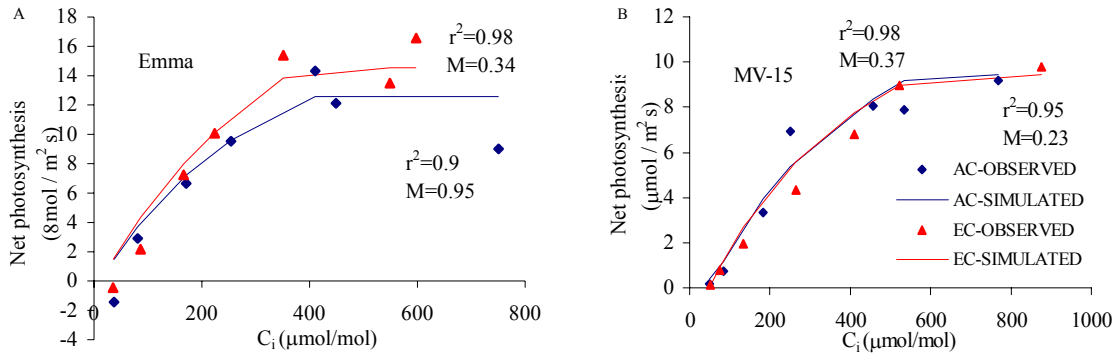

Figure 1. *Measured and simulated net photosynthetic rate of flag leaves of winter wheat (c. Emma A, MV-15 B) grown from germination at ambient, AC (control), or enhanced, EC CO_2 concentration.* r^2 *denotes determination coefficient and M denotes average deviation between observed and simulated values.*

The acclimation of P_N to EC varied both between species and over the course of the period of exposure. After two months of exposure upward acclimation was exhibited by all EC plants, the degree of which was greater in the dicot species. After 36 months of exposure the monocot species *F. rupicola* showed a downward acclimation in Rubisco capacity and its P_N/C_i curve did not reach saturation. The dicot species *F. vulgaris* showed upregulation for both Rubisco capacity and RuBP regeneration capacity.

Simulations were done for both grassland species studied. The parameter values used in the model were set the same after two and 36 months of CO_2 exposure but differed in the two species. The model simulated P_N accurately in all cases when the plants were grown at AC (for both species and after both exposure times). After two months of exposure the model did not adequately simulate P_N when the plants were grown at EC, but after 36 months the simulation results were accurate.

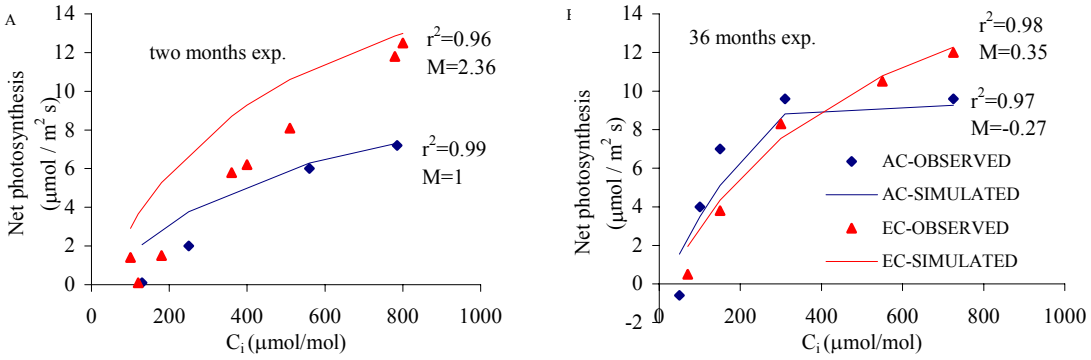

Figure 2. *Measured and simulated net photosynthetic rate of leaves of F. rupicola grown at AC or at EC after two (A) or 36 (B) months of exposure.* r^2 *denotes determination coefficient and M denotes average deviation between observed and simulated values.*

http://www.ecology.uni-corvinus.hu ● ISSN 1589 1623

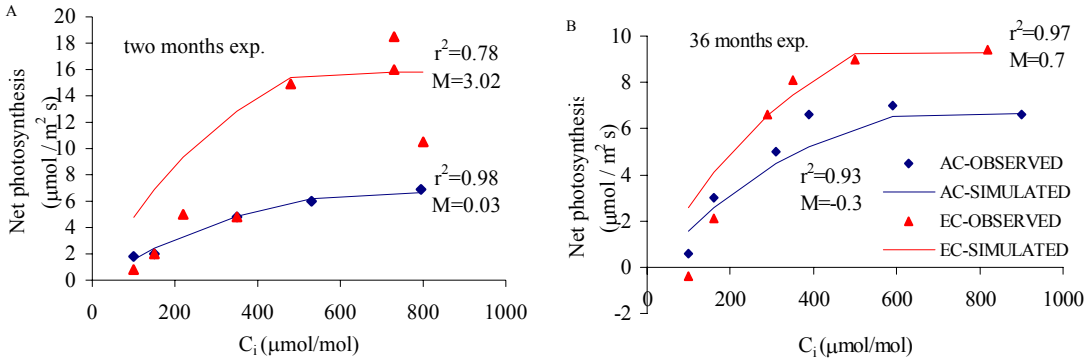

Figure 3. *Measured and simulated net photosynthetic rate of leaves of F. vulgaris grown at AC or at EC after two (A) or 36 (B) months of exposure. r2 denotes determination coefficient and M denotes average deviation between observed and simulated values.*

Discussion

The aim of the experiment was to obtain information on how the model of Farquhar *et al.* (1980) and Farquhar and Caemmerer (1982) modified by Sharkey (1985) and Harley and Sharkey (1991), described the P_N of Hungarian winter wheat cultivars and grassland species. The results of P_N measurements revealed two important facts: first, there was a large increase in P_N as a result of EC, and second, gas exchange acclimation responses were influenced by the length of exposure to EC.

The study also supports the use of the model for describing the P_N of various C_3 plants under several types of environmental conditions. Separate parameterization and validation for individual plant species is essential, but the results show that the same parameterization can be used for two different Hungarian winter wheat cultivars grown in different years.

In conclusion, the Farquhar model is able to describe the P_N of different plant species under various environmental conditions (irradiance, temperature, CO_2), but parameterization has to be done very carefully in all cases, especially for long-term examinations. Hence, the Farquhar model should be included in various plant growth simulation models.

Acknowledgements. The present study was carried out in the framework of the ESPACE-Grass Project (EU Brussels Contract No. EV5V-CT93-0292) and was supported by the ECOCRAFT Environment R&D Programme (EU Brussels), by the MEGARICH Project, EU contract ENV4-CT97-0503, the Hungarian Scientific Research Fund (OTKA, Nos. F020704, T18595, T22723), and the Research Development of Higher Education (FKFP0472/97).

REFERENCES

[1] Brooks, A., Farquhar, G.D. (1985): Effect of temperature on the CO_2 / O_2 specificity of ribulose-1,5-bisphosphate carboxylase/oxygenase and the rate of respiration in the light: estimates from gas-exchange experiments on spinach. - Planta 165: 397-406.

http://www.ecology.uni-corvinus.hu ● ISSN 1589 1623

[2] Farquhar, G.D., von Caemmerer, S. (1982): Modelling of photosynthetic response to environmental conditions. - In: Lange, O.L., Nobel, P.S., Osmond, C.B., Ziegler, H., (Szerk.): Physiological plant ecology II. Water relations and carbon assimilation. Encyclopedia of plant physiology, New series, Berlin: Springer-Verlag, Vol. 12B. 549-587. p.
[3] Farquhar, G.D., von Caemmerer, S., Berry J.A. (1980): A biochemical model of photosynthetic CO_2 assimilation in leaves of C_3 species. - Planta 149: 78-90.
[4] Harley, P.C., Sharkey, T.D. (1991): An improved model of C_3 photosynthesis at high CO_2 : Reversed O_2 sensitivity explained by lack of glycerate re-entry into the chloroplast. - Photosynthesis Research 27: 169-178.
[5] Harnos, N., Tuba, Z., Szente, K. (2002): Modelling net photosynthetic rate of winter wheat in elevated air CO_2 concentrations. – Photosynthetica 40(2): 293-300.
[6] Johnson, F., Eyring, H., Williams, R., (1942): The nature of enzyme inhibitions in bacterial luminescence: sulfanilamide, urethane, temperature and pressure. - Journal of Cell Comparative Physiology 20: 247-268.
[7] Jordan, D.B., Orgen, W.L. (1984): The CO_2 / O_2 specificity of ribulose 1,5-bisphosphate carboxylase/oxygenase: dependence on ribulose-bisphosphate concentration, pH and temperature. - Planta 161: 308-313.
[8] Nagy, Z., Szente, K., Tuba, Z. (1997): Acclimation of dicot and monocot temperate grassland species to long-term elevated CO_2 concentration. - Abstracta Botanica 21(2): 297-304.
[9] Sharkey, T.D. (1985): Photosynthesis in intact leaves of C_3 plants: Physics, physiology and rate limitations. - The Botanical Review 51: 53-105.
[10] Smith, E. (1937): The influence of light and carbon dioxide on photosynthesis. - General Physiology 20: 807-830.
[11] Tuba Z., Szente K., Koch J. (1994): Response of photosynthesis, stomatal conductance, water use efficiency and production to long-term elevated CO_2 in winter wheat. - Journal of Plant Physiology 144 (6): 669-678.

Appendix

Symbols and units:

RuBP: ribulose-1,5-bisphosphate
RuBPCO: RuBP carboxylase/oxygenase
P_N [μmol m^{-2} s^{-1}]: net photosynthetic rate of leaf
V_c [μmol m^{-2} s^{-1}]: rate of carboxylation at RuBPCO
V_o [μmol m^{-2} s^{-1}]: rate of oxygenation at RuBPCO
τ: specifity factor for RuBPCO [7]
C_i [Pa]: partial pressure of CO_2 in the intercellular space
O_i [kPa]: partial pressure of O_2 in the intercellular space (O_i = 30 kPa)
R_{day} [μmol m^{-2} s^{-1}]: day respiration rate (excluding photorespiration) [1]
W_c [μmol m^{-2} s^{-1}]: RuBPCO (amount, activation state and kinetic properties) limited carboxylation rate
W_j [μmol m^{-2} s^{-1}]: RuBP regeneration-limited carboxylation rate
T [μmol m^{-2} s^{-1}]: rate of phosphate release in triose phosphate utilisation (starch and sucrose production)
W_p [μmol m^{-2} s^{-1}]: T-limited carboxylation rate [4; 9]
V_{cmax} [μmol m^{-2} s^{-1}]: maximum rate of carboxylation

http://www.ecology.uni-corvinus.hu ● ISSN 1589 1623

K_c [μmol m^{-2} s^{-1}]: Michaelis constant of C_i for carboxylation
K_o [μmol m^{-2} s^{-1}]: Michaelis constant of O_i for oxygenation
J [μmol m^{-2} s^{-1}]: potential rate of electron transport [10]
I [μmol m^{-2} s^{-1}]: quantum flux density absorbed by the leaf
α: efficiency of light energy conversion on an incident irradiance basis [mol(electron) mol^{-1}(photon)]
J_{max} [μmol m^{-2} s^{-1}]: radiation saturated rate of electron transport

P_N can be expressed by Farquhar model:

$$P_N = V_c - 0.5V_o - R_{day} = V_c(1 - \frac{0.5O_i}{\tau \cdot C_i}) - R_{day},$$

where the rate of carboxylation, V_c, is assumed to be limited by one of three factors:

$$V_c = \min\{W_c, W_j, W_p\}$$

$$W_c = \frac{V_{cmax} \cdot C_i}{C_i + K_c(1 + O_i / K_o)},$$

where the carboxylation is limited by the amount, activation state and kinetic properties of RuBPCO.

$$W_j = \frac{J \cdot C_i}{4(C_i + O_i / \tau)}$$

In the W_j formula above, it is assumed that four electrons generate sufficient STP and NADPH for the regeneration of RuBP in the Calvin cycle [2]. The radiation dependency in the model is on electron transport [10]:

$$J = \frac{\alpha \cdot I}{(1 + \frac{\alpha^2 \cdot I^2}{J_{max}^2})^{1/2}},$$

and

$$W_p = 3T + 0.5V_o = 3T + \frac{V_c \cdot 0.5O_i}{C_i \cdot \tau \cdot C_i \cdot \tau}$$

Temperature dependence of K_c, K_o, R_d, τ, J_{max},, V_{cmax},and T are:

$$\text{parameter } (K_c, K_o, R_d, \tau) = e^{c - \frac{\Delta H_a}{R \cdot T_k}}$$

and

$$\text{parameter } (J_{max}, V_{cmax}, T) = \frac{e^{c - \frac{\Delta H_a}{R \cdot T_k}}}{1 + e^{\frac{\Delta S \cdot T_k - \Delta H_d}{R \cdot T_k}}}$$

[6], where c is a scaling constant, ΔH_a is an activation energy, R is the gas constant (R = 0.00831 kJ K^{-1} mol^{-1}), T_k is leaf temperature [K]. τ is a declining function of temperature whose activation energy is negative. ΔH_d is the energy of deactivation, and ΔS is an entropy term.

http://www.ecology.uni-corvinus.hu ● ISSN 1589 1623

APPLICABILITY OF THE AFRCWHEAT2 WHEAT GROWTH SIMULATION MODEL IN HUNGARY

N.HARNOS

Agricultural Research Institute of the Hungarian Academy of Sciences
P.O.Box 19. H-2462, Martonvásár, Hungary
(phone: +36-22-569-508)

e-mail: noemi@mail.mgki.hu

(Received 10th Sep 2005, accepted 10th Oct 2006)

Abstract. The aim of the present work was to determine the applicability of the AFRCWHEAT2 wheat growth model under Hungarian conditions. The Farquhar model, which, when properly calibrated, gives a satisfactory description of the net photosynthesis of Hungarian winter wheat varieties at various atmospheric CO_2 concentrations, temperatures and light conditions, was incorporated into the model. Both the original AFRCWHEAT2 model and the modified AF2MOD model were tested on long-term yield and climatic data series from Győr-Moson-Sopron County.

It was observed that the average yield over the period 1980-1990 was well simulated by both models, but the AF2MOD simulated the annual fluctuations much better: the determination coefficients describing the correlation between the actual wheat yield in Győr-Moson-Sopron county over the whole period and the values generated using the models were $r^2 = 0.32$ for the AFRCWHEAT2 model and $r^2 = 0.86$ for AF2MOD.

A comparison of the results simulated using the AFRCWHEAT2 and AF2MOD models demonstrated that detailed physiological submodels are required for the mathematical description of plant growth if yields are to be accurately estimated and the effects of environmental changes adequately described. A good example of this is the description of the effect of atmospheric CO_2 concentration on simulated yield figures, which depended on the climate of the given year in the AF2MOD model, but was described by a simple linear function in the AFRCWHEAT2 model.
Keywords: *winter wheat, modelling, calibration, elevated CO_2 concentration*

Introduction

Plant growth models with various degrees of complexity have been elaborated for the use of plant growers and breeders, ranging from simple statistical regression models to models with a complicated mechanism, capable of simulating anything from a simple process to the behaviour of the whole plant. In addition to experimental research, many scientists also use simulation models to gain a better understanding and description of environmental stress effects, such as high temperature, drought stress, and their effects on the development and yield of plants grown at elevated atmospheric CO_2 concentration.

In recent decades more than 70 wheat models have been published internationally, including AFRCWHEAT2, Ceres-Wheat and SIRIUS [9]. These models require detailed weather data, soil characteristics and agronomic descriptions (variety, sowing date, mineral fertilization, irrigation, etc.), which are often not available.

Before the models can be applied, they must be adapted to and calibrated for the given environment and plant variety.

The aim of the present work was to determine the applicability of the AFRCWHEAT2 wheat growth model under Hungarian conditions. The Farquhar

http://www.ecology.uni-corvinus.hu ● ISSN 1589 1623

model, which, when properly calibrated, gives a satisfactory description of the net photosynthesis of Hungarian winter wheat varieties at various atmospheric CO_2 concentrations, temperatures and light conditions, was incorporated into the model. Both the original AFRCWHEAT2 model and the modified AF2MOD model were tested on long-term yield and climatic data series from Győr-Moson-Sopron County.

Abbreviations: EC = elevated air CO_2 concentration; M = average deviation; r^2 = determination coefficient.

Materials and methods

Models

AFRCWHEAT2 is a complex model of wheat growth and development, describing the phenological development, dry matter production and dry matter distribution between the organs for various environmental parameters on a daily time scale [12, 13, 17]. The model includes a description of plant transpiration and soil evaporation, water and nitrogen movement in the soil, and their uptake by the plant in the course of growth.

Description of net photosynthesis: The photosynthetically active radiation (PAR) reaching the plant stand is calculated from the daily incoming short-wave radiation. This and the leaf area index (LAI) are used to calculate the incoming PAR at each leaf canopy level, using the method reported by Charles-Edwards (1978). The extent of photosynthesis, P_s [mg (CO_2) m^{-2} s^{-1}] is described using a quadratic equation fitted to the photosynthesis–light response curve [11], after subtracting the photorespiration [17].

Direct effect of elevated atmospheric CO_2 concentration (EC): EC causes a linear increase in the maximum net CO_2 assimilation [17] and the rate of electron transport.

In the course of the present work, the photosynthesis section of the AFRCWHEAT2 model was replaced by the Farquhar model [2, 3, 5, 14], thus creating the **AF2MOD** model. This alteration was possible because the AFRCWHEAT2 model is written in Fortran, and the full code is freely available for scientific purposes.

In order to incorporate the Farquhar model, new parameters had to be defined in the AFRCWHEAT2 model, and these were edited into the initialization data file. This required changes in the parameter-loading program (init.for), the parameter file and the program section describing photosynthesis (phosyn.for).

Data

Wheat yield and weather data from Győr-Moson-Sopron County were used for the analysis. In order to test the reliability of the models, climatic and mean yield data for the 1961–1990 period were employed. As there was a significant improvement in the cultivation techniques and average yield during this period, these effects were eliminated with the help of a logistic function, so that the yield figures applied would only reflect variations in the weather [8, 6]. The logistic function was as follows:

$$y(t) = c_1 + \frac{c_2 - c_1}{1 + e^{\alpha(c_3 - t)}} \qquad \text{(Eq. 1)}$$

where c_1 and c_2 were the lower and higher saturation values, c_3 the point of inflection, indicating the year when the growth rate was most rapid, α the parameter

http://www.ecology.uni-corvinus.hu ● ISSN 1589 1623

representing the growth rate and *t* the time in years. The magnitude of the deviation from the mean was corrected using a linear function taking into account the greater deviation of higher values.

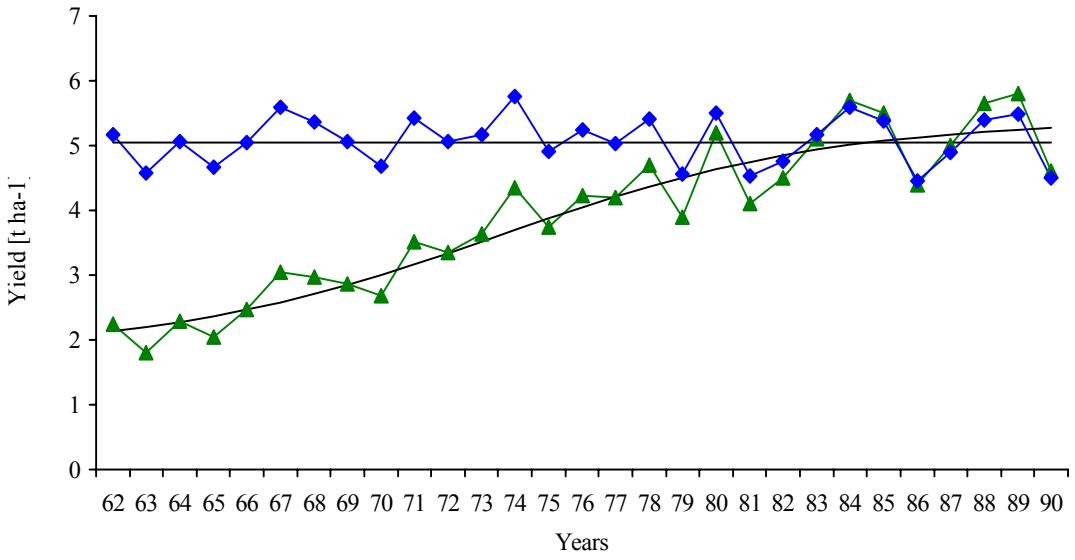

Figure 1. *Average wheat yields recorded in Győr-Moson-Sopron County in 1962–1990 (▲), the y(t) logistic function, the average yield over the last 10 years (horizontal line) and the yield quantity used in the models (♦)*

Daily weather data are available for the period examined. These include daily maximum (T_{max}) and minimum (T_{min}) temperatures, rainfall sums (P), the number of sunshine hours (n) and the relative humidity (RH). As the selected simulation models also require other climatic data, these were calculated using the relevant equations. These data were the wet (T_{wet}) and dry (T_{dry}) temperatures and the global radiation (R_g).

$$Tdry = T_{\min} + (T_{\max} - T_{\min}) \cdot \sin \frac{\Pi \cdot (h - 12 + N/2)}{N + 3} \qquad \text{(Eq. 2)}$$

where N is the number of astronomically possible sunshine hours, and h the hour of the day for which the T_{dry} values were calculated.

$$T_{wet} = T_{dry} + Y, \text{ where}$$

$$Y = [-0.05833 + (-0.00333 \cdot T_{dry})] \cdot RH + [5.833 + (0.333 \cdot T_{dry})]$$

(4; Kempenaar 1997, personal communication).

$$R_g = R_{\max} \cdot (a + b \cdot \frac{n}{N}), \qquad \text{(Eq. 3)}$$

where N is the number of astronomically possible sunshine hours, n the number of actual sunshine hours, R_{max} the maximum possible global radiation on the given area, and a and b empirically determined constants which, based on the data of Takács

http://www.ecology.uni-corvinus.hu ● ISSN 1589 1623

(1967), had values of a = 0.41 and b = 0.46 in the summer half-year and a = 0.35 and b = 0.694 in the winter half-year in Hungary [16]. It should be noted here that during the given period the number of sunshine hours was often recorded subjectively, so in many cases the accuracy of these data leaves much to be desired.

In both models parameter values given by Porter (1993) were used, and in the AF2MOD model the parameterization of the Farquhar photosynthesis model was based on experiments. Mineral fertilizer supplies were set at 90 %, so nitrogen limitation was also taken into account in the calculations. In the course of modelling the damage caused by pests, diseases and weeds was ignored. The mean plant density per square metre was taken as 300 and the sowing date as October 10th. For the choice of variety, the data of the wheat variety Martonvásári 8, which is widely grown in Hungary, were used [10].

Results

It was observed that the average yield over the whole experimental period was well simulated by the models (*Table 1*), but not the annual fluctuations: the determination coefficients describing the correlation between the actual wheat yield in Győr-Moson-Sopron county over the whole period and the values generated using the models were r^2 = 0.28 for the AFRCWHEAT2 model and r^2 = 0.37 for AF2MOD (*Fig. 2*).

Table 1. *Measured and simulated regional yields in Győr-Moson-Sopron County over the average of 28 years (1962–1990) and their deviations*

	Measured	AFRCWHEAT2	AF2MOD
Yield average [t ha^{-1}]	5.08	4.97	4.99
Deviation	*0.43*	*0.43*	*0.34*

The AF2MOD model gave an extremely good approximation to the yields of the last 10 years (r^2 = 0.86), while the mean deviation between data pairs was also acceptably low (M_{AF2MOD} = 0.16). This can be attributed to the fact that due to the advanced technologies and intensive varieties introduced in the 1980s the yield potential was so stable that the yield depended only on the weather conditions. When testing the AF2MOD model it was found that over the first 20 years of the tested period the variability in the wheat yield was influenced not only by the weather, but also by annual changes in the technology and varieties. This means that the elimination of cultivation techniques and variety effects with the help of a mathematical function is not necessarily the best method to use for model testing. Instead it is advisable to select a period like the 1980s in the present case, when the applied technology and choice of variety remained constant from year to year.

Testing indicated that the AF2MOD model gave a better simulation of historical yield data than the original AFRCWHEAT2 model, so it could be assumed that the AF2MOD model would also provide a more reliable simulation of the probable effects of climate change.

http://www.ecology.uni-corvinus.hu ● ISSN 1589 1623

The purpose of model testing was to analyze the effect of climate change, one of the main causes of which is elevated CO_2 concentration (EC). For this reason, it was important to determine the efficiency with which the AFRCWHEAT2 and AF2MOD models simulated the effect of EC. Both models were thus run on the original climatic data for Győr-Moson-Sopron County applying CO_2 concentrations of 350 and 515 µmol mol^{-1}. The differences between the results, presented in *Fig. 3*, were investigated for both models. It is clear from the *Fig. 3* that the yield-increasing effect of EC did not depend on the climatic data in the case of AFRCWHEAT2, while for AF2MOD a lower yield increase was predicted as the result of EC and the yield increase was a function of the climatic conditions in the given year.

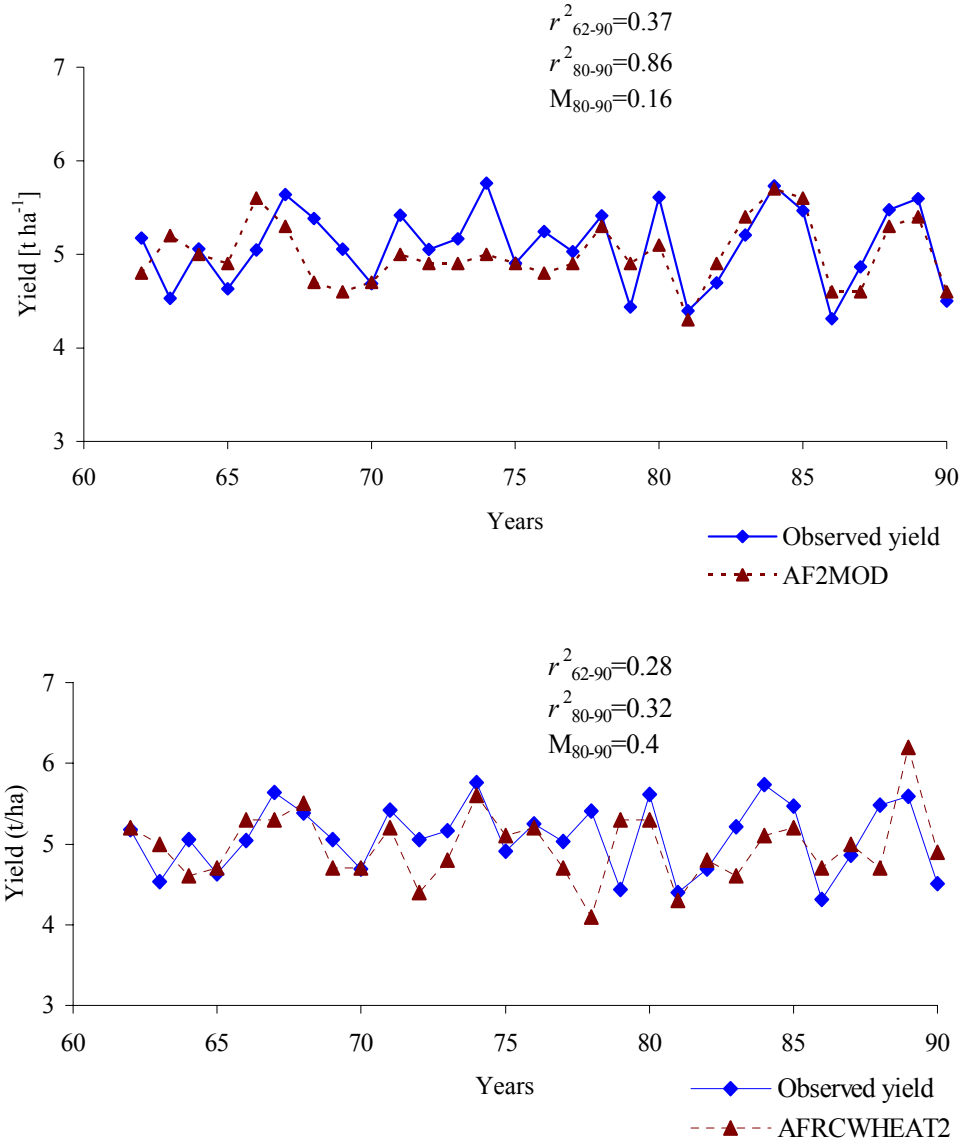

Figure 2. *Measured yields and the regional yield quantities simulated each year for Győr-Moson-Sopron County using the AFRCWHEAT2 and AF2MOD models in the period 1961–1990.*

http://www.ecology.uni-corvinus.hu ● ISSN 1589 1623

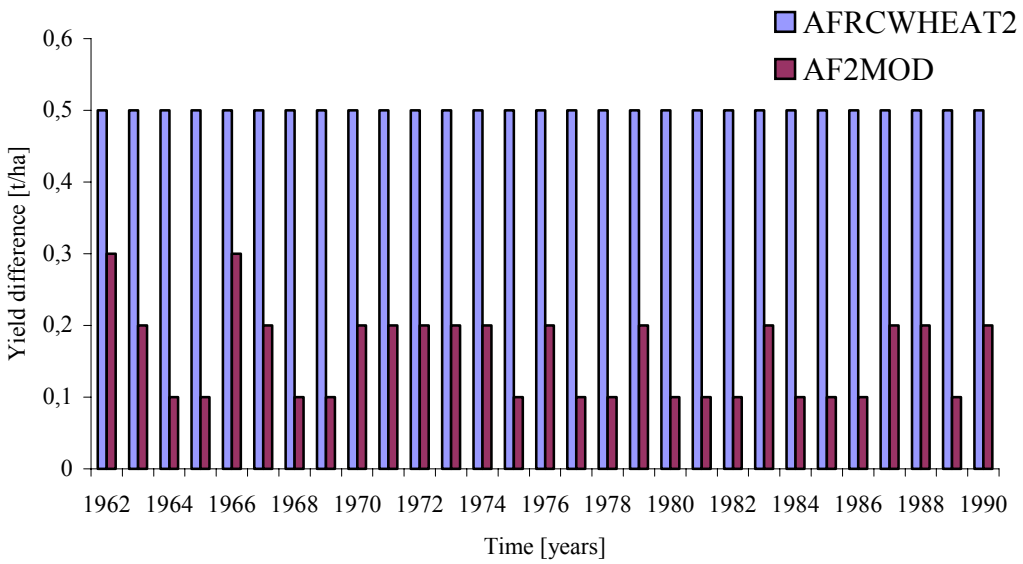

Figure 3. *Wheat yield simulation achieved for Győr-Moson-Sopron County using the AFRCWHEAT2 and AF2MOD models with weather data series for 1962–1990 at two CO_2 concentrations. The simulations were run at concentrations of 350 μmol mol^{-1} and 515 μmol mol^{-1} CO_2. The figure illustrates differences in the yields.*

Discussion

Earlier results suggested that the Farquhar model was suitable for the description of the net photosynthesis of winter wheat under various environmental conditions (radiation, temperature, atmospheric CO_2 concentration) and could thus be usefully incorporated into wheat growth simulation models [7]. In the course of the present work the Farquhar model was thus incorporated into the module of the AFRCWHEAT2 model that describes net CO_2 assimilation, thus developing the AF2MOD model.

A comparison of the results simulated using the AFRCWHEAT2 and AF2MOD models demonstrated that detailed physiological submodels are required for the mathematical description of plant growth if yields are to be accurately estimated and the effects of environmental changes adequately described. A good example of this is the description of the effect of atmospheric CO_2 concentration on simulated yield figures, which depended on the climate of the given year in the AF2MOD model, but was described by a simple linear function in the AFRCWHEAT2 model.

In the course of validation it was observed that the yield averages recorded in the first half of the tested period were well simulated by the models, by not the annual figures**.** By contrast, the yield obtained in Győr-Moson-Sopron County over the last 10–15 years was far better approximated by the AF2MOD model than that of earlier years. This could be explained by the fact that in the 1980s, when advanced technologies and intensive varieties were introduced, the yield potential became so stable that where the yield depended almost entirely on the climatic conditions. It is thus recommended that models should be tested on periods when the technology applied and the varieties chosen remained constant from year to year, such as the 1980s in the present case [6].

http://www.ecology.uni-corvinus.hu ● ISSN 1589 1623

REFERENCES

[1] Charles-Edwards, D.A. (1978): An analysis of the photosynthesis and productivity of vegetable crops in the United Kingdom. - Annals of Botany 42: 717-731.

[2] Farquhar, G.D., von Caemmerer, S. (1982): Modelling of photosynthetic response to environmental conditions. - In: Lange, O.L., Nobel, P.S., Osmond, C.B., Ziegler, H., (Szerk.): Physiological plant ecology II. Water relations and carbon assimilation. Encyclopedia of plant physiology, New series, Berlin: Springer-Verlag, Vol. 12B. 549-587. p.

[3] Farquhar, G.D., von Caemmerer, S., Berry J.A. (1980): A biochemical model of photosynthetic CO_2 assimilation in leaves of C_3 species. - Planta 149: 78-90.

[4] Goudriaan, J., van Laar, H.H. (1994): Modelling Potential Crop Growth Processes. Textbook with Exercises. - Kluwer Academic Publishers. 238 p.

[5] Harley, P.C., Sharkey, T.D. (1991): An improved model of C_3 photosynthesis at high CO_2 : Reversed O_2 sensitivity explained by lack of glycerate re-entry into the chloroplast. - Photosynthesis Research 27: 169-178.

[6] Harnos, N. (2003): A klímaváltozás hatásának szimulációs vizsgálata őszi búza produkciójára. „AGRO-21" Füzetek, 2003. 31: 56-73.

[7] Harnos, N., Tuba, Z., Szente, K. (2002): Modelling net photosynthetic rate of winter wheat in elevated air CO_2 concentrations. - Photosynthetica 40(2): 293-300.

[8] Harnos, Zs. (1996): Modelling crop response in Hungary. - In: Harrison, P.A., Butterfield, R.E., Cowning, T.E. (ed.): Climate Change, Climatic Variability and Agriculture in Europe. Annual Report. Environmental Change Unit, University of Oxford. 179-189. p.

[9] Jamieson, P.D., Porter, J.R., Goudriaan, J., Ritchie, J.T., van Keulen, H., Stol W. (1998): A comparison of the models AFRCWHEAT2, CERES-Wheat, Sirius, SUCROS2 and SWHEAT with measurements from wheat grown under drought. - Field Crops Research 55: 23-44.

[10] Kovács, G.J., Németh, T., Ritchie, J.T. (1995): Testing Simulation Models for Assessment of Crop Production and Nitrate Leaching in Hungary. - Agricultural Systems 49(4): 385-397.

[11] Marshall, B., Biscoe, P.V. (1980): A model for C_3 leaves describing the dependence of net photosynthesis on irradiance. I. Derivation. - Journal of Experimental Botany 31: 29-39.

[12] Porter, J.R. (1984): A model of canopy development in winter wheat. - Journal of Agricultural Science 102: 383-392.

[13] Porter, J.R. (1993): AFRCWHEAT2 A model of the growth and development of wheat incorporating responses to water and nitrogen. - European Journal of Agronomy 2: 69-82.

[14] Sharkey, T.D. (1985): Photosynthesis in intact leaves of C_3 plants: Physics, physiology and rate limitations. - The Botanical Review 51: 53-105.

[15] Takács, L. (1967): A globálsugárzás számítása. Az Országos Meteorológiai Intézetben 1967-ben elhangzott referátumköri előadás. Kézirat.

[16] Varga-Haszonits, Z. (1977): Agrometeorológia. - Mezőgazdasági Kiadó, Budapest.

[17] Weir, A.H., Bragg, P.L., Porter, J.R., Rayner, J.H. (1984): A winter wheat model without water or nutrient limitations. - Journal of Agricultural Sci. 102: 371-383.

http://www.ecology.uni-corvinus.hu ● ISSN 1589 1623

KERNEL-BASED CLASSIFICATION OF TISSUES USING FEATURE WEIGHTINGS

A. KERTÉSZ-FARKAS* – A. KOCSOR

Research Group on Artificial Intelligence of the
Hungarian Academy of Sciences and University of Szeged
H-6720 Szeged, Aradi vértanúk tere 1., Hungary
(phone: +36-62-544-140; fax: +36-62-425-508)

**e-mail: kfa@inf.u-szeged.hu*

(Received 10th Sep 2005, accepted 10th Oct 2006)

Abstract. In high-dimensional spaces classification methods could be more effective using various feature selection methods. The training procedure could be speeded up by decreasing the dimension of the feature space, and the classification method could be improved by removing noisy or irrelevant features. In this paper we present a new method which weights the features according to their importance instead of removing the negligible ones via kernel functions. It could be applied to a range of real-world problems. We tested it on several biological datasets like a small part of the UCI Learning Repository and SCOP and the Leukaemia AML-ALL databases, and obtained a significantly better classification performance than that using the usual unweighted method.
Keywords: *Support Vector Machines (SVMs), classification, kernel functions, feature ranking algorithms*

Introduction

Biological databases like those generated by a DNA microarray consist of some thousands of features (i.e. components) that are not equally important. During classification, some features may be considered crucial while others can be safely ignored. It is obvious that the various features should have different weights in the classification procedure, i.e. the features should be weighted according to their importance. One such method is the Fisher Correlation Coefficients which assigns the following weighting value to the *i*th feature:

$$\frac{(\mu_i^+ - \mu_i^-)^2}{(\sigma_i^+)^2 + (\sigma_i^-)^2}$$

where μ_i^+, μ_i^-, σ_i^+, σ_i^- are the mean and standard deviations of the *i*th feature value for the positive and negative examples, resepectively [4].

In this paper we give a feature weighting method that is based on feature ranking. To rank the features here several methods are used and the corresponding weight calculation is based on this rank. A sample vector which is weighted by the given weights is computed via a kernel function. We carried out several experiments on a DNA microarray database and a part of the Astral databases of the SCOP protein sequence databases. We employed Support Vector Machines (SVM) with kernel functions as the classification method to obtain the experimental results.

The article is organised as follows. In Section 2 we discuss SVMs, feature weightings via kernels. In Section 3 we provide a summary of widely-used feature ranking methods. Section 4 describes the results of our method on real-world databases then, in Section 5, we discuss these results and their implications.

http://www.ecology.uni-corvinus.hu ● ISSN 1589 1623

SVM and kernels

SVM is a supervised binary classifier first introduced by Vapnik et al [1]. Let $D = \{(x, y) : x \in \Re^n, y \in \{-1,1\}\}$, where x is a n-dimensional training vector and y is the class label of x. $\Re^n$ is called the input space and D is referred to as the training database. Training an SVM amounts to solving an optimisation problem that determines a linear classification rule $f(x) = \langle w, x \rangle + b$. A test example z is classified as positive (or negative) if $f(z) > 0$ (or $f(z) < 0$). Such a classification rule determines a linear hyperplane decision boundary with normal vector w and bias term b that separates positive and negative classes.

The key part of SVM is the inner product $\langle x_i, x_j \rangle$ of two vectors x_i, x_j over $\Re^n$, which is used for the classification of samples. Given a feature map Φ from an input space to a (possibly infinite dimensional) dot product space (referred to as the kernel feature space), we obtain a inner product $\langle \Phi(x), \Phi(y) \rangle$. If a function $\kappa(x, y)$ is symmetric, continuous and positive definite, which is called the kernel function, then exist a Φ mapping so that $\kappa(x, y) = \langle \Phi(x), \Phi(y) \rangle$. We can directly and efficiently compute the kernel values $\kappa(x, y)$ without explicitly representing the feature vectors. The inner product $\langle x_i, x_j \rangle$ in SVM when replaced by $\kappa(x, y)$ leads to a linear hyperplane in the kernel feature space and a nonlinear one in the original input space. This gives us a tremendous computational advantage for high-dimensional feature spaces.

Let $K(\Re^n)$ denote the class of kernel functions for the mapping $\Re^n \times \Re^n$ to $\Re$. This class is not empty, because $\kappa(x, y) = x^T y$ is a trivial kernel function. The following proposition provides a way for generating additional kernels from an existing kernel.

Proposition 1 $K(\Re^n)$ is closed under addition, multiplication, composition of a continuous function, and addition and multiplication with a positive scalar, i.e. if $\kappa_1, \kappa_2 \in K(\Re^n)$, $\kappa_0 \in K(\Re^m)$ and $\varphi : \Re^n \to \Re^m$ is continuous, then the following five functions again belong to $K(\Re^n)$.

i) $\kappa(x, y) = \kappa_1(x, y) + \kappa_2(x, y)$,

ii) $\kappa(x, y) = \kappa_1(x, y) \cdot \kappa_2(x, y)$,

iii) $\kappa(x, y) = \kappa_1(x, y) + \delta$ for any positive $\delta \in \Re_+$,

iv) $\kappa(x, y) = \kappa_1(x, y) \cdot \delta$ for any positive $\delta \in \Re_+$.

v) $\kappa(x, y) = \kappa_0(\varphi(x), \varphi(y))$.■

For further reading and details of kernel function properties see [3].

Now, we will list the most well-known and useful kernels used in classification tasks in the following table.

http://www.ecology.uni-corvinus.hu ● ISSN 1589 1623

Table 1. *Some well-known kernels*

Gaussian RBF kernel:	$\kappa(x,y)=\exp\left(-\frac{\|x-y\|^2}{\sigma}\right)$, where $\sigma\in\Re_+$
Polynomial kernel:	$\kappa(x,y)=(x^Ty+\sigma)^q$, where $\sigma\in\Re, q\in\mathbf{N}$
Rational quadratic kernel:	$\kappa(x,y)=1-\frac{\|x-y\|^2}{\|x-y\|^2+\sigma}$, where $\sigma\in\Re$
Inverse multi-quadratic kernel:	$\kappa(x,y)=\frac{1}{\sqrt{\|x-y\|^2+\sigma}}$, where $\sigma\in\Re$
Cosine polynomial kernel:	$\kappa(x,y)=\cos\left(\frac{x^Ty}{\|x\|\|y\|}+\sigma\right)^q$, where $\sigma\in\Re, q\in\mathbf{N}$

Weighted kernel functions

When the inner product is computed, one might weight the features such that more important features are given higher weightings than the less important ones. Let $\Re^n$ be an n-dimensional feature space, and $w_1, w_2, \ldots, w_n$ the weights where w_i corresponds to the ith feature. Afterwards the weighted inner product of two vectors $x, y \in \Re^n$ is evaluated in the following way. Let $U = diag(w_1, w_2, \ldots w_n)$ be a diagonal matrix constructed from weights $w_1, w_2, \ldots, w_n$. Then x^TUy is the weighted inner product of vectors x and y.

This idea is also applicable to kernel functions. If κ is a kernel, then $\kappa(Ux,Uy)$ will be a weighted kernel. The following proposition states this in a more general way.

Proposition 2 Let U be a $m \times n$ matrix and $x, y \in \Re^n$ be two vectors. If $\kappa_0 \in K(\Re^n)$ is a kernel, then $k(x,y) = k_0(Ux,Uy)$ is also a kernel function and belongs to $K(\Re^m)$.

Proof. Let the function $\varphi : \Re^n \to \Re^m$ be defined by $\varphi(x) = Ux$. This function is continuous and, because $\kappa_0 \in K(\Re^n)$, $\kappa(x,y) = \kappa_0(\varphi(x),\varphi(y)) = \kappa_0(Ux,Uy)$ is again a valid kernel. This follows from v) of Proposition 1.

Feature ranking methods

Here we describe the feature ranking methods which are used in experiments to rank the features, so that if a feature is more important or less important in a classification then it is ranked accordingly. Most of these methods are traditionally known as feature selection methods because they retain only a small number of features from the top of the ranked list. With this trick, classification will hopefully be speeded up and be more accurate.

http://www.ecology.uni-corvinus.hu ● ISSN 1589 1623

Table 2. *Feature ranking methods used in experiments*

Method name	Description
Std. dev.	The standard deviation method computes the deviation along the direction of the basis vectors. Then it ranks the features according to their values.
Fisher	The Fisher Correlation Coefficient [4] is described in the introduction of this article.
R^2W^2	This method is based on a minimising generalisation bound through gradient descent and is feasible computationally via SVMs. This allows several new possibilities: one can speed up time-critical applications and one can perform feature selection. This method scales the input parameters with a real-valued vector σ, larger values of σ_i indicating more useful features [6]. For further details see [5].
RFE	Recursive Feature Elimination (RFE) is a recently proposed feature selection method described in [7]. The method, given that one wishes to have only $r < n$ input dimensions in the final decision rule, attempts to find the best subset *r*. The method seeks to choose the 'best' *r* features that lead to the largest margin of class separation using an SVM classifier. For each iteration of the training, this combinatorial problem is solved in a greedy fashion by removing those input features that decrease the margin the least until just *r* input features remain. This is known as backward selection [6].
L0	Zero-Norm feature selection can be expressed as the following minimisation problem: $\min_{w \in \Re^n} \quad \|w\|_p$ subject to : $y_i (w \cdot x_i + b) \geq 1$ and $\|w\|_0 \leq r$ where $p = \{1,2\}$ and *r* is the desired number of features. This method can be approximated by minimizing the zero norm using the ℓ_2-AROM or ℓ_1-AROM methods, halting the step-wise minimisation when the constraint $\|w\|_0 \leq r$ is met [6]. One can then re-train a *p*-norm classifier on those features corresponding to the nonzero elements of *w*. In this way one is free to choose the parameter *r* which dictates how many features the classifier will see. This method is based on SVM.
FSV	In the Feature Selection via the concaVe minimisation (FSV) [8] approach, a separating plane is generated by minimising the weighted sum of distances of misclassified points to two parallel planes that bound the set, and which determine the separating plane midway between them. The number of dimensions of the space is used to determine how the plane is minimised. SVM is used in this method.
Entropy	The basic concept of entropy in information theory, first introduced by Shannon, has to do with how much randomness there is in a signal or in a random event. Let $H(f_i) = -p_1 \log_2(p_1) - p_2 \log_2(p_2)$ be the entropy for the *i*th feature, where p_1, p_2 is the rate of the positive and negative examples in the *i*th feature, respectively. The feature ranking is based on these entropy values.

http://www.ecology.uni-corvinus.hu ● ISSN 1589 1623

Experimental Results

We tried out our feature weighting methods on three selected databases, namely two biological datasets of the UCI Machine Learning Repository, the AML/ALL leukaemia dataset at http://lara.enm.bris.ac.uk/colin and the Structural Classification of Proteins (SCOP) database.

We made use of SVM Light as a classification algorithm, and most of the feature ranking methods which are part of SpiderSVM. These algorithms are also available at http://www.kernel-machines.org/software.html and http://www.kyb.tuebingen.mpg.de/bs/people/spider/index.html, respectively. The Standard Deviation and Entropy weighting methods were implemented by us.

To weight the features, the features are first ranked by each ranking method mentioned in the previous section. Afterwards, the ranked features are weighted by the $g(i) = 2^{-i}$ monotonic decrease function, i.e. the *i*th feature of the ranked list is assigned a weight of 2^{-i} except in the Fisher method. With the latter, it has its own feature weighting procedure. The given weights corresponding to features are stored in a diagonal matrix, and it is used for weighting the kernel in the way described above.

In order to measure the performance of these weighted kernel methods we applied an accuracy analysis followed by a receiver operating characteristic (ROC) analysis [11]. The accuracy for a method is simply the fraction of the true predictions of the total number of predictions. The ROC score is the normalized area under a curve that plots sensitivity as a function of specificity for varying classification thresholds. A perfect classifier that puts all the positives at the top of the ranked list will receive an ROC score of 1, while a random classifier will receive an ROC score of 0.5.

Ranking a lot of features naturally requires a lot of time. Hence we apply a dimensionality reduction method called Locally Linear Embedding (LLE) [15]. This is an unsupervised learning method that computes low dimensional, neighbourhood preserving embeddings of high dimensional data. We used this on high dimensional datasets like the leukaemia dataset and SCOP [14]. Details of this method and the Matlab code of the LLE are available at http://www.cs.toronto.edu/~roweis/lle/. Because the LLE preserves the neighbourhoods, the SVM classification does not change significantly because it is based on the inner product of two vectors.

The methods were implemented in Matlab and were run on an IBM PC machine with a 3GHz Intel Pentium IV processor, 4Gbyte RAM and a Windows XP operating system.

Feature weighting and SVM parameters

For the SVM classification we chose the Gaussian RBF kernel function with a σ parameter defined as the median Euclidean distance in the input space from any positive training example to the nearest negative example. The parameter *c* of SVM was set to 1, and a 2-*norm* with value 0.01 was used.

Tests on the AML/ ALL database

The challenge here is to distinguish acute myeloid leukaemia (AML) from acute lymphoblastic leukaemia (ALL). The databases consist of 47 and 25 bone marrow or peripherial blood samples taken from 72 patients of type ALL and AML respectively, with 7129 features per sample, also available at http://lara.enm.bris.ac.uk/colin [9].

http://www.ecology.uni-corvinus.hu ● ISSN 1589 1623

These samples were produced by AFFymetrix high-density oligonucleotid microarrays [10].

First of all, we reduced the features from 7129 to 10 using LLE. The training set and the test set contained 39 and 34 samples respectively. The results are given in the following table and figures.

Table 3. *Results for the Leukeamia AML-ALL database*

	Unweighted	Std. dev.	Fisher	R^2W^2	RFE	L0	FSV	Entropy
Accuracy	0.67	0.74	0.73	0.88	0.88	0.88	0.59	**0.94**
ROC score	0.93	0.98	0.97	0.99	**1.00**	0.99	0.45	0.99
Time(s)	0.06	0.03	0.04	0.08	0.03	0.08	0.05	0.05

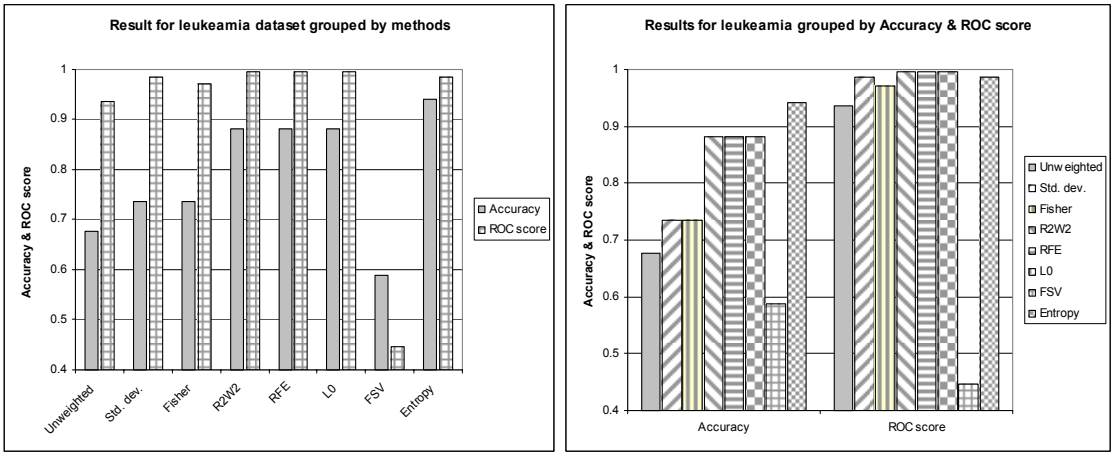

In this database the feature weighting methods perform significantly better than the usual unweighted method. As can be seen, the best accuracy results are given by the feature weighting algorithm based on entropy. We also significantly improved the ROC scores by using a feature weighting method that achieved an ROC score of 1.

Tests on the SCOP databases

The SCOP databases designed by Jakkoola et al. [13] for the remote protein homology are simulated by retaining all members of a target SCOP family from a given superfamily [2]. The sequences were selected using the Astral databases (http://astral.stanford.edu) [14]. Here, positive training examples are chosen from the remaining families in the same superfamily, and negative test and training examples are chosen from disjoint sets of folds outside the target family's fold [12]. Details of the datasets are available at http://www.soe.ucsc.edu/research/compbio/discriminative. The dataset can also be found at http://cs.columbia.edu/compbio/svm-pairvise. In the following *Table 4* we summarise the main details of the dataset used.

Table 4. *Description of the SCOP datasets*

ID	Family name	Positiv train	Negativ train	Positiv test	Negative test	Dimension numbers
SCOP 2.1.1.5	E set domains	94	194	27	39	270
SCOP 2.44.1.2	Eukaryotic proteases	11	14	140	183	25
SCOP 3.32.1.13	Extended AAA-ATPase domain	43	184	8	32	227
SCOP 7.41.5.1	Rubredoxin	10	112	9	98	112

http://www.ecology.uni-corvinus.hu ● ISSN 1589 1623

A numerical database was obtained from this protein sequence database in the following way. A protein sequence A is represented by a vector $F_A = a_1, a_2, \ldots, a_n$, where n is the number of training proteins, and a_i is the similarity score of A and A_i proteins by Smith- Watermann algorithm, as implemented on the BioXLP hardware accelerator (www.cgen.com).

Before we carried out the classification procedure, every high-dimensional dataset was reduced to an 8-dimensional input space, except for the SCOP 2.44.1.2 dataset because its dimensionality was low.

Table 5. *Results for the SCOP datasets*

	Unweighted	Std. dev.	Fisher	R^2W^2	RFE	L0	FSV	Entropy
	SCOP 2.1.1.5							
Accuracy	0.66	0.68	**0.75**	0.67	0.67	0.67	0.68	0.67
ROC score	0.79	**0.89**	0.88	0.85	0.84	0.84	0.86	0.85
Time(s)	7.2	7.9	7.9	8.0	8.0	7.8	6.3	8.4
	SCOP 2.44.1.2							
Accuracy	**0.59**	0.48	0.52	0.54	0.54	0.54	0.51	0.49
ROC score	0.35	0.14	**0.72**	0.47	0.47	0.47	0.70	0.59
Time(s)	0.13	0.13	0.13	0.14	0.13	0.14	014	0.13
	SCOP 3.32.1.13							
Accuracy	0.86	0.86	0.81	**0.89**	**0.89**	**0.89**	0.86	0.86
ROC score	0.85	0.92	0.85	**0.93**	**0.93**	**0.93**	0.87	0.81
Time(s)	3.0	2.8	2.0	2.5	2.6	2.5	2.4	1.9
	SCOP 7.41.5.1							
Accuracy	0.92	0.92	0.92	0.92	0.92	0.92	0.92	0.92
ROC score	0.61	0.80	**0.84**	0.75	0.75	0.75	0.74	0.73
Time(s)	0.53	0.64	0.64	0.66	0.66	0.64	0.58	0.43

With these datasets better results were indeed obtained by applying feature weighting methods. The ROC scores achieved by using weighted feature methods were significantly better than those for the usual unweighted case. The accuracy scores using the weighted methods were also better than the baseline but no significant improvement was obtained. This may be because there were too many dimensions and too few training and test examples for a learning method to work effectively.

Tests on the UCI Machine Learning Repository

The UCI Machine Learning Repository is a database that contains millions of records and thousands of field types widely used in business, medicine, engineering, and the sciences. This datasets is available at http://www.ics.uci.edu/~mlearn. We chose the Heart and Hepatitis biological and medical databases, which are listed in *Table 6*. These databases were not divided into train and test sets originally, so we used 10-fold cross validation for testing.

Table 6. *Description of the heart and Hepatitis UCI datasets*

Dataset name	# Features	#Instances	Class #1 name	Class #2 name
Heart	13	270	Absence of heart disease	Presence of heart disease
Hepatitis	19	155	Die	Live

http://www.ecology.uni-corvinus.hu ● ISSN 1589 1623

The performance of the feature weighting methods on each of these datasets is presented in the table below. In these experiments the baseline unweighted methods provided the best results. A reason for this might be because all of these features were equally important or that another weighting function should be applied here.

Table 7. *Results for the UCI datasets*

	Unweighted	**Std. dev.**	**Fisher**	**R^2W^2**	**RFE**	**L0**	**FSV**	**Entropy**
				HEART				
Accuracy	**0.84**	0.79	0.82	0.76	0.76	0.76	0.81	0.77
ROC score	**0.91**	0.85	0.88	0.85	0.85	0.85	0.89	0.85
Time(s)	23.0	6.7	7.5	8.5	8.0	8.0	8.9	6.7
				HEPATITIS				
Accuracy	**0.83**	0.79	0.81	0.76	0.76	0.76	0.80	0.80
ROC score	**0.92**	0.85	0.89	0.82	0.82	0.82	0.83	0.86
Time(s)	4.9	1.6	1.2	3.3	3.2	3.3	2.0	3.1

Conclusions and further work

Here we introduced a feature weighting method for SVMs that is based on a feature ranking methodology. To enable us to do this, several feature ranking procedures were applied, and then the weights were assigned to these ranked features. In some real-world biological classification experiments we showed that we could obtain more accurate predictions using this method, and in a very short time.

In this paper we focused on feature rankings using the weighting function $g(i) = 2^{-i}$. This, of course, is unsuitable in high dimensional features spaces which may be of order ten/hundred/thousand, because most of the features are assigned almost zero weights. On the other hand, the importance of certain features could not be represented exactly by this weighting function as the importance of ranked features did not, for instance, decrease in quite the same way as the weighting function. Further study is needed to learn the effect of our approach on special databases and to find out whether other good methods exist that allow us to determine the weights for each ranked feature.

REFERENCES

[1] Bosser, B.E., Guyon, M., Vapnik, V.N. (1992): A Training Algorithm for Optimal Margin Classifiers. - Proc. Of the Fifth Annual ACM Conference on Computational Learning Theory

[2] Leslie, C., Eskin, E., Cohen, A., Weston, J., Stafford Noble, W. (2004): Mismatch string kernels for discriminative protein classification. - Bioinformatics

[3] Berg, C., Christensen, J., Ressel, P. (1984): Harmonic Analysis on Semigroups: Theory of Positive Definite and Related Functions. - Springer

[4] Bishop, C. (1995): Neural Networks for Pattern Recognition. - Oxford UP, Oxford, UK

[5] Weston, J., Mukherjee, S., Chapelle, O., Pontil, M., Poggio, T., Vapnik, V. (2001): Feature Selection for SVMs, Advances in Neural Information Processing Systems 13. - MIT Press, Cambridge, MA, USA,

[6] Weston, J., Elisseff, A., Schölkopf, B., Tipping, M. (2003): Use of the zero-norm with linear models and kernel methods. - Journal of Machine Learning Research

http://www.ecology.uni-corvinus.hu ● ISSN 1589 1623

[7] Guyon, I., Weston, J., Branhill, S., Vapnik, V. (2002): Gene Selection for Cancer Classification using Support Vector Machines. - Machine Learning 46.
[8] Bradley, P.S., Mangasarian, O.L. (1998): Feature Selection via Concave Minimization and Support Vector Machines. - INFORMS Journal on Computing 10.
[9] Shevade, S.K., Keerthi, S.S., (2002): A Simple and Efficient Algorithm for Gene Selection using Sparse Logistic Regression. - Bioinformatics
[10] Furey, T.S., Cristianini, N., Duffy, N., Bednarski, D.W., Schummer, M., Haussler, D. (2000): Support Vector Machine Classification and Validation of Cancer Tissue Samples Using Microarray Expression Data. - Bioinformatics 16.
[11] Gribskov, M., Robinson, N. (1996): The Use of Receiver Operating Characteristic (ROC) Analyisis to Evaluate Sequence Matching. - Computers and Chemistry 20
[12] Lialo, L., Noble, W.S. (2003): Combining Pairwise Sequence Similarity and Support Vector Machines for Detecting Remote Protein Ecolutionary and Structural Relationships. - Journal of Computational Biology
[13] Jaakkola, T., Diekhans, M., Haussler, D. (2000): A discriminative framework for detecting remote protein homologies. - Journal of Computational Biology
[14] Brenner, S.S., Koehl, P., Levitt, M. (2000): The ASTRAL compendium for sequence and structure analysis. - Nucl. Acad. Sci. 28 USA.
[15] Saul, L., Roweis, S.T. (2000): Nonlinear dimensionality reduction by locally linear embedding. - Science 290

http://www.ecology.uni-corvinus.hu ● ISSN 1589 1623

GENERATION OF TEMPORALLY AND SPATIALLY HETEROGENEOUS LANDSCAPES FOR MODELS OF POPULATION DYNAMICS

Á. KUN

Department of Plant Taxonomy and Ecology, Eötvös University
Pázmány Péter sétány 1/C, H-1117 Budapest, Hungary
(phone: +36-1-209-555/1708; fax: +36-1-381-2188)

e-mail: kunadam@ludens.elte.hu

(Received 10th Sep 2005, accepted 10th Oct 2006)

Abstract. There is an increased interest in the use of spatial explicit modelling techniques in ecological research. One of the strength of this technique is the possibility to explicitly study the effect of environmental heterogeneity on the dynamics of populations or whole communities. Most of these studies focused on aspects of spatial heterogeneity, and studies focusing on environmental change employed other modelling techniques. Only recently were these two aspects of heterogeneity coupled within the same framework. The paper aims to review algorithms for generating spatially and temporarily heterogeneous landscapes that can be used in studies of population dynamics. These models have the potential to give new insight into the dynamics of populations living in a fragmented and changing environment.
Keywords: *Cellular automata, percolation map, heterogeneous landscape, dynamic landscape, habitat fragmentation*

Introduction

Recently the number of ecological studies investigating the effects of environmental heterogeneity is increasing. Both experimental and modeling techniques are advanced enough to cope with the added complexity of heterogeneity. Spatially explicit models [1] are convenient tools for investigating the effect of environmental heterogeneity on the dynamics of populations or whole communities. However, until recently even if a lattice model considered environmental heterogeneity, it included only spatial aspects of it and the landscape was otherwise static. Even if there was a change in the landscape it was disturbance, meaning that populations or individuals were unselectively removed from part of the landscape [2, 3, 4, 5]. Fires, hailstorms, herbivory or windfall can cause such effect [6].

Here I define temporal change as a process that rearranges the distribution of resources, but which does not affect the static characteristic of the landscape, i.e. the characteristics (indices) that can be measures on a one-time snapshot of the landscape. For example With and Crist [7] studied habitat destruction with the continuous removal of habitat patches. While this study employed a spatially explicit technique and the resource (habitat) pattern changed over time, the dynamics led to a homogeneous landscape (one where all habitats were removed). This kind of environmental change is not considered here. Unless we wish to study habitat degradation or climatic change we should employ an algorithm which do not remove heterogeneity from the landscape, and preferably do not affect the overall measures of the spatial pattern.

http://www.ecology.uni-corvinus.hu ● ISSN 1589 1623

In order to introduce heterogeneous landscape into a model of population dynamics an algorithm generating the landscape is required. In the following I will present a number of algorithms for generating heterogeneous landscapes. The main focus of the present paper is to demonstrate that most of the commonly used algorithm can accommodate temporal heterogeneity as well. This paper offers, for the first time, methods that extend the capabilities of these landscapes to accommodate temporal changes. Furthermore the Ising model known in statistical physics [8] is proposed here as a novel landscape generating method.

The landscapes used as illustration throughout the paper are generated by the HETEROLAND landscape generating program developed by the author.

Components of heterogeneity

Please note that I do not attempt to define heterogeneity in a general sense, only pertaining to spatially explicit lattice models (e.g. cellular automata), even thought these descriptors have been or could be defined also for a general heterogeneous landscape. The definitions utilize the fact that a lattice is a regular grid of sites (cells), and thus space is discreticized. While it can be objected that the natural environment is not divided into lattice cells, but this kind of discretization is deeply ingrained in the methodology. For example landscape analysis using GIS data (aerial or space-photos) are discretized as the pixels form a grid. Thus studies using such data employ the lattice representation. Furthermore in most of the green-house experiments, where heterogeneous environment were created it was achieved by separating the experimental box into smaller parts, and assigning a quality (for example watered and not watered) to each of the parts. Again the lattice representation is there. Finally in cellular automata – and in other lattice models as well – the lattice is an integral part of the method.

Source of heterogeneity: Heterogeneity can be defined as the uneven distribution of biotic or abiotic resources or conditions in time and space. The first descriptor of heterogeneity is the statement of which resource or condition has a heterogeneous distribution. Most experiments and models focuses on heterogeneous distribution of a resource (e.g. light, mineral nutrients, water, preys, etc.), but studies on other factors are not unknown (e.g. cover, competitors, pathogen, etc.).

Component of spatial heterogeneity

Spatial grain/Elementary scale/Cell size: Traditionally spatial grain is defined as the smallest scale at which the organism can still sense the heterogeneity of the environment [9]. While it is exceedingly important to define heterogeneity from the point of view of the studied / modeled organism, but the determination of grain according to the above definition is often difficult and cumbersome. In landscape ecology spatial grain is defined as the finest resolution of the dataset [10]. In models this corresponds to the size of one cell, which I term *elementary scale* here.

Spatial extent: The definition of extent as relating to an organism is the largest scale of heterogeneity to which the organism can still react [9]. The same is defined in landscape ecology as the physical size of the study area [10]. In models this corresponds to the lattice size (N, usually an $L \times L$ array of cells).

Quality of the resource patches: Let us assume that the quality of an arbitrary resource patch can be classified into a finite number of discrete types. In the simplest

http://www.ecology.uni-corvinus.hu ● ISSN 1589 1623

case a patch is assumed to be either good (favourable, resource rich) or bad (unfavourable, resource poor). Naturally, more than two quality classes can be considered.

Patch size (s): The smallest scale at which the environment is heterogeneous. This scale can be larger than the elementary scale. Thus on a rectangular grid a patch is defined as an $s \times s$ area, and each of those patches are assigned a resource status (usually good or bad).

Frequency of resource quality classes ($\underline{p}$): The vector $\underline{p}$ gives for each distinguished resource quality class the percentage of the whole habitat having the given quality. If there are only good and bad sites, then let p be the percentage of the habitat covered by good sites, and consequently $q = 1 - p$ is the percentage cover of the bad sites. In this case the frequency of the good sites measures the average resource richness of the habitat.

Contrast ($\underline{m}$): The vector $\underline{m}$ gives the difference between the succeeding quality classes, and also defines an absolute value for one of the classes, so that the difference can be applied to obtain an absolute value. In models contrast can measure differences in reproductive rates, survival or competitive ability. The actual definition of this parameter is closely linked with effect of the heterogeneous environment on the performance of the modeled populations.

Spatial aggregation: Spatial aggregation can be measured in a number of different ways. The easiest index is pair correlation, i.e. the conditional probability that a patch with the same quality is found next to a given patch. This probability is 0 in a totally overdispersed pattern. In a random environment the value of pair correlation is equal to the probability of encountering a patch with the given resource quality (p). Furthermore, in an aggregated pattern pair correlation has a value higher than p.

Components of temporal heterogeneity

Temporal heterogeneity can be characterized with the same parameters as in the case of spatial heterogeneity. Naturally, here they refer to changes and differences in time, instead of space [11].

Temporal grain: In the case of a dynamics landscape temporal grain can be defined as the time interval between samples, or the time steps used in the simulation of the population dynamics. With respect to an organism temporal grain is determined by its response [11].

Temporal extent: In a modeling context it is defined as the length of a simulation. With respect to an organism, its lifespan determines its temporal extent [11].

Severity/Degree of the change (temporal contrast): This component defines the degree of the change in quality. If there are only two patch types then temporal contrast and spatial contrast are the same.

Expected lifespan of a patch (temporal patch size): This parameter gives the time interval in which there would be no change in the quality of a patch. Having a low frequency of environmental change causes the patch to remain in the same resource quality class for a longer time, thus having a higher temporal patch size.

Temporal aggregation of change events: This parameter gives the frequency of environmental changes in the quality of a patch. The expected lifespan of a patch is the inverse of the frequency of quality changes. An environment is termed positively

http://www.ecology.uni-corvinus.hu ● ISSN 1589 1623

autocorrelated in time if the probability of changing the patch quality is less than 0.5, otherwise it is negatively autocorrelated in time.

Landscape generating methods

Checkerboard landscape

The simplest landscape is the checkerboard landscape, which is a periodic pattern of good and bad patches, where each good patch is surrounded by bad patches and *vice versa*. The good and bad patches are maximally over-dispersed, a pattern that are absolutely unlikely to be found in nature. Nevertheless such landscapes are used in experimental plant ecology [12, 13, 14], because they can be easily set up, and the pattern can be faithfully reproduced as there is no stochasticity involved in the generation of the landscape.

As the checkerboard landscape is the simplest landscape it is nice to point out that two of the spatial heterogeneity elements: patch size (*Fig. 1*) and contrast can be varied. The ratio of good and bad patches is always 1:1, and thus the frequency of them cannot be changed; nor can the patch types be raised above two, as then the fully over-dispersed pattern cannot be realized.

Temporal change can only be defined as the total inversion of the patter, meaning that every good patch turns into a bad patch, and at the same time every bad patch turns into a good patch. The frequency of environmental change (f) gives the probability of the change described above.

Such landscape was used for example in the study of Rácz and Karsai [15].

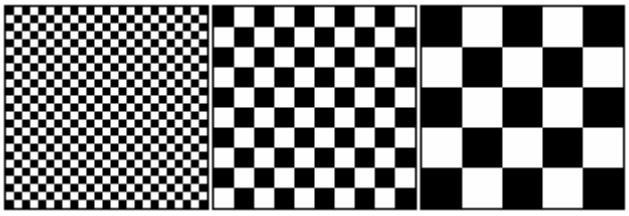

Figure 1. *Checkerboard landscape with different patch sizes. From left to right, s = 4, 10 and 20.*

Percolation map

In a percolation map [16] patches are randomly arranged. If we distinguish only good and bad patches, then a patch is chosen to be good with probability p, and bad otherwise (with probability $1-p$). The frequency of good sites (p), patch size (s) and contrast (m) can be varied (*Fig. 2*). The generated pattern is random at the scale of the patch size, thus spatial aggregation cannot be varied.

Percolation maps got its name from percolation theory in physics [17]. For such maps, with each site being either habitable (good) or non-habitable (bad), it is known that there exists a critical fraction of habitable sites ($p_c = 0.5923$ for the four-neighbor case), below which the landscape consists of isolated habitat clusters [17]. Thus a critical transition occurs from a continuous habitat to a fragmented habitat as the overall habitat density is reduced [18, 19, 20]. Furthermore models based on percolation maps have also proved useful in studies on the effects of habitat heterogeneity on the

http://www.ecology.uni-corvinus.hu ● ISSN 1589 1623

dynamics of spatially distributed populations [7, 18, 21-33]. It is interesting to note that percolation maps have been realized even in experimental studies [34-37].

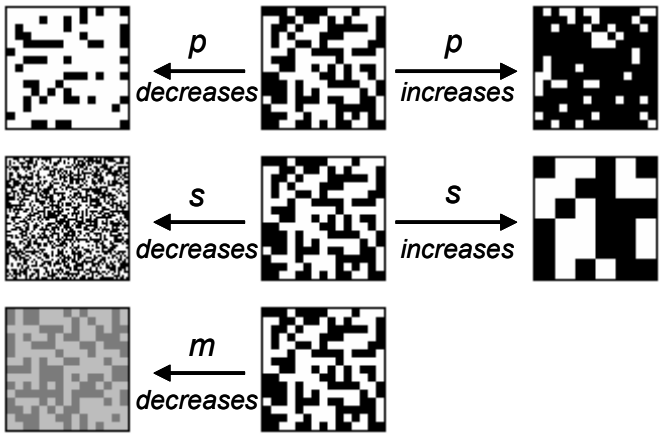

Figure 2. *Percolation maps. Dark colour denotes good quality sites, light colour denotes bad sites. Compared to the reference panels in the middle column (p = 0.5; s = 4; m = maximal) the frequency of the good sites can be higher (p = 0.8) or lower (p = 0.2); patch size can be bigger (s = 10) or smaller (s = 1); and contrast can be decreased (m = intermediate).*

The inclusion of temporal change is straightforward. If the site is good, then its quality is changed to bad with probability $½ \cdot f \cdot p^{-1}$; if the focal site is bad, then a change to good occurs with probability $½ \cdot f \cdot (1-p)^{-1}$. This transition rule ensures that the fraction of habitable sites in the whole area converges to p, while the distribution of habitable sites remains spatially uncorrelated. The rule also means that the frequency at which a site's quality changes, averaged across the whole landscape, is f. Because, in order to conserve p, for every good site turned to bad an equal number of bad sites has to be turned into good sites f, cannot take an arbitrary values. The inequalities $f \le 2p$ and $f \le 2(1-p)$ has to be obeyed.

Percolation maps can be generalized to include more than two patch quality types. The frequency of resource quality classes ($\underline{p}$) vector unambiguously partitions the 0-1 interval. Thus by generating an evenly distributed random number on the interval 0-1 for each site the quality of the sites can be determined. In the multiple patch types percolation maps the probability of a site with the ith quality changing is $f/d \cdot p_i$, where d is the number of distinct quality classes. If a site changes its quality it is turned into one of the other possible qualities with equal probabilities. Please note that – as above - not all values of f are possible for a given $\underline{p}$ quality frequency vector. Plotnick and Gardner [38] used a static multiple patch types percolation map to study the effect of landscape heterogeneity on community patterns.

Hierarchical random landscapes

Real landscape are heterogeneous on multiple scales [9], thus it was natural to develop landscape generating algorithm that can generate such a landscape.

http://www.ecology.uni-corvinus.hu ● ISSN 1589 1623

First the number of hierarchical levels (L) has to be specified. Then for each hierarchical level the frequency of good sites ($p_1, p_2, ..., p_L$) and the patch sizes ($s_1, s_2, ..., s_L$) are specified. Beginning from the highest hierarchical level (coarsest scale) a percolation map is generated with p_1 and s_1. At the second scale a percolation map is generated with p_2 and s_2, within the good patches of the highest scale. In this landscape, the availability of good sites at coarser scales constraint the availability of good sites at finer scales. The landscape generation is continued with the finer scales, and at each scale a percolation map is generated within the good patches of the scale one level up. In the final landscape (*Fig. 3*) the frequency of good sites is $p_{overall} = \prod_{i=1}^{L} p_i$.

All parameters that can be varied in a percolation map can be varied in a hierarchical random landscape (i.e. frequency of good sites, contrast and patch size). Furthermore the autocorrelation of the good sites will not be random at the finest scale. The introduction of temporal variation is similar to the one described previously for the percolation map. At the coarsest scale a good patch is turned into a bad patch with the probability $½ \cdot f_1 \cdot p_1^{-1}$; and if the focal patch is bad then a change to good occurs with the probability $½ \cdot f_1 \cdot (1 - p_1)^{-1}$. If a new good patch is formed then its finer scale structure has to be generated as above. If a good patch does not change its state then its finer structure can change. At each lower scale f_i percentage of the sites are changed, but only in places that are considered good patch at a scale one level higher. While this method is straightforward, the resulting pattern of changes can be quite abrupt as large patches can disappear and new ones formed.

Hierarchical random landscapes can be generalized to include more than two types of patches [39]. First we assign patch types at the coarsest scale according to a frequency vector ($\underline{p}_1$). Then each patch is subdivided according to the patch size (s_2) of the next scale, and each of those patches are assigned a type according a frequency matrix ($\underline{\underline{p}}_2$), where the row is chosen randomly and the column depends on the patch type assigned for the previous scale. This kind of assignment is then repeated for each specified lower scales.

Hierarchical random landscape was employed for example to investigate the effect of seed dispersal and seed dormancy on the competition of two annual plants [3].

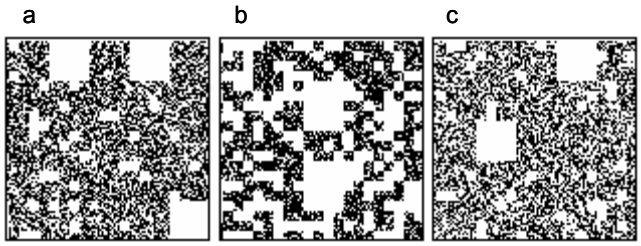

Figure 3. *Hierarchical random landscapes. In each of the presented 3 landscape the overall frequency of good sites (black) is p = 0.4; and s_1 = 20, s_2 = 5 and s_3 = 1.*
a. *p_1 = 0.80; p_2 = 0.90; p_3 = 0.56;* ***b.*** *p_1 = 0.90; p_2 = 0.75; p_3 = 0.60;*
c. *p_1 = 0.90; p_2 = 0.90; p_3 = 0.49.*

http://www.ecology.uni-corvinus.hu ● ISSN 1589 1623

Pair correlation landscape

The simples landscape where the aggregation of patches can be directly varied is presented here according to Hiebler [23, 40]. Spatial aggregation of patches with similar quality is measured as the conditional probability (p_{GG}) of finding a good patch next to a good patch. Please note that if $p_{GG} = p$ then we get a percolation map. Similarly, if $p_{GG} < p$ then the resulting landscape is overdispersed, and if $p_{GG} > p$ then the resource pattern is aggregated.

The landscape is generated by an iterative procedure. First a percolation map is generated whit a predefined frequency of good sites (p). Then the conditional probability of having a good site next to another good site is computed for every possible site-pair. Then a good and a bad site are chosen randomly. If exchanging these two sites brings the landscape closer to the defined pattern, i.e. the $p_{GG,actual}$ value of the resulting landscape is closer to the desired $p_{GG,desired}$ value, and then we accept the exchange. Otherwise the exchange is accepted with the probability $Exp\left(-\lambda\left|p_{GG,actual} - p_{GG,desired}\right|\right)$, where λ is chosen so that such exchanges are accepted sometimes, but not too often. This ensured that an exchange is accepted with a small probability even if do not improve $p_{GG,actual}$, but is might help to reach the $p_{GG,desired}$, and avoid being having a landscape where $p_{GG,actual}$ cannot be improved. Continue selecting sites and exchanging them until the difference between the desired and the actual probabilities are less than some predefined tolerance ($D = \left|p_{GG,actual} - p_{GG,desired}\right| \le \varepsilon$) or some specified number of iterations has been performed. *Figure 4* shows examples of the generated landscape with different agregateddness.

The generating algorithm offers a way to introduce temporal change. Simply try to exchange patches according to the above rules till the predetermined fraction of sites (f) have been changed (the quality of a site should not be changed more than once in one time step). Assigning a relatively lower value to λ results in a higher number of exchanges being accepted, but $p_{GG,actual}$ will still remain close to $p_{GG,desired}$.

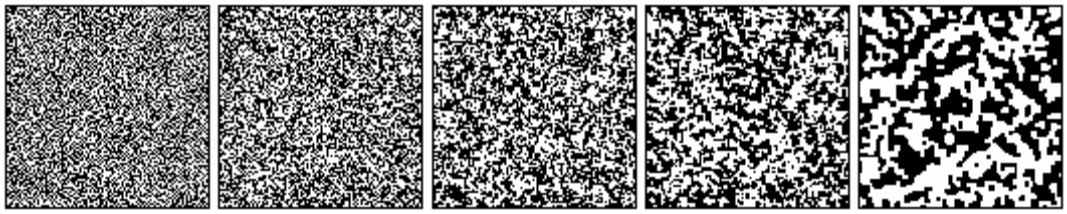

Figure 4. *Pair correlation landscapes. The frequency of good sites (black) is p = 0.5.The ratio* p_{GG} / p *is 0.9; 1.0; 1.1; 1.2 and 1.35 from left to right. In the first landscape the patches are overdispersed, in the second they are randomly distributed, the remaining landscapes show aggregated pattern.*

http://www.ecology.uni-corvinus.hu ● ISSN 1589 1623

Ising landscape

The so called Ising model is used in statistical mechanics to describe ferromagnetism [8]. Here I will use it to generate a heterogeneous landscape consisting of good and bad sites. The landscape derived from the Ising model has varying degree of autocorrelation between sites of the same quality. Here I present the algorithm without describing the Ising model, albeit I will use the symbols traditionally used in statistical physics.

Let us have a lattice, where each cell of the lattice can be either good (+1) or bad (-1). A site's quality depends on the qualities of the neighbouring sites via the parameter J. If $J > 0$ then neighbouring sites are more likely to have the same quality. On the other hand a landscape generated with $J < 0$ is overdispersed with regard to the patch types. The landscape is generated by the so-called Metropolis algorithm, where a state is changed (1) if it lowers the energy of the system (thus it gets closer to some desired state), or (2) with a probability less than 1 if the energy would rise. This probability function has the form $e^{-\Delta E}$, where ΔE is the change in energy (in a landscape context is measures the difference between the actual state and the desired state, c.f. the previous landscape generating algorithm). The energy of a state is given by

$$E = -J \sum_{<i,j>} s_i s_j - H \sum_{i=1}^{N} s_i ,$$

where J is the interaction parameter; H is the outside magnetic field; s_i is the state of the i[th] site and $\langle i, j \rangle$ are neighbouring sites. The probability that the quality (s_i) of the i[th] site is changed is

$$P_i = \frac{1}{1 + Exp\left(2 s_i \beta \left(J \sum_j s_j + H \right) \right)},$$

where s_j is the quality of a site neighbouring site i and β is proportional to temperature. Actually $\beta = \frac{1}{k_B T}$, where T is the absolute temperature and k_B is the Boltzman constant.

Let assume that $J = +1$, and then the properties of the landscape is determined by β and H. It is know that in some parameter range the Ising model results in a homogeneous landscape, thus the inequality $\beta J < -0,5 \ln\left(\sqrt{2} - 1\right) \approx 0,44069$ has to be observed. The Metropolis algorithm can be started from a percolation map.

If $H = 0$ then half of the sites will be good and the other half of the sites will be bad, accordingly $p = 0.5$. The frequency of the good sites (p) can be varied by varying H. Unfortunately changes in H will also affect the aggregatedness of the landscape, thus the two parameter cannot be changed independently. Here the aggregatedness of the landscape is measured with the correlation length (ξ), which gives the average radius of the clusters of good patches. In order to compute correlation length we have to compute for each site the fraction of sites at distance r that have the same quality. Note that in a percolation map p portion of the sites are good independent of the distance from a good site. In the Ising landscape the percentage of good sites at distance r from a good site is an exponentially decreasing function of r, and tends toward the average frequency of good sites (p) in the landscape. Correlation length is then the exponent of

http://www.ecology.uni-corvinus.hu ● ISSN 1589 1623

this decreasing function $\left(p + a\mathrm{Exp}\left(-r/\xi\right)\right)$. *Figure 5* shows Ising landscapes with different correlation lengths.

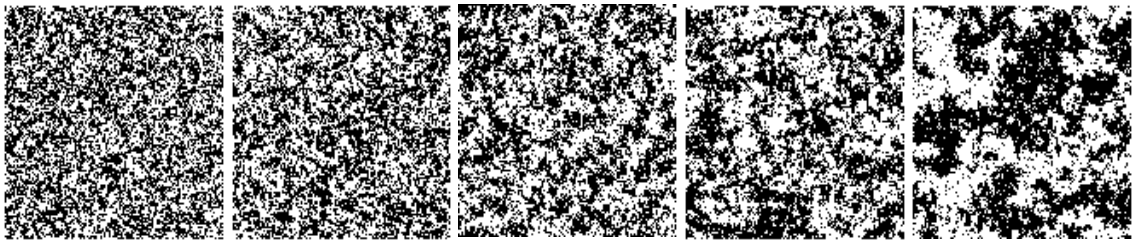

Figure 5. *Ising landscape. Correlation lengths (ξ) are from left to right 0.75; 1.01; 1.80; 2.02 and 3.74. For each landscape s = 1 and p = 0.5.*

To my knowledge, there isn't any mathematical formula that describes the relationship between H, β and ξ, p. I have simulated the Ising dynamics on a 512 × 512 lattice. For a number of parameter combination I have made 21 repetitions. An empirical graph showing the relationship between the parameter of the Ising model and the heterogeneity parameters is shown in *Figure 6*. It can be seen that the relationship is quite complex, but it is symmetrical around $H = 0$ (in the case of p, the absolute value of the difference from $p = 0.5$ is symmetrical).

Temporal change can be included in a similar way as in the pair correlation landscape. The Metropolis algorithm is continued until the desired amount of state change occurs.

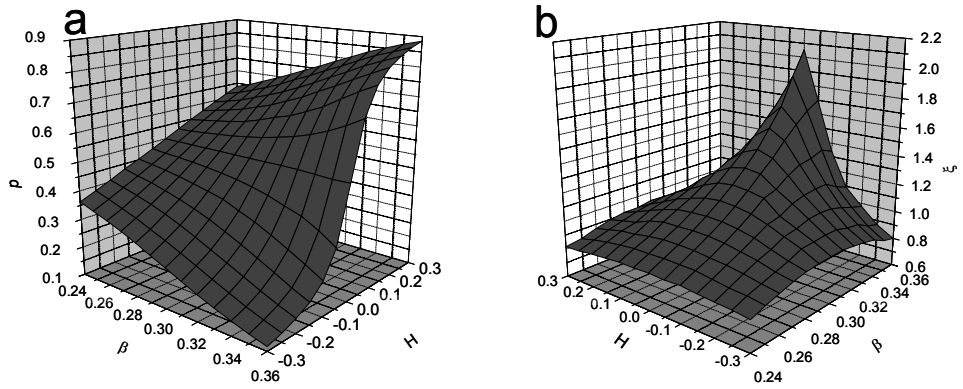

Figure 6. *Heterogeneity parameters as functions of Ising parameters.*
a*. Frequency of good patches.* ***b****. Correlation length.*

Summary

Here I presented five algorithms to generate heterogeneous landscapes for spatially explicit simulations of population dynamics. *Table 1* summarizes the heterogeneity components that can be varied in these landscapes. Furthermore the possibility to have more than two kinds of patch qualities is also included. In the table I have included fractal landscapes, that are employed in studies of population dynamics [30, 31, 33, 38,

http://www.ecology.uni-corvinus.hu ● ISSN 1589 1623

41, 42]. However I was unable to devise a method for the generated pattern to be changed and, at the same time, retain its fractal nature. Thus fractal landscapes were excluded from this study. One of the strength of the fractal landscape is the possibility to vary the autocorrelation of patch qualities. The most frequently employed percolation map while exhibits an interesting phenomenon (percolation [17]), that makes it ideal for studies of habitat fragmentation, produces a rather unrealistic random distribution of resource patches. However, both the pair correlation landscapes and the Ising landscapes can accommodate aggregated or overdispersed pattern of resource distribution, and unlike the fractal landscape this pattern can be rearranged without changing other aspects of the pattern. Thus both of these algorithms have a great potential for studied of population dynamics.

A common feature of the discussed landscapes is the possibility to model temporal heterogeneity. This is a major methodological step forward in spatially explicit modeling as – for example - there is a novel interest of studying the effects of habitat fragmentation and disturbance or climate change.

Table 1. *Summary of landscape generating algorithms*

Landscape	**Can be varied?**					**multiple patch type**
	p	***m***	***s***	***f***	***aggregation***	
Checkerboard	no	yes	yes	yes	no	no
Percolation map	yes	yes	yes	yes	no	yes
Hierarchical random landscapes	yes	yes	yes	yes	no	yes
Pair correlation landscape	yes	yes	yes	yes	yes	no
Ising landscape	yes	yes	yes	yes	yes	no
Fractal landscape	yes	yes	yes	no	yes	yes

Acknowledgements. I am grateful to Beáta Oborny, Géza Meszéna, Ulf Dieckmann, Josef Stuefer, István Scheuring, Gabriella Magyar and Miklós Kertész for valuable and enjoyable discussions about this project and their helpful comments. Á.K. is a postdoctoral fellow of OTKA (D048406).

REFERENCES

[1] Czárán, T. (1998): Spatiotemporal models of population and community dynamics. - Chapman and Hall, New York

[2] Inghe, O. (1989): Genet and ramet survivorship under different mortality regimes. - A cellular automata model - Journal of Theoretical Biology 138: 257-270.

[3] Lavorel, S., O'Neill, R.V., Gardner, R.H. (1994): Spatio-temporal dispersal strategies and annual plant species coexistence in a structured landscape. - Oikos 71: 75-88.

[4] Savage, M., Sawhill, B., Askenazi, M. (2000): Community dynamics: What happens when we rerun the tape. - Journal of Theoretical Biology 205: 515-526.

[5] Winkler, E., Fischer, M. (2002): The role of vegetative spread and seed dispersal for optimal life histories of clonal plants: a simulation study. - Evolutionary Ecology 15: 281-301.

[6] Pickett, S.T.A., Thompson, J.N. (1978): Patch dynamics and the design of nature reserves. - Biological Conservation 13: 75-37.

http://www.ecology.uni-corvinus.hu ● ISSN 1589 1623

[7] With, K.A., Crist, T.O. (1995): Critical threshold in species responses to landscape structure. - Ecology 76: 2446-2459.
[8] Huang, K. (1994): Statistical mechanics. - John Wiley & Sons, New York
[9] Kotliar, N.B., Wiens, J.A. (1990): Multiple scales of patchiness and patch structure: a hierarchical framework for the study of heterogeneity. - Oikos 59: 253-260.
[10] Turner, M.G., Gardner, R.H., O'Neill, R.V. (2001): Landscape Ecology. - Springer-Verlag, New York
[11] Stuefer, J.F. (1996): Potential and limitations of current concepts regarding the responses of clonal plants to environmental heterogeneity. - Vegetatio 127: 55-70.
[12] Fransen, B., de Kroon, H., Berendse, F. (2001): Soil nutrient heterogeneity alters competition between perennial grass species. - Ecology 82: 2534-2546.
[13] Wijesinghe, D.K., Hutchings, M.J. (1997): The effects of spatial scale of environmental heterogeneity on the growth of a clonal plant: an experimental study with Glechoma hederacea. - Journal of Ecology 85: 17-28.
[14] Wijesinghe, D.K., Hutchings, M.J. (1999): The effect of environmental heterogeneity on the performance of Glechoma hederacea: the interactions between patch contrast and patch scale. - Journal of Ecology 87: 860-872.
[15] Rácz, É.V.P., Karsai, J. (2005): Effect of initial patterns on competitive exclusion - Community Ecology (in press)
[16] Gardner, R.H., Milne, B.T., Turner, M.G., O'Neill, R.V. (1987): Neutral models for the analysis of broad-scale landscape pattern. - Landscape Ecology 1: 19-28.
[17] Stauffer, D., Aharony, A. (1994): Introduction to percolation theory. Revised second edition. - Taylor and Francis
[18] Bascompte, J., Solé, R.V. (1996): Habitat fragmentation and extinction threshold in spatially explicit models. - Journal of Animal Ecology 65: 465-473.
[19] Gustafson, E.J., Parker, G.R. (1992): Relationships between landcover proportions and indices of landscape spatial pattern. - Landscape Ecology 7: 101-110.
[20] Boswell, G.P., Britton, N.F., Franks, N.R. (1998): Habitat fragmentation, percolation theory and the conservation of a keystone species. - Proceedings of the Royal Society of London B 265: 1921-1025.
[21] Dytham, C. (1995): The effect of habitat destruction pattern on species persistence: a cellular model. - Oikos 74: 340-344.
[22] Neuhauser, C. (1998): Habitat destruction and competitive coexistence in spatially explicit models with local interaction. - Journal of Theoretical Biology 193: 445-463.
[23] Hiebler, D. (2000): Populations on fragmented landscapes with spatially structured heterogeneities: landscape generation and local dispersal. - Ecology 81: 1629-1641.
[24] Oborny, B., Kun, Á. (2002): Fragmentation of clones: How does it influence dispersal and competitive ability? - Evolutionary Ecology 15: 319-346.
[25] Kun, Á., Oborny, B. (2003): Survival and competition of clonal plant populations in spatially and temporally heterogeneous habitats. - Community Ecology 4: 1-20.
[26] Hoverstadt, T., Messer, S., Poethke, H.J. (2001): Evolution of reduced dispersal mortality and 'fat-tailed' dispersal kernels in autocorrelated landscapes. - Proc. Roy. Soc. Lond. B. 268: 385-391.
[27] Piqueras, J., Klimeš, L., Redbo-Torstensson, P. (1999): Modelling the morphological response to nutrient availability in the clonal plant Trientalis europaea L. - Plant Ecology 141: 117-127.
[28] Sutherland, W.J., Stillman, R.A. (1988): The foraging tactics of plants. - Oikos 52: 239-244.
[29] Turner, M.G., Gardner, R.H., Dale, V.H., O'Neill, R.V. (1989): Predicting the spread of distrubance across heterogeneous landscapes - Oikos 55: 121-129.
[30] With, K.A., Gardner, R.H., Turner, M.G. (1997): Landscape connectivity and population distribution in heterogeneous environments. - Oikos 78: 151-169.

http://www.ecology.uni-corvinus.hu ● ISSN 1589 1623

[31] With, K.A., King, A.W. (1999): Dispersal success on fractal landscapes: a consequence of lacunarity threshold. - Landscape Ecology 14: 73-82.
[32] Oborny, B., Meszéna, G., Szabó, G. (2005): Dynamics of populations on the verge of extinction. - Oikos 109: 291-296.
[33] Pearson, R.G., Dawson, T.P. (2005): Long-distance plant dispersal and habitat fragmentation: identifying conservation targets for spatial landscape planning under climate change. - Biological Conservation 123: 389-401.
[34] Wijesinghe, D.K., Handel, S.N. (1994): Advantages of clonal growth in heterogeneous habitats: an experiment with Potentilla simplex. - Journal of Ecology 82: 495-502.
[35] Bowers, M.A., Doley, J.M.J. (1999): A contrtolled, hierarchical study of habitat fragmentation: responses at the individual, patch, and landscape level. - Landscape Ecology 14: 381-389.
[36] McIntyre, N.E., Wiens, J.A. (1999): Interaction between habitat abundance and configuration: experimental validation of some predictions from percolation theory. - Oikos 88: 129-137.
[37] Wiens, J.A., Schooley, R.L., Weeks, D., Jr. (1997): Patchy landscapes and animal movements: do beetles percolate. - Oikos 78: 257-264.
[38] Plotnick, R.E., Gardner, R.H. (2002): A general model for simulating the effects of landscape heterogeneity and disturbance on community patterns. - Ecological Modelling 147: 171–197.
[39] Johnson, G.D., Myers, W.L., Patil, G.P. (1999): Stochastic generating models for simulating hierarchically structured multi-cover landscapes. - Landscape Ecology 14: 413-421.
[40] Hiebler, D. (2004): Competition between near and far dispersers in spatially structured habitats. - Theoretical Population Biology 66: 205–218.
[41] Keitt, T.H., Johnson, A.R. (1995): Spatial heterogeneity and anomalous kinetics: emergent patterns in diffusion-limited predator-prey interaction. - Journal of Theoretical Biology 171: 127-139.
[42] Gardner, R.H., Gustafson, E.J. (2004): Simulating dispersal of reintroduced species within heterogeneous landscapes. - Ecological Modelling 171: 339–358.

http://www.ecology.uni-corvinus.hu ● ISSN 1589 1623

THE EFFECT OF CLIMATE CHANGE ON THE POPULATION OF SYCAMORE LACE BUG (CORYTHUCA CILIATA, SAY, TINGIDAE HETEROPTERA) BASED ON A SIMULATION MODEL WITH PHENOLOGICAL RESPONSE

M. LADÁNYI* – L. HUFNAGEL

Corvinus University of Budapest, Department of Mathematics and Informatics
H-1118 Budapest, Villányi út 29-43., Hungary
*(*phone: +36-1-482-6261; fax: +36-1-466-9273*)*

**e-mail: marta.ladanyi@uni-corvinus.hu*

(Received 10th Sep 2005, accepted 10th Oct 2006)

Abstract. Climate change affects on insect populations in many ways: it can cause a shift in geographical spread, abundance, or diversity, it can change the location, the timing and the magnitude of outbreaks of pests and it can define the phenological or even the genetic properties of the species. Long-time investigations of special insect populations, simulation models and scenario studies give us very important information about the response of the insects far away and near to our century. Getting to know the potential responses of insect populations to climate change makes us possible to evaluate the adaptation of pest management alternatives as well as to formulate our future management policy. In this paper we apply two simple models, in order to introduce a complex case study for a Sycamore lace bug population. We test how the model works in case the whether conditions are very different from those in our days. Thus, besides we can understand the processes that happen in present, we can analyze the effects of a possible climate change, as well.
Keywords: *climate change, insects, pest management, simulation, agriculture*

Introduction and Aims

Simulation is the ultimate tool for forecasting the effect of climate and other environmental factors on the ecosystem, since the real circumstances of future cannot be examined empirically. However, it may take several years to reach the stage when these forecasts will be usable in the agriculture since the longer climate forecasts are not yet good enough [18], [15], [39]. There have been made several projects in Hungary with simulation model applications and with valuable results about the effects of climate change on the yield of arable crops [16], [17], [29], [27], [30], [31], [32], but there are very rare references on plant – pest populations.

In our paper we refer to one of our earlier population dynamical food web biomass model together with a phenology model based on the food web model [33], [34]. In the food web model the seasonal weather aspects, the nutrient content of soil and the biotic interactions are considered. To simulate the interactions, a discrete difference equation system was used. The general equation of the model is based on three terms: the first one is to express the activity of the individual depending on the temperature, the second one is to describe the effect of the quality and the quantity of the nutrient of the populations and the third one is to display the effect of the predators.

Besides quantitative (biomass) changes, however, there are also seasonal qualitative changes during the evolution of the entities. These changes are described by phenology.

http://www.ecology.uni-corvinus.hu ● ISSN 1589 1623

It is obvious to ask, how the number of entities can be derived from a given amount of biomass. More exactly, if the phenological phases of the population, together with their biological properties, are known, how can one define the number of the entities of each phenophase at a given point of time? Our phenology model is to solve this problem.

In what follows, we apply the above two models in a drastically simplified form, in order to introduce a complex case study for a *Sycamore lace bug* (*Corythuca ciliata*) population.

In addition to the foregoing, we found it very useful to ask, how the model works in case the whether conditions are very different from those in our days. Thus, besides we can understand the processes that happen in present, we can analyze the effects of a possible climate change, as well.

Sycamore lace bug can be an excellent indicator for the climate researchers as it has much less biotic interactions comparing with other native species or with species having native host. *Sycamore lace bug* has other advantages, too, namely, that it is monophagous in Europe and it can quite easily be monitored, due to its way of life [55], [44].

Obviously, our contemporary knowledge does not make us possible to *predict* the future, even for the quite well known *Corythuca ciliata - Sycamore tree (Platanus hybrida)* populations. A reasonable aim can be, however, to find out, what is predicted by our model for simulated weather data with different parameters for different assumptions. This aim corresponds to the aims of VAHAVA project of the Hungarian Academy of Sciences, as well as to those of international climate change projects [4, 5, 20, 21, 35, 54].

To explore the possible effects of an unknown climate change in future, we need not real but realistic alternative climate scenarios. First, we define the concept of climate scenario.

Climate scenarios are possible future climates in a set. Each of them is made consistently by applying scientific principles; however any of them has a fixed (calculable) possibility. A climate scenario is one of the possible climates and it is by no means a prediction [3, 21].

After having recognized the ecological consequences of climate change, together with UNEP, WMO (World Meteorological Organization) has established IPCC (Intergovernmental Panel on Climate Change) with the task of giving unbiased and detailed information about climate change and its expected effects.

During our research, we applied the principles defined by IPCC and we used some of the most commonly accepted scenarios presented in international reports. The most serious scenarios, themselves, are results of simulation models. For generating scenarios the so-called GCMs are generally used (General Circulation Model or Global Climate Model). GCMs have been successfully used to estimate the climate change on arable crops yield in Hungary in a 15- and a 30-year scenario [26].

In our research we applied six different scenarios, such as:

- - Scenario BASE is a simulated weather data series with the same conditions as we have at present.
- Scenarios GFDL2535 and GFDL5564 have been created by *Geophysical Fluid Dynamics Laboratory* (U.S.A.) with the assumption that CO_2 concentration doubles in atmosphere. The difference between the scenarios is their resolution level. (The later has higher resolution.)

http://www.ecology.uni-corvinus.hu ● ISSN 1589 1623

- Three very different scenarios have been worked out by United Kingdom Meteorological Office (UKMO), namely UKHI (high-resolution equilibrium climate change experiment), UKLO (low-resolution equilibrium climate change experiment) and UKTR (high-resolution transient climate change experiment). The first two scenarios of UKMO (UKHI, UKLO) are so-called equilibrium models, that is to say, assumed that CO_2-concentration doubles in atmosphere, GCM runs until an equilibrium state with stable surface temperature. The third scenario of UKMO (UKTR) is a transient model that describes the gradually changing climate assuming a gradually increasing CO_2 content of atmosphere [4, 24].

Note that the results of GCMs should be scaled on the examined region with the help of empirical statistical methods [5]. In our paper, we present the results of the 15th year of each 30-year period scenario concerning the years around 2050. The scaling of the scenarios for the region of Hungary was made in the frame of CLIVARA project (Climate Change, Climatic Variability and Agriculture in Europe). The database and the references were made available for us by professor Zs. Harnos, the Hungarian leader of the project.

To sum it up, in this paper we followed two main aims:

- To create a complex population dynamical model with phenology responses for Sycamore lace bug based on an earlier field-work [44].
- To introduce a case study for the above model applied for some widely accepted climate-change scenarios.

Review of literature

In our century increasing societal, environmental, and economic pressures force us to develop new agricultural pest management strategies. Interdisciplinary approaches have the aim to find the way, how the environmental degradation caused by the use of chemicals can be decreased, how the productivity can be increased by reducing insect and disease damage to cultivated plants, and how the competition with weeds can be reduced. Crop and forestry population system models are useful tools to examine the interrelationships among plants, pests and the environment. With simulation models we can find optimal strategies that meet individual and societal goals.

Improved techniques for managing pests require weather and insect data from thoroughly maintained monitoring as well as climate information and forecast to determine their suitability. Climatic change, including global warming and increased variability require improved analyses that can be used to assess the risk of the existing and the newly developed pest management strategies and techniques, and to define the impact of these techniques on environment, productivity and profitability. Each technique has to be evaluated whether and how it is suitable in the farming system where they are to be applied.

Nowadays, several studies are investigating the impact of climatic change on insect populations. Some of the effects can be discovered in laboratories, only (e.g. the effect of humidity [6]), some of them need field observations maintenance. The impact of climate change, moreover, alters from region to region, from species to species. Quite a lot of new methods from different disciplines are used to detect the most important

http://www.ecology.uni-corvinus.hu ● ISSN 1589 1623

effects. Therefore, the studies of climate change effects are considering different aspects, such as palaeontological, agricultural, medical, geological, biological as well as the aspects of forestry management. This widespread research work requires interdisciplinary cooperation of researchers from several fields [53]. We give a short review of the main approaches.

The aspect of palaeontology

One of the most important ways to find out what climate change can bring us is to look back into the very past. A few thousand years ago some regions were characterized by such kind of vegetations that existed within warming thermal conditions analogous to those today. For example, the transition from parkland vegetation and insects to the one of coniferous forest of south-western Ontario region indicates that the climate continued gradually warm through the mid-Holocene [48].

The Lateglacial-Holocen transition is characterized by major changes in the insect fauna, too, reflecting an extremely rapid climate change in South-Sweden, as well as in Swiss-Alps. In these regions the cold-adapted species assemblage was immediately replaced by temperate species [36], [37]. During the same time period most of temperate species of Chihuahuan Desert (Texas) were replaced either by desert species or more cosmopolitan taxa [12]. The above studies pointed out the dependency of the changes in climate and fauna. The question of how these kinds of responses proceed was studied by Amman [1].

The approaches with models, simulations and scenarios

Developing ecological and simulation models is a very useful tool to find out the response of a system to an event or a series of events. Ecological or meteorological models describe biological or climate properties mathematically, while simulations make a computer based models system supplied with a great amount of empirical data.

To reach his above mentioned palaeontological results in Swiss-Alps, Lemdahl [37] applied a so-called climatic reconstruction (MCR) method that simulates realistic climate data in the past. Simulated weather data, however, are most commonly used to examine the potential future effects. These approaches are called scenario studies.

The main problems that have to precede scenario studies are, nevertheless, the evaluation, the validation and verification of the applied models. Though several models have been developed e.g. for the carbon budget of boreal forests, enormous problems remain in incorporating pest effects in these models. These problems have their origins, partly in scaling. The common problems of verification and validation of model results are particularly troublesome in projecting future productivity [56].

A main point of scenario studies is, therefore, how the applied model should be scaled. Hanson [19] noticed that although early model predictions of climate change impacts suggested extensive forest dieback and species migration, more recent analyses suggest that catastrophic dieback will be a local phenomenon, and changes in forest composition will be a relatively gradual process. Better climate predictions at regional scales, with a higher temporal resolution (months to days), coupled with carefully designed, field-based experiments that incorporate multiple driving variables (e.g. temperature and CO_2); will advance our ability to predict the response to climate change.

Time-dependent models developed at fine spatial resolution of experimental studies are widely used to forecast how plant - insect populations will react over large spatial

http://www.ecology.uni-corvinus.hu ● ISSN 1589 1623

extents. Usually the best data available for constructing such models comes from intensive, detailed field studies. Models are then scaled-up to coarser resolution for management decision-making. Scaling-up, however, can affect model predictions and dynamical behaviour which can result misinterpretation of model output. The potential negative consequences of scaling-up deserve consideration whenever data measured at different spatial resolutions are integrated during model development, as often happens in climate change research [13].

Chen [7] investigates the integrated effects of insect infections, management practices, carbon cycle and climatic factors both at regional and global scales.

To see that there can be great difference between the responses of even similar species, we refer to Conrad et al [8]. They examined the garden tiger moth (Arctia caja) that was widespread and common in the UK in the last century, but its abundance fell rapidly and suddenly after 1984. The most UK butterflies are expected to increase under UK climate change scenarios of global warming. Contrary to them, garden tiger is predicted to decrease further because of warm wet winters and springs, to which it is very sensitive [38].

Ecological models serving climate change studies

We give a short list of the most widely applied ecological models focused to insect populations.

The Forest Vegetation Simulator (FVS) is a distance-independent, geographic region dependent individual-tree forest growth model that has been widely used in the United States for about 30 years to support management decision making. It has been continuously extended, improved and adapted to further management tasks like prediction of climate change effects. Component models predict the growth and mortality of individual trees, and extensions to the base model represent disturbance agents including insects, pathogens, and fire. The geographic regions are represented by regionally specific model variants. The differences are due to data availability and the applicability of existing models. The model supports specification of management rules in the input [10], [11].

The Phenology and PopulatIoN SIM (INSIM) is an age - structured model that needs biological information on the insect species and gives calculations on the number of individuals and the development of the population. It involves a complex pest – natural enemies model, as well [41], [42].

Agro – ECOsystem ManagemenT and OPtimization Model (ECOTOPE) is a typical simulation model, which describes processes of an agricultural ecosystem for crop growth, nitrogen dynamics in soil and pest population. It is used to derive optimum management strategies [49], [50], [51].

Boundary LAYER Model (BLAYER) simulates atmospheric flows and it has been adapted to forecast the timing and location of insect pest migrations into the United States corn belt. It is very useful to study the possible changes in pest populations like migration or dispersal patterns resulted by climate change [45].

Boll Weevil DISPersal Model (BWDISP) is a stochastic simulation model that predicts the spread of boll weevil populations on cotton. Because the development and dispersal of this insect is sensitive to temperature, it is important to understand how this insect will potentially respond to climate change. In addition, without proper management of this pest, other secondary pests may attack the crop [40].

http://www.ecology.uni-corvinus.hu ● ISSN 1589 1623

Northern Corn ROOTWORM Model (ROOTWORM) is a process – oriented simulation model that examines the population dynamics of corn – rootworm in the northern United States. The rootworm attacks both the roots and tassels of corn, decreasing yields. The model examines how planting date affects the population dynamics of the insects. It gives information on phenology and the number of individuals in each growth state of corn. The model can analyze global change impact on the population levels and distribution of the insects, as well as the potential economic impacts [43].

The potential responses of insects to climate change

Climate and weather can substantially influence the development and distribution of insects. Current estimates of changes in climate indicate an increase in global mean annual temperatures of 1°C by 2025 and 3°C by the end of the next century. Such increases in temperature have a number of implications for temperature-dependent insects, especially in the region of Middle - Europe. Changes in climate may result changes in geographical distribution, increased overwintering, changes in population growth rates, increases in the number of generations, extension of the development season, changes in crop-pest synchrony of phenology, changes in interspecific interactions and increased risk of invasion by migrant pests.

Under the climatic changes projected by the Goddard Institute for Space Studies general circulation model, northward shifts in the potential distribution of the European corn borer of up to 1220 km are estimated to occur, with an additional generation found in nearly all regions where it is currently known to occur [46].

Several results on the effect of climate change on insects were published in the field of forestry sciences, since insects cause considerable loss of wood that has an adverse effect on the balance of carbon sequestered by forests. Volney and Fleming [56] state that pests are major, but consistently overlooked forest ecosystem components that have manifold consequences to the structure and functions of future forests. Global change will have demonstrable changes in the frequency and intensity of pest outbreaks, particularly at the margins of host ranges.

Ayres and Lombardero [2] have shown that climate change has

- direct effects on the development and survival of herbivores and pathogens;
- physiological changes in tree defenses; and
- indirect effects from changes in the abundance of natural enemies (e.g. parasitoids of insect herbivores), mutualists (e.g. insect vectors of tree pathogens), and competitors.

Because of the short life cycles of insects, mobility, reproductive potential, and physiological sensitivity to temperature, even modest climate change will have rapid impacts on the distribution and abundance of many kinds of insects. To consider scenario studies, some of them predict negative, but many forecast positive effects on insects. E.g. global warming accelerates insect development rate and facilitate range expansions of pests, moreover, climate change tends to increase the vulnerability of plants to herbivores. One alarming scenario is that climate warming may increase insect outbreaks in boreal forests, which would tend to increase forest fires and exacerbate further climate warming by releasing carbon stores from boreal ecosystems [2].

Hanson and Weltzin [19] studied especially the drought disturbances caused by climate change. They showed that severe or prolonged drought may render trees more susceptible to insects.

http://www.ecology.uni-corvinus.hu ● ISSN 1589 1623

Climate variability at decadal scales influences the timing and severity of insect outbreaks that may alter species distributions. Coops and al. [9] have presented a spatial modelling technique to infer how a sustained change in climate might alter the geographic distribution of the species. Using simulations they produced a series of maps that display predicted shifts of zones where the species they examined might expand its range if modelled climatic conditions at annual and decadal intervals were sustained.

The connection between temperature tolerance and phenology of insects was investigated by Klok and Chown [25]. They defined how current climate change like increased temperature and decreased rainfall affect on physiological regulation and susceptibility.

Powell and Logan [47] have reviewed the mathematical relationship between environmental temperatures and developmental timing and analyzed circle maps from yearly oviposition dates and temperatures to oviposition dates for subsequent generations. Applying scenarios for global warming they proved that adaptive seasonality may break down with little warning with constantly increasing (and also decreasing) temperature.

Forecasted increases in atmospheric CO_2 and global mean temperature are likely to influence insect – plant interactions. Plant traits important to insect herbivores, such as nitrogen content, may be directly affected by elevated CO_2 and temperature, while insect herbivores are likely to be directly affected only by temperature. Flynn et al. [14] stated that insect populations did not change significantly under elevated CO_2, but tended to increase slightly. Average weight decreased at high temperatures. Plant height and biomass were not significantly affected by the CO_2 treatment, but growth rates before infestation were enhanced by elevated CO_2. These results indicate that the combined effects of both elevated CO_2 and temperature may exacerbate pest damage to certain plants, particularly to plants which respond weakly to increases in atmospheric CO_2.

Up to this time, as we have seen, mainly two climatic factors – temperature and humidity have been investigated. Though, it is possible that some parts of solar radiation have at least the same importance in controlling insect populations [6].

Last, but not least, changes in climate increases the likelihood of insect transport from regions to regions, as well [22, 23, 55, 57].

The special agricultural aspects of climate change effect on insects

Global climate change impact on plant - pest populations depends on the combined effects of climate (temperature, precipitation, humidity) and other components like soil moisture, atmospheric CO_2 and tropospheric ozone (O_3). Changes in agricultural productivity can be the result of direct effects of these factors at the plant level, or indirect effects at the system level, for instance, through shifts in insect pest occurrence. With respect to crops, the data suggest that elevated CO_2 may have many positive effects, including yield stimulation, improved resource - use efficiency, more successful competition with weeds, reduced O_3-toxicity, and in some cases better pest and disease resistance. However, many of these beneficial effects may be lost - at least to some extent - in a warmer climate. Warming accelerates plant development and reduces grain-fill, reduces nutrient-use efficiency, increases crop water consumption, and favours weeds over crops. Also, the rate of development of insects may be increased. A major effect of climate warming in the temperate zone could be a change in winter survival of insect pests, whereas at more northern latitudes shifts in phenology in terms

http://www.ecology.uni-corvinus.hu ● ISSN 1589 1623

of growth and reproduction, may be of special importance. However, climate warming disturbs the synchrony between temperature and photoperiod; because insect and host plant species show individualistic responses to temperature, CO_2 and photoperiod, it is expected that climate change will affect the temporal and spatial association between species interacting at different trophic levels. Although predictions are difficult, it seems reasonable to assume that agro - ecosystem responses will be dominated by those caused directly or indirectly by shifts in climate, associated with altered weather patterns, and not by elevated CO_2 per se. Overall, intensive agriculture may have the potential to adapt to changing conditions, in contrast to extensive agricultural systems or low - input systems which may be affected more seriously [18].

Crop protection in Europe became strongly chemically oriented in the middle of the last century. An excellent climate for fast reproduction of pests and diseases demanded high spray frequencies and, thus, resulted in quick development of resistance against pesticides. This initiated a search for alternatives of chemical pesticides, like natural enemies for control of pests. A change from chemical control to very advanced integrated pest management programs (IPM) in European greenhouses took place at the end of the last century [38]. For the main greenhouse vegetable crops in northern Europe, most insect problems can now be solved without the use of insecticides. IPM without conventional chemical pesticides is a goal that will be realized for most of the important vegetables in Europe, not limited to greenhouse vegetables. At the same time, however, climate change affects the distribution, the phenology, the susceptibility and the interrelationship of insects drastically, which emphasize the risk of sustainable crop protection by loosing the control on pests - natural enemies' populations.

Materials and Methods

The methods of modelling

In a former work [33] we have introduced a food web population dynamical model that describes the biomass change of the members of a food web with a cultivated plant and two kinds of weed, monophagous and polyphagous pests and a predator. In what follows, we apply this model for our *Corythuca ciliata – Sycamore tree* population with three purposes:

- we show, how the model works in practise
- we find out the model-parameters for a *Corythuca ciliata – Sycamore tree* population and
- with the help of the food web population dynamical model, we try to get information out of weather parameters for plant protection purposes.

The examined *Corythuca ciliata – Sycamore tree* population shows a very simple case of the general food web seasonal population dynamical model:

- Though there exist several natural enemies of Sycamore lace bug, under natural circumstances they do not appear at all in Hungary, or they are playing no limiting role in reproduction. Thus, we consider Sycamore lace bug in the model, as a pest of Sycamore tree having no predator.
- Though the rate of Sycamore lace bug infection can be quite high in Hungary, the size of the population has never been limited by the Sycamore tree population. Thus, we assume in the model, that there is no nutrient limitation of Sycamore lace bug.

http://www.ecology.uni-corvinus.hu ● ISSN 1589 1623

- Sycamore lace bug is monophagous and nowadays it is the most important pest of Sycamore trees.

To simulate the population of *Sycamore lace bug*, we used a model with discrete-time (with daily scale), deterministic and weather-dependent difference equations.

The model has a format of MS Excel so that it can widely be applied. The parameters of the model were fitted to the empirical data with the help of MS Excel Solver. The empirical data were gathered between 1989 and 1999 in public parks of Budapest, Hungary [44].

Results

General biomass model

Our drastically simplified food web biomass seasonal population dynamical model applied for the examined *Corythuca ciliata – Sycamore tree* population is generally as follows:

$$M_{t+1} = M_t \cdot R_t$$

where

the amounts of the biomass of *Sycamore lace bug* population at the $(t+1)^{\text{th}}$ and at the t^{th} points of time are denoted by M_{t+1} and M_t, respectively

the activity term of the entities of M is denoted by R_t is depending on the daily average temperature T.

In what follows the terms of the general equation are introduced.

The activity term R_t and the cumulated activity $\underset{t \geq t_s}{cum}\, R_t^{Ph}$

Activity term R_t expresses that the agro-ecological process – that was represented by the general biomass model above – is depending on the daily average temperature; nevertheless, the effect of the same temperature on the entities can be different in different phenological phases (*Table 1 and 2*).

Let us denote by t_s the so-called 'first spring day of the population' and by t_w the 'first winter day of it'. We say, that the vegetation period of a population lies between t_s and t_w.

The cumulated activity is defined by

$$\underset{t \geq t_s}{cum}\, R_t^{Ph} = \begin{cases} 0 & \text{if } t < t_s \\ \sum_{i=t_s}^{t} R_i^{Ph} \cdot SW_i^{Ph} & \text{if } t \geq t_s \end{cases}$$

Cumulated activity $\underset{t \geq t_s}{cum}\, R_t^{Ph}$ cumulates the values of *activity terms* R_t of *Sycamore lace bug* from a starting point of time, t_s (from 'the first spring day of *Sycamore lace bug*'), in the case phase *Ph* holds. *Ph* denotes one of L_{ij} (for the j^{th} larva state of the i^{th} generation, i=1, 2, j=1, 2, ... ,5) and I_i (for the imago state of the i^{th} generation i=1, 2, 3).

Cumulated activity $\underset{t \geq t_s}{cum}\, R_t^{Ph}$ of *Sycamore lace bug* is calculated with the help of a characteristic function SW_t^{Ph}:

http://www.ecology.uni-corvinus.hu ● ISSN 1589 1623

$$SW_t^{Ph} = \begin{cases} 0 & \text{if} \quad t = 0 \quad and \quad Ph > I_1 \\ \prod_{\underline{Ph} > I_1} \left(1 - SW_t^{\underline{Ph}}\right) & \text{if} \quad Ph = I_1 \\ \min\left[\max\left\{\left(CumR_t^{Ph} - T_m^{Ph}\right), 0\right\}, 1\right] \prod_{\underline{Ph} > Ph} \left(1 - SW_t^{\underline{Ph}}\right) & \text{if} \quad t > 0 \quad and \quad Ph > I_1 \end{cases}$$

where

T_m^{Ph} denotes the minimum of cumulated activity of *Sycamore lace bug* $\underset{t \geq t_s}{cum}\, R_t^{Ph}$ that is necessary to enter phase *Ph*

and relation $\underline{Ph} > Ph$ means that „*for all phases later than phase Ph* ”.

For a fixed point of time *t* and a phenophase *Ph*, SW_t^{Ph} shows, whether the phase *Ph* holds at a point of time *t*, that is to say:

$$SW_t^{Ph} = \begin{cases} 0 & \text{if } Ph \text{ holds} \\ 1 & \text{if } Ph \text{ does not hold} \end{cases}$$

(*Figures 1, 2, 3 and 4*)

Table 1. *The values of activity term* R_t *of the daily average temperature T. Activity term expresses that the agro-ecological process* $M_{t+1} = M_t \cdot R_t$ *is depending on the daily average temperature differently in different phenophases.*

	Conditions	R_t
Earlier than the first spring day	$t < t_s$	0.90
In the third Imago phase	$22 < \underset{t}{cum}\, R_{t-1}^{I_3} < 33$	0.90
	$\underset{t}{cum}\, R_{t-1}^{I_3} > 33$	1
Else	$T < 5$	0.98
	$5 \leq T < 10$	0.99
	$10 \leq T < 15$	1.06
	$15 \leq T < 21$	1.08
	$21 \leq T < 26$	1.04
	$26 \leq T$	0.80

http://www.ecology.uni-corvinus.hu ● ISSN 1589 1623

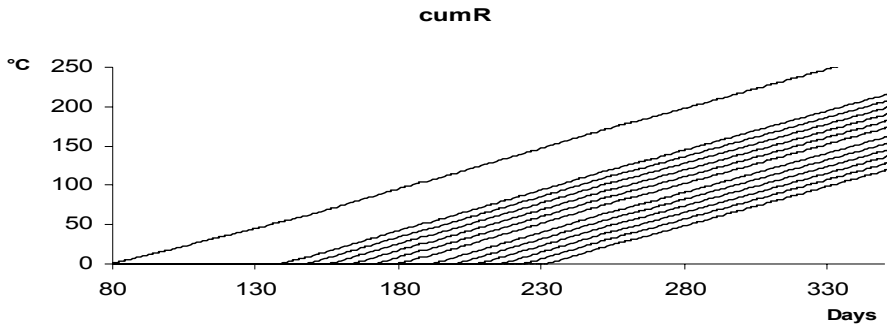

Figure 1. *The graphs of cumulated activities* $\underset{t \geq t_{s,M}}{cum}\, R_t^{Ph}$ *for Ph =* I_1, L_{11}, L_{12} , L_{13},, L_{14},, L_{15} *as well as for Ph =* I_2, L_{21}, L_{22} , L_{23} , L_{24} , L_{25}, I_3.. $\underset{t \geq t_s}{cum}\, R_t^{Ph}$ *cumulates the values of activity terms* R_t *of Sycamore lace bug from a starting point of time,* t_s .
Note that though the graphs of $\underset{t \geq t_{s,M}}{cum}\, R_t^{Ph}$ *seem to be straight lines, it is not the fact.*

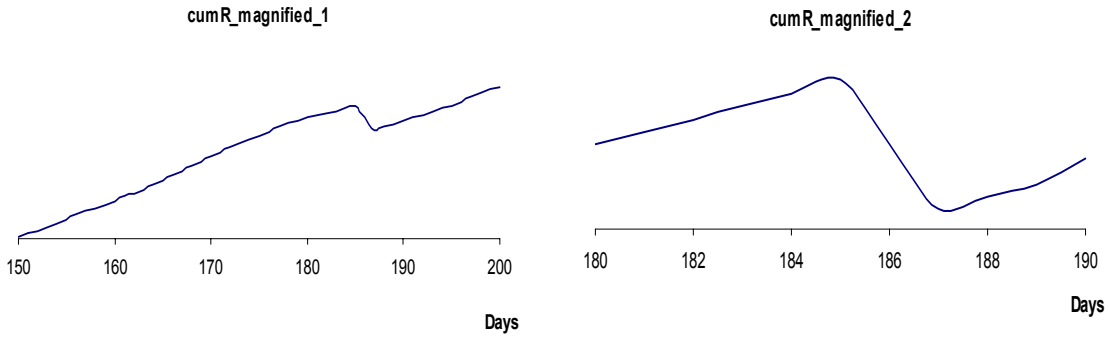

Figure 2. *The graphs of cumulated activities* $\underset{t \geq t_{s,M}}{cum}\, R_t^{Ph}$ *seem to be straight lines, it is not the fact. Their lines brake several times.*

First, we assume that the phenophases of the population are disjunctive, that is to say each entity of the population belongs to an only phase *Ph*. (Later we omit this condition.) Function SW_t^{Ph} equals to 1 if and only if the *Sycamore lace bug* population has more than zero number of entities in phase *Ph* at a given point of time *t*, and equals to 0, else. The change of the values of function SW_t^{Ph}

- from 0 to 1 is caused by the fact cumulated activity $\underset{t \geq t_s}{cum}\, R_t^{Ph}$ has reached the minimum that is necessary for the entities to enter phase *Ph* +1, that is to say $\underset{t \geq t_s}{cum}\, R_t^{Ph} > T_m^{Ph}$.
- from 1 to 0 is caused by the fact the next phase has been entered.

http://www.ecology.uni-corvinus.hu ● ISSN 1589 1623

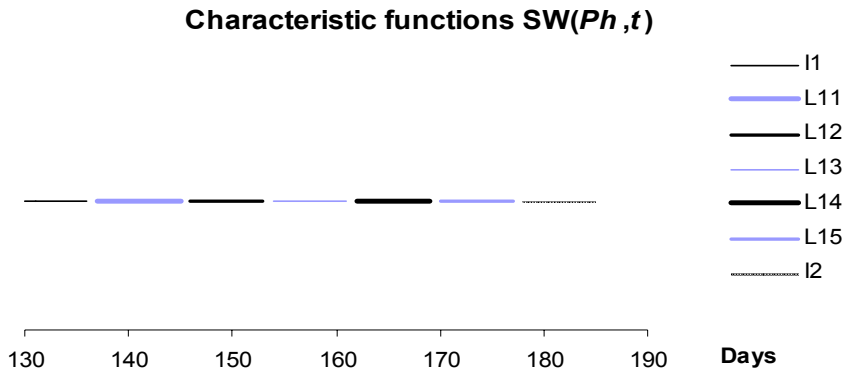

Figure 3. *The graphs of characteristic functions* SW_t^{Ph} *for Ph =* I_1, L_{11}, L_{12}, L_{13}, L_{14}, L_{15}, *and* I_2

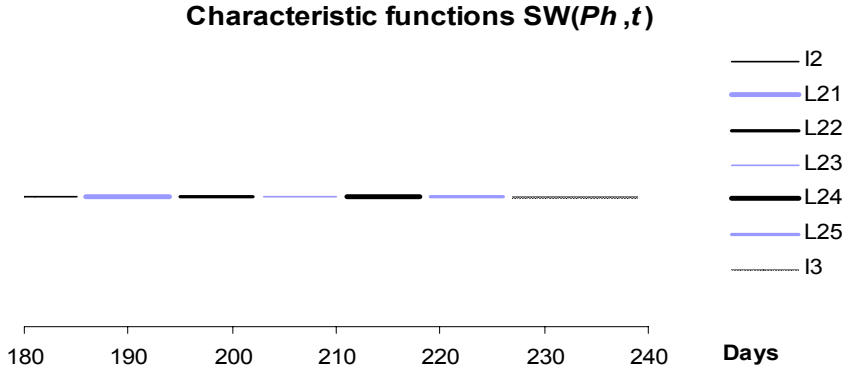

Figure 4. *The graphs of characteristic functions* SW_t^{Ph} *for Ph =* I_2, L_{21}, L_{22}, L_{23}, L_{24}, L_{25}, *and* I_3

The smoothed characteristic function SSW_t^{Ph}

Our main aim is to define the current number of the entities if we know the current biomass of *Sycamore lace bug*. On the way to our goal we have to keep in mind that there is a point of time a phase is entered *first*, and there is another one at which the process of metamorphosis is *finished for the whole population*. This means that there can usually appear more than one phenological phases at the same time (as opposed to our earlier assumption). Thus, function SW_t^{Ph} that 'switches' on/off the phases has to be '*smoothed*' in order to get the number of entities later more exactly. The smoothed characteristic function SSW_t^{Ph} is defined as follows:

At $t = 0$, we have $SSW_t^{I_1} = 1$ and $SSW_t^{Ph} = 0$ for all phases $Ph > I_1$. (At the beginning of spring there are entities in the first Imago phase, only.) At the point of time the minimal value of cumulated activity $\underset{t}{cum}\, R_t^{Ph-1}$, that is necessary to enter phase Ph (denoted by T_m^{Ph-1}, see *Table 2*), has been exceeded ($\underset{t}{cum}\, R_t^{Ph-1} > T_m^{Ph-1}$), the entities of phase $Ph-1$ are starting to enter phase Ph. (We say, that at the point of time t, when $\underset{t}{cum}\, R_t^{Ph-1} > T_m^{Ph-1}$ first, phase Ph is entered *first*.) During the time of metamorphosis

http://www.ecology.uni-corvinus.hu ● ISSN 1589 1623

from $Ph-1$ to Ph, the value of SSW_t^{Ph} is growing from zero to 1 (though, it is not necessary that SSW_t^{Ph} reaches 1, indeed. We can say only that $0 \le SSW_t^{Ph} \le 1$). The value of SSW_t^{Ph} reaches its potential maximum ($pot \max SSW_t^{Ph} = 1$), if $\underset{t}{cum}\, R_t^{Ph-1} > T_M^{Ph-1}$ and if $\underset{t}{cum}\, R_t^{Ph} < T_m^{Ph}$, that is to say, the metamorphosis to the next phase, $Ph + 1$ has still not began. (At this point of time the process of metamorphosis from $Ph - 1$ to Ph is *finished for the whole population*.) In the case the minimal value of cumulated activity $\underset{t}{cum}\, R_t^{Ph}$, that is necessary to enter phase $Ph + 1$ (denoted by T_m^{Ph}), has been exceeded ($\underset{t}{cum}\, R_t^{Ph} > T_m^{Ph}$), then SSW_t^{Ph} starts to decrease monotonously to zero.

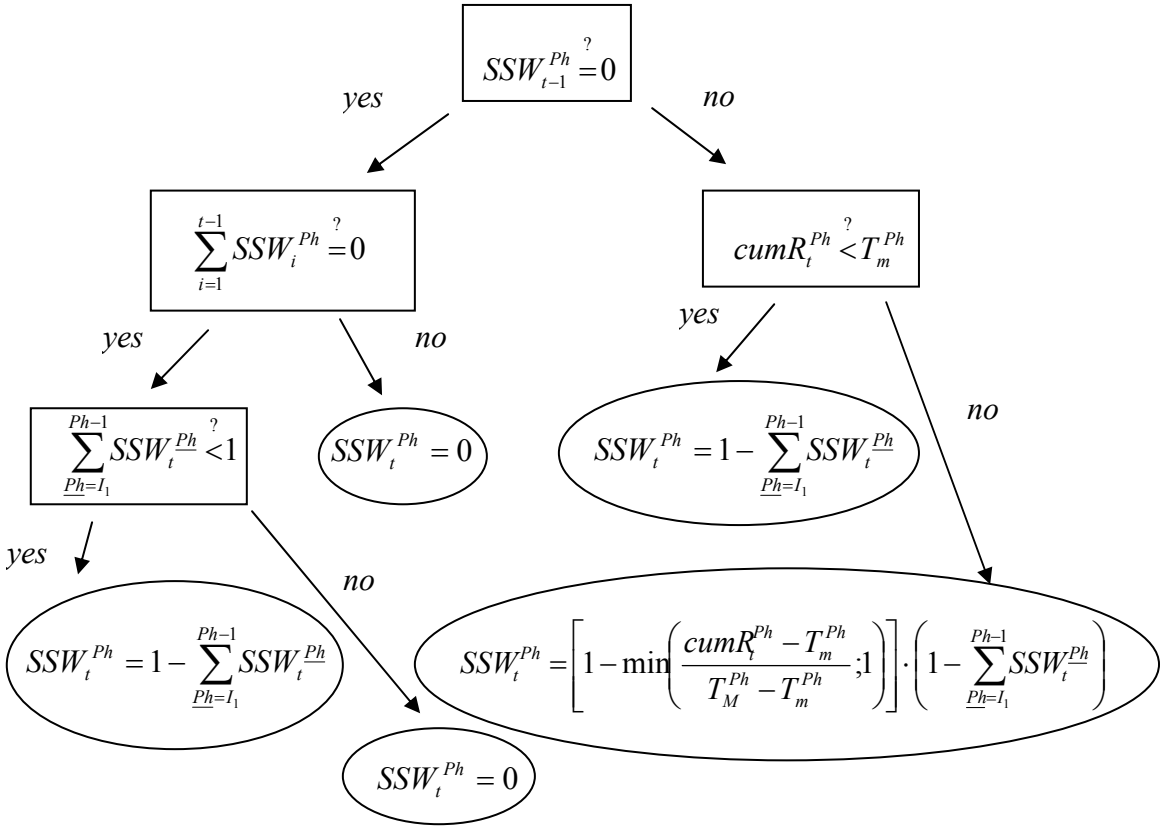

Figure 5. *The way of evaluation of function SSW_t^{Ph}. Considering that the metamorphosis from phase Ph to phase Ph + 1 is a continuous process, characteristic function SW_t^{Ph} that 'switches' on/off the phases has to be smoothed in order to get the number of entities later more exactly. (For $Ph=I_1$ we say that $SSW_t^{Ph-1} = 0$ for each t.)*

If $\underset{t}{cum}\, R_t^{Ph} > T_m^{Ph}$ at the point of time t when $\underset{t}{cum}\, R_t^{Ph-1} > T_M^{Ph-1}$ first, then SSW_t^{Ph} cannot reach its potential maximum value ($\max SSW_t^{Ph} < pot \max SSW_t^{Ph} = 1$), because the metamorphosis from Ph - 1 to Ph ends later than the metamorphosis from Ph to $Ph + 1$ starts.

http://www.ecology.uni-corvinus.hu ● ISSN 1589 1623

At the point of time at which the whole process of metamorphosis from *Ph* to *Ph* + 1 is finished, namely, when $\underset{t}{cum}\, R_t^{Ph} > T_M^{Ph}$, the value of SSW_t^{Ph} becomes to be equal to, and keeps to be, zero (*Figures 5, 6 and 7*).

It is easy to see that $\sum_{\text{for all phases } Ph} SSW_t^{Ph} = 1$.

Table 2. *The values of T_m^{Ph} and T_M^{Ph}. At the point of time t, when $\underset{t}{cum}\, R_t^{Ph-1} > T_m^{Ph-1}$ first, phase Ph is entered first. At the point of time $\underset{t}{cum}\, R_t^{Ph-1} > T_M^{Ph-1}$ first, the process of metamorphosis from Ph – 1 to Ph is finished.*

Phase	I_1	L_{11}	L_{12}	L_{13}	L_{14}	L_{15}	I_2	L_{21}	L_{22}	L_{23}	L_{24}	L_{25}
T_m^{Ph}	52	7	7	7	7	7	7	7	7	7	7	7
T_M^{Ph}	67	27	32	37	37	37	37	37	42	42	42	42

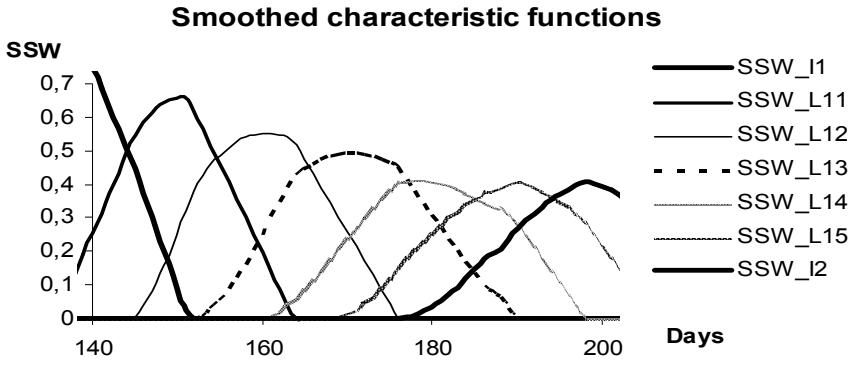

Figure 6. *The graphs of smoothed characteristic functions SSW_t^{Ph} for Ph = I_1, L_{11}, L_{12}, L_{13}, L_{14}, L_{15}, and I_2*

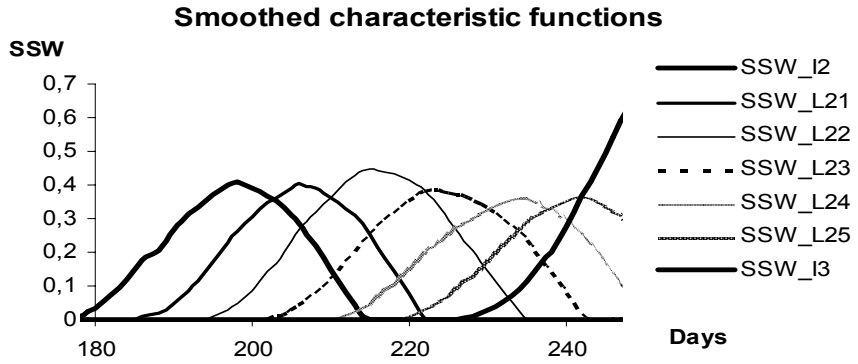

Figure 7. *The graphs of smoothed characteristic functions SSW_t^{Ph} for Ph =I_2, L_{21}, L_{22}, L_{23}, L_{24}, L_{25}, and I_3*

http://www.ecology.uni-corvinus.hu ● ISSN 1589 1623

The number of entities of Sycamore lace bug (NoI_t^{Ph})

Finally, the numbers of entities of *Sycamore lace bug* in all phenophases will be calculated as follows. Set out from an estimated value of the number of entities of phase I_1 at the point of time $t_0 = 0$:

$$NoI_0^{I_1} = \frac{M_0}{\overline{m}^{I_1}}$$

where $\overline{m}^{I_1}$ denotes the average mass of an only entity of *Sycamore lace bug* in phenophase I_1.

The number of entities of *Sycamore lace bug* for a phenophase *Ph*) at a point of time $t > 0$ is obtained as:

$$NoI_t^{Ph} = \begin{cases} \min\left(\dfrac{M_t}{m_{t-1}^{Ph}} \cdot SSW_t^{Ph} \quad , \quad k^{Ph} \cdot \max\limits_{t \in \{Ph-1\}} NoI_t^{Ph-1} \right) & \text{if} \quad Ph \neq L_{i1} \quad (i = 1, 2) \\ \dfrac{M_t}{m_{t-1}^{Ph}} \cdot SSW_t^{Ph} & \text{if} \quad Ph = L_{i1} \quad (i = 1, 2) \end{cases}$$

where m_t^{Ph} denotes the current average mass of an only entity of *Sycamore lace bug* in the phenophase *Ph* at a point of time *t*:

$$m_t^{Ph} = \frac{M_t}{NoI_t^{Ph}}$$

$t \in \{Ph-1\}$ means: "for all *t* for which $SSW_t^{Ph-1} > 0$",

and the multiplier term k^{Ph} expresses the standard mortality during the metamorphosis from phase $Ph-1$ to phase Ph (*See Figures 8 and 9*).

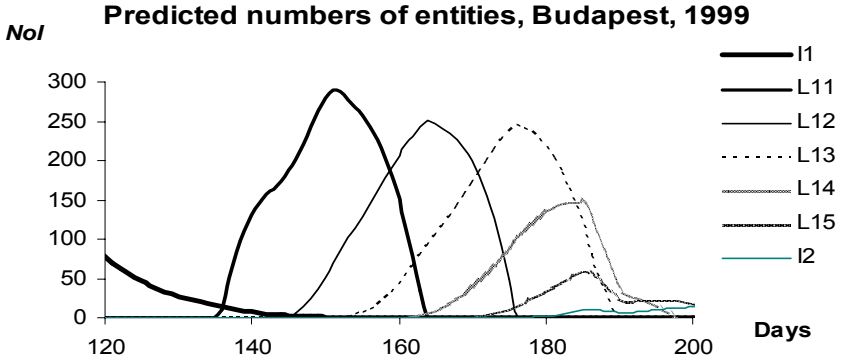

Figure 8. *The numbers of Sycamore lace bug entities NoI_t^{Ph} in Budapest, between the 120th and 200th days of year 1999, predicted by the model for $Ph = I_1, L_{11}, L_{12}, L_{13}, L_{14}, L_{15}$ and I_2*

http://www.ecology.uni-corvinus.hu ● ISSN 1589 1623

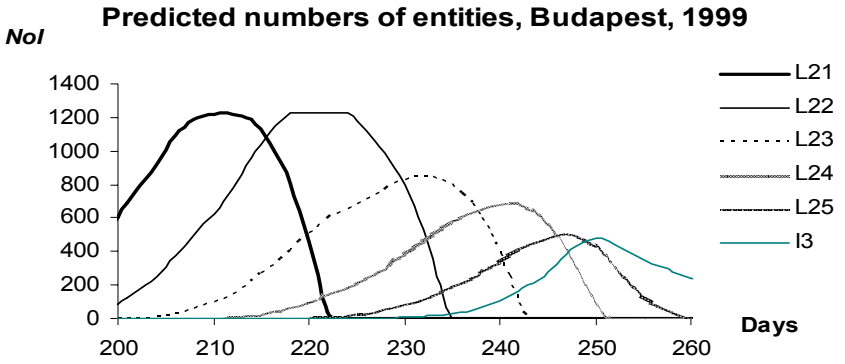

Figure 9. *The numbers of Sycamore lace bug entities* NoI_t^{Ph} *in Budapest, between the 200th and 260th days of year 1999, predicted by the model for Ph =* L_{21}, L_{22}, L_{23}, L_{24}, L_{25}, *and* I_3

The properties of the function NoI_t^{Ph} *of the number of entities (of day t):*

1. The sum of the numbers of entities does not increase in any phase except if $Ph = L_{i1}$ $(i = 1, 2)$, that is to say there is no reproduction except in phases I_1 and I_2.
2. During the metamorphosis from a phase Ph into the next one (denoted by $Ph+1$), the number of entities in phase Ph is decreasing tending to 0, while the number of entities in phase $Ph+1$ is increasing.
3. During the metamorphoses there is a given rate of mortality.
4. The change of the biomass of *Sycamore lace bug* of phenophase Ph can be caused by two facts:
   a. the entities are losing/putting on their weights
   b. the entities of the population is changing their phase (reproduction or mortality during the metamorphosis)
5. The number of entities does not change in the first case, while in the second one it is decreasing for phenophase Ph and increasing for phenophase $Ph+1$.

The predictions of the model for the daily number of entities of each phenological phase can be seen in *Figures 8* and *9*. In order to compare the predictions with the empirical data we displayed the average numbers of entities referred to a leaf (*Figure 10*). It can be seen that the model follows the empirical data quite well. Its advantage is, however, that it gives such information about each single phenophase that has not been measured.

http://www.ecology.uni-corvinus.hu ● ISSN 1589 1623

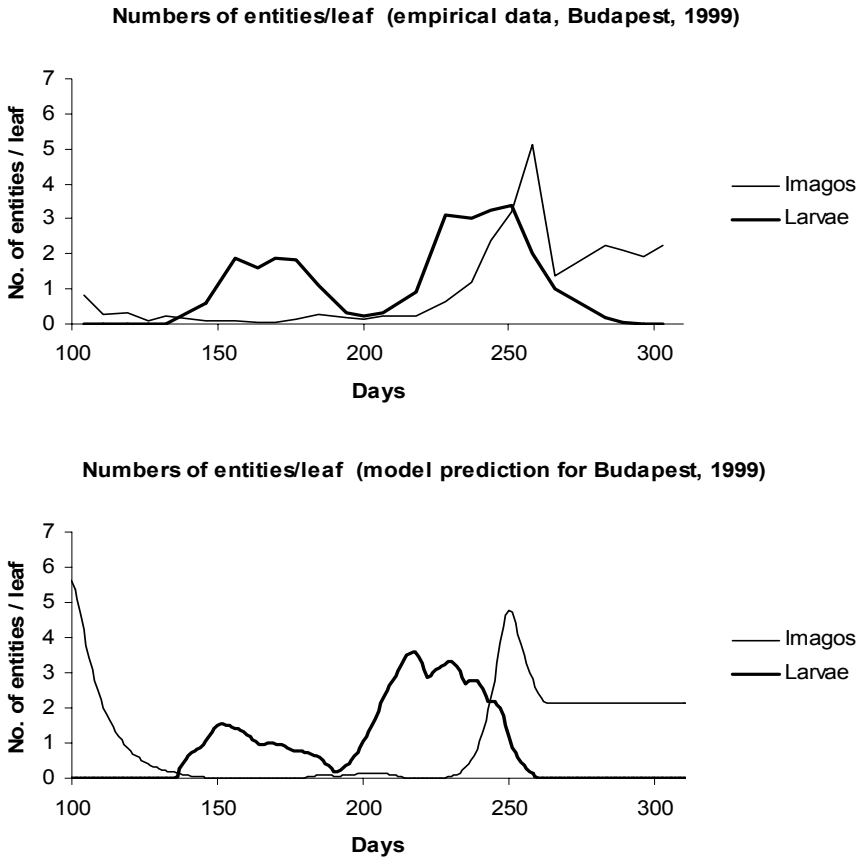

Figure 10. *The numbers of Sycamore lace bug imagos and larvae per leaf in Budapest, between the 100th and the 300th days of year 1999*
Upper figure: empirical data; Lower figure: model prediction

http://www.ecology.uni-corvinus.hu ● ISSN 1589 1623

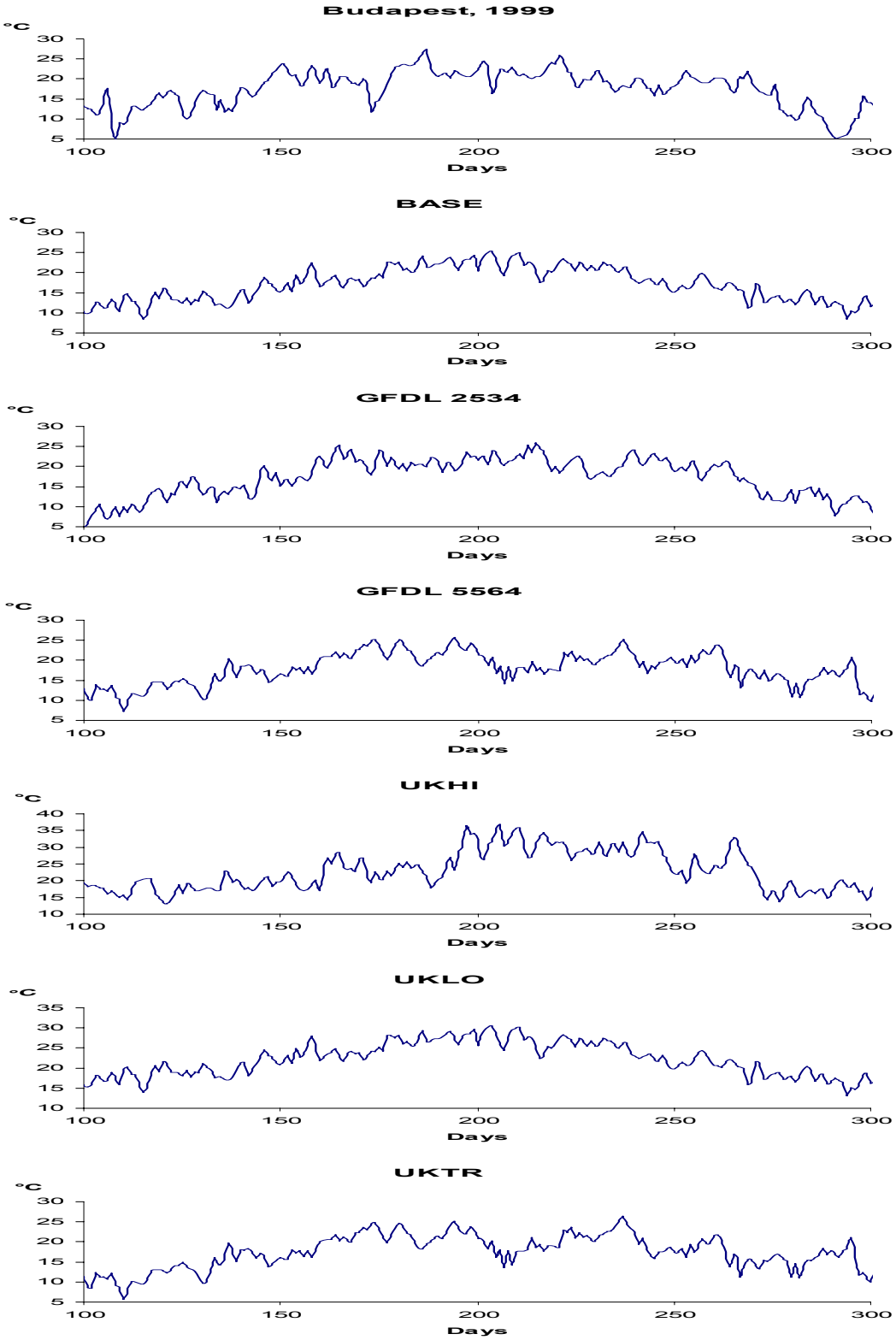

Figure 11. *Daily average temperature data of year 1999 and of the 15th years of the scenarios. Note that the scale of axis y of UKLO and UKHI is different because of the essentially higher values.*

http://www.ecology.uni-corvinus.hu ● ISSN 1589 1623

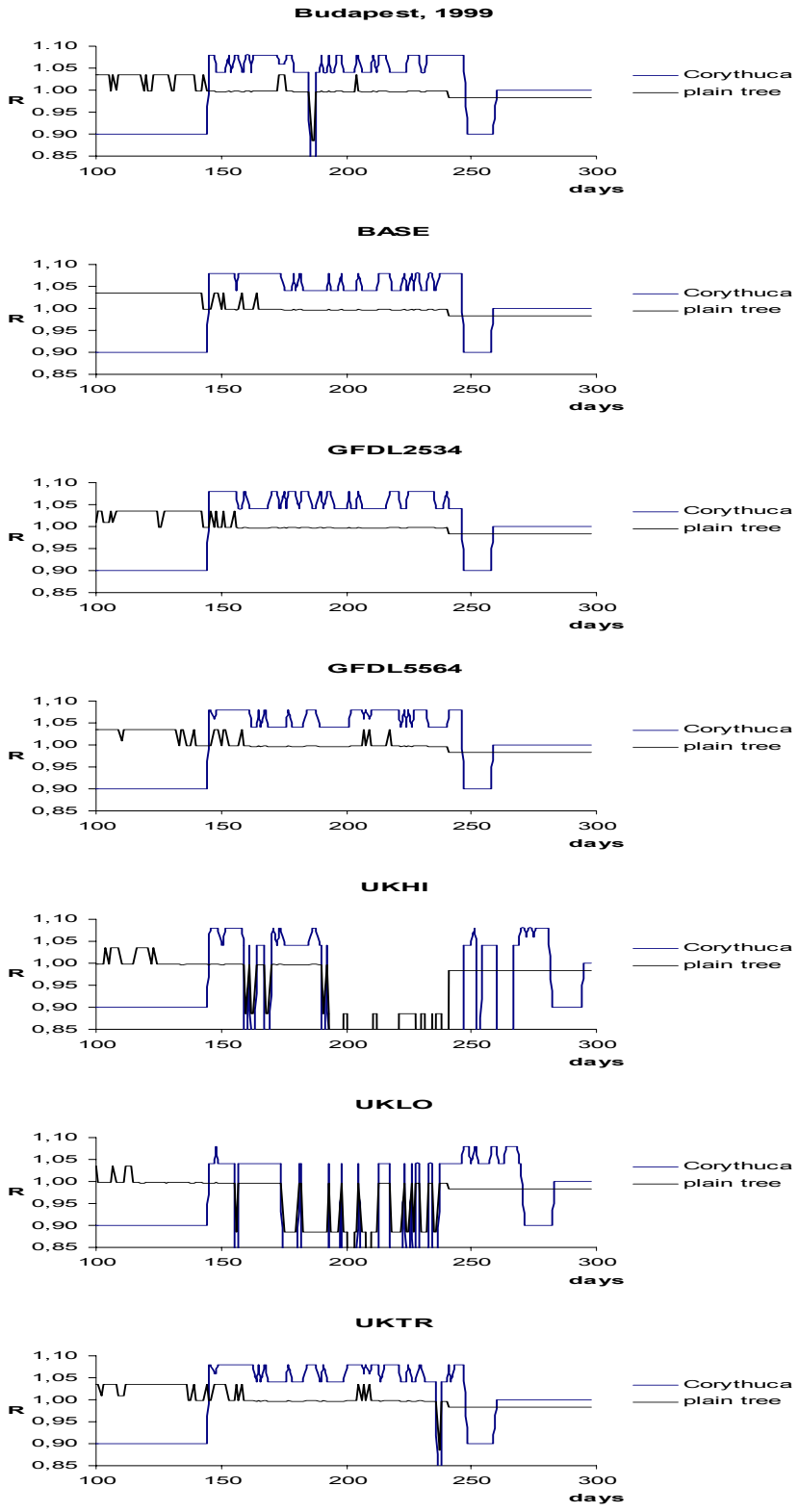

Figure 12. *Activity terms R_t of the 15th years of the scenarios. In order to see the effect of the climate better, we displayed the activity terms of Corythuca ciliata as well as the ones of Sycamore trees.*

http://www.ecology.uni-corvinus.hu ● ISSN 1589 1623

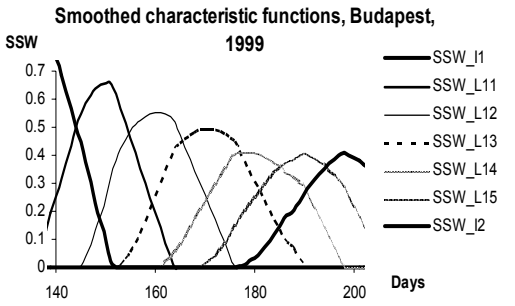

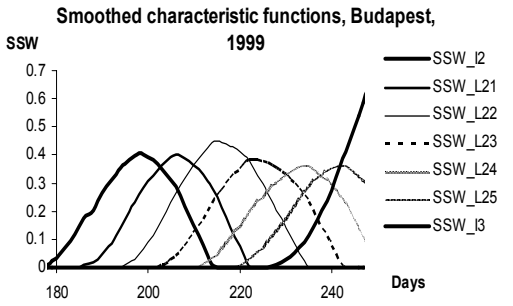

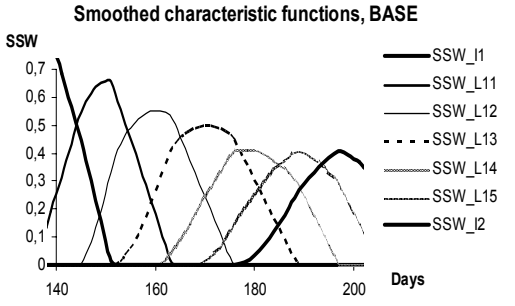

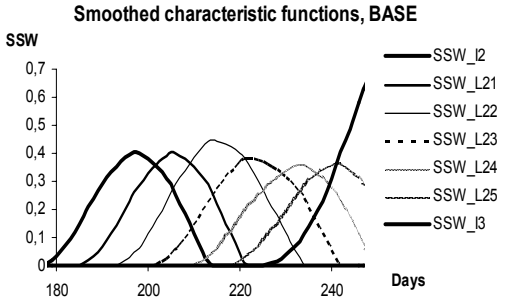

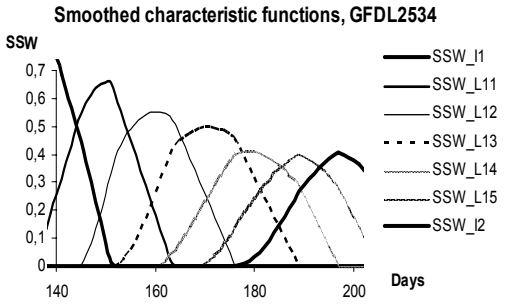

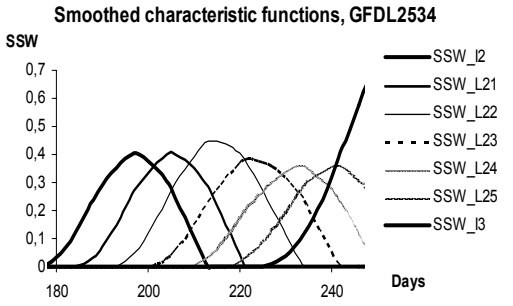

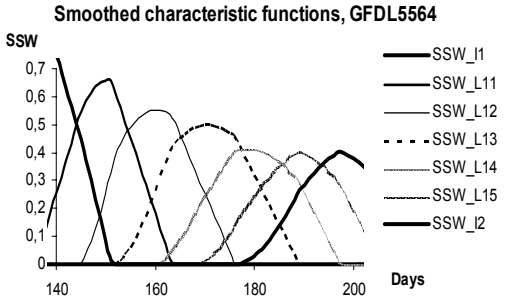

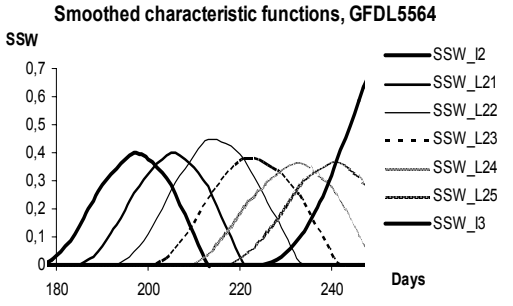

http://www.ecology.uni-corvinus.hu ● ISSN 1589 1623

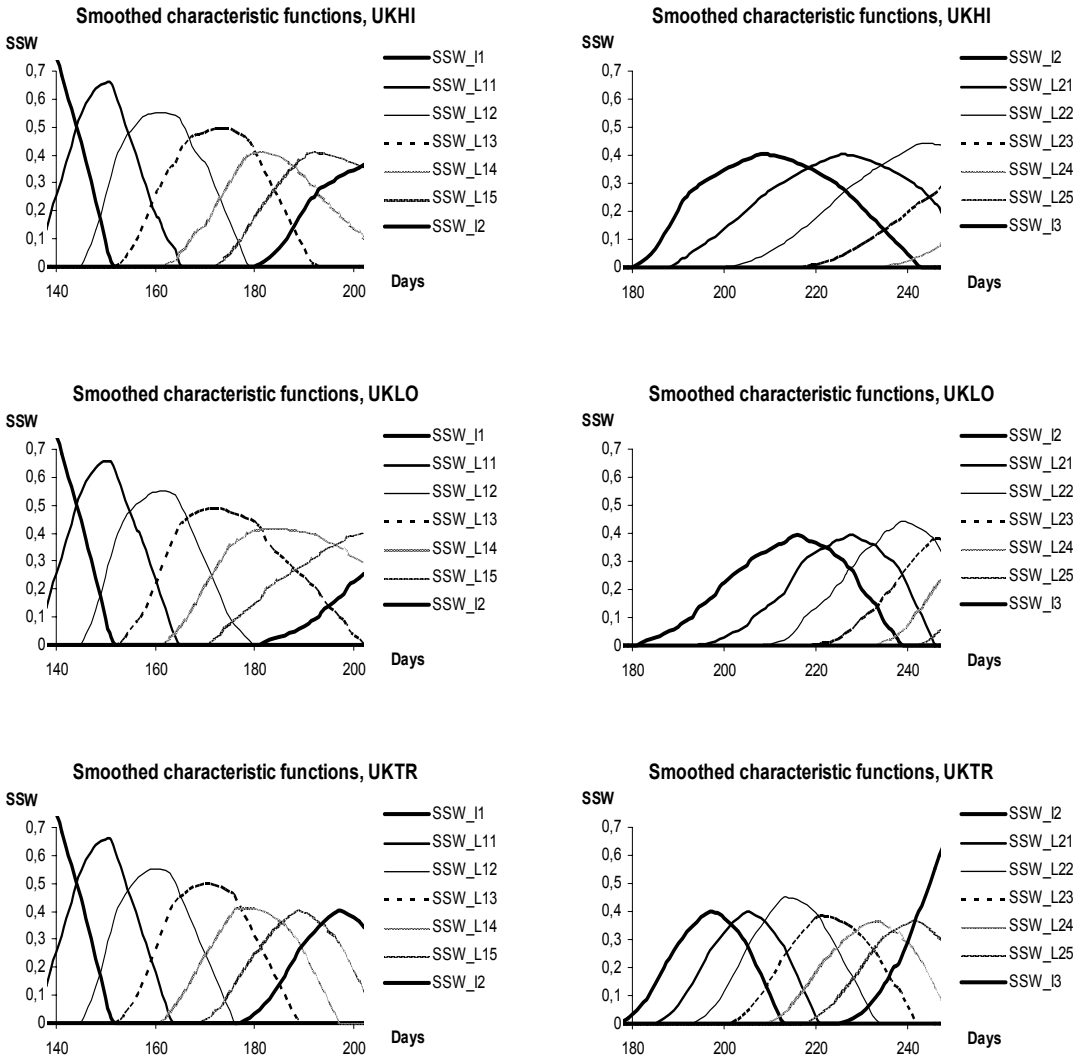

Figure 13. *The graphs of smoothed characteristic functions* SSW_t^{Ph} *for each phenophase, predicted by the model for Budapest, for 1999 and for the* 15^{th} *years of the scenarios.*

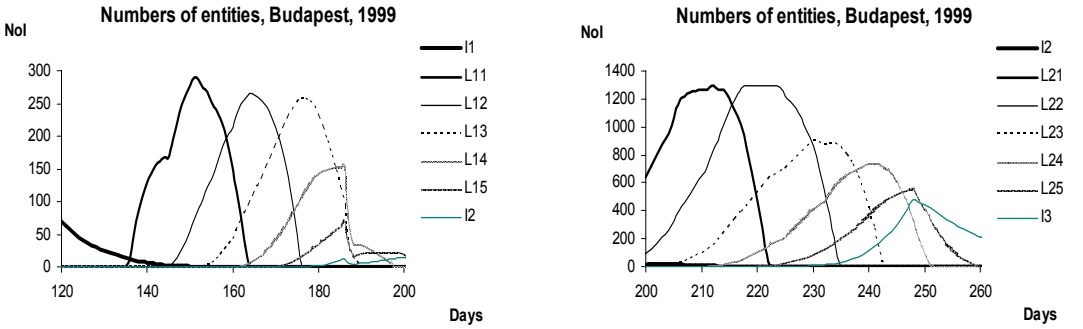

http://www.ecology.uni-corvinus.hu ● ISSN 1589 1623

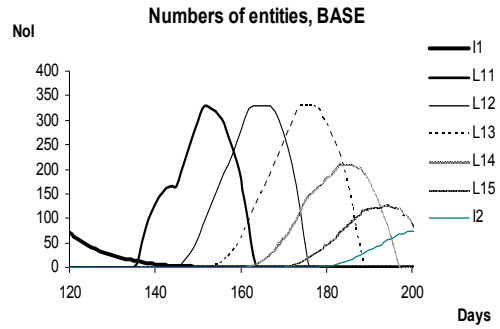

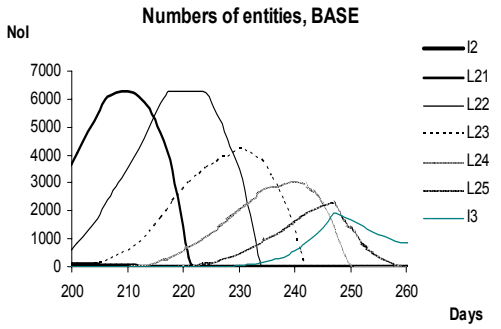

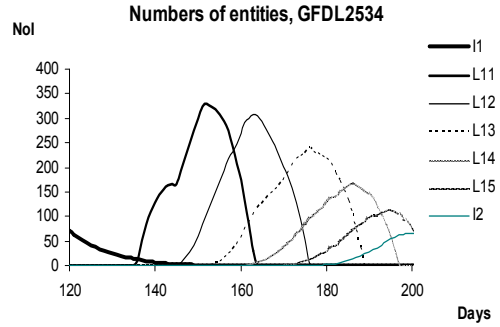

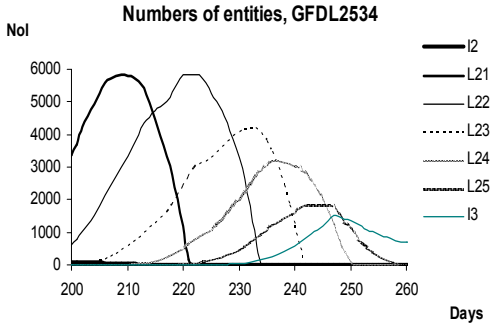

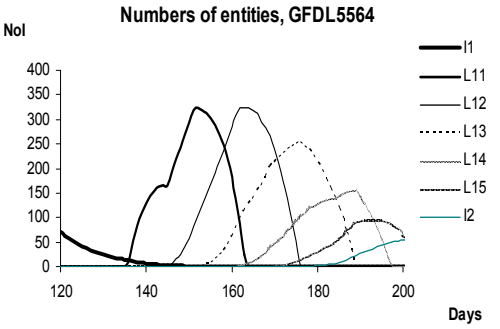

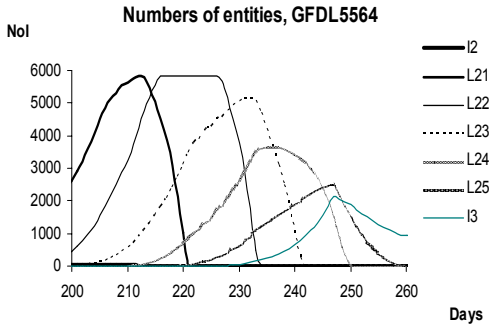

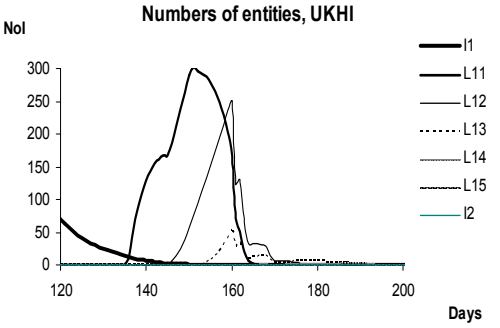

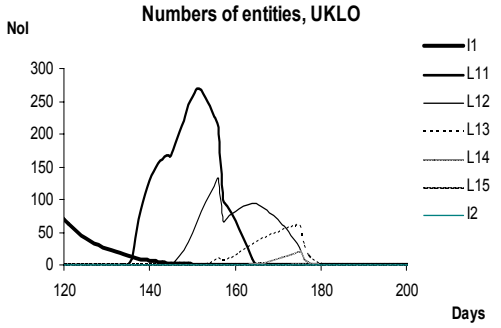

http://www.ecology.uni-corvinus.hu ● ISSN 1589 1623

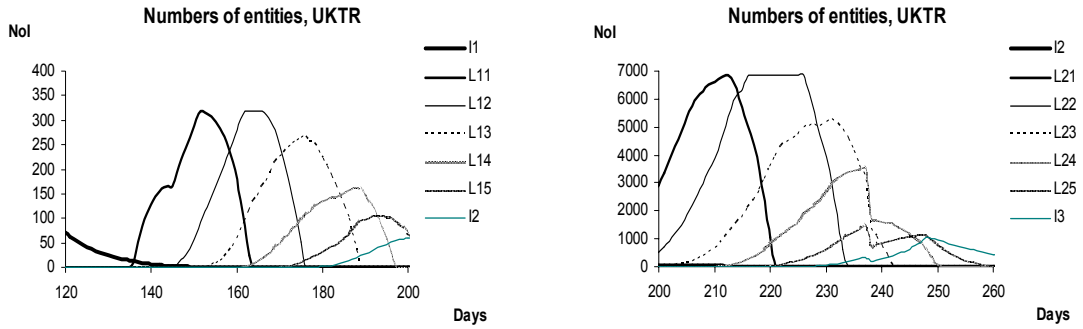

Figure 14. *The numbers of Sycamore lace bug entities in each phenophase* NoI_t^{Ph}*, predicted by the model for Budapest, for 1999 and for the* 15^{th} *years of the scenarios.*

Phenological pattern of Sycamore lace bug and climate change scenarios

In order to compare the predictions of the model related to the different climate scenarios we have checked the model behaviour for the data of all the 30 years of each scenario. In what follows, we display the results of the 15^{th} year of each scenario, together with the ones of year 1999. First, we give the temperature data (*Figure 11*), then the values of activity terms R_t (*Figure 12*), the smoothed characteristic functions SSW_t^{Ph} (*Figure 13*), the numbers of entities NoI_t^{Ph} (*Figure 14*), and finally the numbers of imagos and larvae per leaf (*Figure 15*).

Discussion

Activity term R_t

The activity terms of scenarios Base, GFDL2535 and GFDL5564 are very similar to the one of the empirical data of Budapest, 1999. Moreover, they do not even have extremely low values as the one of year 1999 (caused by some extremely hot days in the middle of summer). Thus, we expect the results of these scenarios quite similar to the one of year 1999. The weather data of scenarios UKHI and UKLO are such extreme that even at the beginning of spring it is unbearable for both *Corythuca ciliata* and *Sycamore tree* populations, that is to say the values of the activity the terms are very low in long periods of the vegetation. The activity term of scenario UKTR is similar to the one of year 1999, except at the end of August. Then, there is a short period with extreme weather conditions. For both population it is very hard to get over, though they are not threatened by extinction.

Smoothed characteristic function SSW_t^{Ph}

As it was expected, the smoothed characteristic functions of scenarios Base, GFDL2535, GFDL5564 and UKTR are very similar to the one of the empirical data of Budapest, 1999. The smoothed characteristic functions of scenarios UKHI and UKLO are not very different in case of the first generation. The curves of SSW_t^{Ph} of the phenophases of the second generation are fatter and sluggish, the metamorphosis takes longer. (For scenario UKLO it is true for a greater extent.) Note, that the effect of the smoothed characteristic function can be detected only if the population survives.

http://www.ecology.uni-corvinus.hu ● ISSN 1589 1623

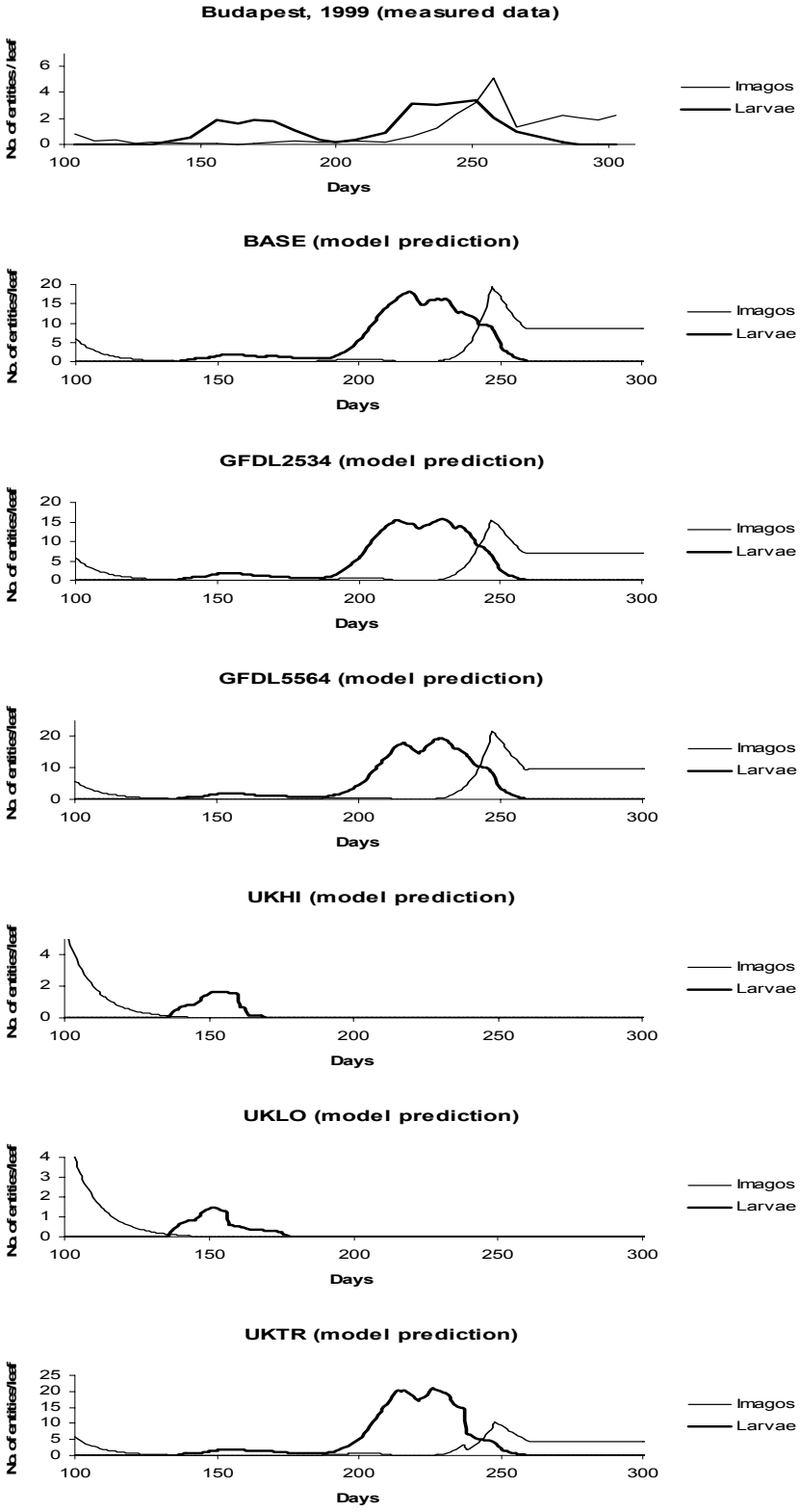

Figure 15. *The numbers of Sycamore lace bug imagos and larvae per leaf, measured in Budapest, 1999 (uppermost figure), predicted by the model for Budapest, for 1999 (second figure) and for the 15th years of the scenarios.*

http://www.ecology.uni-corvinus.hu ● ISSN 1589 1623

The number of entities NoI_t^{Ph}

The shapes of the characteristic curves of the functions NoI_t^{Ph} are quite similar for scenarios Base, GFDL2535 and GFDL5564. The number of entities of the first generation increases 15-20% (compared with its value of 1999), while the one of the second generation increases about 500%. The date of the first appearance of the phenophases are shifted 2-5 days earlier. The balance does not tip yet.

Considering curve of the number of entities for scenarios UKLO and UKHI we can observe that the entities of first generation practically extinct in their $L_{14} - L_{15}$ phase. We can assume that some entities can survive till their I_2 phase, but there is no chance for the second generation. This can be explained by the extreme weather.
The phenophases in the years of scenario UKTR begin slightly earlier. The effect of the extreme weather in August can be seen on the curves, a lot of entities die. Just after that, a balancing process can be observed.

The numbers of imagos and larvae per leaf

The numbers of the imagos of the first generation for scenarios Base, GFDL2535 and GFDL5564 are very similar to the one of the empirical data of Budapest, 1999, however, the numbers of the second generation are higher. The third generation appears a little later with a very speedy increase. Thus, the number of the third generation reaches its maximum 5-7 days earlier and the value of the maximum is about five times higher than the one of year 1999. These entities are going to winter.

The numbers of the larvae of the first generation for scenarios Base, GFDL2535 and GFDL5564 do not differ essentially from the one of the empirical data of Budapest, 1999, but the second generation appears about 7 days earlier, the increase in number is quicker, the maximum is five times higher.

The larvae of the first generation for scenarios UKLO and UKHI extinct in their $L_{14} - L_{15}$ phase, as we have seen before.

The shapes of the characteristic curves of the numbers of the imagos and larvae per leaf for scenario UKTR is similar to the ones of scenarios Base, GFDL2535 and GFDL5564. The effect of the extreme weather in August can be seen on the curves. Just after that, a balancing process can be observed.

Acknowledgements. Our work was supported by the VAHAVA project of Hungarian Academy of Sciences, the KLIMAKKT project of NKFP "Jedlik Ányos" program, the FKFP 0087/2002 and OTKA T042583 projects and the ADAM project of EU.

REFERENCES

[1] Ammann, B. (2000): Biotic responses to rapid climatic changes; Introduction to a multidisciplinary study of the Younger Dryas and minor oscillations on an altitudinal transect in the Swiss Alps. - Palaeogeography, Palaeoclimatology, Palaeoecology 159(3-4): 191-201.

[2] Ayres, M.P., Lombardero, M.J. (2000): Assessing the consequences of global change for forest disturbance from herbivores and pathogens. - The Science of The Total Environment 262(3): 263-286.

[3] Barrow, E.M. (1993): Scenarios of climate changes for the European Community – European Journal of Agronomy, 2(4): 247-260.

http://www.ecology.uni-corvinus.hu ● ISSN 1589 1623

[4] Barrow, E.M., Hulme, M., Semenov, M.A., Brooks, R.J. (2000): Climate change scenarios, In: Downing, T.E. (ed.) Climate Change, Climatic Variability and Agriculture in Europe - Environmental Change Institute, University of Oxford.

[5] Butterfield, R.E., Bindi, M., Brooks, R.J., Carter, T.R., Delécolle, R., Downing, T.E. (2000): Review and comparison od scaling-up methods, In: Downing, T.E. (ed.) Climate Change, Climatic Variability and Agriculture in Europe - Environmental Change Institute, University of Oxford

[6] Buxton, P.A. (2004): The effect of climatic conditions upon populations of insects. - Transactions of the Royal Society of Tropical Medicine and Hygiene 26: 325-356.

[7] Chen, W., Chen, J., Cihlar, J. (2000): An integrated terrestrial ecosystem carbon-budget model based on changes in disturbance, climate, and atmospheric chemistry. - Ecological Modelling 135(1): 55-79.

[8] Conrad, K.F., Woiwod, I.P., Perry, J.N. (2002): Long-term decline in abundance and distribution of the garden tiger moth (Arctia caja) in Great Britain. - Biological Conservation 106(3): 329-337.

[9] Coops, N.C. Waring, R.H., Law, B.E. (2005): Assessing the past and future distribution and productivity of ponderosa pine in the Pacific Northwest using a process model, 3-PG. - Ecological Modelling 183(1): 107-124.

[10] Crookston, N.L., Dixon, G. E. (2005): The forest vegetation simulator: A review of its structure, content, and applications. - Computers and Electronics in Agriculture 49(1): 60-80.

[11] Dyck, M. van (1999): Keyword Reference Guide for the Forest Vegetation Simulator. - WO-TM Service Center, USDA Forest Service. Fort Collins, CO. September 1, 1996. 134 pp.

[12] Elias, S.A., Devender, T.R. van (1990): Fossil insect evidence for late Quaternary climatic change in the Big Bend region, Chihuahuan Desert, Texas. - Quaternary Research 34(2): 249-261.

[13] Fleming, R.A., Barclay, H.J., Candau , J.N. (2002): Scaling-up an autoregressive time-series model (of spruce budworm population dynamics) changes its qualitative behaviour. - Ecological Modelling 149(1-2): 127-142.

[14] Flynn, D.F.B., Sudderth, E.A., Bazzaz, F.A. (2005): Effects of aphid herbivory on biomass and leaf-level physiology of Solanum dulcamara under elevated temperature and CO_2. - Environmental and Experimental Botany (in press).

[15] Fodor N., Kovács G.J. (2005): Sensitivity of crop models to the inaccuracy of meteorological observations. - Physics and Chemistry of the Earth. Special issue: Agrometeorology. Dunkel, Z. (ed.) Elsevier Science, Amsterdam, The Netherlands. 30(1-3): 53-58.

[16] Fodor N., Máthéné-Gáspár G., Pokovai K., Kovács G.J. (2002): 4M - software package for modelling cropping systems. - European J. of Agr. 18(3-4): 389-393.

[17] Fodor N., Rajkai K. (2004): Talajfizikai tulajdonságok becslése és modellezésben való alkalmazásuk. - Agrokémia és Talajtan 53: 225-238

[18] Fuhrer, J. (2003): Agroecosystem responses to combinations of elevated CO_2, ozone, and global climate change. - Agriculture, Ecosystems & Environment 97(1-3): 1-20.

[19] Hanson, P.J., Weltzin, J.F. (2000): Drought disturbance from climate change: response of United States forests. - The Science of The Total Environment 262(3): 205-220.

[20] Harnos, Zs., Bussay, A., Harnos, N. (2000): Modelling climate change impacts on wheat and potato in Hungary - In: Downing, T.E. (ed.) Climate Change, Climatic Variability and Agriculture in Europe - Environmental Change Institute, University of Oxford.

[21] Harnos, N. (2003): A klímaváltozás hatásának szimulációs vizsgálata őszi búza produkciójára, - "Agro-21" Füzetek 31: 56-73.

[22] Hufnagel, L., Mészáros, Z. (1999): Lehetséges természetvédelmi problémák, a faunánkra idegen állatfajok növényvédelmi célú mesterséges betelepítésével kapcsolatban - Növényvédelem, 35. évf, 11. sz. 563-565

http://www.ecology.uni-corvinus.hu ● ISSN 1589 1623

[23] Hufnagel, L., Mészáros, Z. (2000): Viszontválasz egy válaszcikk nyomán - Növényvédelem, 36. évf 1. sz 9-11.
[24] IPCC (1996): Climate Change 1995: The Science of Climate Change, Cambridge University Press, Cambridge.
[25] Klok, C.J., Chown, S.L. (2001): Critical thermal limits, temperature tolerance and water balance of a sub-Antarctic kelp fly, Paractora dreuxi (Diptera: Helcomyzidae). - Journal of Insect Physiology 47(1): 95-109.
[26] Kovács G.J. (1998): Estimation of the Effect of Global Warming on Yields and Environment of Arable Crops in Hungary. - Agrokémia és Talajtan 47(1-4.): 133-144.
[27] Kovács G.J. (1997): Nitrate leaching study in a long term experiment; combination of field- and simulation experiments. - Agrokémia és talajtan 46(1-4): 135-143.
[28] Kovács G.J. (2004): Application of models to development of decision support tools. - In: Improving the Balance Between Economic Agricultural Production and Environmental Quality through Enhanced Decision Making, Hatfield, J.L. (ed.) OECD. Ames, USA
[29] Kovács, G.J. (1995) Application of CERES model in soil science and agricultural chemistry. - Agrokémia és Talajtan. 44(1-2): 249-262.
[30] Kovács, G.J., T. Németh (1995c): Modeling of nitrogen regime based on long term field experiments. - Agrokémia és Talajtan. 44(3-4): 545-551.
[31] Kovács, G.J., T. Németh, J.T. Ritchie (1995a): Testing Simulation Models for Assessment of Crop Production and Nitrate Leaching in Hungary. - Agricultural Systems, (ELSEVIER Sci. Ld., Oxford, England) 49(4): 385-397.
[32] Kovács, G.J., T.Németh (1995b) Modeling of yield and nitrate accumulation comparing with measurements in long term experiments. - Agrokémia és Talajtan. 44(1-2): 89-100.
[33] Ladányi, M., Horváth, L., Gaál, M., Hufnagel, L. (2003): An agro-ecological simulation model system. - Applied Ecology and Environmental Research, 1(1-2): 47-74.
[34] Ladányi, M., Hufnagel, L. (2003): A phenology model embedded in an ecosystem model for agroecological processes. - In: Harnos, Zs. et al. (eds) EFITA 2003 Conference, Debrecen-Budapest, Hungary. Information technology for a better agri-food sector, environment and rural living, pp. 876-881.
[35] Láng, I. (2003): Bevezető gondolatok "A globális klímaváltozással összefüggő hazai hatások és az arra adandó válaszok" című MTA-KvVM közös kutatási projekthez, - "Agro-21" Füzetek 31: 3-8.
[36] Lemdahl, G. (1991): A rapid climatic change at the end of the Younger Dryas in south Sweden - palaeoclimatic and palaeoenvironmental reconstructions based on fossil insect assemblages. - Palaeogeog., Palaeoclimat., Palaeoecology 83(4): 313-331.
[37] Lemdahl, G. (2000): Lateglacial and Early Holocene insect assemblages from sites at different altitudes in the Swiss Alps - implications on climate and environment. Palaeogeography, Palaeoclimatology, Palaeoecology 159(3-4): 293-312.
[38] Lenteren, J.C. van (2000): A greenhouse without pesticides: fact or fantasy? - Crop Protection 19(6): 375-384.
[39] Máthé-Gáspár G., Fodor N., Pokovai K., Kovács G.J. (2005): Crop modelling as a tool to separate the influences of the soil and weather on crop yields. - Physics and Chemistry of the Earth. Special issue: Agrometeorology. Dunkel, Z. (ed.) Elsevier Science, Amsterdam, The Netherlands. 30(1-3): 165-170.
[40] McKibben, G.H., Willers, J.L. Smith, J.W., Wagner, T.L. (1991): Stochastic model for studying boll weevil dispersal. - Environ.Ent. 20(5) pp.1327-1332.
[41] Mols, P.J.M. (1990): Forecasting orchard pests for adequate timing of control measures. - Proc. Exp. & Appl. Entomol., NEV. Amsterdam 1: 75-81.
[42] Mols, P.J.M. (1992): Forecasting an indispensable port of IPM in apple orchards. - Acta Phytop. Entom. H. 27(1-4): 449-460.
[43] Norango, S.E., Sawyer, A.J. (1989): A simulation model of northern corn rootworm. Diabrotica barberi, population dynamics, oviposition: significance of host-plant phenology. - Can. Ent. 121: 169-191.

http://www.ecology.uni-corvinus.hu ● ISSN 1589 1623

[44] Őszi, B., Ladányi, M., Hufnagel, L. (2005): Population dynamics of the sycamore lace bug, Corythucha ciliata (Say) (heteroptera: tingidae) in Hungary. -Applied Ecology and Environmental Research, 4(1): 135-150.
[45] Paegle and McLawhorn (1983): Correlation of nocturnal thunderstorms and boundary-layer convergence. - Monthly Weather Review 101: 877-933.
[46] Porter, J.H., Parry, M.L., Carter, T.R. (1991): The potential effects of climatic change on agricultural insect pests. - Agricultural and Forest Meteorology 57(1-3): 221-240.
[47] Powell, J.A., Logan, J.A (2005): Insect seasonality: circle map analysis of temperature-driven life cycles. - Theoretical Population Biology 67(3): 161-179.
[48] Schwert, D.P., Anderson, T.W., Morgan, A., Morgan, A. V., Karrow, P. F. (1985): Changes in late Quaternary vegetation and insect communities in southwestern Ontario. - Quaternary Research, 23(2): 205-226.
[49] Seppelt, R. (1999): Applications of optimum control theory to agro-ecological modelling. - Ecological Modelling 121(2-3): 161-183.
[50] Seppelt, R. (2000): Regionalised optimum control problems for agro-ecosystem management. - Ecological Modelling. 131(2-3): 121-132.
[51] Seppelt, R. (2001): Agro-ecosystem Management. - In: J. Pinter (ed.): Global Optimization & Selected Case Studies, Kluver, Dordrecht, New York.
[52] Sharon, R., Degani, G., Warburg, M. (2001): Comparing the soil macro-fauna in two oak-wood forests: does community structure differ under similar ambient conditions? - Pedobiologia 45(4): 355-366.
[53] Strand, J.F. (2000): Some agrometeorological aspects of pest and disease management for the 21st century. - Agricultural and Forest Meteorology 103(1-2): 73-82.
[54] Varga-Haszonits, Z. (2003): Az éghajlatváltozás mezőgazdasági hatásának elemzése, éghajlati szcenáriók, - "Agro-21" Füzetek 31: 9-28.
[55] Vásárhelyi, T., Hufnagel, L. (1990): A platánfa légies átka. - Élet és Tudomány 1990(30): 940-942.
[56] Volney, W.J.A., Fleming, R.A. (2000): Climate change and impacts of boreal forest insects. - Agriculture, Ecosystems & Environment 82(1-3): 283-294.
[57] Whinam, J., Chilcott, N., Bergstrom, D.M. (2005): Subantarctic hitchhikers: expeditioners as vectors for the introduction of alien organisms. - Biological Conservation 121(2): 207-219.

http://www.ecology.uni-corvinus.hu ● ISSN 1589 1623

REDUNDANCY ANALYSIS OF THE INFLUENCE OF METAL CONTENT AND OTHER EDAPHIC PARAMETERS ON THE CO-EXSISTENCE OF *TRICHODERMA* SPECIES

Z. NAÁR* - A. DOBOS

Eszterházy Károly College
H-3300 Eger, Leányka str. 6., Hungary
(phone: +36-36-520-400; fax: +36-36-520-446)

**e-mail: naarzo@ektf.hu*

(Received 10th Sep 2005, accepted 10th Oct 2006)

Abstract. The growth requirements of *Trichoderma* fungi that are wide spread saprotrophic soil micro-organisms, are quite similar, therefore it is essential to define the environmental factor(s) along which they divide the available ecological niches. For this reason, we determined chemical and physical properties of 24 soil samples from different localities of Hungary, the presence of *Trichoderma* species and the relationships between two groups of data were analyzed with different statistical methods. The coexistence of 13 identified *Trichoderma* spp. proved to be a general phenomenon, which provided a good opportunity to explore the dividing environmental factors. Only redundancy analysis gave a reasonable model from 26 abiotic soil parameters. However, the number of variables was two times higher than that of species, thus the model was built in step-by-step process during which the explanation power of parameters was assessed with Monte Carlo permutation test. The best possible model of 13 soil properties explained 66.19 % of variance in the occurrence of *Trichoderma* species. Their positions in the triplots showed the separation of their niches along some of the investigated abiotic environmental variables. The available Zn-content had the highest explaining power however the in vitro zinc tolerance test did not justify its importance.
Keywords: *Trichoderma spp., coexistence, edaphic parameters, redundancy analysis, niche separation*

Introduction

Trichoderma species are worldwide spread common soil microorganisms and have a potential in biological control of plant pathogenic fungi [1]. In spite of their abundance and importance as litter decomposers as well as biocontrol tools, their ecology is not well understood considering their occurrence and coexistence. Although these species are often isolated from various samples containing organic materials [8], difficulties of their exact taxonomic identification have slowed the development of their ecology. The morphologically and physiologically similar *Trichodermas* are often represented by more than one species in the same habitat [24, 25, 26]. This phenomenon raises the need for detailed study, how they avoid the competitive exclusion [11]. The possibilities for niche separations are the differences in exploited microhabitat, utilized substrates and/or period of activity [21]. Advances on the coexistence of *Trichoderma* spp. were restricted to the clarification of the role of temperature. It was established that the sympatric species might share their available ecological space along the fluctuating temperature through seasons: the cold adapted ones like *T. polysporum* and *T. viride* proliferated from autumn to spring, whereas the other species having higher growth temperature optima (like *T. harzianum* and *T. koningii*) were more active during

http://www.ecology.uni-corvinus.hu ● ISSN 1589 1623

summer [26]. To our knowledge, no further abiotic environmental parameters were investigated in details to explain the coexistence of *Trichoderma* spp.

The aims of this study were to clarify the possible role of several abiotic soil characteristics on the occurrence of *Trichoderma* spp. in various soil types and to reveal whether the expected niche separation can be observed along those environmental parameters.

Materials and methods

Soil samples

Soil samples were collected late Spring at 24 localities to represent each main soil types occurring in Hungary. All of sampling sites were arable fields of various cultivation history with exception of site Sopron where the sample was collected from a beech forest. After removing plant debris from the surface, about 10 kg soil of A-horizon was taken in plastic bag from 1 m^2, and was left opened to preserve aerobic conditions. Soil samples were stored at a dry cool place until using within two weeks.

Physico-chemical analysis of soil samples

Each sample was thoroughly homogenized and subsample of 1 kg was taken to determine the following 24 physico-chemical properties of soil: $pH_{(KCl)}$, compaction (according to Arany), $CaCO_3$ content, total water soluble salt content, amount of organic carbon as humus content; KCl-soluble Mg, nitrite+nitrate nitrogen, and ammonium content; EDTA+KCl soluble Cu, Zn, Mn content; ammonium-lactate soluble K_2O, Na, and P_2O_5 content; granulometric composition: pebble (>5 mm), gravel (2-5 mm), total sand (0.02-2 mm) separated to coarse sand (0.5-2 mm), medium sand (0.2-0.5 mm), small sand (0.1-0.2 mm), fine sand (0.05-0.1 mm), very fine sand (0.02-0.05 mm), silt (0.002-0.02 mm), clay (<0.002 mm). The measurement of the above parameters was made by Hajdú-Bihar County Station of Plant Protection and Soil Preservation Department (Debrecen) according to the Hungarian Standards.

Isolation and identification of **Trichoderma** *fungi*

A modified washing and plating method [20] was used to check the presence of *Trichoderma* fungi in soil. Subsample of 200 g soil was blended for 30 s with 350 cm^3 sterile tap water and sieved through 0.1 mm mesh. The remained material were placed in the apparatus and washed with continuous flow of sterile tap water (0.3 dm^3min^{-1}) to obtain particles that are colonized by growing hyphae. After 20 min washing during which the apparatus was gently shaken on orbital shaker (20 rev min^{-1}), 50 randomly chosen particles of 1-2 mm fraction were plated in *Trichoderma*-selective medium [2] containing Petri dishes (120 mm diam.) in five replicates. Plates were than incubated for 10 days at 22 ºC under continuous fluorescent light. Pure culture of each developing colonies were prepared by transferring of hyphal inoculum on PDA (Oxoid) slants. For identification, the macroscopic features of pure grown colonies were observed on oatmeal agar, potato-dextrose agar, or malt-extract agar, and the microscopic ones were surveyed with lactophenol cotton-blue staining. *Trichoderma* isolates were taxonomically identified [22, 3, 4, 5, 6].

http://www.ecology.uni-corvinus.hu ● ISSN 1589 1623

Measurement of zinc tolerance of T. harzianum *strains*

The zinc content proved to the most effective explanatory factor for variance of *Trichoderma* spp. therefore we assessed their reaction to the zinc concentration measured in the particular soils, and determined the minimum inhibitory concentration that cause total lack of spore germination. *T. harzianum* strains were used because this species occurred in 22 of 24 soil samples. Spore suspensions were prepared from 5 days old cultures and 1-15 mM concentration series of $ZnSO_4$ solution made in 2 % pepton water was inoculated in microtiter plates with three replications. Lack of germination was registred after 48 hours of incubation at 25 ºC.

Statistical analysis

Although the population density of *Trichoderma* spp. was counted as number of colony developing soil particles, the presence data (+ or -) of particular species were used for statistical analysis because some unmeasured environmental factors (such as season history of soil temperature and water content) might greatly influence the population size of particular species. The incidence of species was summarized in a co-occurrence matrix that showed the numbers of soils, from which two particular species could have been isolated. The theoretical probability of coexistence was calculated with multiplication of their observed incidence rates (number of incidence divided with 24, the number of soil samples). The observed probability was obtained with division of coexistence cases and the number of soil samples (24). Pearsons's non-parametric correlation analysis was performed to reveal the relationships between the occurrence of particular *Trichoderma* species and each of soil parameters as single factors. Before analysis, the data of 24 soil properties were classified into four groups according to quartiles. The soil type as complex parameter and the vegetation of collection site were also tested with codes listed in *Table 1*. The presence of *Trichoderma* species was introduced as presence-absence value of 1 or 0. Because of insignificant result of correlation analyses, redundancy analyses were performed to quantify the extent to which the occurrence of *Trichoderma* spp. can be explained by combinations of soil properties. The number of environmental variables was too high to introduce all of them in one analysis because it might not be higher than 13, the number of *Trichoderma* species. Therefore, a forward selection of variables was achieved, in tandem with Monte Carlo Permutation test. The randomization was performed as similar as McCune [18] did it. Shuffle of the environmental matrix (variables on the right) by rows preserved the species matrix and the structures of correlations among soil parameters but it destroyed the relationship between species and environmental data. One hundred randomizations of 576 possible different permutations were used for each analysis. Those ordinations were accounted to be significant, of which total explained species matrix variation were higher than that of at least 95 randomizations. The RDA process was carried out with SYNTAX 2000 [1].

Results

Occurrence of Trichoderma fungi in various soil types

Trichoderma fungi were present in all of 24 soil samples.The number of species inhabiting the same soil ranged from 1 to 5. No conspicues relationship could be found

http://www.ecology.uni-corvinus.hu ● ISSN 1589 1623

between the soil type and the species composition. Three species hosting soils were found most commonly, in 7 of 24 cases. It was followed by single and two species hosting soils (5-5 samples). Four species were found in four samples, five species were isolated from three ones. Soils hosting single species had some extreme properties: high salt content in solonchak-solonetz (Sample 16), solonchak (Sample 17), high organic matter content in peat soil (Sample 24), raw texture in alluvial soil (Sample 22). However, one of two pseudomycelier chernozem soils (Sample 4) that had neither extreme property hosted also only one species. In contrast, three species could be isolated from the other sample of this soil type (Sample 5). In four of five cases, *T. harzianum* was found in these soils, and *T. viride* was isolated from one single species hosting soil. The five species hosting soils belonged also to different main soil types: meadow chernozem with salt accumulation in the deeper layers (Sample 8), rust-colored forest soil (Sample 13), and solonetzic meadow soil (Sample 21). Their species composition differed greatly; no common species were detected.

Coexistence of Trichoderma spp.

Trichoderma spp. associated with different ranges of other species (not shown) suggesting some associability. There was no species, which would associate with all the other 12 species or with no other species. Although *T. harzianum* was detected in 20 of 24 soil samples, and it coexisted with 10 of 12 other species. *T. harzianum* never coupled with *T. koningii* or *T. hamatum* raising the possibility of their competitive exclusion by *T. harzianum*. However, it coupled frequently with *T. virens*: in 13 soil samples of possible 14 cases, which gave higher observed probability ($p = 0.542$) than the theoretical one ($p = 0.486$) for common occurrence. Similar tendency was found for the relationship of *T. harzianum* to *T. atroviride*. The theoretical probability of coexistence of *T. harzianum* with *T. viride* was the same as the observed one, thus, their coexistence seemed to be rather a random phenomenon. In contrast, the difference between the observed and the theoretical frequency of common existence of *T. harzianum* with *T. tomentosum* was considerably (by 9.7 %) lower, suggesting some competence between them. The case was similar for the occurrence of *T. tomentosum* with *T. virens*, which was not a surprise considering the common occurrence of *T. harzianum* and *T. virens*. The rare species (*T. koningii*, *T. hamatum*, *T. longipilis*, *T. polysporum*, *T. strigosum,* and *T. strictipilis,*) that have only one representative, never coupled with one another, with the exception of the first two species that were found in the same soil sample.

Table 1. *Collection site, soil type, vegetation and occurring Trichoderma fungi of applied soil samples in Hungary.*

No.	Origin	Soil type (code)	Vegetation (code)	Trichoderma species
1	Gödöllő	humous sandy soil (1)	tomato 81)	*T. harzianum, T. virens*
2	Mélykút	chernozem-type sandy soil (1)	wheat (2)	*T. harzianum, T. virens*
3	Izsák	calcareous blown sand (1)	rye (2)	*T. harzianum, T. virens*
4	Nagyigmánd	pseudomycelier chernozem (2)	corn (1)	*T. harzianum*
5	Érd	pseudomycelier chernozem (2)	corn (1)	*T. harzianum, T. virens, T. viride*
6	Martonvásár	chernozem brown forest soil (2)	wheat (2)	*T. atroviride, T. harzianum, T. virens, T. viride,*

http://www.ecology.uni-corvinus.hu ● ISSN 1589 1623

No.	Origin	Soil type (code)	Vegetation (code)	Trichoderma species
7	Kondoros	lowland chernozem (2)	wheat (2)	*T. harzianum, T. virens, T. viride, T. minutisporum*
8	Nagyszénás	lowland chernozem with salt accumulation in the deeper layers (2)	corn (1)	*T. atroviride, T. harzianum, T. virens, T. longipilis, T. tomento-sum,*
9	Csanádapáca	meadow chernozem (2)	wheat (2)	*T. harzianum, T. virens, T. viride, T. polysporum*
10	Székkutas	meadow chernozem with salt accumulation in the deep (2)	sunflower (1)	*T. harzianum, T. virens*
11	Kapoly	brown earth (3)	potato (1)	*T. tomentosum, T. minutisporum*
12	Sopron	brown forest soil (3)	beach forest (3)	*T. atroviride, T. harzianum, T. viride, T. tomentosum*
13	Máriabesnyő	rust-coloured forest soil (3)	wheat (2)	*T. viride, T. tomentosum, T. hamatum, T. koningii, T. spirale*
14	Nagyrécse	brown forest soil with clay illuviation (3)	corn (1)	*T. harzianum, T. virens, T. viride*
15	Lenti	pseudogley (3)	corn (1)	*T. harzianum, T. virens, T. spirale*
16	Kunszentmik-lós	solonchak-solonetz (4)	rape (2)	*T. harzianum*
17	Apaj	solonchak (4)	sunflower (1)	*T. viride*
18	Mezőtúr	meadow solonetz turning into steppe formation (4)	corn (1)	*T. harzianum, T. strigosum, T. viride*
19	Szentes	meadow solonetz (4)	sunflower (1)	*T. harzianum, T. virens, T. viride*
20	Szászberek	meadow soil (5)	alfalfa (3)	*T. atroviride, T. harzianum, T. virens,*
21	Szarvas	solonetzic meadow soil (5)	corn (1)	*T. atroviride, T. harzianum, T. strictipilis, T. virens, T. viride*
22	Vág	alluvial soil (6)	alfalfa (3)	*T. harzianum*
23	Pörböly	alluvial soil with high humus content (6)	corn (1)	*T. atroviride, T. harzianum, T. viride*
24	Nádasdladány	partly decomposed peat (7)	sunflower (1)	*T. harzianum*

Selection of important environmental variables with redundancy analysis

Redundancy analyses were performed to find significant relationships between soil parameters and the presence of *Trichoderma* fungi, because the correlation analysis between did not reveal any noteworthy relationship. There was a problem during the redundancy analyses (RDA): the number of soil parameters two fold exceeded the maximum testable number of environmental variables that may not be higher than number of species. Thus, selections were carried out among the parameters in two groups of 13 chemical properties and the other 13 ones (11 physical properties, soil main type and the vegetation of collection site as categories) and. At first, the weight of soil parameters (as explaining environmental variables on the right side) was assessed with exclusion of one at a time. Those variables were used as first one in model building of which exclusion resulted in the highest decrease of eigenvalue of axis 1 (having the highest explaining power for variance of species data). RDA of physical properties without pebble and that of chemical ones without zinc content had the least explaining power, thus, these two parameters were used for model building with

http://www.ecology.uni-corvinus.hu ● ISSN 1589 1623

stepwise selection. For this process, all of the soil properties (with exception of starting ones) were used. They were tried to introduce one by one, RDA was carried out, and the sum of eigenvalues of axis 1 and 2 was calculated. In each step, that variable was built in, which caused the highest increase in summed eigenvalue. All new ordinations were tested for significance with Monte Carlo Method as described in Materials and methods. The model based on the pebble content proved not to be significant when the zinc content was not introduced, thus, we finished the model building only with zinc content based one. The introduction order of further variables was as follows: clay, K_2O, P_2O_5, Cu, $CaCO_3$, Mn content, rate of silt, NH_4 content, vegetation, rate of coarse sand, total sand rate, and $pH_{(KCl)}$. The ordination remained statistically significant until the introduction of the thirteenth variable. Moreover, further variables seemed to be introducible, when they were changed with the last one, however, they should have been omitted because of reaching of the maximum number of the model.

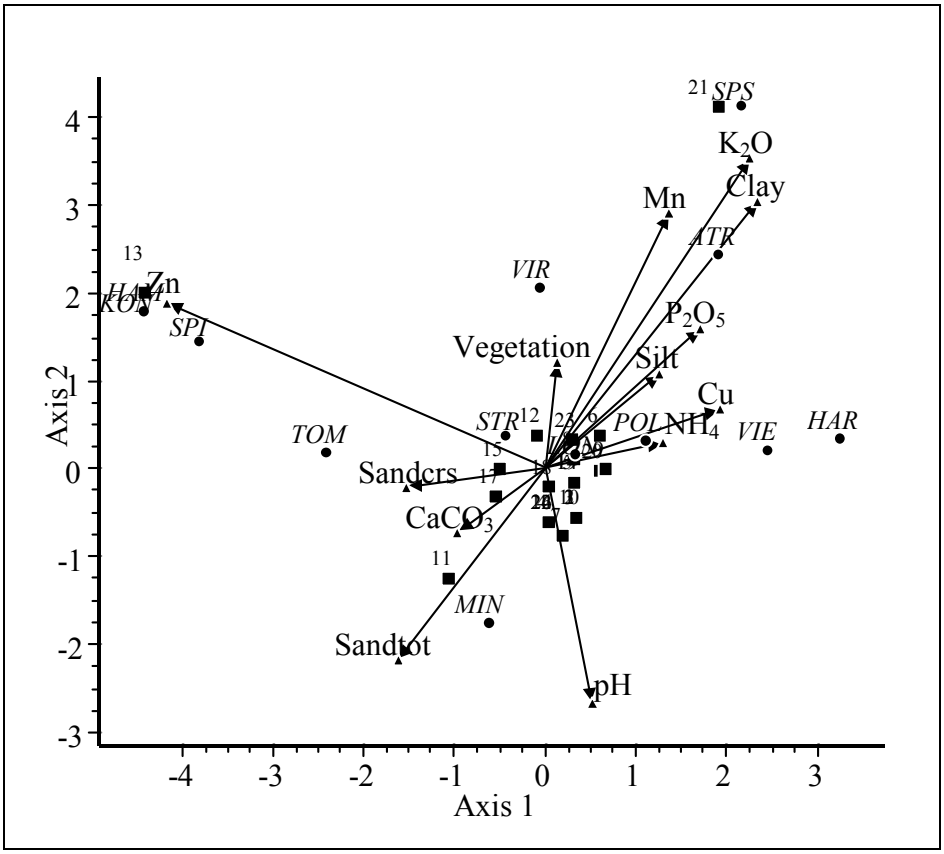

Figure 1. *The most effective ordination of 24 soil samples as objects, 13* Trichoderma *species as variables on the left, and 13 soil parameters as variables on the right. Soil samples as objects are marked with rectangles and numbers (Table 1).* Trichoderma *species are marked with circles and abbreviations in italic as follows: ATR – T. atroviride, HAM – T. hamatum, HAR – T. harzianum, KON – T.koningii, LON – T. longipilis, MIN – T. minutisporum, POL – T. polysporum, SPI – T. spirale, SPS– T. strictipilis, STR – T. strigosum, TOM – T. tomentosum, VIE – T. virens, VIR – T. viride. Soil parameters are marked with triangles.*

The abovementioned environmental variables of the best ordination (*Fig. 1*) explained total 66.18 % of variance in the species data. The eigenvalues of Axis 1 and 2

http://www.ecology.uni-corvinus.hu ● ISSN 1589 1623

were 3.17 and 1.99, respectively, and these axes together explained 39.71 % of species data variance. According to the high explaining power, they correlated closely (r = 0.957 and 0.937, respectively) with the occurrence of *Trichoderma* species. As the arrows show, the introduced environmental variables influenced the occurrence of *Trichoderma* spp. differently both in direction and the extent. According to the previous selection of the environmental variable, Axis 1, which is the most important in the evaluation of ordinations, was predominantly determined by the extractable Zn content of soil with r = -0.786 value (*Table 2*). Axis 2 was determined by more variables: extractable K_2O, Mn content, rate of clay, and $pH_{(KCl)}$.

Table 2. *Correlation of environmental variables with ordination axes obtained with redundancy analyzis and showed on Fig. 1.*

	Correlation with	
Environmental variables	Axis 1	Axis 2
Zn content (available)	-0.786	0.354
Clay content	0.443	0.574
K_2O content (available)	0.426	0.669
P_2O_5 content (available)	0.325	0.301
Cu content (available)	0.365	0.129
$CaCO_3$ content	-0.181	-0.138
Mn content (available)	0.26	0.549
Silt content	0.239	0.202
NH_4 content (available)	0.247	0.057
Vegetation of collection site	0.028	0.229
Coarse sand content	-0.288	-0.038
Total sand content	-0.304	-0.41
$pH_{(KCl)}$	0.1	-0.506

The species were rather scattered in the triplot, however, some associations also seemed to be present. The proximity of *T. harzianum* and *T. virens* supported their associability suspected from the coexistence matrix. The other frequent species (*T. viride* and *T. atroviride*) having representatives in at least 25 % of the soil samples were clearly separated from them. The close position of *T. hamatum* and *T. koningii*, or *T. strictipilis* and *T. strigosum* might be only random phenomenon, because they have only one representative pro species.

Measurement of zinc tolerance of Trichoderma *fungi*

The growth of the tested *T. harzianum* strains did not change significantly due to the zinc level measured in the originating soil samples. The minimum inhibitory concentration (MIC) that cause total lack of spore germination was always above the zinc content of given soil samples and differed by strains in the range 5-14.3 mM. No marked correlation could be revealed between available zinc content of soil and the MIC value of *T.harzianum* strain isolated from the particular soil sample (*Fig. 2*).

http://www.ecology.uni-corvinus.hu ● ISSN 1589 1623

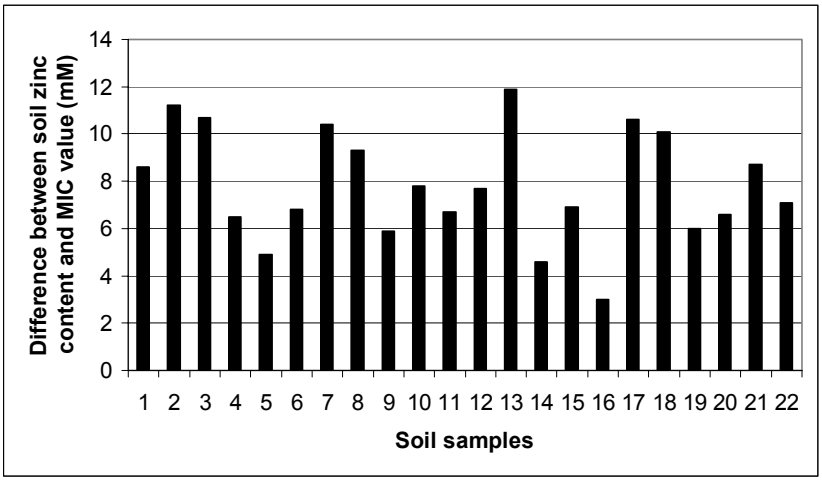

Figure 2. *The difference between available zinc content of soil samples and the minimum inhibitory concentration (MIC) of* T. harzianum *strains from the particular soil samples.*

Discussion

Trichoderma species were present in all of the 24 investigated soil samples even in the raw textured soil types, which allowed a detailed analysis of the influence of soil characteristics. There are only a few similar works dealing with detailed analysis of *Trichoderma* population of soils. In the most comparable work [23] the analysis of the *Trichoderma* population of 12 soil samples collected from apple orchards at various sites of Wisconsin was performed and the data about co-occurrence of *Trichoderma* species was also investigated and reported. Although the tested range of soil texture was wider in our investigation, we found a similar species co-occurrence. They found that the number of species occurring in any one soil varied from two to five. The rates of the soils hosting a particular number of *Trichoderma* species were similar. Also in the Wisconsin soils, the three species hosting soils were the most frequent. *T. harzianum* was found to be the most frequent species. The occurrence of *T. virens* was somewhat lower in Wisconsin (50 %) than in Hungary (58 %). A further disagreement that *T. viride* was rarer (25 % comparing to our 50 % data),

The common occurrence of *Trichoderma* spp. coupling with moderate number of species of the genus (compared to that of similarly common *Penicillium*) gave an excellent opportunity to test the influence of abiotic soil characteristics on their incidence. In redundancy analyzis (RDA), available zinc content of soil proved to be the most effective soil parameter as explanative environmental variable for the variance in the occurrence of *Trichoderma* species. Without it no significant ordination could be computed from those soil parameters (pH, organic matter or humus content, rate of sand, silt and clay) that were determined and published in the most soil microbiological and biocontrol studies. No other researchers observed that the amount of zinc exert so strong influence on the incidence of any soil fungus. Although there are numerous works dealing with impact of heavy metals among them zinc, on the growth and activity of *Trichoderma* fungi [10, 13, 14, 15, 16], no characteristic difference in the reaction to zinc was found among *Trichoderma* species. Our data on the zinc reaction of *T. harzianum* species agree with that statement. We assumed that the available zinc content lower than the minimum inhibitory concentration influences the growth and the survival indirectly through physiological processes in which this metal ion is involved.

http://www.ecology.uni-corvinus.hu ● ISSN 1589 1623

Further investigations are needed to clarify the fine differences between the studied species in the zinc requirement for survival in soil.

In earlier investigations, not all soil parameters that were combined with zinc content during redundancy analysis had been prove to exert more or less influence on the activity or population size of indigenous or applied *Trichoderma* fungi. The results of our work partly supported the findings of Duffy et al. [9]. The impact of percent clay, copper content, soil pH and available phosphorous content was strengthened, but not that of nitrate-nitrogen and soluble magnesium, which were omitted during our ordination analysis because of their less explanative value. Significant partial correlations between *Trichoderma* population size and calcium, magnesium, or manganese content of soil were found[7], but not for potassium content, agreeing with Duffy et al. [9]. Contrary, we found the extractable potassium content to be the third most important environmental variable (see *Table 2*). Beyond litter quality, organic matter, pH, KCl-extractable ammonium and phosphate were responsible for the differences in fungal communities of different birch stand sites [17]. All of these soil characteristics were among the thirteen most effective environmental variables in our investigation. Earlier it was concluded that the abiotic characteristics of soil are of less importance on the population size of *Trichoderma* species [23, 26]. In our investigation, however, the combinations of the abiotic soil parameters explained 66.19 % of variation of species occurrence, and further soil parameters seemed to have influence, but their introduction was not allowed because of number restriction of explanative variables in RDA.

The niche separation of *Trichoderma* spp. was supported by our work: the species were widely scattered trough the triplot (*Fig. 1*). In accordance with many works, it was found that their co-occurrence is a common phenomenon, which had to be accounted for type of niche separation [11]. It was summarized that the possibilities of separation in three types: exploited microhabitat, utilized substrates, time of activity [21]. The seasonal fluctuation of the soil water content and the temperature might be among of the abiotic environmental variables along which the sympatric *Trihoderma* spp. shared their microhabitat [26]. These findings were demonstrated under laboratory conditions, too [25]. To our knowledge, however, there were no studies carried out that would give evidence for niche separation along other abiotic soil characteristics. The relative position of the detected species are quite fare from one another with exception of *T. harzianum* and *T. virens* suggesting that they share the ecological niche along the studied soil parameters. These two species may do it along other, not investigated environmental parameter(s). Thus, the often-used soil parameters such as organic matter content, pH, sand-silt-clay ratio appeared to be good predictors, but not the best for the occurrence of *Trichoderma* spp, because the combination of zinc, clay, copper, potassium and phosphorous content explained considerably higher part of variance in species occurrence data. The often-isolated species seemed to have fairly separated niches that might explain their co-occurrence.

Acknowledgement. The partial support of the Hungarian Research Fund (OTKA F036445) is highly acknowledged. The authors wish to thank for valuable comments of J. Podani and B. McCune on ordination tests.

http://www.ecology.uni-corvinus.hu ● ISSN 1589 1623

REFERENCES

[1] Anonymous (2001): SYNTAX 2000. Computer programs for data analysis in ecology and systematics. User's Manual. - Scientia, Budapest. pp. 67.
[2] Askew, D.J., Laing, M.D. (1993): An adapted selective medium for the quantitative isolation of *Trichoderma* species. – Plant Pathology 42: 686-690.
[3] Bissett, J. (1991a): A revision of the genus *Trichoderma*. II. Infrageneric classification. – Canadian Journal of Botany 69: 2357-2372.
[4] Bissett, J. (1991b): A revision of the genus *Trichoderma*. III. Section *Pachybasium*. – Canadian Journal of Botany 69: 2373-2417.
[5] Bissett, J. (1991c): A revision of the genus *Trichoderma* IV. Additional notes on section Longibrachiatum. – Canadian Journal of Botany 69: 2418-2420.
[6] Bissett, J. (1992): *Trichoderma atroviride*. – Canadian Journal of Botany 70: 639-641.
[7] Bulluck III, L.R., Brosius, M., Evanlyo, G.K., Ristaino, J.B. (2002): Organic and syntehtic fertility amendments influence soil microbial, physical and chemical properties on organic and conventional farms. – Applied Soil Ecology 19: 147-160.
[8] Domsch, K.H., Gams, W. Anderson, T.H. (1980): Compendium of soil fungi. Vol. 1. - Academic Press, London, England. pp. 794-809.
[9] Duffy, B., Ownley, B.H., Weller, D.M. (1997): Soil chemical and physical properties associated with suppression of take-all of wheat by *Trichoderma koningii*. – Phytopathology 87: 1118-1124.
[10] Gadd, G.M., Ramsay, L., Crawford, J.W., Ritz, K. (2001): Nutritional influence on fungal colony growth and biomass distribution in response to toxic metals. – FEMS Microbiology Letters 204: 311-316.
[11] Hardin, G. (1960): The competitive exclusion principle. - Science 131: 1292-1297.
[12] Köhl, J., Schlösser, E. (1988): Occurrence and temperature requirements of four Trichoderma species from different regions and substrates. - Angewandte Botanik 62: 301-309.
[13] Kredics, L., Dóczi, I., Antal, Zs., Manczinger, L. (2001): Effect of heavy metals on growth and extracellular enzyme activities of mycoparasitic *Trichoderma* strains. – Bulletin of Environmental Contamination and Toxicology 66: 249-254.
[14] Kredics, L., Antal, Zs., Manczinger, L., Nagy, E. (2001): Breeding of mycoparasitic *Trichoderma* strains for heavy metal resistance. – Letters in Applied Microbiology 33: 112-116.
[15] Kredics, L., Antal, Zs., Manczinger, L., Nagy, E. (2001): Isolation and characterization of heavy metal resistant mutants from mycoparasitic *Trichoderma* strains. – IOBC-WPRS Bulletin 24: 233-236.
[16] Ledin, M., Krantz-Rülcker, C., Allard, B. (1999): Microorganisms as metal sorbents: comparson with other soil constituents in multi-compartment systems. – Soil Biology and Biochemistry 31: 1639-1648.
[17] McLean, M. A., Huhta, V. (2002): Microfungal community structure in anthropogenic birch stands in central Finland. – Biology and Fertility of Soils 35: 1-12.
[18] McCune, B. (1997): Influence of noisy environmental data on canonical correpondence analysis. – Ecology 78: 2617-2623.
[19] Papavizas, G.C. (1985): *Trichoderma* and *Gliocladium*: biology, ecology, and potential for biocontrol. – Annual Review of Phytopathology 23: 23-54.
[20] Parkinson, D., Williams, S.T. (1961): A method for isolating fungi from soil microhabitats. – Plant and Soil 13: 347-355.
[21] Pianka, E. R. (1978): Evolutionary ecology. - Harper and Row, New York. pp. 416.
[22] Rifai, M.A. (1969): A revision of the genus *Trichoderma*. – Mycological Papers of Commonwealth Mycological Institute, Kew, Surrey, England, 116: 1-56.

http://www.ecology.uni-corvinus.hu ● ISSN 1589 1623

[23] Roiger, D.J., Jeffers, S.N., Caldwell, R.W. (1991): Occurrence of *Trichoderma* species in apple orchard and woodland soils. – Soil Biology and Biochemistry 23: 353-359.
[24] Söderström, B.E., Bååth, E. (1978): Soil microfungi in 3 Swedish coniferous forests. – Holarctic Ecology 1: 62-72.
[25] Widden, P. (1984): The effects of temperature on competition for spruce needles among sympatric species of *Trichoderma*. – Mycologia 76: 873-883.
[26] Widden, P., Abitbol, J.-J. (1980): Seasonality of *Trichoderma* species in a spruce-forest soil. – Mycologia 72: 775-784.

http://www.ecology.uni-corvinus.hu ● ISSN 1589 1623

DEVELOPMENTAL STAGE RESPONSE OF PEARL MILLET DOWNY MILDEW (SCLEROSPORA GRAMINICOLA) TO FUNGICIDES

S.A. DEEPAK[1] – P. BASAVARAJU[1] – G. CHALUVARAJU[1] – N.P. SHETTY[1] - G. OROS[2] - H. SHEKAR SHETTY[1]*

[1]*Downy Mildew Research Laboratory, Department of Studies in Applied Botany, Seed Pathology and Biochemistry, University of Mysore Manasagangotri, Mysore 570 006, Karnataka, India*

[2]*Plant Protection Institute HAS H-1525 Budapest 114, Pf. 102, Hungary*

**e-mail: hss@appbot.uni-mysore.ac.in*

(Received 10th Sep 2005, accepted 10th Oct 2006)

Abstract: Inhibitory effect of 21 commercial and 6 experimental fungicides was assessed in model experiments against pearl millet downy mildew disease. Chemicals differed strongly by their anti-mildew activity, however neither the pathogen nor the host plant showed complete tolerance to any of compounds tested. Nevertheless, the plants outgrew depressant effect of compounds observed in germling stage and this activity did not significantly influence the yield. There was a significant correlation between yield performance and disease inhibitory effects assessed either *in vitro* or *in vivo* tests. The response of pathogen to investigated compounds varied during ontogeny, where zoosporangium formation was found to be the most sensitive ontogenetic event. When comparing responses of pathogen and host with fungicides by means of principal component analysis, the presence of two independent components has been demonstrated accounting for 86% of the total variation to which responses of host and pathogen contributed differently.

The antisporulant activity of compounds evaluated on detached leaf segments and their positive effect on yield significantly correlated allowing to predict the expectable grain yield significantly ($p>0.05$). Beside acylanilides andoprim, drazoxolon and efosit offered efficacy on the level requested. Metalaxyl and tridemorph as well as andoprim and cymoxanil acted synergistically against *S. graminicola.*

Keywords: *ontogeny, fungicide screening, yield performance, synergy*

Introduction

Pear millet (*Pennisetum glaucum* (L.) R. Br.), a crop of international importance, is indigenous to areas in North Africa [2]. Today, its production is centred in semiarid-tropical zone [49] but it is a reliable double-crop after wheat for some regions of Holarctic.zone, particularly at the southern altitudes 50° in Europe and 40° in USA [16]. This plant has good drought tolerance, so it could withstand some of the late summer droughts in the marked area. The vegetation period of highly productive pearl millet varieties and hybrids is short; it is possible to harvest a mature crop 60 to 65 days after plantation. Many diseases of pearl millet have been described worldwide [65], however, catastrophic fungal diseases had not been known before Indian pandemic caused by downy mildew in 1985. The disease was known in most of the pearl millet growing areas but it remained sporadic until introduction of high yielding hybrids with susceptible parent line [49]. The causative agent *Sclerospora graminicola* (Sacc.) Schroet., originally described from Europe [44], was probably introduced into new

http://www.ecology.uni-corvinus.hu ● ISSN 1589 1623

areas in infected seeds various weeds contaminating grains [61]. Pearl millet downy mildew recently is distributed worldwide and one of the most important diseases causing losses up to 60% of grain yield [32].

Review of literature

S. graminicola, like other oomycetes, has a complex life cycle where developmental forms differ essentially in their anatomy and physiology, as well as having different impacts host/parasite interactions, survival and distribution in space and time. Zoosporangia produced during the night, and at over 70 percent relative humidity [60], germinate directly either by germ-tubes, or by releasing 1 to 12 zoospores, which encyst and germinate by a germ-tube. Sexual oospores are produced in colonised plant tissue and can survive to several years. Asexual spores spread the disease between plants, whilst within plants the pathogen spreads intercellularily. Sexual oospores can travel large distances and can survive several seasons [26, 47, 49]. Progenies of the same oospore could be classified into several distinct pathotype groups [55] indicating that it shows high natural variation in agressivity [7]. One could expect the similar variation in sensitivity to chemical control measures as well. Widespread and regular cultivation of susceptible F_1 hybrids led to accumulation of oospore inoculum in the soil that resulted in epidemics in 1971-72. Since than PDMD epidemics cause considerable economic losses in India [3, 43, 49]. Epidemics have also been reported from Asia and Africa [65] and this disease has been the major biotic factor affecting grain yield for the last decades [51, 53]. The pathogen can be transmitted to new areas by wind and infected seeds [53].

S. graminicola can be controlled efficiently with systemic fungicide metalaxyl [14, 31, 63]. Seed dressing with Apron 35SD (6 kg/t seeds) in pearl millet growing regions of India and foliar application of Ridomil MZ72 (2 kg/ha) for seed crop were recommended [50]. Possibilities of biocontrol measures [57] and enhancement of plant resistance with chemical treatment [46] has also been explored.

Resistance to PMDM in some pearl millet cultivars was found [54, 56] which have been cultivated widely [3, 47]. However, the vulnerability of their resistance to the disease has been a major cause of concern, as even 10 % disease incidence cause economic loss. New pathogenic races may overcome the genetic resistance. In the populations of phylogenetically related pathogens (*Bremia* [12, 62], *Peronosprora* [29], *Plasmopara* [40, 59] and *Phytophthora* [36]) resistance to metalaxyl has observed demonstrating the necessity to have alternative fungicides for PMDM control as well.

Responses of *S. graminicola* to various fungicides have been repeatedly tested, however there were difficulties to compare data obtained by different authors because of alterations in screening methods, moreover, the tests were limited in most of cases to screening only one of ontogenetic developmental stages. For this reason, anti-mildew efficacy of 21 commercial and 6 experimental compounds, with known and diverse mode of action, were compared in a highly standardized model experiment. Spectrum of activity on various developmental forms of *S. graminicola* was investigated, the responses of subsequent ontogenetic stages were compared and the effects on host plant as well as on the yield performance were evaluated.

http://www.ecology.uni-corvinus.hu ● ISSN 1589 1623

Materials and Methods

Host-parasites system

The downy mildew pathogen *S. graminicola* (pathotype 1) was isolated from naturally infested plants (hybrid HB3) in Bogadi village of Mysore district (Karnataka state, India) during 1970 by Shetty. The strain was maintained on greenhouse grown plants before being used as inoculum for the experiments. The pearl millet hybrid HB3 - highly susceptible to downy mildew - was used throughout the experiments. The plants for *in vitro* studies were grown on in 4 kg pots (20 plant per pot) filled with a mixture of soil, sand and manure (1:1:1) in green-house.

Preparation of inoculum. Leaves were collected from systemically infected 21 day-old plants in the evening. Previously formed zoosporangia were eliminated from the surface by washing in tap water and the exess of water was removed. Then leaves were incubated in a moist chamber at 25±2 ^{o}C overnight (12-14 hours). Zoosporangia were collected by washing them off with sterile distilled water, and the resulting suspension incubated for 15 min to release zoospores. The concentration of zoospores was adjusted by adding sterile distilled water to 4×10^4 cells/ml using haemocytometer, and this suspension was used for inoculation of the plants at first true leaf stage. The method was described in detail by Safeulla [42].

Chemicals

The compounds tested are listed in *Table 1*. Stock solutions (0.2 M) were prepared and the dilutions of the same were used for all the experiments.

Biological activity studies

Developmental stage dependent responses of the pathogen and reactions of the host plant to chemicals were studied both *in vitro* and *in vivo*. The activity of compounds determined according to appropriate scale was transformed into percent inhibiton at the given dose. The dose response lines were fitted using log probit function and the biological activities expressed as EC_{50} values. The protective effect of compounds (percent disease control) was measured both in greenhouse and field conditions at maximum dose tolerated by the host plant.

The effect of fungicides on host-dependent (HD) stages of *S. graminicola* was determined by following methods:

Sporulation (zoosporangiogenesis): Leaves with disease symptoms were collected from infected plants and washed in distilled water, exess water was then removed. The leaves were cut into ≈1 cm^2 pieces which were subsequently smeared with solution of test compound of appropriate concentration (10 μL of 0.01, 0.25, 0.5, 1.0 and 2.0 μM for a single piece). Treated pieces were incubated in moist chambers (plastic trays lined with wet filter paper) at 22 ^{o}C in the dark. To determine the intensity of sporulation, a 0-4 scale was used where the proportion of leaf area covered by zoosporangia was graded as follows: 0, no sporulation; 1-4, sporulation appearing on < 25, 25-75, 75-<100 % and total area, respectively.

Production of zoospores: Zoosporangia were collected from leaf segments in each treatment (1 mL sterile distilled water per piece). The sporangial suspension was incubated for 15 min, than centrifuged at 20-40 g for 10 min. The number of zoospores released was counted in the supernatant using a haemocytometer.

http://www.ecology.uni-corvinus.hu ● ISSN 1589 1623

To assess the effect of fungicides on host-independent (HI) stages in the fungal life-cycle, the effects on zoospore release and zoospore motility were recorded. Both events were observed microscopically in suspensions of spores mixed in 1:1 ratio (v/v) with fungicide solutions of appropriate concentrations to achieve a final spore number at 10-50 $\times 10^4$ cell per ml as well as 0.1, 0.5, 1.0, 2.0 and 4.0 mM concentration of test chemicals. After 15 min the proportion of empty sporangia was determined microscopically.

Zoospore motility: Released zoospores were separated from the zoosporangium suspension prepared as above by centrifugation at 20-40 g. The resulting supernant was adjusted with distilled water to 5×10^4 zoospores per ml. This suspension was treated with the test chemicals as above, and intensity of motion assessed after 15 min incubation.

Phytotoxicity limits for test compounds were determined by examining their effects on seed germination and seedling vigour. Pearl millet seeds were soaked in solutions of test compounds at appropriate concentrations (1 g per 2 ml for 6 hours). After treatment the seeds were used for further experiments. Seeds treated with sterile distilled water by the same manner served as control. Effects on seed germination *in vitro* were determined according to rules of ISTA [4] counting the number of germinated seeds after 4 days of incubation. The ratio of inhibiton was expressed as a percentage related to the watery control. The vigour index was calculated according to following formule [1];

Seedling vigour (SV) = (RL + SL) × SG where RL and SL = average length of roots and shoot of seedlings after seven days, SG = percentage ratio of germinated seeds in the given Petri dish (n=25 per set).

Preventive anti-mildew activity of test compounds was evaluated both in greenhouse and field experiments. The pearl millet seeds treated at maximum tolerated concentration of chemical were sowed into soil and the seedlings artificially infected with *S. graminicola*. All plants lacking visible symptoms (sporulation, yellowing, stunted growth and malformed ear-heads) were taken as healthy. The activity of each compound was calculated as percent decrease in disease incidence as compared to water control. Field trials were conducted in experimental station of Mysore University (N12°18', E76°39', 733 m altitude, red loam soil) during the rainy seasons Monsoon.

Greenhouse grown two-day-old seedlings were inoculated at whorl region with zoospore suspension (4×10^4 cell/ml) and maintained in daylight regime. Disease incidence was recorded after 10^{th} days. The field screening was conducted in the downy mildew nursery plot by adopting the procedures of Williams [64]. The treated seeds were sown in a randomised block design with four replicates. Normal agronomic practices were followed. The disease incidence was evaluated at 60 days after sowing. The ratio of diseased vs. healthy plants was calculated as compared to the water control in both cases.

Assessment for pearl millet grain yield. The treated seeds with untreated checks were sown in subplots (12 m^2 of each) consisting of four 4 m rows 75 cm apart. Plants were about 15 cm apart with in the rows. Four replicates were maintained for each treatment in a randomised split plot design. The grain yield was collected from the central 3.8 m of the two central rows (net plot size 5.7 m^2), measured and the result provided into kg/ha.

http://www.ecology.uni-corvinus.hu ● ISSN 1589 1623

Table 1. *List of chemicals tested*

No.	Common name	Chemical Name	Log P[f]	Trade name	Producer
1[b]	Metalaxyl	methyl *N*-(2-methoxyacetyl)-*N*-(2,6-xylyl)-*DL*-alaninate	1.86	Ridomil 25 wp	Ciba-Geigy, Swiss
2[c]	CGA29212	methyl *N*-(2,6-dimethylphenyl)-*N*-chloroacetyl-*DL*-alaninate	2.11	experimental	Ciba-Geigy
3[c]	RE-26745	*N*-(2,6-dimethylphenyl)-2-methoxy-*N*-(2-oxo-tetrahydro-furan-3-yl)-acetamide	1.47	experimental	Chevron, USA
4[b]	Ofurace	α-2-chloro-*N*-2,6-xylylacetamido-γ-butyrolactone	1.80	Milfuram 50 wp	Chevron
5[b]	Furalaxyl	methyl-*N*-(2,6-xylyl)-N-(2-furanylcarbonyl)-*DL*-alaninate	3.64	Fongarid 25 wp	Ciba Geigy
6[a]	LAB14202F	2-[(2,6-dimethyl-phenyl)-(oxazole-5-carbonyl)-ami-no]-propionic acid methylester	2.41	experimental	BASF AG, BRD
7[b]	Benalaxyl	methyl-*N*-phenylacetyl-*N*-2,6-xylyl-*DL*-alaninate	3.09	Galben 25 wp	Montedison, Italy
8[c]	Cyprofuram	(±)-α-[*N*-(3-chloro-phenyl) cyclopropanecarboxamido]-γ-butyrolactone	1.95	Vinicur 50 wp	Schering AG
9[a]	Oxadixyl	methoxy-*N*-(2-oxo-1,3-oxazolidin-3-yl)acet-2',6'-xylidide	1.47	Sandofan	Sandoz AG, BRD
10[a]	Dimethomorph	4-[3-(4-chlorophenyl)-3-(3,4-dimethoxyphenyl)acryloyl]morpholine	4.06	Acrobat 50 wp	ICI, UK
11[a]	Andoprim	4,6-dimethyl-pirimidin-2-yl)-(4-methoxyphenyl)-amine	2.55	experimental	Fahlberglist, BRD
12[a]	Cymoxanil	1-(2-cyano-2-methoxyiminoacetyl)-3-ethylurea	1.53	Curzate 50 wp	Du Pont, USA
13[d]	Propamocarb[e]	propyl (3-dimethylamino-propyl)-carbamic acid propyl ester	0.37	Previcur N 70 LS	Schering AG
14[a]	Prothiocarb	(3-dimethylamino-propyl)-thiocarbamic acid *S*-propyl ester	1.50	Previcur	Schering AG
15[b]	TMTD	tetramethylthiuram disulfide	2.37	Perthiram 500 SC	Bayer, BRD
16[b]	Drazoxolon	(4-(2-chlorophenylhydraxono)-3-methyl-1,2-oxazol-5(4*H*)-one	2.43	Mil-Col 300	ICI
17[d]	Efosit[e]	ethyl hydrogen phosphonate	0.41	Aliette 80 wp	Rhone Poulenc Agro, France

APPLIED ECOLOGY AND ENVIRONMENTAL RESEARCH 4(2): 125-149.

No.	Common name	Chemical Name	Log P[f]	Trade name	Producer
18[a]	BKF-3[e]	propyl hydrogen phosphonate	1.49	experimental	BorsodChem, HU
19[d]	Thiomersal	ethyl-(2--mercaptobenzoato-*S*)mercury sodium salt	3.52	experimental	Sigma-Aldrich
20[c]	Ziram	zinc*bis*(dimethyldithiocarbamate)	2.04		
21[c]	$Zn(PDC)_2$	zinc*bis*(pirrolidine-1-carbodithioate)	4.58	experimental	
22[b]	Dodemorph-*cis*	4-cyclododecyl-2,6-dimethylmorpholine	6.10	Meltatox 75 ec	BASF
23[b]	Dodemorph-*trans*	4-cyclododecyl-2,6-dimethylmorpholine	6.10	Meltatox 75 ec	
24[b]	Tridemorph-*cis*	2,6-dimethyl-4-tridecylmopholine	6.54	Calixin 75 ec	BASF
25[b]	Tridemorph-*trans*	2,6-dimethyl-4-tridecylmopholine	6.54	Calixin 75 ec	
26[b]	Fenpropimorph	*cis*-4-[3-*tert*-butylphenyl)-2-methylpropyl-2,6-dimethylmorpholine	4.54	Corbel 75 ec	BASF
27[a]	Dodine	dodecylguanidinium acetate	4.42	Efuzin 500 FW	Agrokemia, HU

Stock solutions of compounds 12, 15, 16, 20 and 21 were prepared in acetone, while those of 13, 14 and 19 in water and all others in methanole.

[a] = supplied by manufacturer, [b] = extracted from marketed product, [c] = synthesised in PPI HAS by known manner, [d] = purchased, [e]= commercial preparation was used, [f]= Log P values were calculated by Interactive Analysis LogP and LogW (water solubility) predictor website [6].

Table 2. *Activity of fungicides against various developmental stages of Sclerospora graminicola.*

Compounds		Developmental stages															
		Abiotrophic (HID)								Biotrophic (HD)							
No	Name	EC_{50}		m		EC_{50}		m		EC_{50}		m		EC_{50}		m	
1	Metalaxyl	236	*a*	2.841	*a*	305	*a,b*	2.747	*a*	36.2	*a,b*	1.953	*a,b*	234	*d*	4.16	*d,e*
2	CGA29212	277	*a,b*	2.783	*a*	277	*a,b*	2.783	*a*	46.4	*b*	1.815	*a,b*	202	*d*	3.85	*c,d*
3	RE26745	277	*a*	2.783	*a*	132	*a*	2.350	*a*	15.5	*a*	1.614	*a*	72.4	*b,c*	2.29	*b*
4	Ofurace	277	*a*	2.783	*a*	201	*a*	2.375	*a*	46.4	*b*	1.815	*a,b*	86.1	*c*	2.45	*b*
5	Furalaxyl	252	*a*	2.380	*a*	592	*b,c*	4.500	*b*	21.6	*a,b*	1.681	*a,b*	8.4	*a*	1.51	*a,b*
6	LAB149202F	236	*a*	2.841	*a*	277	*a,b*	2.783	*a*	46.4	*b*	1.815	*a,b*	40.3	*b*	2.03	*b*
7	Benalaxyl	236	*a*	2.841	*a*	132	*a*	2.350	*a*	46.4	*b*	1.815	*a,b*	81.4	*c*	2.38	*b*
8	Cyprofuram	236	*a*	2.841	*a*	277	*a,b*	2.783	*a*	46.4	*b*	1.815	*a,b*	46.6	*a*	2.09	*b*
9	Oxadixyl	613	*a,b*	4.424	*b*	548	*b,c*	4.402	*b*	166	*b,c*	2.936	*c,d*	100	*c*	2.57	*b,c*
10	Dimethomorph	236	*a*	2.841	*a*	277	*a,b*	2.783	*a*	36.2	*a,b*	1.953	*a,b*	65.3	*b,c*	2.33	*b*
11	Andoprim	548	*a,b*	4.402	*b*	567	*b,c*	4.523	*b*	25.8	*a*	2.182	*a,b,c*	31.6	*a,b*	2.55	*b*
12	Cymoxanil	2783	*d*	5.093	*b,c*	1496	*d*	6.860	*d*	1121	*d,e*	3.139	*d*	979	*f*	4.29	*d*
13	Propamocarb	1337	*c*	6.860	*c*	2938	*c,d*	6.644	*c,d*	2520	*f*	5.531	*e,f*	1735	*f,g*	2.16	*a,b*
14	Prothiocarb	2095	*d*	11.062	*d*	1414	*d*	7.082	*d*	585	*d*	4.670	*d,e,f*	794	*f*	7.44	*e*
15	TMTD	519	*a,b*	4.832	*b*	735	*c,d*	4.072	*b*	519	*c,d*	4.832	*e,f*	258	*d*	3.48	*c*

APPLIED ECOLOGY AND ENVIRONMENTAL RESEARCH 4(2): 125-149.

Compounds		Developmental stages															
		Abiotrophic (HID)								Biotrophic (HD)							
No	Name	EC_{50}		m		EC_{50}		m		EC_{50}		m		EC_{50}		m	
16	Drazoxolon	955	*b,c*	11.062	*d*	1337	*d*	6.860	*d*	36.2	*a,b*	1.953	*a,b*	9.45	*a*	1.77	*b*
17	Efosit	644	*b*	4.870	*b,c*	669	*b,c*	4.160	*b*	134	*b,c*	2.916	*c,d*	214	*d*	3.63	*c*
18	BKF-3	562	*a,b*	4.869	*b*	1337	*d*	6.860	*d*	514	*c,d*	5.084	*e,f*	241	*d,e*	3.82	*c*
19	Ziram	519	*a,b*	4.832	*b*	1337	*d*	6.860	*d*	186	*c*	2.890	*b,c,d*	86.4	*c*	2.42	*b*
20	$Zn(PDC)_2$	1337	*c*	6.860	*c*	1414	*d*	7.082	*d*	519	*c,d*	4.832	*e,f*	243	*d*	3.39	*c*
21	Thiomersal	1496	*c*	6.860	*c*	2477	*c,d*	4.587	*b,c*	1469	*e,f*	6.644	*f*	1518	*f,g*	2.39	*a,b*
22	Dodemorph-*cis*	1337	*c*	6.860	*c*	1496	*d*	6.860	*d*	519	*c,d*	4.832	*e,f*	36.6	*b*	2.42	*b*
23	Dodemorph-*trans*	1337	*c*	6.860	*c*	2719	*d,e*	6.644	*b,c, d*	585	*d*	4.670	*d,e,f*	287	*d,e*	3.35	*b,c*
24	Tridemorph-*cis*	1337	*c*	6.860	*c*	2938	*d,e*	6.644	*c,d*	2520	*f*	5.531	*e,f*	1127	*f*	1.26	*a,b*
25	Tridemorph-*trans*	1337	*c*	6.860	*c*	1479	*d*	7.270	*d*	1360	*d,e*	6.644	*f*	351	*e*	1.16	*a*
26	Fenpropimorph-*cis*	1337	*c*	6.860	*c*	2477	*d,e*	4.587	*b,c*	2520	*f*	5.531	*e,f*	2248	*f*	1.54	*a,b*
27	Dodine	669	*b*	4.160	*b*	1414	*d*	7.082	*d*	398	*c,d*	5.546	*e,f*	198	*c,d*	3.96	*c,d*

Sensitivity to fungicides (inhibition) is expressed as EC_{50} value in micromol, m = slope of dose response line at log/probit scale.
Values labelled by the same letter are not significantly different at P=5% level.

http://www.ecology.uni-corvinus.hu ● ISSN 1589 1623

Data analysis

All tests were carried out at least in triplicate. Reliability of assessments was evaluated by analysing variation coefficients (C.V.%= 100×[stdev/mean]) using statistical functions of Excel 6 (Microsoft, Redmondton, USA). Disease inhibitory effects were analysed by MANOVA. Averages of grain yield were compared by Student's *t*-test.

In vitro efficacy of each chemical tested was characterised by EC_{50} value and slope of dose response line, the latter relates to specific activity of compounds. Both values were calculated from basic data expressed as a percentage, using a curve-fitting method based on log/probit function. Therapeutic value of tested chemicals was calculated by following formula (Eq.1):

$$\text{Therapeutic index (TI)} = MTC_{host}/MIC_{parasite} \quad \text{(Eq.1)}$$

where MTC_{host}=maximum tolerated concentration by germinating seeds of pearl millet and $MIC_{parasite}$=minimum inhibitory concentration determined on germinating zoosporangia of *S. graminicola* have been replaced with EC_{01} and EC_{99} values, both expressed in molar concentrations.

The experimental data were also analysed by employing bivariate linear regression, multiple correlation, multivariate linear regression and principal component analyses to disclose differences in developmental stage dependent responses. Excel97 statistical functions (Microsoft, Redmondton, USA) and Statistica5 program (StatSoft, Tusla, USA) were used for calculations and graphic presentation of data.

Results

Reliability of assessments

The coefficient of variation of the parallel measurements ranged from 0 to 6 % in most of cases. It exceeded 10 % just in 77 of 4023 cases mostly in the range of maximum tolerated concentrations when screening inhibitory effects against asexual spores, which verifies the reliability of the measurements. The correlation coefficient of dose/response lines was over 0.707 (r^2=0.50) in all cases, and it was lower than 0.775 ($r_{0.001}$=0.597) only in 10 cases. The major variation in curve fitting was found for screening activities against zoospores (*Fig 1*). The goodness of fitting of the activities of acylanilides was lower than that of other compounds. Nevertheless all lines could be fit at P<5 % level verifying the reliability of toxicological parameters; EC_{50} and slope (specific activity).

Responses of the pathogen

The responses of various developmental stages of *S. graminicola* to the tested compounds are shown in *Table 2*. Fungicides inhibited the two types (HI and HD) of ontogenetic development differently. Zoosporangium germination (ZG) was more sensitive to systemic acylanilides (**1-9**) and dimethomorph (EC_{50} < 500 μM) than to the other compounds (EC_{50}=500-2500 μM). Free moving zoospores (ZM) responded similarly. The organo-metallic compounds (**17-21**), as well as dimethyl-morpholine derivatives (**22-26**) contrary to expectations, were not most active against asexual spores

http://www.ecology.uni-corvinus.hu ● ISSN 1589 1623

of *S. graminicola*. These molecules exhibited high efficacy against *P. infestans* and *P. halstedii* zoospores [35], which were much less sensitive to acylanilides [37].

Treatments on established thallus of *S. graminicola* inhibited the intensity of sporulation (SP) within large limits (EC_{50}=15-2500 μM). In addition to acylanilides (**1-9**) andoprim, dimethomorph and drazoxolon proved to be highly active (EC_{50}=15-50 μM). The remaining compounds were two or three order of magnitude less effective in this respect (EC_{50}=100-2500 μM). The number of zoospores (PZ) arising from zoosporangia originated from the exposed leaf areas was also decreased by various degrees. Furalaxyl and drazoxolon separate from others with particularly high (EC_{50} < 10 μM) while propamocarb, thiomersal and fenpropimorph with low activity (EC_{50} > 1500 μM) on zoospore production.

When evaluating similarity of responses of various developmental stages to fungicides on the base of EC_{50} values (*Table 5*) the correlation did not deviated significantly from the linear one (P=0.1-5 %). The similarity in spectrum of sensitivity was significant ($r_{0.001}$=0.597 < $r_{SP,PZ}$= 0.816 < $r_{ZG,ZM}$=0.871 < $R_{[ZG+ZM],[SP+PZ]}$= 0.901) between HD and HID stages. Differences in the slope of dose response lines indicate qualitative dissimilarities in reaction of the parasite to test compounds in dependence of its ontogenetic stage. In general, the differences in steepness of dose response lines for activities against asexual spores (HID) were smaller for acylanilides than for other compounds (*Table 2*). The spectrum of sensitivity in HD stages as evaluated by specific activities differed greatly ($r_{SP,PZ}$= 0.051 < $r_{0.001}$=0.597 < $r_{ZG,ZM}$=0.729).

Responses of the host plant

Phytotoxity of tests compounds varied within large limits (EC_{50}=0.5-280 mM), and the systemic anti-oomycete fungicides were less toxic than the other ones (*Table* 3). Pearl millet did not tolerated well (EC50 < 10 mM) the thiocarbamate derivatives (**15**, **19**, **20**), thiomersal, tridemorph isomers (**24**, **25**) and fenpropimorph. Cymoxanil and drazoxolon proved to be also surprisingly toxic. Variations in the structure of acylanilide derivatives greatly influenced their phytotoxicity; replacement of methoxyacetyl group to chloroacetyl one (**2**, **4**) increased, while coupling methylester moiety into butyrolactone ring (**3**, **4**) decreased this activity. The cationic tenside type dodemorph isomers (**22**, **23**) and dodine as well as the phosphonic acid salts (**17**, **18**) were also well tolerated by pearl millet germlings. With few exceptions (**1**, **13, 15, 17** and **20**) the retardant effect of fungicides (EC_{50} mM) applied as seed dressing was slightly increased during first steps of seedling growth (EC_{50} for SG=1-115 mM > EC_{50} for SV=0.5-42 mM, $t_{SG,SV}$=2.90 > $t_{0.01}$=2.80).

The slope of dose response lines showed great variations (SG=1.29-5.45 and SV=1.28-6.88 probits in both cases), and except compounds **1**, **5**, **7, 13** and **24** either decreased or increased (14 and 8 cases, respectively) by development of seedlings. Nevertheless pear millet plants outgrew the depressant effect of fungicides. None of compounds exhibited phytotoxic effects when applied on leaf surface (2 mM).

Activity against downy mildew disease

Only acylanilide derivatives exhibited adequate protective effect (<95%) against downy mildew of pearl millet (*Table 4*). Although the activity of oxadixyl was slightly lower than other members of this group of fungicides, there were not significant differences in their efficacy. Among the other test compounds andoprim, drazoxolon

http://www.ecology.uni-corvinus.hu ● ISSN 1589 1623

and salts of phosphonic acid (**17**, **18**) exhibited some disease control (>30%) while all others proved to be ineffective. The field activity of fungicides with few exceptions (**10**, **11**, **17**, **18**) was lower than the greenhouse one but this difference was not significant ($\Delta_{GH,F}$=(1-10)% < $LSD_{0.05}$=12%). Otherwise the field activity of compounds was closely related to their greenhouse effect (F_{regr}=927.6, p<0.001).

The therapeutic index of compounds (*Table 3*) varied between 0.02-29. Differences in the structure of acylanilides characteristically influenced this parameter; the presence of chloroacetyl group (**2**, **4**) decreased their therapeutic value. Changes in structure increasing the hydrophobicity of molecules (**2**, **4**, **7**, **18** and **21**) lead to increase in phytotocity and a reduction of the therapeutic value.

Seed treatments influenced radically the grain yield of pearl millet (*Table 4*). With exception of cationic surfactant type molecules **24-26** all compounds increased the yield. The acylanilide derivatives (**1-9**) were the most effective increasing yield by more than 60%. Significant correlation was revealed between antimildew efficacy of compounds and their effect on the yield with special regard to disease inhibition as evaluated either in greenhouse or in provocation field ($F_{Y,GH}$=927,7; $F_{Y,\ F}$=118.5 > $F_{0.001}$=13.8). Contrarily, reverse correlation was revealed between the yield of plants treated on the level of maximum tolerated concentrations of conpounds and their depressant on host plant effect ($r_{Y,\ [SG+SV]}$= -0.747; F_{regr}=15.12 > $F_{0.05}$=3.40).

The effect of treatments correlated significantly ($r_{lg(TI),Y}$=0.728 > $r_{0.001}$=0.59) with therapeutic value of fungicides: Y= [4.369±0.108] + [0.873±0.159]*X (F_{regr}=30.27 > $F_{0.001}$=13.61, t_a=38.83, t_m=5.502 > $t_{0.001}$=3.73); where Y= yield increase in percent (probits) related to the untreated control, X = logarithm of therapeutic index). The compound with higher therapeutic index tends to influence more beneficially onto the grain yield of downy mildewed pearl millet than those of lower index (p <0.001).

The synergetic action of combined preparations containing systemic fungicides metalaxyl+tridemorph as well as andoprim+cymoxanyl has been demonstrated against oomycetes [18, 58]. In our model experiments the joint action of these fungicides against *S. graminicola* proved to be also synergetic (*Table 6*).

The compounds for present investigations were selected on the basis of studies with other oomycetes [34, 59, 62] that made possible to compare sensitivity spectra of various genera. There were significant differences between responses: asexual spores of *S. graminicola* were more sensitive to acylanilides than the analogous cells of *P. halstedii* or *P. infestans* while the cationic surfactant type molecules (**23-26**) exhibited much less activity to *S. graminicola*. The sensitivity of the biotrophic *S. graminicola* to acylanilides was non selective contrary to *P. halstedii* [62] and *Phytophthora* species [59]. Cymoxanil exhibited good activity against SDM [62] and poorly inhibited the PMDM while drazoxolon acted oppositely. The sunflower tolerated all compounds better than pearl millet. The rank order of therapeutic values for PMDM shows few similarities with that established for sunflower downy mildew ($\rho_{PMDM,SDM}$=0.517, F_{regr}=4.36, P=5-10%). Nevertheless, some similarities occurred; the replacement of methoxylacetyl group for chloroacetyl one decreased the therapeutic value for SDM as well [62].

http://www.ecology.uni-corvinus.hu ● ISSN 1589 1623

Table 3. *Phytotoxic effect of various fungicides on pearl millet*

Compounds		Inhibition of								Therapeutic
		Seed germination				Seedling vigour				Index
No.	Name	EC_{50}		m		EC_{50}		m		SG/SP
1	Metalaxyl	69.7	*h*	1.697	*a,b,c*	26.3	*f*	1.391	*a*	5.23
2	CGA29212	17.5	*e*	1.768	*b*	12.8	*e*	3.346	*c,d*	0.945
3	RE26745	64.1	*g,h*	3.305	*c,d,e*	87.9	*i*	1.276	*a*	29.4
4	Ofurace	38.2	*f*	1.974	*b,c*	20.6	*e,f*	3.870	*c,d,e*	2.83
5	Furalaxyl	80.7	*h,i*	1.641	*a,b*	32.4	*g,h*	1.445	*a*	5.84
6	LAB149202F	113.4	*i*	1.286	*a*	33.3	*g,h*	1.778	*a,b,c*	1.97
7	Benalaxyl	41.5	*f,g*	1.857	*a,b,c*	28.9	*g,h*	1.636	*a,b*	2.59
8	Cyprofuram	56.4	*f,g*	1.519	*a,b*	20.3	*e,f*	2.776	*b,c,d*	1.85
9	Oxadixyl	93.9	*i*	1.334	*a*	28.8	*f,g*	1.648	*a,b*	1.63
10	Dimethomorph	65.2	*g,h*	1.394	*a,b*	27.6	*f,g*	1.574	*a*	2.46
11	Andoprim	69.7	*h*	1.697	*a,b,c*	26.9	*f,g*	5.282	*e,f*	9.79
12	Cymoxanil	14.2	*d,e*	1.994	*b,c*	7.22	*d*	2.144	*b*	0.156
13	Propamocarb	69.3	*h*	1.378	*a*	41.9	*h,i*	1.396	*a*	0.212
14	Prothiocarb	22.4	*e,f*	5.448	*e*	17.8	*e*	2.454	*b,c*	4.53
15	TMTD	2.56	*b*	5.081	*e*	1.68	*b*	3.895	*d*	0.566
16	Drazoxolon	14.2	*d,e*	1.994	*b,c*	13.9	*d,e*	3.270	*c,d*	1.71
17	Efosit	29.1	*e,f*	2.133	*b,c*	19.2	*e,f*	6.876	*f*	2.79
18	BKF-3	44.8	*f,g*	1.585	*a,b*	21.5	*e,f*	5.614	*e,f*	1.03
19	Ziram	12.2	*d*	2.227	*c*	9.24	*d,e*	2.916	*c*	0.923
20	$Zn(PDC)_2$	4.01	*c*	3.988	*e*	4.99	*c*	4.916	*e*	0.663
21	Thiomersal	2.53	*b*	4.947	*e*	1.83	*b*	3.626	*d*	0.260
22	Dodemorph-*cis*	30.2	*e,f*	2.395	*c,d*	11.1	*e*	1.807	*b,c*	2.04
23	Dodemorph-*trans*	26.1	*f*	4.701	*e*	18.9	*e,f*	1.605	*a,b*	4.52
24	Tridemorph-*cis*	1.09	*a*	2.993	*d*	0.874	*a*	2.962	*c*	0.0273
25	Tridemorph-*trans*	1.08	*a*	4.971	*e*	1.09	*a,b*	3.829	*d,e*	0.120
26	Fenpropimorph	1.31	*a*	4.527	*e*	0.574	*a*	3.102	*c,d*	0.0603
27	Dodine	15.2	*d,e*	1.750	*b*	14.7	*d,e*	2.310	*b,c*	0.675

Sensitivity to fungicides (inhibition) is expressed as ED_{50} value in millimol, m = slope of dose response line at log/probit scale. Values labelled by the same letter are not significantly different at P=5% level. Therapeutic index = the ratio (EC_{01} for seed germination)/(EC_{99} for intensity of sporulation).

http://www.ecology.uni-corvinus.hu ● ISSN 1589 1623

Table 4. *Antimildew activity of compounds and their effect on the grain yield of pearl millet*

No.	Compound	Conc.[a] (mM)	Activity (%)[b] in the Glasshouse	Field	Yield[c] kg/ha	Increase[d] kg/ha
1	Metalaxyl	10	98.0	97.9	1864±88	728*f*
2	CGA29212	5	98.4	98.7	1864±96	728*f*
3	RE26745	10	99.3	98.8	1875±94	739*f*
4	Ofurace	10	97.3	97.5	1856±96	720*f*
5	Furalaxyl	10	98.6	98.7	1906±94	770*f*
6	LAB149202F	10	97.0	98.0	1838±90	702e*f*
7	Benalaxyl	10	97.9	97.9	1864±88	728*f*
8	Cyprofuram	10	99.1	98.7	1872±96	736*f*
9	Oxadixyl	10	95.8	94.4	1842±102	706*f*
10	Dimethomorph	10	12.8	26.0	1427±64	291*c*
11	Andoprim	10	35.9	46.7	1474±69	338*d*
12	Cymoxanyl	10	14.7	3.9	1272±64	136*bc*
13	Propamocarb	10	12.2	9.5	1346±70	210*bc*
14	Prothiocarb	10	20.1	13.4	1400±64	264*c*
15	TMTD	1	27.3	26.4	1456±72	320*c*
16	Drazoxazolon	10	32.9	28.5	1600±80	464*d*
17	Efosit	10	32.4	40.0	1496±72	360*cd*
18	BKF-3	10	44.4	50.4	1384±64	248*bc*
19	Ziram	1	13.1	14.7	1288±64	152*bc*
20	Zn-PDC	1	16.5	22.4	1288±67	152*bc*
21	Thiomersal	1	13.7	18.1	1256±58	120*ab*
22	Dodemorph-cis	10	13.0	14.8	1360±56	224*c*
23	Dodemorph-trans	10	8.3	8.8	1288±64	152b*c*
24	Tridemorph-cis	0.2	3.1	4.3	1139±53	3*a*
25	Tridemorph-trans	0.5	6.6	12.4	1192±64	56*a*
26	Fenpropimorph	0.5	9.6	3.5	1208±64	72*ab*
27	Dodine	10	9.0	8.7	1256±64	120*ab*

[a]= Maximum tolerated doses by pearl millet. Preventive seed treatments were made in each case (see Materials and Methods).
[b]= For efficacy of compounds in different locations $LSD_{5\%}$= 11.9 (F_{exp}= 43.9 < $F_{5\%}$=1.26).
[c]= Yield of the untreated control was 1136±56 kh/ha. [d]= as compared to untreated control plots. The values marked by the same letter are not significantly different at P=5% level.

http://www.ecology.uni-corvinus.hu ● ISSN 1589 1623

Table 5. *Correlation in sensitivity to fungicides between different developmental of Sclerospora graminicola and pearl millet basen on their responses to fungicides*

	Matrix A (FG=27) Inhibition of					
Matrix B (FG=27)	**Zoospore Release**	**Zoospore Motility**	**Sporulation**	**Zoospore production**	**Seed germination**	**Seedling vigour**
Inhibition of	**1**	**2**	**3**	**4**	**5**	**6**
1. Zoospore release	1.0	0.872	0.793	0.630	-0.600	-0.579
2. Zoospore motility	0.7296	1.0	0.872	0.653	-0.597	-0.607
3. Sporulation	0.5670	0.6734	1.0	0.854	-0.644	-0.649
4. Zoospore production	0.2167	0.1725	0.0513	1.0	-0.571	-0.523
5. Seed germination	0.5520	0.3069	0.6257	0.2027	1.0	0.933
6. Seedling vigour	0.1547	0.1517	0.1987	0.0962	0.1496	1.0

Matrix A = Pearson's correlation coefficients calculated on the base of log EC_{50} values.
Matrix B = Pearson's correlation coefficients calculated on the base of slope values of dose respose lines. ($r_{0.001}$=0.597)
The underlined coefficient indicates significant relationship between the activities of compounds evaluated by the given parameter ($100 \times R^2 > 50$).

Table 6*. Joint action of systemic fungicides against Sclerospora graminicola*

	Treatments	**Efficacy (mgl^{-1})**	
No.	**Compounds**	**EC_{99}**	**Co.T.I.[a]**
1	Metalaxyl (M)	72.9	
2	Tridemorph (T)	640.7	
	1M+4T[b]	62.3	3.36
3	Andoprim (A)	117.8	
4	Cymoxanil (C)	1788.9	
	3A+7C[b]	105.4	3.43

[a]=Co.T.I. = Comparative toxicity index according to Sun [52]. The inhibition of sporulation was determined on detached leaf segments (see Materials and methods).
[b]= Weight parts.

http://www.ecology.uni-corvinus.hu ● ISSN 1589 1623

***Table 7**. Principal components of the Spearman's correlation matrix between responses of downy mildew fungus and pearl millet to fungicides*

No.	Evaluated events[a] (variable)	Principal component[b] 1	2
1	Zoosporangium germination (ZG)	0.822	0.314
2	Zoospore motion (ZM)	0.892	0.299
3	Intensity of sporulation (SP)	0.859	0.382
4	Production of zoospores (PZ)	0.695	0.354
5	Seed germination (SG)	-0.368	-0.911
6	Seedling vigour (SV)	-0.351	-0.916
7	Disease inhibition in vitro (GH)	0.856	0.301
8	Disease inhibition in vivo (F)	0.892	0.335
9	Yield increase (Y)	0.859	0.414
	Eigenvalue	5.215	2.504
	Percentage of variation	57.9	27.8
	Cumulative percentage	57.9	85.7

[a]= Events correspond to those given in Tables 2, 3 and 4.
[b]= The Varimax rotated principal components are shown in order of the amount of variation they represent; eigenvalues having percentage variation less than 5 are omitted.

***Table 8**. Variations in the efficacy of seed dressings against pearl millet downy mildew in various regions of India*

Location[a]		Geographic coordinates		Disease Incidence (%)[b]		Disease Inhibition
No.	Name	N	E	Untreated Control	Apron 35SD 3 kg/t	Rate (%)[c]
1	Jaipur	26°55'0"	75°49'0"	24.3	4.3	82
2	Gwalior	25°55'60"	78°28'0"	81.8	62.4	24
3	Jamnogar	22°28'0"	70°4'0"	85.5	82.2	4
4	Anand	22°13'0"	71°10'0"	82.2	91.2	1
5	Aurangabad	19°52'60"	75°19'60"	85.3	9.8	89
6	Patancheru	17°31'60"	78°16'0"	9.0	5.0	44
7	Mysore	12°18'0"	76°39'0"	27.0	7.7	71
8	Coimbatore	11°0'0"	76°58'0"	82.0	14.0	83

http://www.ecology.uni-corvinus.hu ● ISSN 1589 1623

In accordance to official reports [5] and multitudinous observations cited the standard metalaxyl treatment (2 kg/t) showed in earlier times excellent protective effect in all plots inhibiting the PMDM at rate >95%.

[a]The trials were conducted in ICAR-AICPMIP research stations [5].

[b]Disease incidence was recorded at tillering, $LSD_{0.05}$= 10.2 ($F=231.7$, $p<0.001$).

[c]The disease inhibition rate was calculated following formula DIR=100*(C-T)/C, where C and T are disease incidences in control and treated variants, respectively.

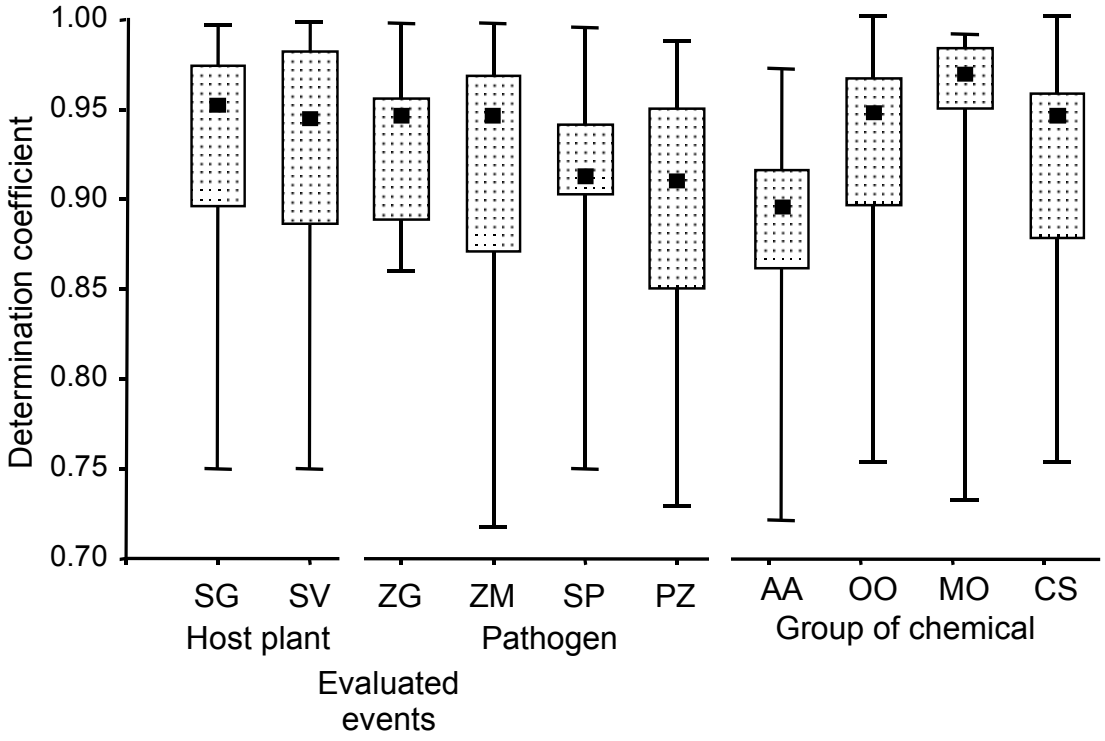

Figure 1. *Evaluation of the goodness of curve fitting of dose response lines for characterising activity of test compounds screened by different methods.*
The graph was built up based on median (central point), second and third quartiles (box) and extremum values (whiskers) of determination coefficients of log/probit function used for calculation of dose response lines (Tables 2, 3 and 4). Evaluated events are SG = seed germination, SV = seedling vigour, ZG = zoosporangium germination, ZM = zoospore motility, SP = intensity of sporulation, PZ = zoospore production. Responses of pathogen to the chemicals tested are grouped as follows; AA = acylanilides, OO = other antioomycete compounds, MO = metallo-organics, CS = cationic type surfactants.

Multivariate analysis

The responses of parasite and host plant to fungicides evaluated by different manners were compared and subjected as variates to PCA (*Table 7*). The first PC accounted for 58 % of the total variation comprising all events where the pathogen was presented with positive weights and plant responses with negative ones. The second PC accounted for less of the variation (28 %) and related mainly to host plant which was less sensitive to test compounds than the parasite. The two organisms have been presented in both cases

http://www.ecology.uni-corvinus.hu ● ISSN 1589 1623

with opposite signs that relates to the reverse relationship between groups of variates; observations for pathogens and for host plant.

The multivariate regression analysis revealed positive correlation of different power between disease inhibitory effect on the field (F) and the capacity of compounds to inhibit host independent and host dependent developmental form of *S. graminicola* as well as their phytotoxicity; $R_{F,[ZG+ZM]}=0.884 > R_{F,[SP+PZ]}=0.815 > r_{0.001}=0.652 > R_{F,[SG+SV]}=0.614 > r_{0.05}=0.427$. All these are in accordance to the result of bivariate regression and PC analyses (see *Tables 5 and 7*). When omitting from calculation observations for disease inhibitory actions determined in greenhouse (G) and field (F) as well as yield increase (Y) the resulted PC-s are derived only from *in vitro* activity data. The first PC in this case accounted 74.5 % of variation of the correlation matrix of EC_{50} values (reduced *Table 5*). Plotting effects of treatments on the yield of pearl millet versus variables of this first PC (*Fig 2*) revealed significant linear correlation ($p < 0.001$).

The comparative analysis of multivariate determination coefficients showed that the number of parameters in screening might be decreased, and involvement of two, correctly selected variables was satisfactory for prediction of the effect on the yield of pearl millet ($\rho_{Y,[SP+SG]}=0.84$, $p<0.01$). All the above indicates the possibility of limiting the number of parameters for selection of compounds in primary screening against PMDM.

Discussion

The tested fungicides exerted different impacts on *S. graminicola* at different stages in its life cycle, where the zoosporangiogenesis was more sensitive than other events. Inhibition of asexual spores of *S. graminicola* is important, because these provide the greatest opportunity for rapid built up in the number of infective propagules and subsequently, the high potential for infection of new plants. Therefore, any chemical that significantly suppresses the zoosporangium formation reduces the ability of disease expansion as well. Indeed, there was a significant correlation between the inhibition of this event and the effect of a single seed treatment on the grain yield ($r_{SP,Y}=0.83 > r_{P=0.1\%}=0.54$). The sensitive response of asexual spores to acylanilides is particularly interesting property of *S. graminicola*. These chemicals are thought to inhibit a single enzyme system, the α-amanitine RNA polymerase [15]. The inhibition of this receptor site leading to stop of protein synthesis and consequently to discoupling of the life cycle dominates over other metabolic effects. There was demonstrated that transcription in *Peronospora tabacina* started before the differentiation of sporangia [25] and that mRNA continued to be synthesised during HD stages. Similarly, this pause occurred also with *Bremia lactucae* sporangia [13]. Although the zoosporangium formation of *S. graminicola* was found to be more sensitive to the tested set of chemicals than other ontogenetic events, the developmental stage dependent variations in its response were less pronounced than in the case of *Plasmopara* or *Phytophthora*. Contrary to the latter species the ontogenetic forms of *S. graminicola* had many commons in their sensitivity to fungicides. The high activity of acylanilides against PMDM is likely to involve active transcription and translation (protein synthesis) in parasiting thallus, while the sensitivity of asexual spores indicates that both ratio and intensity of the above steps in protein synthesis would occur at the previous level during host independent stages. However, the selective inhibition of mitochondrial respiration by phenylamide

http://www.ecology.uni-corvinus.hu ● ISSN 1589 1623

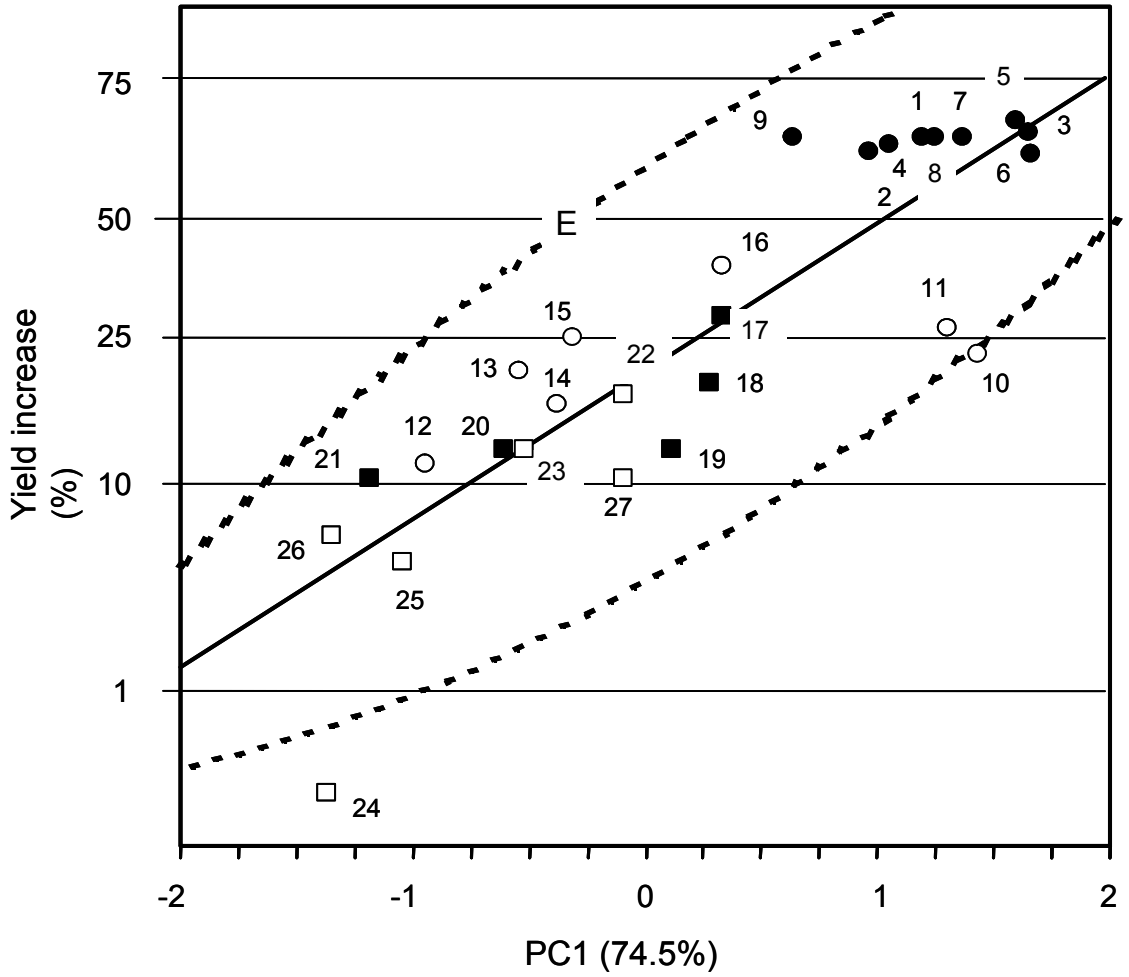

Figure 2. *Relationship between the effect of fungicides on the yield of pearl millet and their antimildew activity measured in vitro.*
Arabic numerals represent compounds and correspond to those given in Table 1. Chemical groups of acylanilides and other antioomycete fungicides are marked with filled and opened circles while metallo-organics and cationic tensides with filled and opened squares, respectively. The trend line was drawn according to the equation y=b+mx as follows: Yield increase (%) = [4.4289±0.0806]+[0.7039±0.0821]×PC1; (F_{regr}=73.51 > $F_{0.1}$= 13.74, R^2_{adj}= 0.7361, t_a=54.98, t_b=8.57)
where Y= Yield increase in percent (probits) related to the untreated control (Derived from data of Table 4), X = Principal component (PC1) of Spearman's correlation matrix calculated from in vitro response data (Tables 2-3). E = 99.5 % normal bivariate confidence ellipse.

http://www.ecology.uni-corvinus.hu ● ISSN 1589 1623

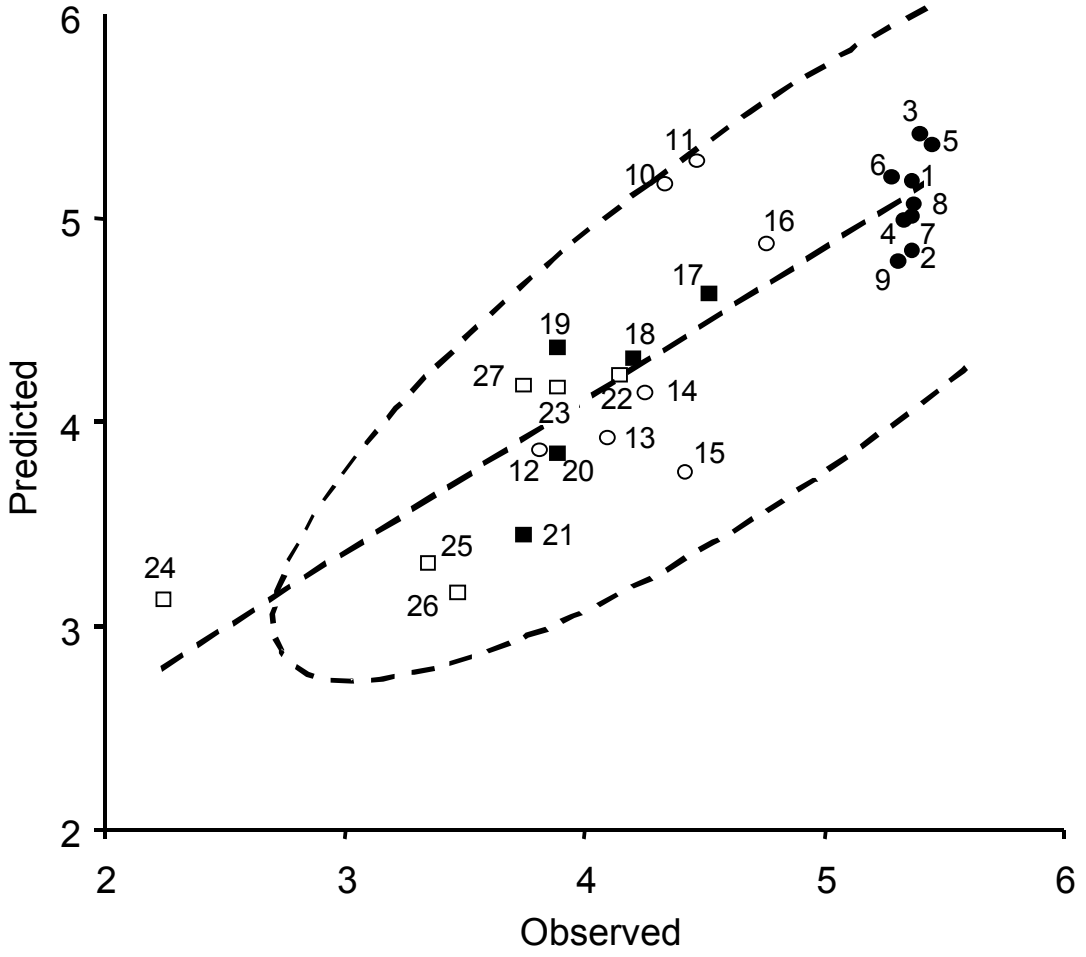

***Figure 3**. Relationship between observed and predicted effects of fungicides on the yield of downy mildewed pearl millet.*
Arabic numerals represent compounds and correspond to those given in Table 1. Chemical groups of acylanilides and other antioomycete fungicides are marked with filled and opened circles while metallo-organics and cationic tensides with filled and opened squares, respectively. E = 99.5 % normal bivariate confidence ellipse. The trend line was drawn according to the equation y=b+mx as follows:
$Y= [1.0961\pm0.3384] + [0.7525\pm0.0863]*X$; ($F_{regr}=76.02 > F_{0.001}=13.61$, $R^2_{adjusted}=0.7426$, $t_b=2.82$, $t_m=8.72 > t_{0.01}=2.80$) where X= Yield increase in percent (probits) related to the untreated control (derived from data of Table 4), Y = the predicted yield increase calculated from activities against SP and SG stages.

fungicides [41] might also be the factor of sensitivity of asexual spores of *S. graminicola*. The extent of lipophilic properties of different phenylamide fungicides varies; this is probably the reason why the most lipophilic member of this group (benalaxyl) is active also against zoospores of *Phytophthora* and *Plasmopara* [11, 24, 62]. Although the importance of zoospores in sustaining of disease cycle of PMDM is reduced because of dual character of zoosporangia, the high tolerance of *S. graminicola* spores to cationic type surfactants is very interesting, with special regard of its cell wall

http://www.ecology.uni-corvinus.hu ● ISSN 1589 1623

less zoospores, that might be related to alterations in membrane structure as compared to other peronosporas.

None of the compounds tested was tolerated completely by HB3 hybrid, however the depression observed on germinating seeds was soon overcome; the negative effect on the grain yield was seemingly unimportant. Nevertheless, an antimildew compound to be used in the control of pearl millet should provide better therapeutic properties than majority of acylanilides (*Table 3*). The influence of the host plant on the performance of biological activity of any compound can be determinative in the case of biotrophic endoparasites. By this reason it is very important to study the effects on the host plant. The risk of application of compounds shown to prove satisfactory control of other Peronosporas can be high when applied against PMDM because of different therapeutic indices. The ratio of non-effective dose on host and lethal dose on parasite is an important measure (T.I.). If it is high, than the pesticide is relatively safe. This means that there is a big difference between these parameters of the compound affecting two partners at the same time. The anilopyrimidine derivative (andoprim) and the dimethomorph being highly active in other relations [21, 28, 45, 56] exerted, in our experiments, good activity against *S. graminicola in vitro*. Nevertheless, they can't be recommended for controlling PMDM because of their low T.I. Similar studies on metalaxyl have been reported wherein, the higher concentrations, which offered higher protection but had effect on seed quality parameters [48]. The other compounds exhibited good sporocidal and antisporulant activity against taxonomically related pathogens [11, 20, 22, 30, 63], however, for controlling *S. graminicola* these compounds were not efficacious at the requested level.

Among systemically active antimildew compounds only the acylanilides were efficient at economically acceptable levels (*Table 4*). Regrettably, apart of their high efficacy these compounds (**1-9**) possess some unfavourable properties when using them against PMDM. Metalaxyl has low therapeutic value because of the sensitivity of pearl millet [53]. Although modifications in molecule of metalaxyl advantageously affected the therapeutic value (*Table 3*), the cross-tolerance has been complete for these analogues [19, 59]. Consequently new compounds with different mode of action should be developed for resolution of this problem. In populations of phylogenetically related to *S. graminicola* pathogens this type of tolerance was reported with probability between 10^{-6}–10^{-7} in model experiments [59, 62]. Although in the case of PMDM has not been reported yet, one can expect the appearance of strains of *S. graminicola* acquired tolerance to acylanilides in near future. Significant shift of PMDM incidence was in the recent vegetation recorded [5] in some plantations treated with metalaxyl (*Table 8*). There is, therefore, a need to find new systemic fungicides with activity against *S. graminicola*. The high variation in genetic background of *S. graminicola* [8, 27, 47, 55] also impress on searching new possibilities.

The screening activity against an obligate endoparasite is complicated. The comprehensive analysis of the effect against *S. graminicola* involve, in our opinion, evaluation effects both on host and parasite (zoosporangiogenesis, zoosporogenesis), disease syndrome and grain yield. Measurements on intact plants are time and work consuming. Moreover, the costs are also higher than studying responses of spores and germinating seeds or assessments of detached leaf segments. Similarities in the response of various developmental forms of *S. graminicola* to diverse chemicals as well as the close relationship between predicted activities and experimental values indicate the possibility of reduction of parameters for characterising the effect of compounds for use

http://www.ecology.uni-corvinus.hu ● ISSN 1589 1623

against PMDM. The results of calculations showed that characterisation of biological activity by two parameters (SP and SG) gave possibility ($p < 0.01$) to discriminate between compounds with acceptable or negligible antimildew effect (*Fig 3*).

The yield loss due to PMDM disease is attributed to loss of diseased plants during early developmental stages, poor tillering, and ear-head malformation [63]. Singh (1983) has made observation on grain yield increase upon seed treatment with metalaxyl [28]. It was shown that greatest yield increase was occurred in PMDM susceptible varieties. The present study also demonstrated the dominant effect of disease inhibition by fungicides, as it was indicated by a positive relation between efficacy of downy mildew control and yield enhancement (*Table 4*). The compounds with efficacy over 30% against PMDM in vitro may be useful for protecting pearl millet as seed applicants, while the compounds with disease inhibitory activity less than 25 % at maximum tolerated dose by pearl millet are considered useless as protectants. Therefore, the compounds with ED_{50} values more than 50 μM (about 10-20 mgL^{-1}) in test for sporulation are ineffective to prevent economic loss caused by *S. graminicola*.

Basing on our results the use of some acylanilides (furalaxyl, RE26745) is proposed for controlling PMDM. The chemicals with different mode of action that offered protection to considerable extent were andoprim (45%), efosit (39%), BKF-3 (49%) and drazoxolon (27%). The possible exploitation of them in the form of combinations with other fungicides would be promising for preventing the risk of resistance development in pathogen populations to fungicides. However, there are no such preparations available in the control of pearl millet downy mildew pathogen, by our results (*Table 6*) the effect of synergetic mixtures was reassuring. The value of these combinations for PMDM control should be rectified.

Conclusions

The present control technologies of downy mildews disrupt infection cycles either by killing asexual spores or by inhibition of growth of the parasite within its host. The infection of germlings and basal tillers of pearl millet is detrimental, while infection of secondary tillers does not contribute greatly to yield [63]. In our experiments both incidence and severity of PMDM were dramatically decreased by a single seed treatment, protecting germlings from seed and early soil borne infections. The phenological phase related susceptibility of pearl millet [50] was revealed with maximum in germling stage, which finding supports the importance of seed treatment as well. Consequently, the primary screening in the case of PMDM should concentrate on prevention of soil- and seed-borne infections as well as early air-borne infections of seedlings, because the control of diseases of primary tillers is fundamental in the production of pearl millet. On our opinion the effects on zoosporangiogenesis, zoosporogenesis, disease syndrome, seed germination and grain yield should be studied for screening compounds to be included into PMDM management. However, the expected yield performance can be roughly estimated ($P<1\%$) evaluating effects on seed germination and sporulation on detached leaf segments that can short-circuit the process for decision from 70 days to 4 days in pesticide development.

Seed treatment is the only feasible method to this disease [63]. This technology easiest to transfer to the farmers to promote sustained millet production [33], because it requests minimum participation and collaboration of farmers as well as the performance of the effect and impact of results do not depend essentially on participants in

http://www.ecology.uni-corvinus.hu ● ISSN 1589 1623

production. Moreover, the contamination with residual amounts of fungicide is also negligible [39] and the exposition of beneficial soil microflora associated to pearl millet [29] remains at low level. In arid climate and poor nutritional conditions the beneficial microflora associated to plants is extremely important [23, 38] so the use of compounds with broad spectrum of activity against soil borne pathogens should be excluded. Although the downy mildew tolerance of pearl millet can be enhanced by diverse methods [17, 66] the use of selective antimildew compounds with systemic activity can not be evaded.

Acknowledgements. This research was supported by the co-operation project "Theoretical base of integrated pest control methods" between Indian National Science Academy and Hungarian Academy of Sciences (Grant No. 11). Authors express thans to The Co-ordinator, All India Co-ordinated Pearl Millet Improvement Project, Jodhpur, India for facilities extended.

REFERENCES

[1] Abdul Baki, A.A., Anderson, J.D. (1973): Vigour determination in soybean seed by multiple criteria. - Crop Science 13: 630-633.
[2] D'Andrea, A.C., Klee, M., Casey, J. (2001): Archaeobotanical evidence for pearl millet (*Pennisetum glaucum*) in sub-Saharan West Africa. - Antiquity 75(288): 341-348.
[3] Anonymous (1977): Pearl millet Pathology. - In: ICRISTAT Annual Report 1976-77 pp 64-68, International Crop Research Institute of Semi-Arid Tropics, Hyderabad, India.
[4] Anonymous (1993): ISTA, International rules for seed testing. - Seed Science and Technology 13: 309-333.
[5] Anonymous (2001): Report of the All India Coordinated Pearl Millet Improvement Project. - Indian Council of Agricultural Research, Project Coordinating Unit, Agricultural Research Station, Mandor, Jodhpur, India.
[6] Anonymous: http://esc.syrres.com/interkow/kowdemo.htm (Syracuse Research Corporation, Syracuse, USA)
[7] Ball, S.L., Pike, D.J. (1984): Intercontinental variation of *Sclerospora graminicola*. - Annales of Applied Biology 104: 41-51.
[8] Ball, S.L., Pike, D.J., Burridge, C.Y. (1986): Characterization of populations of *Sclerospora graminicola*. – Annales of Applied Biology 108: 519-526.
[9] Bruck, R.I., Goodeng, A.V., Main, C.S. (1982): Evidence for resistance to metalaxyl in isolates of *Peronospora hyoscyami.* – Plant Disease 66: 44-45.
[10] Chabane, K., Leroux, P., Bompeix, G. (1993): Selection and characterization of *Phytophthora parasitica* mutants with ultraviolet-induced resistance to dimethomorph or metalaxyl. – Pest Science 39: 325-329.
[11] Cohen, Y., Coffey, M.D. (1986): Systemic fungicides and the control of Oomycetes. – Annual Review of Phytopathology 24: 311-338.
[12] Crute, I.R. (1987): The occurrence, characteristics, distribution, genetics and control of metalaxyl resistant pathotypes of *Bremia lactucae* in the United Kingdom. – Plant Disease 71: 763-767.
[13] Crute, I.R., Wolfman, S.A., Davis, A.A. (1977): A laboratory method of screening fungicides for systemic activity against *Bremia lactucae.* – Annales of Applied Biology 85: 147-152.
[14] Dang, J.K., Thakur, D.P., Grover, R.K. (1983): Control of pearl-millet downy mildew caused by *Sclerospora graminicola* with systemic fungicides in an artificially-contamined plot. – Annales of Applied Biology 102: 99-106.

http://www.ecology.uni-corvinus.hu ● ISSN 1589 1623

[15] Davidse, L.C., Hofman, A.E., Velthuis, G.C.M. (1983): Specific interference of metalaxyl with endogenous RNA polymerase activity in isolated nuclei from *Phytophthora megasperma* f. sp. *medicaginis*. – Experimental Mycology 7: 344-361.
[16] Deepak, S.A., Oros, G., Niranjan Raj, S, Shetty N.P., Shetty, H.S. (2004): Iprovalicarb has potential for the control of downy mildew of pearl millet. – Acta Phytopathologica et Entomologica Hungarica 39(1-3): 55-69.
[17] Desmukuh, S.S., Mayee, C.D., Kulkarni, B.S. (1978): Reduction of downy mildew of pearl millet with fertilizer management. – Phytopathology 68: 1350-1353.
[18] Detre, T., Rejto, L., Sos, J., Szego, A., Schuszler, E., Angyan, S., Keller Nee Marmarosi, K., Lyr, H., Zanke, D., Lenner, B., Strump, M., Oros, G., Virányi, F., Ersek, T., Nagy, G., Hornok, L., Molnar, A. (1991): – Fungicide compositions. US Patent 5 043 338.
[19] Diriwachter, G., Sozzi, D., Ney, C., Staub, T. (1987): Cross resistance in *Phytophthora infestans* and *Plasmopara viticola* against different phenylarnides and unrelated fungicides. – Crop Protection 6: 250-255.
[20] Erwin, D.C., Ribeiro, O.K. (1996): *Phytophthora diseases worldwide*. – APS Press, St. Paul, MN.
[21] Farih, A., Tsao, P.H., Menge, J.A. (1981): Fungitoxic activity of efosite aluminium on growth, sporulation and germination of *Phytophthora parasitica* and *P. citrophthora*. – Phytopathology 71: 934-936.
[22] Ferrin, D.M., Wadsworth, M.L. (1992): Effect of metalaxyl on sporulation and growth of metalaxyl resistant and metalaxyl sensitive isolates of *Phytophthora parasitica* in vitro. – Plant Disease 76: 492-495.
[23] Gilijamse, E., Frinking, H.D., Jeger, M.J. (1997): Occurrence and epidemiology of pearl millet downy mildew, *Sclerospora graminicola*, in southwest Niger. – Internatinal Journal of Pest Management 43: 279-283.
[24] Gozzo, F., Barino, L., Scordamaglia, R. (1987): A new approach to understand the logic of N-phenylamides as systemic fungicides. – Tagungsberichte der Akademie der Landwirtschaftwissenschaften DDR, Berlin 253**:** 77-83.
[25] Hollomon, D.W. (1969): Biochemistry of germination in *Peronospora tabacina* (Adam) conidia: evidence for the existence of stable messenger RNA. – Journal of General Microbiology 55: 267-274.
[26] Ingram, D.S. (1981): The biochemistry of host-parasite interactions. – In: D. M. Spencer (ed.) The Downy Mildews, pp. 143-163. Academic Press, London, U.K.
[27] Jeger, M,J., Gilijamse, E., Bock, C.H., Frinking, H. (1998): The epidemiology, variability and control of the downy mildews of pearl millet and sorghum, with particular reference to Africa. – Plant Pathology 47: 544-569.
[28] Krause. G., Klepel, M., Jumar, A., Franke, R. (1984): Quantitative structure - activity relationships of fungicidal pyrimidines. – Tagungsberichte der Akademie der Landwirtschaftwissenschaften DDR, Berlin 222: 229-232.
[29] Kumar, C.P.C., Balasubramanian, K.A. (1981): Phyllosphere and rhizosphere microflora of pearl millet with reference to downy mildew incited by *Sclerospora graminicola* (Sacc.) Schroet. – Plant and Soil 62: 65-80.
[30] Matheron, M.E., Porchas, M. (2000): Impact of azoxystrobin, dimethomorph, fluazinam, fosetyl-Al, and metalaxyl on growth, sporulation and zoospore cyst germination of three *Phytophthora* spp. – Plant Disease 84: 454-458.
[31] Muthusamy, H., Narayanasamy, M. (1981): Fungicidal control of downy mildew of pearl millet. – Indian Journal of Agricultural Sciences 51: 511-514.
[32] Nene, Y. L., Singh, S. D. (1976): Downy mildew and ergot of pearl millet. – Present and News Search 22: 366-385.
[33] Nyemba, J.A. (1997): Sustainable food-crop production in the semi-arid tropics: Strategy for technology transfer in millet research. – Journal of Sustainable Agriculture 9: 25-47.

http://www.ecology.uni-corvinus.hu ● ISSN 1589 1623

[34] Oros, G., Virányi, F. (1987): Glasshouse evaluation of fungicides for the control of sunflower downy mildew *(Plasmopara halstedii)*. – Annales of Applied Biology 110: 53-63.
[35] Oros, G., Érsek, T., Virányi, F. (1988): Effect of tridemorph oy *Phytophthora infestans* and *Plasmopara halstedii*. – Acta Phytopathologica et Entomologica Hungarica 23: 11-19.,
[36] Oros, G., Kőmives, T. (1991): Effects of phenylamide pesticides on the GSH-conjugation system of *Phytophthora* spp. fungi. – Zeitschrift für Naturforchung 46c: 866-874.
[37] Oros, G., Ujvary, I. (1999): Botanical fungicides: natural and semi-synthetic ceveratrum alkaloids. – Pesticide Science 55: 253-264.
[38] Pande, M., Tarafdar, J.C. (1999): Critical level of VAM fungal propagules in different arid crops. – Agrochimie 43: 187-192.
[39] Reddy, M.V.B., Shetty, H.S., Reddy, M.S. (1996): Residue free treatments of metalaxyl for effective control of pearl millet downy mildew. – Discovery and Innovation 8: 53-57.
[40] Roos, H., Buchenauer, H. (1985): Resistance of *Plasmopara viticola* to cyprofuram and metalaxyl. – Proceedings of Bordeaux Mixture Centenary Meeting (5-7 Sept 1985), a BCPC Monograph pp. 331-335.
[41] Roos, H. (1987): Einfluss von Cyprofuram, Metalaxyl und Aluminium-fosetyl auf die Atmung des Myzels von *Phytophthora cactorum* und der Sporangien von *Plasmopara viticola.* – Zeitschrift für Pflanzenkrankheiten und Pflanzenschutz 94: 130-136.
[42] Safeeulla, K.M. (1976): Biology and control of the downy mildews of pearl millet, sorghum and finger millet, Wesley Press, Mysore, 3*0*4 pp.
[43] Safeulla, K.M. (1976): Genetic vulnerability: the basis of recent epidemics in India. – In: Day, P.R. (ed.) Genetic Basis of Epidemics in Agriculture, pp 72-85, Annales of New York Academy of Sciences.
[44] Schroeter, J. (1879): *Protomyces graminicola* Saccardo. *Hedvigia* 18: 82-87.
[45] Schwinn, F., Staub. T. (1995): Oomycete fungicides. Phenylamides and other fungicides against Oomycetes. – In: Lyr, H. (ed.) Modern Selective fungicides. pp 323-346. Gustav Fischer Verlag, Jena
[46] Shailasree, S., Sarosh, B.R., Vasanthi, N.S., Shetty, H.S. (2001): Seed treatment with beta-aminobutyric acid protects *Pennisetum glaucum* systemically from *Sclerospora graminicola*. – Pest Management Science 57: 721-728.
[47] Shetty, S.A., Shetty, H.S., Mathur, S.B. (1995): Downy mildew of pearl millet. Technical bulletin*,* Downy mildew research laboratory. – University of Mysore, Mysore, India.
[48] Singh, S.D. (1983): Variable cultivar response to metalaxyl treatment in pearl millet. – Plant Disease 67: 1013-1015.
[49] Singh, S.D. (1995): Downy mildew of Pearl Millet. – Plant Dis 79:545-550.
[50] Singh, S.D., Shetty, H.S. (1990): Efficacy of systemic fungicide metalaxyl for the control of downy mildew *(Sclerospora graminicola)* of pearl millet *(Pennisetum glaucum)*. – Indian Journal of Agricultural Sciences 60: 575-581.
[51] Singh, S.D., Talukdar, B.S. (1998): Inheritance of complete resistance to pearl millet downy mildew. – Plant Disease 82(7): 791-793.
[52] Sun, Y-P. (1950): Toxicity Index - an improved method of comparing the relative toxicity of insecticides. – Journal of Economic Entomology 1: 45-53.
[53] Sundaram, N.V., Ramasatry, D.V., Nayar, S.K. (1973): Note on the seed-borne infection of downy mildew *Sclerospora graminicola* (Sacc.) Schroet. of pearl millet. – Indian Journal of Agricultural Sciences 43: 215-217.
[54] Talukdar, B.S., Babu, P.P.P., Rao, A.M., Ramakrishna, C., Witcombe, J.R., King, S.B., Hash, C.T. (1998): Registration of ICMP 85410: Dwarf, downy mildew resistant, restorer parental line of pearl millet. – Crop Science 38: 904-905.
[55] Thakur, R,P., Pushpavathi, B., Rao, V.P. (1998): Virulence characterisation of single-zoospore isolates of *Sclerospora graminicola* from pearl millet. – Plant Disease 82: 747-751.

http://www.ecology.uni-corvinus.hu ● ISSN 1589 1623

[56] Thakur, R.P., Rai, K.N., Rao, V.P., Rao, A.S. (2001): Genetic resistance of pearl millet male-sterile lines to diverse Indian pathotypes of *Sclerospora graminicola*. – Plant Disease 85: 621-626.
[57] Umesha, S., Dharmesh, S.M., Shetty, S.A., Krishnappa, M., Shetty, H.S. (1998): Biocontrol of downy mildew disease of pearl millet using *Pseudomonas fluorescens*. – Crop Protection 17: 387-392.
[58] Virányi, F., Oros, G. (1990): Antifungal activity of Andoprim against sunflower downy mildew. – Tagungsberichte der Akademie der Landwirtschaftwissenschaften DDR, Berlin 291 (S): 373-376.
[59] Virányi, F., Oros, G. (1991): Developmental stage response to fungicides of *Plasmopara halstedii* (sunflower downy mildew). – Mycological Research 95: 199-205.
[60] Weston, W.H. (1924): Nocturnal production of conidia by *Sclerospora graminicola*. – Journal of Agricultural Research 27: 771-783.
[61] Weston, W.H. (1928): Downy mildew (*Sclerospora graminicola*) on everglade millet in Florida. – Journal of Agricultural Research 36: 935-963.
[62] Wicks, T.J., Hall, B., Pezzaniti, P. (1994): Fungicidal control of metalaxyl insensitive strains of *Bremia lactucae* on lettuce. – Crop Protection 13: 617-623.
[63] Williams, R.J., Singh, S.D. (1981): Control of pearl millet downy mildew by seed treatment with metalaxyl. – Annales of Applied Biology 97: 263-268.
[64] Williams, R.J., Singh, S.D., Pawar, M.N. (1981): An improved field screening technique for downy mildew resistance in pearl millet. Plant Disease 65: 239-241.
[65] Wilson, J. P. (2000): Pearl millet diseases: A compilation of information on the known pathogens of pearl millet, *Pennisetum glaucum* (L.) R. Br. – Agriculture Handbook No. 716. USDA, Agricultural Research Service.
[66] Wilson, J.P., Gates, R.N., Panwar, M.S. (2001): Dynamic multiline population approach to resistance gene management. – Phytopathology 91: 255-260.

http://www.ecology.uni-corvinus.hu ● ISSN 1589 1623

SCALING PROPERTIES OF EPIDEMIOLOGICAL TIME SERIES

A. HARNOS[1]* - J. REICZIGEL[1] - F. RUBEL[2] - N. SOLYMOSI[1]

[1]*Department of Biomathematics and Informatics, Faculty of Veterinary Science, Szent István University, H-1078, István u. 2. Budapest, Hungary (phone: +36-1-478-4214; fax: +36-1-478-4217)*

[2]*Biometeorology and Mathematical Epidemiology Group Department of Natural Sciences, University of Veterinary Medicine Vienna Veterinärplatz 1, A-1210 Vienna, Austria*

**e-mail: Harnos.Andrea@aotk.szie.hu*

(Received 10th Sep 2005, accepted 10th Oct 2006)

Abstract. The statistical analysis monthly Hungarian (1967-2001) and Austrian (1989-2003) rabies and Hungarian bovine tuberculosis (1950-1979) cases were statistically analyzed. There were eradication campaigns against both diseases, which gave us the unique opportunity to observe how the statistical properties of the time series changed due to the eradication program. The fluctuations around the trend were got by removing the 12 month moving averages from the time series.

In order to characterize the structure of the contacts among the individuals exposed to the diseases and the underlying processes governing the behavior of the epidemics, the fluctuations were analyzed before and after eradication separately. It turned out that the tails of the complementary cumulative distribution functions differ in the rabies cases, and do not differ in the case of tuberculosis. In each case the tail of the distribution follows an Inverse Power Law (IPL) function and describes the distribution of extreme events. It is possible to make conclusions about the dimensions of the processes from the fitted exponents. These dimensions are not related necessarily to the spatial dimensions, but to the possible connections. The knowledge about the distributions give us the opportunity to asses the risk of epidemic outbreaks.
Keywords: *epidemiology, immunization, rabies, time series analysis, IPL distribution*

Introduction

Instead of using the usual statistical models, Rhodes and Anderson [1][2] [3], [4] proposed a new stochastic model, the so called Invers Power Law function (IPL), or otherwise Pareto model for describing time series of the epidemic sizes from small and large vaccinated human populations. Trottier and Philippe [5] applied this model for measles, rubella, pertussis and mumps outbreaks in Canada. IPL is a function with no characteristic scale and self-similar upon rescaling (scale invariance), and it may fit to the extreme values of the distribution (power law tail). The IPL function is self-similar against rescaling (scale invariance), that means that several scales are hiararchically embedded in each other, and this feature can explain the co-existence of small and very large epidemics. Large outbreaks are expected from this type of distributions [6]. One possible explanation of the existence of the IPL interactions assume that the system of the contacts among the individuals (contact network) is not random (Erdős-Rényi type). In scale-free networks, a few node have several connections (supernodes), but for the most only a few have (*Fig. 1*).

One can draw conclusions about the topolgy of the contact network where the epidemic spread from the distribution of the epidemic sizes [5] or can reveal the

http://www.ecology.uni-corvinus.hu ● ISSN 1589 1623

underlying mechanisms [7]. The interactive network of the contacts can explain the temporal and spatial pattern of the epidemic.

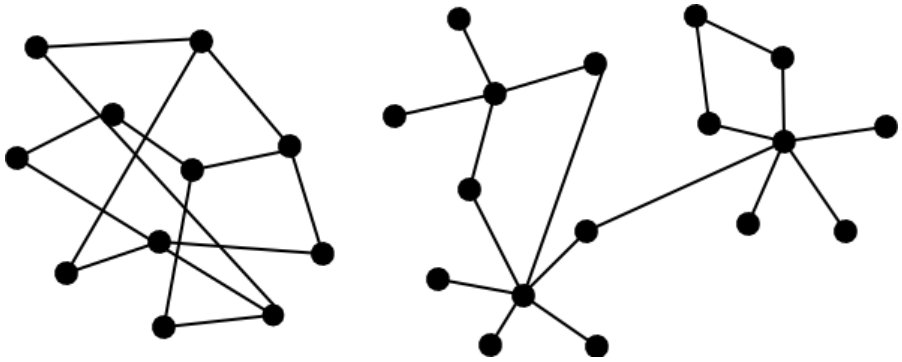

Figure 1. *Exponencial and scale invariant contact network*

Our goal is to prove the hypothesis that like in the case of human epidemics [5], in the cases under investigation, the distribution of the epidemic sizes of animals follows also an IPL function.

Modeling

The method of fitting an IPL function is called scaling analysis [1][2][3] and it consists of fitting the $F_c(l) = al^b$ function to the epidemic size distribution via fitting a linear function on the logarithmic scale $\log F_c(l) = \log a + b \log l$, where l is the epidemic size (in our case normalized with the moving average), a and b (a negative number) are estimable parameters of the epidemic size distribution.

The epidemics

Rabies

Rabies is a lethal viral zoonosis that can spread to humans and other animals through biting. During the last century, rabies has spread throughout parts of Central and Western Europe. Foxes have been the main hosts, but many other animals have also been infected, particularly dogs and cats. The incidence of endemic, fox-adapted rabies in Central and Western Europe has fallen dramatically. This has been largely due to the vaccination of wild and domestic animals.

In Austria and Hungary only the urban type of rabies – spread by dogs – existed until 1954. The sylvatic type rabies – spread by foxes – appeared in 1954 coming from the North-East. The epidemic propagated at a speed of 50-60 km/year until rabies became an endemic disease in 1970 [8].

In 1992, an immunization campaign started in both countries.

http://www.ecology.uni-corvinus.hu ● ISSN 1589 1623

In Hungary the oral vaccination campaign of the red foxes had several steps. In 1996 the whole western part was covered by the program. The eastern part of the country was not eradicated until 2001.

It is convenient to handle separately the western and eastern parts of Hungary because they are separated by the river Danube, a natural barrier for the spread of infection in Hungary, as it is quite unlikely for the foxes to pass through.

Bovine tuberculosis

Bovine tuberculosis is a significant zoonosis that can spread to humans through aerosols and by ingestion of raw milk. In developed countries, eradication efforts have significantly reduced the prevalence of this disease, but reservoirs in wildlife make complete eradication difficult. Bovine tuberculosis is still common in less developed countries, and economic losses can occur in cattle from deaths, chronic disease, and trade restrictions. Infections may also be a serious threat to endangered species [9][11]

Bovine tuberculosis results from infection by Mycobacterium bovis, a Gram positive, acid–fast bacterium.

In Hungary the eradication program against Bovine tuberculosis started in 1962 and it was finished by 1980.

Materials and methods

Data

The Hungarian rabies data have been collected from the rabies case registry of the Animal Health and Food Control Department of the Hungarian Ministry of Agriculture. The resulting data base contains data of all documented rabies cases for the period of 1990-2001, including the location and date of occurrences as well as the species affected. In addition to this detailed data base, we have monthly count data for the period of 1967-1990 for every county.

The bovine tuberculosis data also have been collected from the Animal Health and Food Control Department of the Hungarian Ministry of Agriculture. In this case we have half monthly count data for the whole country (1950-1978).

The Austrian data have been got from the Bundesanastalt für Tierseuchen-bekämpfung in Mödling and the data were processed by the Biometeorology and Mathematical Epidemiology Group Department of Natural Sciences, University of Veterinary Medicine Vienna.

We constructed monthly summarized time series from the Hungarian rabies dataset (1967-2001) for the western (Transdanubia), and for the eastern part (Eastern Hungary) of the country. In *Fig. 2* we show these two time series.

http://www.ecology.uni-corvinus.hu ● ISSN 1589 1623

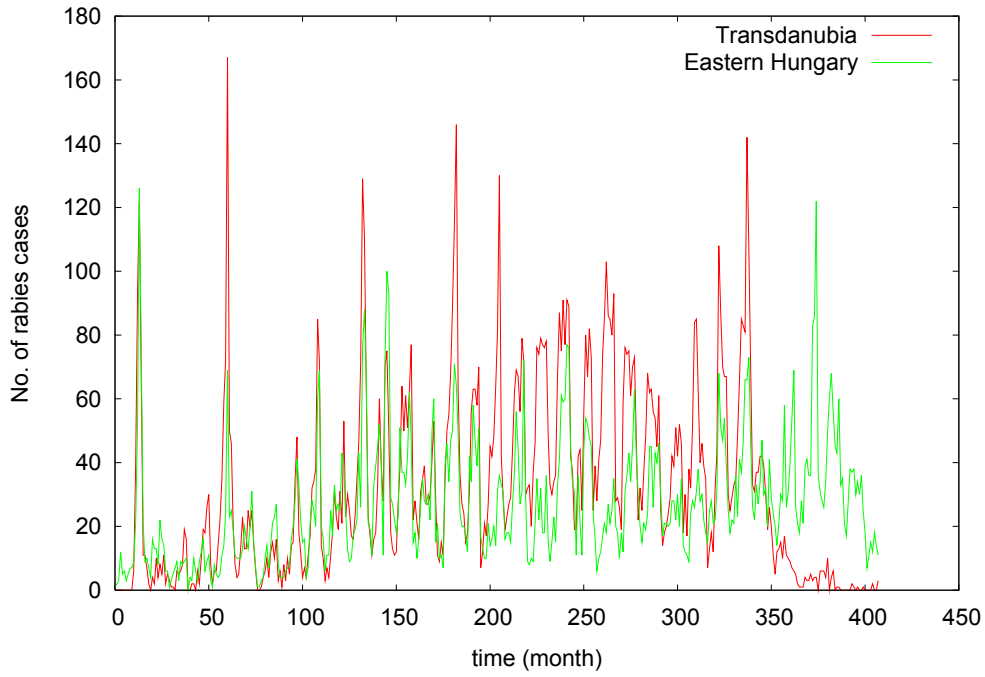

Figure 2. *Monthly number of rabies cases in Transdanubia and in Eastern Hungary (1967-2001)*

In the Austrian case we have summarized count data for the whole country (1989-2001). The constructed time series can be seen on *Fig. 3.*

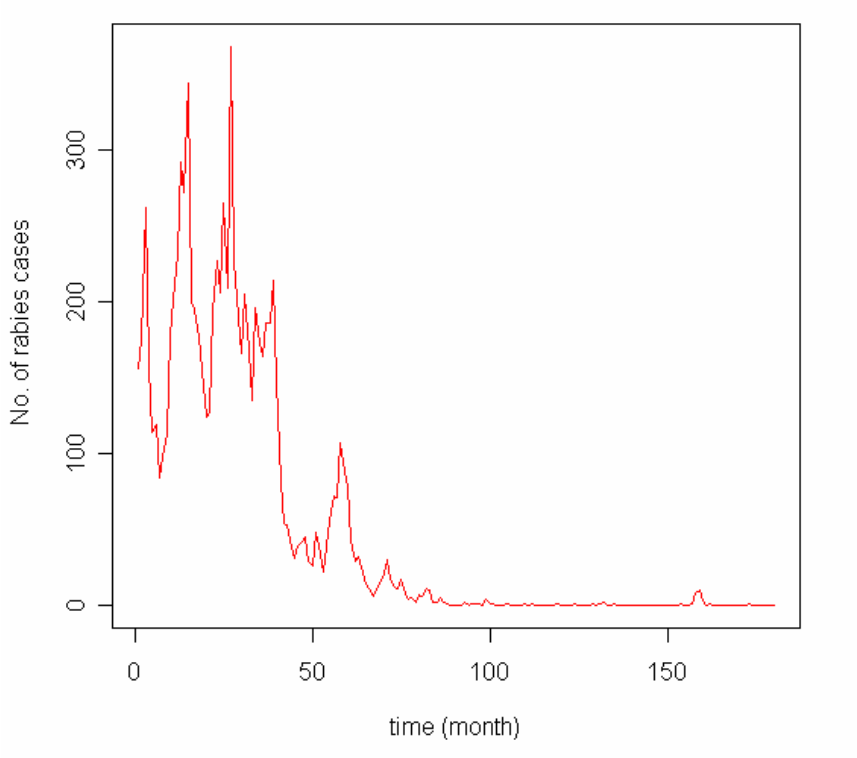

Figure 3. *Monthly number of rabies cases in Austria (1989-2001)*

http://www.ecology.uni-corvinus.hu ● ISSN 1589 1623

In the case of bovine tuberculosis *Fig. 4* shows the time series.

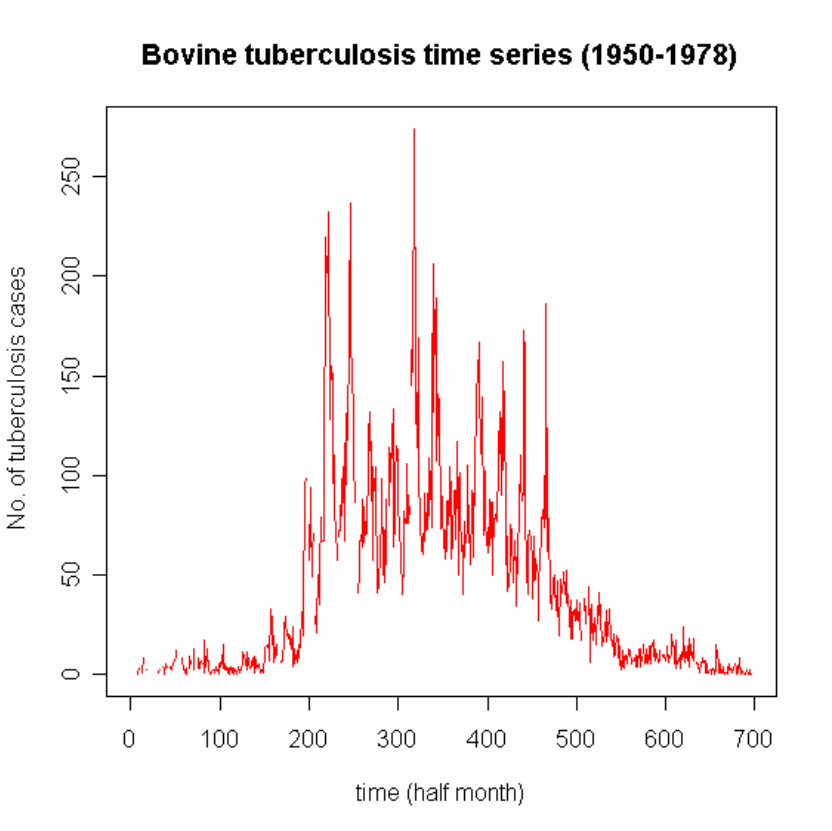

Figure 4. *Half-monthly number of tuberculosis cases (1950-1978)*

Software

The data base was developed using the Microsoft Office XP Professional Edition Microsoft Access software. We performed the analysis with Microsoft Excel XP, R and Gnuplot programs.

Analysis of extreme fluctuations

To analyze the large fluctuations, first we had to identify the trend in the time series. To calculate the moving averages as the trend is a good method if the average of the time series changes rapidly. In such cases it is useful to calculate the fluctuations around the moving average over a preceding period. In our case the external conditions have a 12-month periodicity, so it is natural to consider a 12-month moving average and values relative to the moving average $l(i) = f(i)/\left(\sum_{j=1}^{12} f(i-j)/12 \right)$, where $f(i)$ is the number of cases in the i^{th} month in the series. These are the fluctuations, that we analyse further. It turned out that in each case the fluctuation time series are stationary.

The best way to study the statistics of the extremely large outbreaks is to consider the complementary probability distribution $F_c(l) = \Pr ob\{l(i) > l\}$, which gives the probability that the relative fluctuation is larger than l. By a scaling analysis – fitting

http://www.ecology.uni-corvinus.hu ● ISSN 1589 1623

lines to the tails on double logarithmic plots - it can be shown that this distribution develops an inverse power law tail

In *Fig. 5-7* we show the complementary cumulative distribution for the data series with and without the eradicated parts for rabies in Transdanubia and Austria and for tuberculosis.

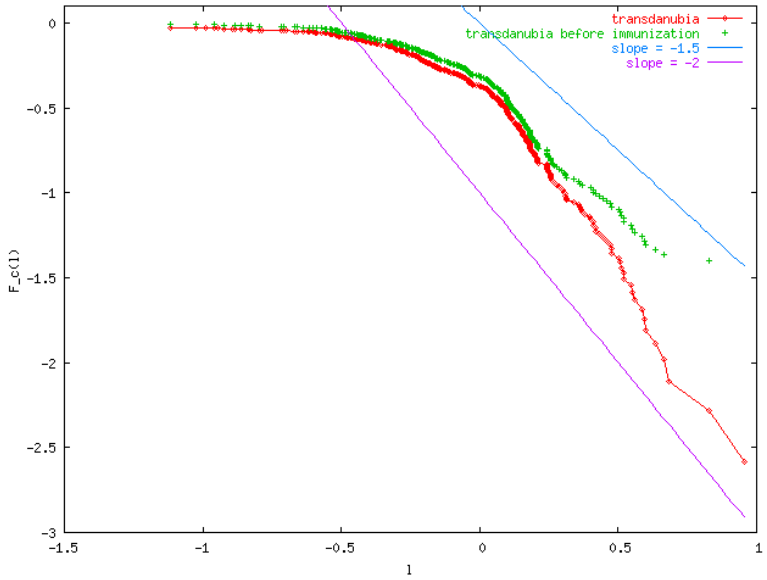

Figure 5. *The complementary cumulative distribution of the fluctuations relative to the 12 months moving average for the Transdanubia data with and without immunization on a doubly logarithmic plot. The straight lines represent the fitted power law tails with exponent b= -2 and b=-1.5..*

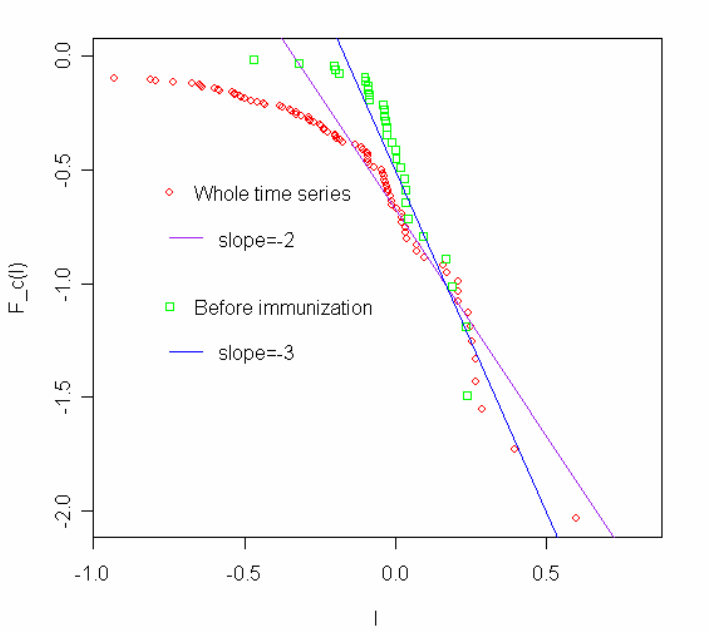

Figure 6. *The complementary cumulative distribution of the fluctuations relative to the 12 months moving average for the Austrian data with and without immunization on a doubly logarithmic plot. The straight lines represent the fitted power law tails with exponent b= -2 and b=-3..*

http://www.ecology.uni-corvinus.hu ● ISSN 1589 1623

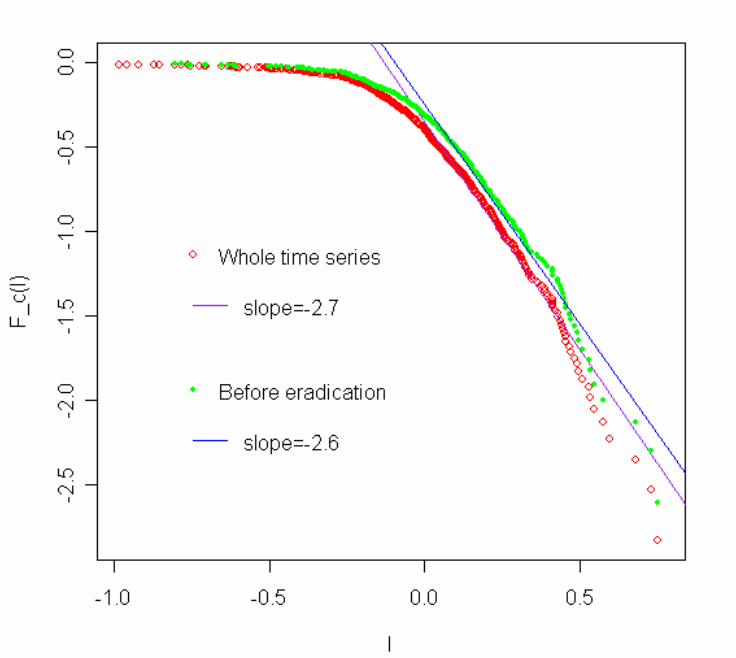

Figure 7. *The complementary cumulative distribution of the fluctuations relative to the 12 months moving average for the tuberculosis data with and without eradication on a doubly logarithmic plot. The straight lines represent the fitted power law tails with exponent b= -2.7 and b=-2.6*

In the Transdanubia case the main effect of immunization on the statistics of large outbreaks is the change of the scaling exponent b of the IPL from about -1.5 before immunization to 2.0 after immunization.

In the austrian case the main effect of immunization on the statistics of large outbreaks is the change of the scaling exponent b of the IPL from about -3 before immunization to -2 after immunization.

In the tuberculosis case there can not be seen significant change in the slopes.

Discussion

Rabies has always been given due respect both in human and veterinary medicine because it is an incurable disease. Most rabies cases in Europe are still diagnosed in red foxes (Vulpes vulpes) because red fox is the reservoir and primary perpetrator of the disease.

Bovine tuberculosis is also a zoonosis that can infect humans seriously.

In this paper we concentrated on extreme fluctuations in the time series constructed by calculating the fluctuations around the trends. Extreme fluctuations are low-probability, high-consequence events [12] representing the majority of total losses. Understanding the size distribution of extreme events makes it possible to assess the risks of outbreaks.

We determined the distributions of extreme fluctuations which is a scale invariant power law distribution for the time series investigated.

Interesting to see that in the rabies cases the exponents (slopes on double logarithmic plots) definitely changed due to the eradication, this is different in the case of bovine

http://www.ecology.uni-corvinus.hu ● ISSN 1589 1623

tuberculosis. Possible explanation is that the contact network of the population did not change in this case, because cattles are domestic animals, and the location of the settlements where they are kept remained the same.

Due to the fact that the exponent of the power law is related to the dimensionality of the process [7] - that is not by all means spatial dimension - we could show how immunization changed the structure of the problem.

The importance of the IPL distribution of the extreme fluctuations (outbreaks of the epidemics) is that from this kind of epidemic spreading contact networks large outbreaks are expectable. As the pathogens of the diseases still exsist in the populations on a very low level, these pathogens may couse serious outbreaks in the future.

This kind of analysis can help to estimate the effects of eradication programs and to asses the risk of epidemic outbreaks.

Acknowledgements: This work was partly supported by the grants OTKA T049157.

REFERENCES

[1] Rhodes, C.J., Anderson, R.M. (1996): A scaling analysis of measles epidemics in a small population. - Philos. Trans. R. Soc. Lond. B Biol. Sci. 351: 1679-1688.

[2] Rhodes, C.J., Anderson, R.M. (1996): Power laws governing epidemics in isolated populations. -- Nature 381: 600-602.

[3] Rhodes, C.J., Jensen, H.J., Anderson, R.M. (1997): On the critical behaviour of simple epidemics. - Proc. R. Soc. Lond. B Biol. Sci. 264: 1639-1646.

[4] Rhodes, C.J., Butler, A.R., Anderson, R.M. (1998): Epidemiology of communicable diseases in small population. - J. Mol. Med. 76: 111-116.

[5] Trottier, H., Philippe, P. (2005): Scaling properties of childhood infectious diseases epidemics before and after mass vaccination in Canada. - Journal of Theoretical Biology Biol. 235: 326-337.

[6] Philippe, P. (2000): Epidemiology and self-organized critical systems: An analysis in waiting times and diseases heterogeneity. - Nonlinear Dyn. Psychol. Life Sci. 4 (4): 275-295.

[7] Harnos, A., Reiczigel, J., Solymosi, N., Vattay, G. (2006): Analysis of the Effect of Immunization in Rabies Time Series. - Journal of Theoretical Biology (in press)

[8] Mocsári, E., Kerekes, B., Heltay, I., Szalay, D., Csabay, L. (1994): Experiences on the oral vaccination of foxes against rabies in Hungary. - Hungarian Veterinary Journal 49: 10–15.

[9] Rubel, F., Höflechner, A. (2004): Documentation of Rabies in Austria 1945-2003. Meeting of the Task Force Subgroup RABIES, Klagenfurt, Austria, 21 - 22 Sept. 2004.

[10] Institute for Internationa Cooperation in Animal Biologic An OIE Collaborating Center Iowa State University, College of Veterinary Medicine (2003): Bovine Tuberculosis 235: 326-337 (http://www.vm.iastate.edu/services/institutes/iicab/iicab.htm)

[11] Varga, J., Tuboly, S., Mészáros, J.(1999): A háziállatok fertőző betegségei. Állatorvosi járványtan II. Mezőgazda Kiadó

[12] Englehardt, J. D. (2002): Scale Invariance of Incident Size Distributons in Response to Sizes of Their Causes - Risk Analysis. 22: 2

http://www.ecology.uni-corvinus.hu ● ISSN 1589 1623

ON THE NUMBER OF RGB COLOURS WE CAN DISTINGUISH PARTITION SPECTRA

E. LÁBOS

Research Group of Neurobiology of Hungarian Academy of Sciences
at the Semmelweis University
1094 Budapest, Tűzoltó u. 58.
(phone: +36-1-215-6920 / 3632; fax: +36-1-215-5158)

E. Lábos
e-mail: labos@ana1.sote.hu

(Received 10th Sep 2005, accepted 10th Oct 2006)

Abstract. Colour vision is a physiological phenomenon, and rays are not coloured (Newton, Wright). While counting hues of solar spectrum is a solved problem, the exact number of colours is unknown. Existing colour systems do not provide automatically colour census methods.
This work addressed only to the 24 bit RGB-colour system. This complete colour space itself is countable. Discovering principles for ordering colours is a prerequisite of any efficient census algorithm. Colours (r, g, b) we define, as a partition of total n = r + g + b amount of intensity into 3 parts also with *r/g* and *g/b* ratios fixed. *Partition spectra* are the lexicographically sorted list of these partitions. Such and also geometrically defined sub-domains of RGB-cube can be transformed into 1D colour spectra by reshuffling according to their HSV-hue-angles in order to bring similar colours into close neighbourhood. These we call pseudo-solar colour spectra. Our estimation for subjectively discriminated RGB-colours is no more than 200000.
Keywords: *partition-colour-spectra, RGB-cube, HSV-space, ordering colours , reshuffling by hues.*

Introduction

To distinguish numerous colours is an ancient experience. The number of hues in rainbow is one of the first related knowledge, associated with Aristotle and Newton [1]. Colour sensation is physiologically founded. No physical arguments for segregation of zones inside the visible electromagnetic continuum exist. Rainbow only appear to be divided. Thus colour is a permanent illusion of normal human subjects. Rays are not coloured (Newton,Wright, [2]). Thus census of colours is finally a human experimental issue. However, preparation of enumerations, that is our actual purpose, should and can be supported with mathematical tools

In any artificial representations, colours are arranged by some regular way in a bounded domain of 1, 2 or 3 dimensions. Inside, points are usually described with 1, 2 or 3 parameters. Such colour-spaces are based on some colour theory. Geometrically, that spaces are either linear spectra, circles, wheels, triangles, cubes, cones, pyramids, cylinders, matrices (charts) or more sophisticated manifolds. Nearly hundred of such historical colour-systems have been constructed. Handbooks like [3] and [4] give good surveys. An incomplete, arbitrary selection may include names from Aristotle to Munsell. While the most important modern colour systems are CIE1931, RGB, HSV [5] and CMYK (see Glossary).

http://www.ecology.uni-corvinus.hu ● ISSN 1589 1623

Neither of colour-systems offers perfect solution for the precise counting of colours or hues we can discriminate. However, all ones provide significant help to approach the answer.

Present considerations are restricted to RGB and partly deals with to HSV system [5].

The RGB model is used to describe colours of computer monitor emissions in a digital fashion. An RGB-colour is a (red, green, blue) vector. Components are either between 0 and 1 or integers between 0 and 255. RGB-system is in close connection with the very consolidated tristimulus colour-vision theory of Young - Helmholtz - Maxwell for human. It is based on 3 cones with maximal sensitivity at 564, 534 and 420 nm supplemented with brightness channel of rods. Different facts hold to other animals. In monitors RGB system describes screen emission of 3 primary colour components through 24 bits per pixel information. Further colours are derived by additive colour mixing.

Intensive use of monitors keeps alive the misbelief that we might distinguish all the $2^{24} = 16777216$ distinct colours simply because the screen display them.

Counting of hues is different from that of colours and it is easier. Here we accept, as the 1st *definition of hue* that one-hue = one-wavelength. Numerous less precise definitions of hue like dominant wavelength, colour-quality, name are not always useful or even misleading. Set of hues becomes finite and countable if perceivable ranges are determined. The estimate for the count of discriminable, almost-monochromatic spectral colours, the hues, arises from psychophysical studies of wavelength discrimination-threshold curves [6, 7, 8, 9]. In 400-800 nm λ–range usually more than 1, often 2, 3, sometimes 6-8 nm $\Delta\lambda$–shift is required (in average 3.1-3.3 nm) to perceive a different hue. Averaging available $\Delta\lambda/\lambda$ curves of Wright and Pitt [6]. approximately 100-120 narrow, i.e. quasi-monochromatic spectral light-ranges (= practical hues) we can encounter or distinguish.

In HSV-systems [5], colours are specified through properties like hue, saturation, and lightness (or value). HSV system provides a *2nd definition of hue* as a computed quantity from parameters of other colour systems. In RGB - system, magnitudes of r, g and b, the so called *primary* components hide values of brightness and saturation and hue. Several conversion formulas between RGB and HSV are available [5]. In HSV, circular hue–spectra is applied., essentially a solar spectrum., closed into a circle.

Further colour-counts are based upon colour charts, collections, catalogues, atlas for painters, printers or recently for web-sites or monitors. Nemcsics [3] and Lukács [4] provide large list of historically important tables of colour - collections. The number of colour in these various catalogues lays between 94 and 25000. Such a list appeared already 450 years ago.

In the CIE1931 diagram, discrimination or MacAdam ellipses or tolerance - spheres serve to separate equivalence classes of colours [10, 3, 4].

It is not the main problem is how to harmonize 7 rainbow-colours, 120 spectral hues, 100 - 25000 catalogue items or 16777216 colours of RGB system. The true problem is the suitable order of colours. However, colour identification is rendered more difficult by additional factors.

- (1#)Various colour-gamuts are different and are roughly in the following relationship:

http://www.ecology.uni-corvinus.hu ● ISSN 1589 1623

CIE1931 ⊂ RGB ⊂ CMYK ⊂ SpectralHues (= rainbow)

Thus in principle colours may exist which are not inside RGB-cube but are present in CIE1931 - space. If an extra RGB - colour was distinguished by a human observer from any monitor-colour, this will enhance reduced RGB - space. Attribute *reduced* would mean a restriction of RGB to pairwise and subjectively discriminated colours. It is paradoxical that monitors display rich CIE-diagrams rather well.

- (2#)Several colour illusions point to contexts which induce perceptual difference of two, physically identical colour stimuli: Bezold-effect, simultaneous or successive chromatic contrast illusion, Mach-bands, spreading, assimilation or shift of colours etc. The related illusions or conditions may be so intensive that are not neutral in definition of colours, hues or colour constancy.
- (3#)Objectively different RGB-colours may appear to be identical. This is mainly a threshold problem. However, discrimination threshold may depend on sophisticated conditions. E.g. additive inverses of undistinguished colours can be discriminated.
  Colour counting is here approached in RGB-cube. Piecewise experimental comparisons of all pairs of $n = 2^{24}$ colours is impossible since involves 2^{47} steps. So tricks for easier mass-comparison. should be elaborated. Colour ordering principle are needed and are possible through various mathematical considerations.

Methods

Image manipulation, coloured spectra and numerical data beyond were generated by own program-codes written in WolframMathematica-5.

Sets of 1D or 2D transitional spectra. 3D colour domains of RGB cube

In any colour-system ordered colour sets are defined. Most often, the solar spectrum is used by closed into colour circles or wheels. In true solar spectrum the control principle is the wavelength. Transitions between colours are mostly determined by the rainbow. In colour charts, homogenous groups of colours are tabulated, often by *ad hoc* principles. Inside groups brightness, or saturation usually change. Complete account of all colours is not guaranted.

It seems an economic way to walk through the RGB - cube or on its surface in the hope to compress the whole into a smaller body of the subjectively distinct RGB-colours.

Interesting 1D colour-transitions arise between 2 saturated primary colours, or between a colour and its additive complement, or between a primary and a secondary colour or between two arbitrary colours A and B which are not necessarily neighbors in solar spectrum or in cube. Examples are given in *Figure 1*. All of these 1D or 2D transitional spectra can be in principle compressed by eliminating undistinguished cases of RGB colours.

http://www.ecology.uni-corvinus.hu ● ISSN 1589 1623

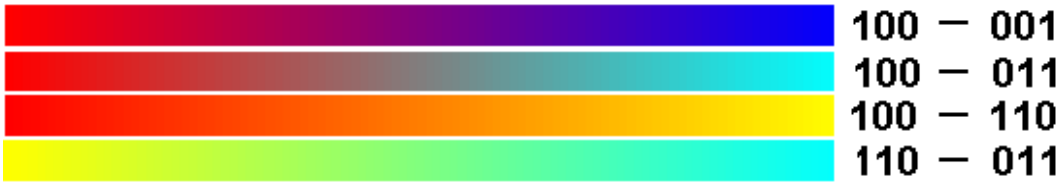

Figure 1. *Spectral 1D- transitions between 2 RGB colours. Examples*

Various 1D, 2D or 3D wandering strategies over the RGB-cube can be chosen. The colour - points are 3D vectors in a unit-cube or discrete lattice points in a cube with side-length = 255 integer, withthe *big grey diagonal* between {0,0,0,} and {255, 255, 255} points. Minings or scans inside cube can be based either on geometrical or even combinatorial principles..

A sensitive point is that close points in Euclidean sense may be close or distant as subjective colours. To get an impression see the 6 sides of this colour cube in *Fig. 2.*

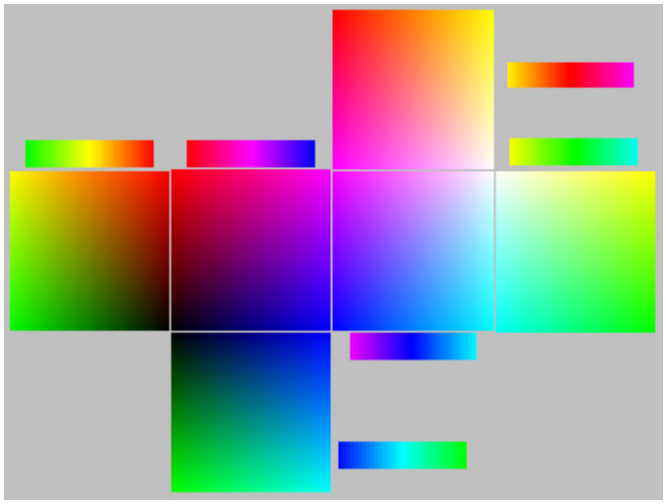

Figure 2. *The 6 sides of the RGB colour cube. Skin of RGB-cube with homogenous zones. Each plane corresponds to a 2D-spectrum, reducible to 1D spectra . Surface contains more than 390000 colours. Only a few hundred subjectively distinguished.*

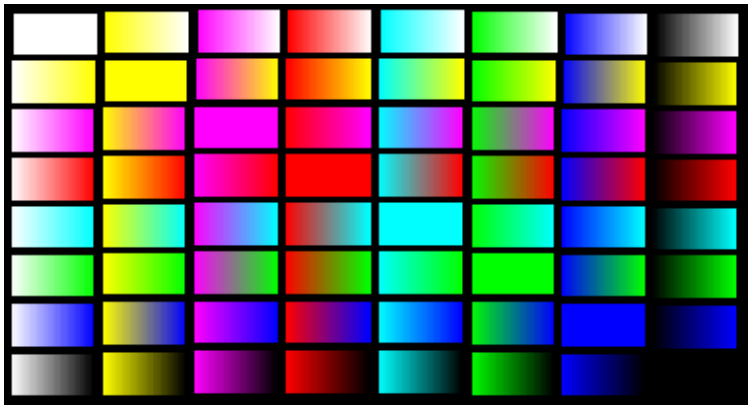

Figure 3. *Matrix of all possible 1D transitions spectra between primary and secondary RGB colours. 64 edges and diagonals between 8 corners of RGB cube. Largest cube-diagonal is the grey-scale. Diagonal of matrix includes the 8 constant corner-colours .*

http://www.ecology.uni-corvinus.hu ● ISSN 1589 1623

A great number of possible 3D-stratagies of wandering are useful. E.g. cut seemingly colour – uniform subsets like {(r ± ε , g ± ε, b ± ε)} even with several thousands of formally different RGB-points, but with only one or a few subjectively monochromous set of pixels.

RGB colours as partitions

This sorting of RGB-colours is radically different from solar spectral transitions as mostly applied previously. RGB-colours are 3D vectors of integer coordinates between 0 and 255. Their linear (=1D) arrangement is possible only in lexicographic manner violating continuum inside the cube. Listing sorted partitions means a reshuffling of geometrical neighbourhoods.

Formal combinatorial background or model

Distribute n cards between three persons, each one receives 0,1,…,n cards. If persons are not distinguished then the solution is the set of partitions of n into 1,2 or three parts. For n=10 we get the following 14 distributions:
{{10,0,0},{9,1,0},{8,2,0},{8,1,1},{7,3,0},{7,2,1},{6,4,0},{6,3,1},{6,2,2},
{5,5,0},{5,4,1},{5,3,2},{4,4,2},{4,3,3}}

The number of solutions p(n) is well known and it is a non-trivial integer [11]:
p(n)= {1,2,3,4,5,7,8,10,12,14,16,19,21,24,27,30,33,37,40,44,48,52,56,61,65,
70,75,80,85,91,96,102}.

As soon as persons are distinguished, more cases arise. If n=10, the 66 ordered partitions
(called also as compositions) are as follows:
{0,0,10},{0,1,9},{0,2,8},{0,3,7},{0,4,6},{0,5,5},{0,6,4},{0,7,3},{0,8,2},{0,9,1},
{0,10,0},{1,0,9},{1,1,8},{1,2,7},{1,3,6},{1,4,5},{1,5,4},{1,6,3},{1,7,2},{1,8,1},
{1,9,0},{2,0,8},{2,1,7},{2,2,6},{2,3,5},{2,4,4},{2,5,3},{2,6,2},{2,7,1},{2,8,0},
{3,0,7},{3,1,6},{3,2,5},{3,3,4},{3,4,3},{3,5,2},{3,6,1},{3,7,0},{4,0,6},{4,1,5},
{4,2,4},{4,3,3},{4,4,2},{4,5,1},{4,6,0},{5,0,5},{5,1,4},{5,2,3},{5,3,2},{5,4,1},
{5,5,0},{6,0,4},{6,1,3},{6,2,2},{6,3,1},{6,4,0},{7,0,3},{7,1,2},{7,2,1},{7,3,0},
{8,0,2},{8,1,1},{8,2,0},{9,0,1},{9,1,0},{10,0,0}

The number of such partitions corresponds to the well-known *triangular numbers* [12]:
P(n) ={1,3,6,10,15,21,28,36,45,55,66,78,91,105,120,136,153,171,190,210,
231,253,276,300,325,351,378,406,435,465,496,528,561,….,32896,…,286146},
from n = 0,1, …, 255,….,755

If n cards are divided into 3 persons then the number of such partitions is:

$$P(n) = (n + 2)(n + 1) / 2 = C(n+1, 2) \qquad \text{(Eq. 1)}$$

Applications triangular partitions to describe RGB colour vectors

Partitions as RGB colours are possible for n < 255+255+255=765. At n > 255, formula of P(n) given in (Eq. 1.) requires corrections. Colours satisfying r+g+b = n are in planes of RGB-cube with identical brightness and all colours in this plane are different because r/g and g/b color ratios are different. Corrected number of colours is R(n) =P(n) - w(n), where w(n), the number of *impossible RGB-partitions* which increases rapidly with n:

http://www.ecology.uni-corvinus.hu ● ISSN 1589 1623

w(n)=0 for n<256, R(n) = 0 if n > 765. Number of colours is maximal in the r + g+ b = 383 plane and it is 49152. E.g. (170,150,190) is a legitimate, while (300,10,200) is an invalid RGB-partition of sum-total = 510 because individual coordinates in cube do not exceed 255. Sequence [13] is involved.

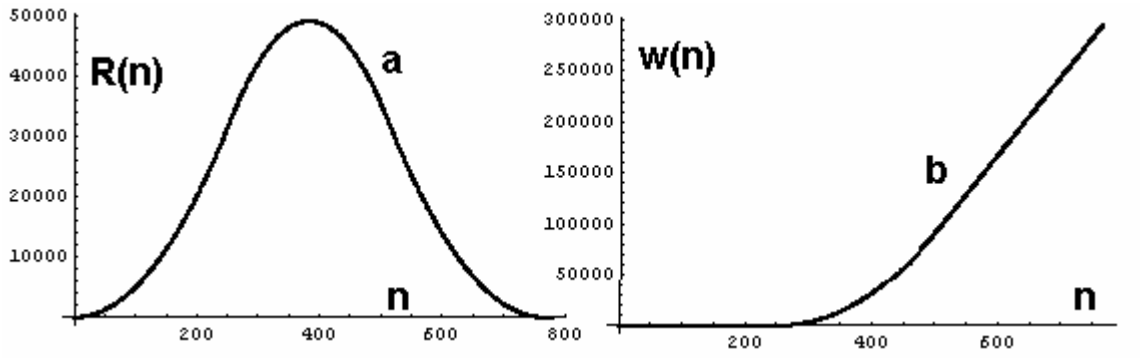

Figure 4. *(a) is the number of valid RGB partitions or different colours, (b) the number of invalid partitions in the 766 luminosity layers of RGB – cube orthogonal to and around the big grey diagonal axis. Plotted against n = r + g + b.*

In a valid RGB partition all components are ≤ 255. Partition of n means luminosity = n. Among the R(n) RGB-solutions for r +g + b = n, pair of ratios $\{k_1=r/g, k_2=r/b\}$ are all different and characterizes colours. Physically these ratios describe emission ratios for a given coloured pixel. Per analogiam, in retina the three cones were activated – or absorb energy or quanta according to analogous characteristic ratios. These two interpretations obviously require further corrections and harmonisation by application of precise emission and absorption spectra of monitor or cones respectively.

- Example 1: n=255; initial colour = (85,111,59), is a relatively dark olive-green. The brightest integer version is (170,222,118).
- Example 2: n=6; initial colour = (3,2,1) is an almost black with invisibly weak reddish/violet shade. Max [{3,2,1}] = 3, thus 255/3=85 colour-shades with invariant r/g, g/b ratios are generated. Spectra are displayed in (*Fig. 5)* Terminal colour is (255,85,170). In the examples ratios are kept invariant, lightness are increases.

Figure 5*. See in text above. Example 1 and 2*

Partitional spectra

Given r + g + b = n. in RGB-space. It is a plane with constant brightness and orthogonal to the *big grey diagonal* of RGB-cube. When (r, g, b) vectors run through all partitions of n and the partitions are lexicographically sorted, then we get a *partition spectrum (p-spectrum)* with resolution 1/n or with lightness n. If n is small, then all generated colours are shaded, darkish. If n ≤ 255, the length of a p-spectrum, i.e. its number of colours is (n + 2)(n +1)/2. At n = {0,1,2,4,8,16,32,64,128,255} these lengths

http://www.ecology.uni-corvinus.hu ● ISSN 1589 1623

are {1,3,6,15,45,153,561,2145,8385,33153} respectively. Inside these spectra at least one of the ratios of {r/g, r/b} and consequently g/b change with particular partitions from (0, 0, n), … to (n, 0, 0) i.e. with individual colours as we define here. The spectrum starts with RGB primary blue and terminates with primary red. In order to get brighter spectral colours, all channel coefficients were further divided by the maximum of {r, g, b} components. Consequently, constancy of brightness disappears, while colour-character and ratios remain invariant. In each colour vector at least one coefficient will have the magnitude 1 (or 255). Therefore colours are projected onto the lighter half-surface of RGB-cube.

These partition spectra show remarkable properties. 1#. - With increasing n, partition - spectrum includes n colour bands. 2#. - Inside a band and also along consecutive bands, regular transitions are observable, bands shorten. 3#. - First half or so bluish - greenish alternation is visible. In the second half, orange-red becomes overwhelming. 4#. At n=1 and at n=3 only the well-known RGB primary and nearly secondary colours (red, green, blue, yellow, magenta, turquoise) emerge. 5#. Colours proximal to white appear in the first series of (1,x,y) colours, while black shades arise among inverted (0,x,y) ones (*Fig. 6b, Fig. 6b1*).

Partition spectra list all distinct colours with 1/n upper bound for deviation of colour-coefficient-ratios. It sorts but did not bring close enough subjectively close colours. Further transformation should be introduced in order to classify colours (not hues!). This better rearrangement was carried out by their *computed hues* as an HSV-parameter. Results see in (a1), (b1) of (*Fig. 6.*)

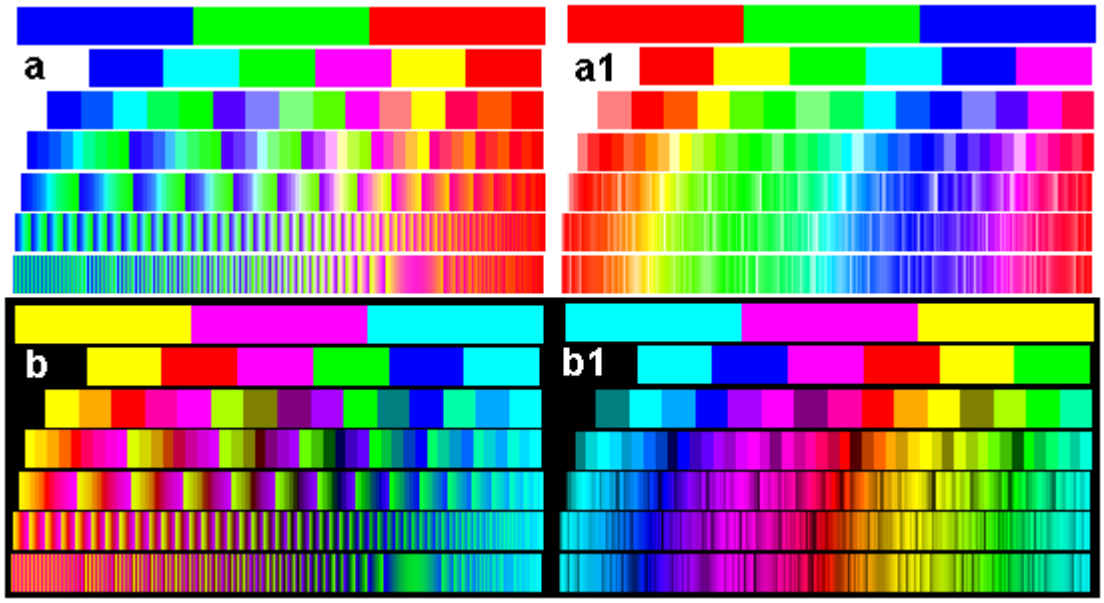

Figure 6. *(a) = Partition spectra with increasing resolutions n = 1, 2, … ,64; max[r,g,b] = 1. (b) = Spectra of (a) are inverted, min[r,g,b]=0. In each spectrum number of colour is (m+2)(m+1)/2. Spectrum (a1) and (b1) rearranged of (a) and (b) according to magnitude of their computed HSV hues-angles*

http://www.ecology.uni-corvinus.hu ● ISSN 1589 1623

A few details of various partition spectra

Partition spectra at different values of n (*Fig. 6*) are similar to each other. Each starts with BTG (blue, turquoise, green) bands. It lasts to 30-40% of the total length. Medial 20% zone keeps green with viola and white. In 3rd zone the bands are composed of lilac-magenta-yellow while green disappears. Finally the bands are dominated with red - orange - yellow. (See *Fig. 7*.) To reach significant colour-number-reduction, comparative psychophysical test of the bands seem here fruitful but are still difficult. Only the completeness of partition-colours is sure.

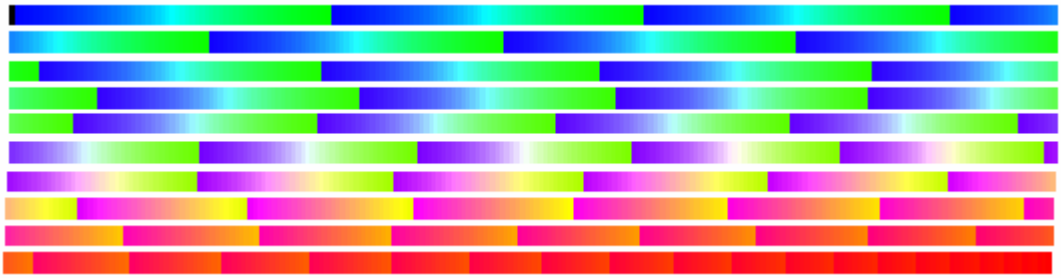

Figure 7*. Single partition spectrum with resolution n = 64. It consists 2145 RGB colours. Observe regular metamorphoses of the 64 bands.*

Hues along partition spectra. Conversions to HSV colour system

Several conversion formula from RGBcolours to HSV colour-representation exist. HSV colour - space [5] describes a colour as a (hue, saturation, value) = (H, S, V) vector. For a given RGB- point, the parameter V is either the maximun or arithmetical mean of RGB coordinates. Saturation S, is either (max - min)/max or standard deviation of RGB coordinates. To compute component H of HSV the most often used formula is applied here:

$$H = b+60(c_1 - c_2)/(\max - \min) \qquad \text{(Eq. 2)}$$

Here c_1-c_2 is G - B, B - R, R - G or b = 0, 2, 4 if max {R,G,B} = R, G, or B respectively. The result is a hue expressed by an angle in degree between 0 and 360, where red = 0, green = 120, blue = 240. It is hard to believe that this concept of hue corresponds to wavelengths with one nm accuracy.It is a 2nd definition of hue.

http://www.ecology.uni-corvinus.hu ● ISSN 1589 1623

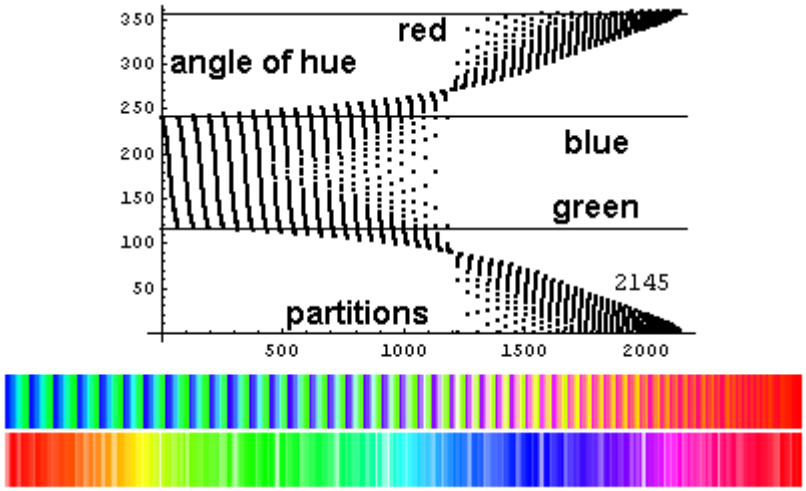

Figure 8. *Hues in degrees of HSV - system plotted against 2145 RGB -colours sorted as partitions of 64. Upper: partition spectrum. Lower pseudo solar spectrum is obtained by reshuffling partition - colours by their computed hues.*

Conclusions

The aim was here to get closer to the number of colours distinguished by a normal human observer. Long history [14] and branches of colour science [15, 16] all suggest that despite of advanced technics available, the most incoherent, diverse solutions are still proposed. Answer is more diversified than it was justified. One possible cause of this uncertainity is the lack of suitable arrangement of colours which would permit the complete and repetition-free survey of a color-space. Here, various geometrical and combinatorial ordering strategies based on sophisticated subsets of RGB-cube were proposed.. E.g. linear arrangement by partitions i.e. also by intensity ratios of RGB-primary channels may achive a regularity, brings closer subjectively similar colours. Only construction of further order algorithms makes worthy to start psychophysical testing identity and difference of colour species.

RGB partition-lists give colour spectra with regularly but still capriciously dispersed colours, albeit these lists are complete with respect of ratios or other aspect. When formal HSV-hues are computed for a given partition sequence or set of other RGB-colours, then this sequences can be simultanously reshuffled by HSV-hues computed with help of (Eq. 2). What we obtain, it is a complete or partial *pseudo-solar spectrum* of colours (not that of hues!) . In *Fig. 8*, the lower spectrum was computed and rearranged from the upper partition spectrum. Also in *Fig. 6a1* and *6b1* the satellite pseudo-solar spectra are obtained from various partition spectra.

Such a rearrangement can be done with an arbitrary initial colour–list as follows: *(1#)* - determine (r, g, b) for each colour. *(2#)* - Compute h = η[r, g, b] sizes of hue-angles. *(3#)* - Arrange h values by their magnitude. List the original and corresponding RGB-colour arguments vectors by this new order of their hues. *(4#)* – Compute and display the new colour-spectrum.

Close colours get physically closer. Now you can start counting colours or you can discriminate with real hope and with efficiency. In pseudo-solar-spectra the similare colours are physically closer along the new 1D arrangement as they were before.

http://www.ecology.uni-corvinus.hu ● ISSN 1589 1623

We emphasize that any colour census is at last a psychophysiological task but impossible to carry out without such preparatory transformations. This work has been initiated.

The more conservative way to reduce colour cube is to generate seemingly uniform RGB colour fields. Count number of its distinct colours. By this way local reduction factors can be collected. E.g. very often in domains with 1000-5000 distinct RGB-colours 1 2 or 3 colours can be subjectively distinguished.

Obviously, several issues are out of our scope. We did not deal with standardization problems related to RGB-cube or monitors, neither with color vision or color blindness. The aim and results are in direct relationships only with and are restricted to those conceptual frameworks which make easier at all any efficient colour census. Better and computerizable colour mining methods inside a colour space chosen for analysis may diminishes gap between 25000 and 250000 our actual rough guesses.

Glossary

CIE1931 = Comission International d'Eclarage from 1931.
RGB = Red - Green - Blue colour system for monitor
HSV = Hue, Saturation, Value or Lightness
CMYK = Cyan - Magenta -Yellow - Black for printers

Acknowledgements. Grateful thanks to M.Csati for valuable help. Grants were supplied by MTA-TKI.

REFERENCES

[1] Wasserman, G.S. (1974): Colour Vision: An Historical Introduction. - Wiley-Interscience, New York.
[2] Wright, W.D. (1967): The Rays are Not Coloured. – Adam Hilger Ltd, Bristol.
[3] Lukács Gy. (1982): Színmérés. - Műszaki Könyvkiadó, Budapest
[4] --- Nemcsics A. (2004): Színdinamika. - Akadémiai Kiadó, Budapest.
[5] --- Smith, A.R. (1978): Colour gamut transform pairs. – Computer Graphics 12(3): 12-19.
[6] --- Wright, W.D. and Pitt, F.H.G. (1934): Hue-discrimination in normal colour-vision. – Proc. Phys. Soc. 45: 459-473.
[7] --- Wright, W.D (1946): Researches on Normal and Defective Colour Vision. - Henrz Kimpton, London.
[8] --- Pitt, F.H.G. (1944): The Nature of Normal Trichromatic and Dichromatic Vision. – Proc.R.Soc. Ser B. 132: 101-117.
[9] --- Krudy, A., Ladunga K. (2001): Measuring Wavelength Discrimination Threshold Along the Entire Visible Spectrum. – Periodica Polytechnica Ser. Mech. Eng. 45: 41-48.
[10] - MacAdam D.L. (1942): Visual sensitivities to colour differences in daylight. - J. Opt. Soc. Am. 32: 247.
[11] - http://www.research.att.com/projects/OEIS?Anum=A000217, triangular numbers.
[12] - http://www.research.att.com/projects/OEIS?Anum=A001399, number of partitions into at most 3 parts.
[13] - http://www.research.att.com/projects/OEIS?Anum=A045943, special triangular numbers.
[14] - Sherman P.D. (1981): Colour Vision in the Nineteenth Century. The Young-Helmholtz-Maxwell Theory. - Adam Hilger Ltd, Bristol.

http://www.ecology.uni-corvinus.hu ● ISSN 1589 1623

[15] - Wyszecki, G., Stiles, W.S. (1967): Colour Science, Concepts and Methods. - Wiley-Interscience, New York.
[16] - Judd, D. B., Wyszecki, G. (1963) : Color in Business, Science, and Industry. - Wiley-Interscience, New York.

http://www.ecology.uni-corvinus.hu ● ISSN 1589 1623

LOGISTIC RIDGE REGRESSION FOR CLINICAL DATA ANALYSIS (A CASE STUDY)

E. VÁGÓ [1]-S. KEMÉNY[1]*

[1]*Department of Chemical Engineering, Budapest University of Technology and Economic H-1111, Budapest, Műegyetem rakpart 3, Hungary*
(phone: +36-1-463-2209; fax: +36-1-463-197)

**e-mail: kemeny@mail.bme.hu*

(Received 10th Sep 2005, accepted 10th Oct 2006)

Abstract. This paper focuses on regression with binomial response data. In these cases logit regression is the most used model. An example is a retrospective biomedical problem, where multicollinearity occurs, thus the variances of the estimated parameters are large.
In this paper we propose to apply the ridge method to the maximum likelihood estimation of the logit model parameters.
The efficiency of the proposed technique was investigated using a biomedical data set. A random sampling technique was used to study the effect of sample size on the ML and the logistic ML estimation.
Keywords: *logit, multicollinearity, bootstrap, restless legs*

Introduction

Logit regression is a widely used method for categorical response data. A typical area of application is biomedical studies, but there are other areas like the prediction of loan returning behaviour of bank clients. A good example is the investigation of the occurrence of a disease (yes/no) as related to different characteristics of the patients.

With logit regression the binary response (y_i) at the i-th setting of independent (regressor) variables is considered as a binomial (Bernoulli) random variable with p_i parameter.

$$y_i \sim Binomial(p_i) \qquad \text{(Eq. 1.)}$$

The *logit* is the link function to the linear predictor [1].

$$\text{logit}[p_i(\boldsymbol{x}_i)] = \log\frac{p_i(\boldsymbol{x}_i)}{1-p_i(\boldsymbol{x}_i)} = \beta_0 + \beta_1 x_{i1} + \ldots + \beta_h x_{ih} \ , \qquad \text{(Eq. 2.)}$$

where x_{ij} is the value of the j-th independent variable (j=1…h) at the i-th measurement point, and β_j is the coefficient of the j-th independent variable. From Eq. 2. the following model relates the probability of occurrence with the regressor variables

$$p_i(\boldsymbol{x}_i) = \frac{\exp(\boldsymbol{x}_i\boldsymbol{\beta})}{1+\exp(\boldsymbol{x}_i\boldsymbol{\beta})} \qquad \text{(Eq. 3.)}$$

where

http://www.ecology.uni-corvinus.hu ● ISSN 1589 1623

$$\boldsymbol{x}_i\boldsymbol{\beta} = \beta_0 + \beta_1 x_{i1} + ... + \beta_h x_{ih} \qquad \text{(Eq. 4.)}$$

p_i is the probability of one of the two specific outcomes at the i-th setting of independent (regressor) variables.

When the number of observations at each $\boldsymbol{x}_i$ is not small weighted least squares estimation method can be used [2]. In case of small sample sizes or ungrouped data (n_i=1 for each i) maximum likelihood estimation is applied. This paper focuses only on the latter case.

Maximum likelihood estimation to logit model

Maximum likelihood estimators are obtained by maximizing the logarithm of the likelihood function [1]:

$$\log(L(\boldsymbol{X},\boldsymbol{\beta})) = l(\boldsymbol{X},\boldsymbol{\beta}) = \sum_{i=1}^{n} y_i \log(p_i) + \sum_{i=1}^{n} (1-y_i)\log(1-p_i) \rightarrow \max(\boldsymbol{\beta}) \qquad \text{(Eq. 5.)}$$

where n is the number of observations and $\boldsymbol{X}$ is an $n \times m$ matrix of the independent variable. The estimator is asymptotically unbiased.

Differentiating Eq. 5. with respect to $\boldsymbol{\beta}$ we obtain [3]:

$$\frac{\partial l(\boldsymbol{X},\boldsymbol{\beta})}{\partial \boldsymbol{\beta}} = \boldsymbol{X}^T(\boldsymbol{Y} - \boldsymbol{p}) \qquad \text{(Eq. 6.)}$$

where $\boldsymbol{Y}$ is an $n \times 1$ vector of observable dependent variables. The maximum likelihood estimator of $\boldsymbol{\beta}$ is obtained by setting the right hand side of these equations equal to zero and then solving them simultaneously and iteratively. Since $\hat{\mathbf{Y}} = \hat{\mathbf{p}}$, Eq. 6. will satisfy

$$\boldsymbol{X}^T(\boldsymbol{Y} - \hat{\boldsymbol{Y}}) = 0 \qquad \text{(Eq. 7.)}$$

Eq. 7. is generally solved using the Newton-Raphson method. Iterative estimates of $\boldsymbol{\beta}$ are obtained as:

$$\hat{\boldsymbol{\beta}} = \left(\boldsymbol{X}^T\boldsymbol{W}\boldsymbol{X}\right)^{-1}\boldsymbol{X}^T\boldsymbol{W}\boldsymbol{Z} \qquad \text{(Eq. 8.)}$$

where $\boldsymbol{Z}$ is an $n \times 1$ column vector with elements:

$$z_i = \text{logit}[\hat{p}_i(\boldsymbol{x}_i)] + \frac{y_i - \hat{p}_i}{\hat{p}_i(1-\hat{p}_i)} \qquad \text{(Eq. 9.)}$$

and the weight matrix is:

http://www.ecology.uni-corvinus.hu ● ISSN 1589 1623

$$\boldsymbol{W} = \mathrm{diag}\left[\hat{p}_i(1-\hat{p}_i)\right] \qquad \text{(Eq. 10.)}$$

The covariance matrix of $\hat{\boldsymbol{\beta}}$ [1]:

$$Var(\hat{\boldsymbol{\beta}}) = \left\{\boldsymbol{X}^T \mathrm{diag}\left[p_i(1-p_i)\right]\boldsymbol{X}\right\}^{-1} \qquad \text{(Eq. 11.)}$$

Ridge regression to least squares estimation of linear models

The purpose of the parameter estimation is to find parameters as close to the true ones as possible. The most used parameter estimation methods lead to unbiased or asymptotically unbiased estimators. It means that the expected value of estimate is the true value of the parameter. However in some cases (e.g. when multicollinearity occurs) the unbiased estimators may have large variance which increases the probability of obtaining estimated parameters largely deviating from the true ones.

The goodness of an estimator is properly quantified by the mean square error function, which is defined for a scalar parameter as [4]:

$$\mathrm{MSE}\left(\hat{\beta}\right) = \mathrm{E}\left[\left(\hat{\beta}-\beta\right)^2\right] \qquad \text{(Eq. 12.)}$$

It is easy to show that MSE algebraically may be split into two parts:

$$\mathrm{MSE} = \mathrm{Var}\left(\hat{\beta}\right) + \left[\mathrm{bias}\left(\hat{\beta}\right)\right]^2 \qquad \text{(Eq. 13.)}$$

where

$$\mathrm{bias}\left(\hat{\beta}\right) = \mathrm{E}\left(\hat{\beta}\right) - \beta \qquad \text{(Eq. 14.)}$$

In multivariate case when $\boldsymbol{\beta}$ is a parameter vector, the mean square error function is defined as (in order to keep it scalar the trace of the covariance matrix is used):

$$\mathrm{MSE} = \mathrm{Tr}\left[\mathrm{Var}\left(\hat{\boldsymbol{\beta}}\right)\right] + \left[\mathrm{bias}\left(\hat{\boldsymbol{\beta}}\right)\right]^T \left[\mathrm{bias}\left(\hat{\boldsymbol{\beta}}\right)\right] \qquad \text{(Eq. 15.)}$$

In this sense a slightly biased estimator with smaller variance may be more advantageous than an unbiased estimator having large variance. Considering this Hoerl and Kennard (1970) have modified the least squares (LS) estimation for linear models and proposed a biased estimation method, called ridge regression [5].

Let us consider a linear model:

$$y_i = \beta_0 + \beta_1 x_{i1} + \beta_2 x_{i2} + \ldots + \beta_h x_{ih} + \varepsilon_i \qquad \text{(Eq. 16.)}$$

where ε_i is the measurement error at the i-th point.

http://www.ecology.uni-corvinus.hu ● ISSN 1589 1623

In matrix notation

$$\boldsymbol{Y} = \boldsymbol{X\beta} + \boldsymbol{\varepsilon} \qquad \text{(Eq. 17.)}$$

where $\boldsymbol{Y}$ is an $n\times1$ vector of observable dependent variables, $\boldsymbol{\varepsilon}$ is an $n\times1$ vector of random errors.

The ordinary least squares (OLS) estimator is obtained by minimizing the following objective function:

$$\phi\left(\hat{\boldsymbol{\beta}}\right) = \left(\boldsymbol{Y} - \boldsymbol{X}\hat{\boldsymbol{\beta}}\right)^{\mathrm{T}} \left(\boldsymbol{Y} - \boldsymbol{X}\hat{\boldsymbol{\beta}}\right) = \sum_{i=1}^{n}\left(y_i - \hat{\beta}_0 - \hat{\beta}_1 x_{1i} - \hat{\beta}_2 x_{2i} - \ldots - \hat{\beta}_h x_{hi}\right)^2 \qquad \text{(Eq. 18.)}$$

The estimated parameter vector is expressed as [6]:

$$\hat{\boldsymbol{\beta}} = \left(\boldsymbol{X}^{\mathrm{T}}\boldsymbol{X}\right)^{-1}\boldsymbol{X}^{\mathrm{T}}\boldsymbol{Y} \qquad \text{(Eq. 19.)}$$

The covariance matrix of $\hat{\boldsymbol{\beta}}$

$$\mathrm{Var}\left(\hat{\boldsymbol{\beta}}\right) = \sigma^2\left(\boldsymbol{X}^T\boldsymbol{X}\right)^{-1} \qquad \text{(Eq. 20.)}$$

Thus with Eq. 15.

$$\mathrm{MSE} = \sigma^2\,\mathrm{Tr}\left[\left(\boldsymbol{X}^T\boldsymbol{X}\right)^{-1}\right] = \sigma^2\sum_{j=1}^{h} 1/\lambda_j \qquad \text{(Eq. 21.)}$$

where λ_j is the j-th eigenvalue of the $\boldsymbol{X}^T\boldsymbol{X}$ matrix.

If any of the λ_j eigenvalues is relatively small (it occurs when they differ in great extent) the value of MSE increases. It means that estimated parameters may be far from the true ones. Using ridge regression a small positive number is added to the diagonal elements of the $\boldsymbol{X}^{\mathrm{T}}\boldsymbol{X}$ matrix:

$$\hat{\boldsymbol{\beta}}^* = \left(\boldsymbol{X}^T\boldsymbol{X} + k\boldsymbol{I}\right)^{-1}\boldsymbol{X}^T\boldsymbol{Y}, \qquad \text{(Eq. 22.)}$$

which may be also obtained by minimising the following objective function:

$$\phi\left(\hat{\boldsymbol{\beta}}^*\right) = \left(\boldsymbol{Y} - \boldsymbol{X}\hat{\boldsymbol{\beta}}^*\right)^T\left(\boldsymbol{Y} - \boldsymbol{X}\hat{\boldsymbol{\beta}}^*\right) + k\hat{\boldsymbol{\beta}}^{*T}\hat{\boldsymbol{\beta}}^* \qquad \text{(Eq. 23.)}$$

$\hat{\boldsymbol{\beta}}$ refers to ML and ridge estimators will be denoted by $\hat{\boldsymbol{\beta}}^*$. The ridge technique enlarges the small eigenvalue(s), thus decreases MSE. It is obvious that with k=0 the OLS estimator is recovered, while at $k\to\infty$ all $\hat{\beta}_j^*$ estimators go to zero.

The ridge estimator is proved to lead to smaller MSE than that obtained by the ordinary least squares method, if small enough positive value is chosen for k, that is

http://www.ecology.uni-corvinus.hu ● ISSN 1589 1623

$\mathrm{MSE}(\mathrm{OLS}) > \mathrm{MSE}(\mathrm{ridge})$.

While the existence of the minimum MSE is proved, the *k* value to which this optimum belongs to may not be calculated. Hoerl and Kennard (1970) proposed to use the ridge trace for deciding on *k*. The ridge trace is the plot of the estimated parameter values as function of *k*. When the $\hat{\beta}_j^*$ values cease to change strongly, the proper *k* is found.

The method is thoroughly discussed and applied in the literature [7-10], simulation studies were also performed.

Ridge method to logit regression

The MSE of asymptotically unbiased $\hat{\boldsymbol{\beta}}$ estimate with ML estimation from Eq. 11.:

$$\mathrm{MSE} = \mathrm{Tr}[\mathrm{Var}(\hat{\boldsymbol{\beta}})] = \mathrm{Tr}\left[\left\{\boldsymbol{X}^T \mathrm{diag}\left[p_i(1-p_i)\right]\boldsymbol{X}\right\}^{-1}\right] = \sum_{j=1}^{h} 1/\lambda_j \qquad \text{(Eq. 24.)}$$

where λ_j is the *j*-th eigenvalue of the $\boldsymbol{X}^T \mathrm{diag}\left[p_i(1-p_i)\right]\boldsymbol{X}$ matrix.

This is analogous to the variance of LS estimation (Eq. 20.). It is known that the eigenvalues of $\boldsymbol{X}^{\mathrm{T}}\boldsymbol{X}$ differ in great extent if the columns of $\boldsymbol{X}$ matrix are correlated [2] (multicollinearity). This occurs when evaluating retrospective biomedical studies, where the regressor variables may not be set properly but may change in almost a random way. In Eq. 24. the estimated covariance matrix related to not simply $\boldsymbol{X}^T\boldsymbol{X}$ but $\boldsymbol{X}^T\boldsymbol{W}\boldsymbol{X}$, where weights depend on $\boldsymbol{X}$ matrix. Thus even with orthogonal $\boldsymbol{X}$ matrix the eigenvalues of the $\boldsymbol{X}^T \mathrm{diag}\left[p_i(1-p_i)\right]\boldsymbol{X}$ matrix may differ. Ridge method is a remedial measure to treat multicollinearity with linear regression, and it can also be applied to the ML estimation as it was proposed by Schaefer [11]. A small positive number is added to the diagonal elements of the covariance matrix given by Eq. 11.:

$$\mathrm{Var}(\hat{\boldsymbol{\beta}}^*) = \left\{\boldsymbol{X}^T \mathrm{diag}\left[n_i p_i(1-p_i)\right]\boldsymbol{X} + k\boldsymbol{I}\right\}^{-1} \qquad \text{(Eq. 25.)}$$

Thus the objective function has the form:

$$\phi(\hat{\boldsymbol{\beta}}^*) = \sum_{i=1}^{n} y_i \log(p_i) + \sum_{i=1}^{n} (1-y_i)\log(1-p_i) - k\hat{\boldsymbol{\beta}}^{*\mathrm{T}}\hat{\boldsymbol{\beta}}^* \rightarrow \max(\hat{\boldsymbol{\beta}}^*) \qquad \text{(Eq. 26.)}$$

the iterative estimate of parameter vector is obtained as:

$$\hat{\boldsymbol{\beta}} = \left(\boldsymbol{X}^T\boldsymbol{W}\boldsymbol{X} + k\boldsymbol{I}\right)^{-1}\boldsymbol{X}^T\boldsymbol{W}\boldsymbol{Z} \qquad \text{(Eq. 27.)}$$

Elements of $\boldsymbol{Z}$ are defined by Eq. 9.

Barker and Brown [12] have compared ridge logit regression to principal component logistic regression and standard logistic regression by simulation studies. In [13] Cessie

http://www.ecology.uni-corvinus.hu ● ISSN 1589 1623

and Houwelingen applied the ridge logistic estimation to a biomedical problem. In this paper we apply the proposed technique both to continuous and discrete regressors, and investigate the effect of extent of correlation between regressors to the estimation error.

Example

We have analysed the data of Molnár M.Z. and co-workers [14]. In a part of their study they investigate the probability of occurrence of restless legs syndrome (RLS) for kidney-transplanted patients. We have fitted a logistic model to their data. The dependent variable is the prevalence of RLS, the covariates (three binomial and three continouos) are: diabetes, sex, modality (its value is 1 for the kidney-transplanted patients, and 0 for the waitlisted dialysis patients), age, albumin and haemoglobin (HGB) level. In this retrospective study the HGB level and modality are strongly correlated, thus the use of ridge regression seems to be recommended. The data set consists of data on 882 patients. (In the original study 992 patients were contained, parts of data for some of them missing. As our aim is to investigate the efficiency of logistic ridge estimators, and the problem of missing data analysis is not the scope of this paper, the cases with missing data were left out from the analysis.)

We have scaled the independent variable. The scaled variables change between 1 and 0. The aim of this transformation was twofold.

- The effect of the *j*-th covariate (on the dependent variable) depends on the range in which $x_j\beta_j$ changes: $effect(x_j) = range(x_j)\beta_j = (x_{j,\max} - x_{j,\min})\beta_j$. If $range(x_j)$ is equal for each *j*, the value of β_j indicates the importance of the *j*-th covariate.
- The model estimates the effect of the *j*-th covariate. The error of this estimated effect is related to $range(x_j)s_{\beta_j}$, where s_{β_j} is the standard deviation of β_j. If $range(x_j)$ is equal for each *j*, s_{β_j} measures the error of the effect of the *j*-th covariate. In the following only the scaled x_j covariates and the β_j scaled model parameters will be used.

Using the data of the 882 patients the $\boldsymbol{\beta}$ parameter vector was estimated both with ML- and with ridge logistic regression. The obtained estimated model parameters do not differ in great extent for the two estimation procedures. Using the bootstrap method [3] a 95% bootstrap interval was calculated for each β_j. The results are shown on *Fig. 1*.

http://www.ecology.uni-corvinus.hu ● ISSN 1589 1623

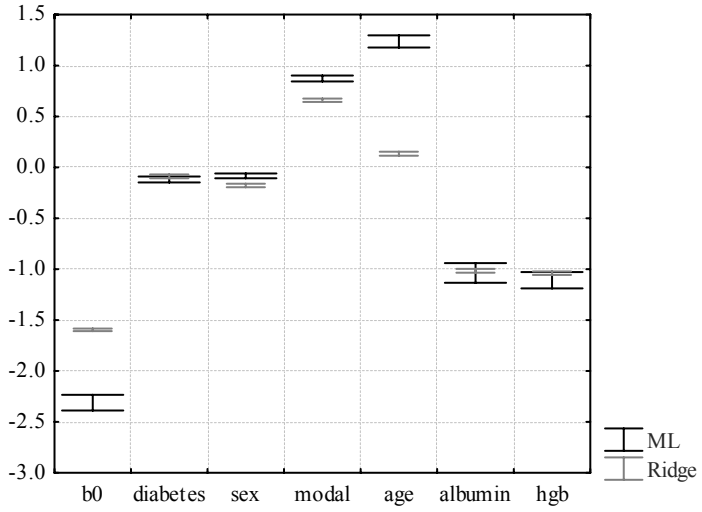

Figure 1. *95% bootstrap intervals for the estimated model parameters with ML and with ridge estimation for the full (882 patients) data set (shorter whiskers belongs to the ridge estimation)*

It can be seen from the figure that 1) the variance of the ridge estimation is smaller than that of the ML estimation, but they are approximately of the same order of magnitude; 2) the means of the parameters estimated by the two regression methods differ considerably, the ridge estimators are shrunken toward 0. In this case the use of ridge regression is not reasonable, because the smaller variance of the ridge estimator do not compensate its bias. Due to the large sample size the variance of ML estimator is relatively small, the use of ridge estimation is not justified. The advantages of using the ridge regression in case of smaller sample sizes may still be a relevant question. This is the scope of this study.

As the full data set is large enough, the ML estimated model parameters from it are close enough to the true model parameters, thus they will be considered as such. These parameters are used to evaluate MSE in further calculations.

We have obtained samples of size n, with replacement, from the original (N=882) dataset. (n:100, 110, 120, 125, 130, 140, 180, 200, 300, 400, 600) Having the sample size fixed, m_n samples were obtained (e.g. for n=100, m_{100} =800 sample were taken, each of size n). We have fitted the logistic model for each sample both with ML and with ridge regression. The estimation error (MSE) is calculated using Eq 28. for each n for both estimation procedures.

$$\mathrm{MSE}(\hat{\boldsymbol{\beta}})_n = \frac{\sum_{i=1}^{m_n}\sum_{j=1}^{h}\left(\hat{\beta}_{j,i} - \beta_j\right)^2}{m_n} \qquad \text{(Eq. 28.)}$$

The results are show in *Fig. 2*.

http://www.ecology.uni-corvinus.hu ● ISSN 1589 1623

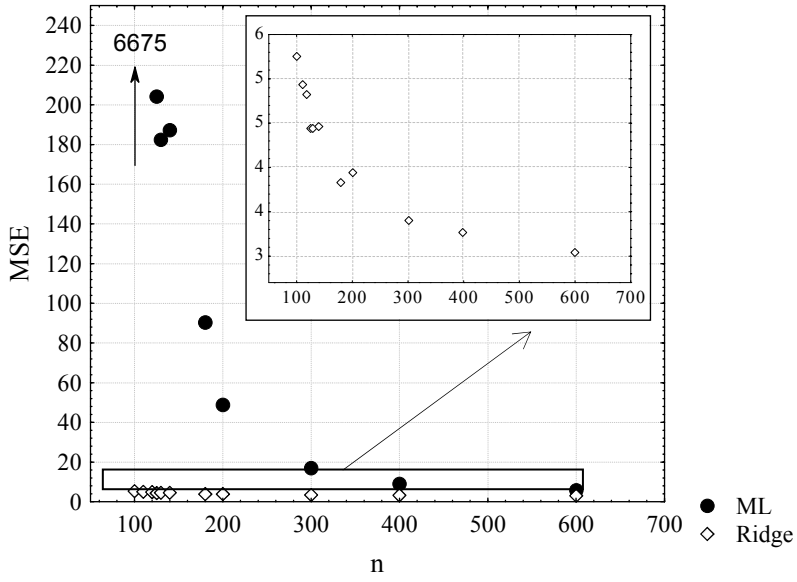

Figure 2. *Error of estimated model parameters with ML and ridge estimation, respectively versus sample size*

The error of the parameter vector ($\mathrm{MSE}(\hat{\boldsymbol{\beta}})$) of ML estimators is exponentially increasing as the sample size is decreasing. The error of ridge estimator changes similarly (*Fig. 2*), but its variation is by orders of magnitude smaller. The use of ridge estimation seems to be useful if the sample size is low, for this example if it is less than about 300.

Conclusions

We have compared the effectiveness of logistic ridge and ML regression using clinical data of kidney-transplanted patients. The use of ridge regression is not recommended for large samples. In these cases the variance of ML estimation is relatively small, thus the variance reduction achieved with ridge estimation dos not compensate the bias of the method. For smaller sample sizes the variance of ML estimator increases strongly as the sample size decreasing, while the variance of ridge estimation hardly changes. Thus for smaller samples the use of ridge method proved to be more effective then the ML estimation.

Acknowledgement. The authors acknowledge Quality of Life Research Team of Institute of Behavioural Sciences, Semmelweis University for providing the data.

REFERENCES

[1] A. Agresti (2002): Categorical data analysis. – John Wiley & Sons, New York, p. 166., 194.

http://www.ecology.uni-corvinus.hu ● ISSN 1589 1623

[2] R.H. Myers (1989): Classical and modern regression with applications. – PWS-KENT, Boston, , p.318., p.126.
[3] T.P. Ryan (1997): Modern regression methods. – John Wiley & Sons, New York, p. 260.
[4] S.H. Ngo, S. Kemény, A. Deák (2003): – Chemometrics and Intelligent Laboratory Systems 67 69-78
[5] A.E. Hoerl and R. W. Kennard (1970): . – Technometrics 12 55-67.
[6] N.R. Draper, H. Smith (1998): . – Applied regression analysis, John Wiley & Sons, New York, , p.136.
[7] J.W. Gorman, R.J. Toman (1966): . – Technometrics 8 27-51.
[8] R.F. Gunst , R.L. Mason (1977): . – Biometrics 33 249-260.
[9] H. Pasternak, Z. Schmilovitch, E. Fallik, Y. Edan (2001), . – Journal of Testing and Evaluation 29 60-66.
[10] J.H. Kalivas (2001): . – Analitica Chimica Acta 428 31-40.
[11] RL. Schaefer (1986): . – Journal of Statistical Computation and Simulation 25 75-91
[12] L. Barker, C.Brown (2001): . – Statistics in Medicine 20 1431-1442
[13] S. Cessie J.C. Houwelingen (1992): . – Applied Statistics 41 No.1191-201
[14] M.Z. Molnár, Novak M., Ambrus C., Szeifert L., Kovacs A., Pap J., Remport A., I. Mucsi (2005): . – Am J Kidney Dis 45(2) 388-96.

http://www.ecology.uni-corvinus.hu ● ISSN 1589 1623

GRAPH THEORY APPLICATION FOR INVESTIGATING AGROECOSYSTEMS EFFECTED BY EXTREM WEATHER CONDITIONS

E. ERDÉLYI

Department of Mathematics and Informatics, Faculty of Horticultural Sciences, Corvinus University of Budapest, H-1118 Budapest, Villányi út 29-33, Hungary (phone: +36-1-482-6179; fax: +36-1-466-9273)

e-mail: eva.erdelyi@uni-corvinus.hu

(Received 10th Sep 2005, accepted 10th Oct 2006)

Abstract. An agro-ecosystem is directed by the interactions among the populations living in it and depending on many abiotic factors. It is needed to investigate as many factors as possible. People are also interested in the effects of predicted climate change, experienced climate variability and frequently present extremal weather conditions nowadays. Elements of the system have direct and indirect influence on each other. Indirect or hidden types of interactions can not be expressed as different kinds of material flow. It would be also nice to combine the optimalisation of the proficiency and environmental protection together with the forecast risk, damages and profit. When extending the already existing models, they become more complex and immense, so simulation and monitoring are not enough for examining and describing the whole interaction process. Application of graph theory - using well known graph theory theorems and having the help of computers - is especially powerful for controlling huge systems that are difficult to survey by other existing methods. Using informatics and electronics agricultural production can be controlled through a complex system, which integrates biological, technological and economical factors.
Keywords: *agriculture, climate, ecosystem, food web, graph, model*

Introduction

An agro-ecosystem is a highly complex system of nature, several different models have already been introduced to investigate it. In ecological research we can distinguish three main trends [14]: describing synbiological patterns and trying to explore their background patterns [22][32][37][38][40][41]; focusing on some alternative hyphoteses of a hyphoteses system through firmly controlled experiments [4][35][36]; and theoretical modelling by mathematical description, when only a fragment of the available knowledge is used [15][26]. These approaches have many advantages, but one of their disadvantage is that it limits the systems complexity.

The interactions in a food web and the structure of a food web have already been studied [15][16][17]. Systems of soil-plant-weather models were also constructed [8][24][26], they were examined empirically, as well [5]. To analyse how the examined agro-ecosystem is functioning, correct simulation models of the complex food web system and continuous monitoring of the processes [1][6][7] were needed. During the simulation there were examined also extremal events [13]. When extending the model, it integrates biological, technological and economical factors and joins the natural circumstances, so it becomes very complex. Agricultural production meeting several requirements such as „precision and sustainability" became more and more in focus. Nowadays investigation of influences explained by climate change and climate variability is of interest and needed, too [33]. Simulation and monitoring are not

http://www.ecology.uni-corvinus.hu ● ISSN 1589 1623

enough. We need to ask for the help of other methods. As in the literature there are plenty of excellent models which describe certain parts of processes quite exactly [9][23][27], our aim was to create a model which describes the whole interaction process: tracking and tracing the effect of an element in an agro-ecosystem. It is also useful in case detailed data are missing, or when extending the model in case more complex data are available. These days discrete mathematics, algorithms and graph theory are very often used in different areas of mathematics, physics, chemistry, molecular biology, economy and other sciences. [3][18][25] and even in ecology [29][42][43]. Informatics and electronics are more and more often applied in different branches of sciences and in agriculture, as well [17][39]. We show that for investigation of several indirect or hidden types of interactions that can not be directly expressed, well known graph theory theorems can be used. There are several softwares for designing and testing networks: e.g. PIGALE (Public Implementation of a Graph Algorithm Library and Editor), Algorithmic Solutions Problem GmbH: LEDA [10], a program dealing with different kinds of e.g. travelling salesman problems [11], an open source project LEMON: Library of Efficient Models and Optimization in Networks [12], which does combinatorial optimization for problems working with graphs and networks using graph theory algorithms in available routines and having a possibility in it of writing programs for a given problem. We only need to translate our question into a mathematical language and use algorithms describing the situation and finding the solution of the given problem. Graph theory can provide us a powerful tool to model several indirect or hidden interactions. These interactions that we integrate in our model are not contained in most existing models or not considered together in the same model. Multidisciplinary sciences are unfurtunately not very popular, but very much needed in future research.

The Effect-Graph

First, we construct the graph of our agro-ecosystem. The vertices of the graph are the elements of the agro-ecosystem. For example in a very simple food web the cultivated plant is our central element, and the others can be its weeds, different types of pests and their predators. Elements of our extended system can also be soil, weather conditions like temperature or precipitation, agrotechniques (watering, fertilization). For describing the interactions between the elements of the system we use the edges of the graph. We put an edge between two elements if there is a relationship between them. We direct the edges form an element to the other one if the certain element has an effect on the other element. We allow to have edges between two elements in both directions. Every edge will get a weight showing how strongly the elements effect one another. The weight is a number that expresses the influence of one element to the other one and it is positive or negative depending on whether this effect acts positively or negatively on the element. On the graph theory language this way we obtain a weighted directed graph. This graph is called the effect graph of our agro-ecosystem [16][17]. We can extend our graphs, influence-diagrams to encode the whole agro-ecosystem into it, labelling the vertices by the quantities of the elements. This graph we call the extended effect graph of our system. It is also possible to set the effective start date and the effective end date (which show when are the relations activated or deactivated). If we are interested in more precise details, the elements of our graph can be considered as subgraphs of the effect-graph with the similar structure. Our center element, the cultivated plant as a subgraph can consist of the elements representing the relative water holding capacity, the

http://www.ecology.uni-corvinus.hu ● ISSN 1589 1623

evapotranspiration of the plant, the biomass growth, etc. The soil element as a subgraph can consist of e.g. water content of soil, different nutrient content of it, temperature of different layers of the soil, the water run-off in it, the evaporation or the water holding capacity of soil. In the same way variables as temperature, percipitation and others can also be included. This way we can get a very complex structure of the agro-ecosystem.

Connections in effect-systems using graph theory

The (extended) effect graph can be analysed from different points of view, like climate change, plant protection and others. In these investigations the most important (centre) element is the cultivated plant, and in the other vertices there are its weeds, pests, needs and many other biotic and abiotic factors.

We would like to examine how the agro-ecosystem takes up a new structure with the quantity change of some elements, turning our attention to the 'centre', the cultivated plant. With the help of the graph we can analyse how the quantities of other elements of the system change from time to time or how some elements compete for „food" with each other, as well.

The starting values, input data of our model can be simply measured (temperature, precipitation, watering, fertilization, global radiation) or obtained by estimation or fitting (constants related to the plant, soil, ionic nutrient, speeds of bioprocesses) easily. For other kinds of data such as the daily growth of biomass, organic substances developed in soil we can use the outputs of other food web models [30]. For the quantity analysis we can use the effect graph itself. For every ecosystem we can construct a vector v_0 where the coordinates of v_0 are the weights of the vertices in one point of time. In the next point of time the weight of a vertex is changing according to the weights of the elements that have effect on it. For the representation of the graph we can use a matrix which have information about the set of components and relationships between them. Let A denote the matrix such that the a_{ij} entry of the matrix is the weight between the vertices i and j. We call it the weighted adjacency matrix of the agro-ecosystem. After the first step (i.e. day) their weights of the vertices – the available quantities of the elements of the system – are given by the coordinates of the vector $v_1 = A v_0$, so after the n^{th} step $v_n = A^n v_0$. In the $(n+1)^{st}$ step we have to raise matrix A to the power of (n+1), which is an easy mathematical excersise. If we write v_0 as a linear combination of the eigenvalues $a_{ij} : v_0 = \sum \lambda_i \underline{a_i}$, then $v_n = \sum \lambda_i^n \underline{a_i}$. For some practical reasoning the eigenvalues of this matrix are of absolute values at most 1.

For other problems we shall use the extended effect graph of the system. Without extensive precise mathematical definition several times we modify the labelling of the edges.

Examples of problems with their possible solution

- What happens if one of the factors is eliminated from the system? (ie. because of no precipitation, the watering prohibition or other conditions). One would think that in this case we have to assign a 0 to the appropriate coordinate of the weight vector. Unfortunately this is not enough. Indeed, the effects of other vertices can result nonzero entries to this element at later points of time, hence

http://www.ecology.uni-corvinus.hu ● ISSN 1589 1623

we have to change the weights of its edges (interactions) to 0. This will result a full 0 row and coloumn in the matrix. Eliminating this row and coloumn we obtain a smaller matrix and we can use this for our model. In matrix calculus this is the same as multiplying our matrix by a projection.

- What happens, if suddenly, unexpectedly the amount of an element of the system undesiredly increases (ie. very high temperature) such that its effect is harmful to our centre? Then, of course we would like to eliminate the effect of this item to our plant. Time to time it happens that we have no direct access to this element. Then we have to examine, how we can alter the indirect interaction between these items. In our graph this can be implemented by examining all the paths from one vertex to the other and try to terminate the flow of effects on all these paths. In graph theory language we have to disconnect the two vertices. To achieve the shortest or fastest or cheapest way one can use the Menger or Ford-Fulkerson type mincut-maxflow theorems [2][20][28] with the help of e.g. lp_maxflow in Lemon [12].
- In case of an expected drought an earlier harvest might be decided. How to find the cheapest and fastest possible way of increasing the yield in the remaining period of time. In our effect system this requires to find the fastest way to increase the yield with our leftover sources. In graph theory language it means finding the shortest paths with largest weights that can be done with e.g. Floyd's algorithm [20]. Here we modify the labelling. The weights will represent the quotient of the effect and the expenses of the desired interactions.
- It would be desired to control or predict all the effects in our system. How can it be done if we have access to the monitoring of a few elements of the system? We would like to choose as few elements as possible to keep a close watch on. In the graph theory language this is equivalent to find a smallest covering set of elements and we can apply Gallai's theorem [2][20][28] to achieve it.
- The reverse procedure, monitoring the effects to control the elements can be a real requirement, as well. The dual of the previous method is a straight application of König's theorem about the independent sets of edges. [2][20][28]

Discussion

In order to understand how an ecological system operates, a matrix or a food web graph is suitable either for description or for analysation of the relations. Based on the problems and their solutions mentioned above, we see that this method is very likely suitable to solve many other ones. Analysing the effecting factors standing behind ecological patterns can be of interest of human society, too. It is very important in planning the future: controlling the vulnerability helps the mitigation and the adaptation for the new circumstances. Graph theory helps us to model and follow the changes of the number of the individuals and the quality of the elements of the complex system. Nowadays apart from environment protection and public health issues the expenses of the agrotechnical methods has to be considered, as well. We do not only have to analyse if the given problem has solution, but we have to examine and decide which of the possible solutions is the most effective one. Application of graph theory in other sciences is a rapidly developing area of mathematics. It is especially powerful for controlling huge systems that are difficult to survey by the existing (manual) methods.

http://www.ecology.uni-corvinus.hu ● ISSN 1589 1623

Today's computers can carry out the necessary calculations in a reasonable amount of time. The complexity of the algorithms we used in our paper are all "easy". The methods offer new possibilities in investigating agro-ecosystems, we presented only a few examples to demonstrate the power of graph theory in this application. Predictions can be given to alternative climate change situations not experienced before. This is important in finding the sensitive points and the role of different creatures in the stability of the system. It is a possibility of decreasing the risks caused by effects of some elements in the system. Our research is still under development and generalization.

REFERENCES

[1] Akiyama, T., Inoue, Y., Shibayama, M., Awaya, Y., Tanaka, N. (1995): Monitoring and predicting crop growth and analysing agricultural ecosystems by remote sensing, Global Climate Change and Agriculture in the North, 367-377

[2] Bollobás B.: Modern graph theory, Springer, 2002.

[3] C. A. van Dorp (2003): A traceability application based on Gozinto graphs, Efita 2003 Conference, Debrecen, 280-285

[4] Fahim, M. A., Hassanien, M. K. & Mostafa, M. H. (2003): Relationships between climatic conditions and Potato Late Blight epidemis in Egypt during winter 1999-2001 - Applied Ecology and Environmental Research, 1(1-2): 159-172.

[5] Gaál, M. (1998): Ökológiai alapú szaktanácsadási információs rendszer, Gazdálkodás, XLII. 50-57.

[6] Gaál, M., Hufnagel, L. (1999): Vízi élőhelyek állapotának monitorozása poloskaközösségek alapján, Agrárinformatika 1999, Debrecen, 346-350

[7] Gaál, M., Hufnagel, L. (2001): Combination of Multivariate Methods and Graphical Database Management in Service of Ecological Monitoring, 3rd EFITA 2001 agroMontpellier ENSA, Montpellier (vol 1), 285-290

[8] Hansen, S., - Jensen, H.E.,- Nielsen, N.E.,-Svedsen, H. (1990): DAISY- Soil Plant Atmosphere System Model, NPo-forskning fra Miljostyrelsen Nr. A10.

[9] Harnos, Zs., Bussay, A., Harnos, N. (2000): Modelling climate change impacts on wheat and potato in Hungary, Climate Change, Climate Variability and Agriculture in Europe, 349-366

[10] http://algorithmic-solutions.com/enleda.htm

[11] http://iwr.uni-heidelberg.de/groups/comopt/software/TSPLIB95

[12] http://lemon.cs.elte.hu

[13] Hufnagel, L., Gaál, M. (2002): Többváltozós állapotsík rendszerek alkalmazása valós és szimulált adatsorok kezelésében, Agrárinformatika Konferencia 2002, Debrecen

[14] Hufnagel, L., Gaál, M. (2005): Seasonal dynamic pattern analysis in service of climate change research (A methodical case-study, monitoring and simulation based on an aquatic insect community) – Applied Ecology and Environmental Research, 3(2): 107-137.

[15] Jordán, F. (2001): Seasonal changes in the positional importance of components in the trophic flow network of the chesapeake Bay, Journal of Marine systems

[16] Jordán, F., - Molnár, I., (1999): Reliable flows and preferred patterns in food webs. Evol. Ecol. Res. 1: 591-609.

[17] Jordán, F.: Comparability: The key to the application of food web research, Applied Ecology and Environmental Research, 2003/1-2:1-18

[18] Jorgensen, E., Höhle, M., Hajsgaard, S. (2003): Diagnostic testing: Model estimation and decision support using graphical models, Efita 2003 Conference, Debrecen, 760-767

http://www.ecology.uni-corvinus.hu ● ISSN 1589 1623

[19] Junttila, O. (1995): Plant adaptation to temperature and photoperiod, Global Climate Change and Agriculture in the North, 251-260
[20] Katona, Gy., Recski, A., Szabó, Cs.: A számítástudomány alapjai, Typotex Kiadó, Budapest, 2002
[21] Kaukoranta, T. (1995): Impact of global warming on potato late blight: risk, yield loss and controll, Global Climate Change and Agriculture in the North, 311-328
[22] Kharkwal, G., Mehrotra, P., Rawat, Y. S. & Pangtey, Y. P. S. (2004): Comparative study of herb layer diversity in pine forest stands at different altitudes of Central Himalaya - Applied Ecology and Environmental Research, 2(2): 15-24.
[23] Kleemola, J., Karvonen, T. (1995): Modelling growth and nitrogen balance of barley under ambient and future conditions, Global Climate Change and Agriculture in the North, 299-310
[24] Kniesel L, W.G., (ed): CREAMS A Field Scale Model for Chemicals, Runoff, and Erosion from Agricultural Management Systems, USA Dept. of Agriculture, Conservation Research Report No. 26., 1980
[25] Lábos Elemér (2005): Neuronhálózatok kaotikus egységekből. Szintézis és analízis feladatok, VII. Magyar Biometriai és Biomatematikai Konferencia, Budapest
[26] Ladányi, M., Horváth, L. Gaál, M. & Hufnagel, L.: An Agro-ecological Simulation Model system, Applied Ecology and Environmental Research, 2(1-2): 52-79.
[27] Ladányi, M.,-Hufnagel, L. (2003): A Fenology Model nested in an Ecosystem Model for Agroecological Processes – EFITA 2003, Debrecen, Hungary
[28] Lovász, L.: Combinatorial Problems and Exercises, Akadémiai Kiadó, Budapest, 1979
[29] Luczkovich, J. J., Borgatti, S. P., Johnson, J. C., Everett, M. G. (2003): Defining and measuring trophic role similarity in food webs using regular equivalence, J. theor.Biol. 220, 303-321
[30] M. Ladányi, É. Erdélyi, A Révész: An ecosystem model to simulate agroecological processes, Efita 2003, Debrecen, Hungary
[31] Máthé-Gáspár, G., Kovács, G. J. (2003): Use of simulation technique to distinguish between the effect of soil and weather on crop development and growth - Applied Ecology and Environmental Research, 1(1-2): 87-92.
[32] Mehrotra, P., Kharkwal, G. & Pangtey, Y. P. S. (2004): Ecological implication of plant traits, strategies and competitive abilities of herbs - Applied Ecology and Environmental Research, 2(2): 1-13.
[33] Mela, T. J. N. (1995): Northern agriculture: constraints and responses to global climate change, Global Climate Change and Agriculture in the North, 229-234
[34] Őszi, B., Ladányi, M., Hufnagel, L. (2005): Population dynamics of the sycamore lace bug, Corythucha ciliata (Say) (Heteroptera: Tingidae) in Hungary - Applied Ecology and Environmental Research, 4(1): 135-150.
[35] Patel, S. R., Awasthi, A. K. & Tomar R. K. S. (2004) Assessmemnt of yield losses in mustard (Brassica juncea L.) due to mustard aphid (Lipaphis erysimi Kalt.) under different thermal environments in Eastern Central India - Applied Ecology and Environmental Research, 2(1): 1-15.
[36] Précsényi, I. (1995): Alapvető kutatásszervezési, statisztikai és projektértékelési módszerek a szupraindividuális biológiában. (Elementary research arranging, statistical and project evaluation methods in supraindividual biology) KLTE, Debrecen
[37] Rédei, D., Harmat, B. & Hufnagel, L. (2004): Ecology of the Acalipta species occuring in Hungary (Insecta: Heteropter: Tingidae) (Data to the knowledge of the ground-living of the Heteroptera of Hungary, No.3) - Applied Ecology and Environmental Research, 2(2): 73-90.
[38] Rifaat, H. M. & Yosery, M. A. (2004): Identification and caracterization of rubber degrading Actinobacteria - Applied Ecology and Environmental Research, 2(1): 63-70.
[39] Salga, P., Herdon, M., Tóth, T. (2004): Intelligent neural grid, XIII. Agrarian Perspectives Conference and Information Technology Workshop, Prague

http://www.ecology.uni-corvinus.hu ● ISSN 1589 1623

[40] Salga, P., Szilágyi, R., Tóth, T., Pokol, A. (2004): Application of CNN-GRID technology, Information Systems for Agriculture, Forestry and Rural Areas – enlargement of EU 10th International Conference, Seč u Shrudimi, Czech Republic
[41] Spellenberg, I. F. (1991): Monitoring ecological change, Cambridge University Press, Cambridge
[42] Ulanowitz, R. E. (1983): Identifying the structure of cycling in ecosystems. Math.Biosci.65, 219-237
[43] Ulanowitz, R. E. (1991): Ecosystem flow networks: loaded dice, Math. Biosci.103, 45-68
[44] Willows, R., Connell, R. (eds.) (2003): Climate adaptation: Risk, uncertainity and decision-making, UK Climate Impacts Programme Technical Report, UKCIP Oxford

http://www.ecology.uni-corvinus.hu ● ISSN 1589 1623

SIMULTANEOUS TEST AND CONFIDENCE SET FOR TWO BINOMIAL PROPORTIONS

ZS. ABONYI-TÓTH., J. REICZIGEL

Szent István University, Faculty of Veterinary Science, Department of Biomathematics and Informatics

e-mail: Abonyi.Zsolt@aotk.szie.hu, Reiczigel.Jeno@aotk.szie.hu

(Received 10th Sep 2005, accepted 10th Oct 2006)

Abstract. Some phenomenons are modelled most naturally by two probabilities, because use of a single combined measure would result in an undesirable loss of information. E.g. diagnostic tests are obligatorily characterized by their sensitivity and specificity, risk of disease is often reported for two subpopulations e.g. males and females rather than for the whole population, etc. Here we present a statistical test and a related method to construct simultaneous two-dimensional confidence sets for two probabilities estimated from independent samples. We also describe a computer algorithm for these calculations.
Keywords: *diagnostic test, confidence, statistics*

Introduction

Suppose we have observed two binomial variables on two independent samples and we want to carry out a statistical test for the binomial parameters (probabilities) with H0: p1=p1(hypot) , p2=p2(hypot). Also, we want to give a simultaneous confidence set.

This problem may come up in situations when a phenomenon cannot be reasonable modelled by a single probability. This is the case e.g. if sensitivity and specificity of a diagnostic test are to be estimated, for sensitivity is calculated from a sample of people having a disease, while specificity is calculated from a sample of people not having the disease. Another example is when risk of a disease is needed separately for males and females, or urban and rural people, etc. If these two risks were combined to have a single measure (e.g. risk for the whole population), then it would be impossible to control for differences in sex ratio or urban/rural ratio between different populations or over time.

Concerning hypothesis testing, a typical question may be whether both sensitivity and specificity of a new diagnostic test exceeds those of a standard test with known sensitivity and specificity, say Se = 92% (p1(hypot)) and Sp = 87% (p2(hypot)), or whether a certain public health measure reduced the risks compared to the preceeding period of time in both parts of the population.

The solution is based on the method suggested by Sterne [5] for the one-dimensional case. The acceptance region is constructed taking the points of the two-dimensional sample-space in descending order of their probabilities (first the one with highest probability, then the one with second highest, etc.) until the probability of the acceptance region reaches the desired level, e.g. 95%. The acceptance region defined this way has a minimal area (it contains the fewest points among all possible regions at the same level). The confidence set can be constructed by inverting the test [4]. This

http://www.ecology.uni-corvinus.hu ● ISSN 1589 1623

means that the confidence set will contain all parameter pairs, for which the observed outcome is in the acceptance region at the level of interest.

The test and confidence region can be used to create exact tests and confidence intervals for functions of the two parameters like e.g. difference of proportions, relative risk, or odds ratio. Exact solutions for these problems are not always readily available [1][3].

The first idea of the computerized solution is to evaluate the whole parameter-space, i.e. [0,1]x[0,1] with a step size providing the desired precision. It needs a lot of computing time, because we have to construct acceptance regions for several pairs of parameters. Our paper describes the possible optimizations of the algorithm and introduces the first version of the program.

The problem

We have two independent samples of size n1 and n2 (each should be less than 300 in the present version of the program) with observed numbers of successes k1 and k2, respectively. What could be the probabilities p1 and p2?

The confidence interval will be created using loops. Given the step size (ss), the program calculates the acceptance region for the probabilities p1 and p2, where p1=i/ss (i=0,1,…,ss) and for every p1 value p2=j/ss (j=0,1,…,ss). Those (p1, p2) pairs are regarded to belong to the confidence region, for which the acceptance region contains the pair (k1, k2). During this process, functions of p1 and p2 are also calculated in order to create confidence intervals for them.

It's clear that (ss+1)2 acceptance regions must be computed. For each of them, we have to calculate the appropriate two-dimensional probability mass function (n1·n2 calculations), order the probabilities, and select them until we reach the desired level.

Of course it is easy to write a program to do this, but as we increase the sample sizes and the step size, the computing time will make the program inapplicable. That's why we have to optimize the program code.

Optimisation

There are several ways to optimize an algorithm and/or the corresponding program code. We used more memory to store temporary results, which were needed several times. We also simplified calculations using theoretical knowledge on the problem.

Important part of optimisation is to eliminate unrelevant points from calculations. For example we have to calculate the acceptance region (ss+1)2 times. Of course it is very important to do it as fast as possible.

With given n1 and n2, the number of possible pairs of outcomes is (n1+1)·(n2+1), that is, the size of the sample space is proportional to the square of the sample size. Calculation of the probability mass function for each pair slows down the program considerably. But we can recognize that, as the sample size increases, the acceptance region will contain just a few percent of the possible pairs. Examining the probability mass function it is not surprising, most probabilities are very close to zero. Selecting a good algorithm, we don't need to calculate the probability mass function for the whole parameter space, it's enough to calculate the highest probabilities to get the acceptance

http://www.ecology.uni-corvinus.hu ● ISSN 1589 1623

region. In this case, we need to know, where we can find higher probabilities without calculating all of them.

Another way of speeding up the program is to recognize that we don't need the whole acceptance region. If we have reached the observed k1 and k2, we can stop.

The program

Our algorithm is using the above 'tricks' to work as fast as possible. We have used the Borland Delphi 2.0 Desktop programming environment to compile a working version, but the algorithm itself is language and platform independent and can be implemented in any programming environment.

After optimization, the computing time is 20 seconds on a 2.6GHz P4 computer for n1=n2=100, stepsize=1000. The maximum value of sample sizes is 300, the maximum of step size is 100000.

The result is written into a space separated text file with a name generated from input data to make it easier to find a result later.

The output of the program consists of four windows. The log window summarizes the results: it shows the file name, input parameters and processing time. The results window displays the results from the results file. The drawing window displays a plot of the acceptance or confidence region denoting points belonging to the region by 'X' and others by '.'. It demonstrates that the confidence interval is generally not convex. It can have both holes and disjoint areas. The main reason for this is the discreteness of the binomial distribution. For practical purposes one can reasonably use the convex hull of the computed confidence set. The last window shows the confidence intervals for some functions of the parameters.

The program is able to give some partial results:

Probability mass function

For given n1, n2, p1, p2 the program calculates the two dimensional binomial probability mass function. As we have shown above, it first calculates the arrays of binomial coefficients, the powers of pi, (1-pi), then calculates the probability of each (k1, k2) pairs.

We were able to save time here by avoiding use of the built-in power function and simply multiplying the previous element in the array with the base of the power to get the next one in a cycle.

Acceptance region

For given n1, n2, p1, p2 the program calculates the acceptance region. The construction is the following: the program calculates the probability mass function, sorts the probabilities of the different (k1, k2) pairs in descending order, and adds these pairs to the region until the sum of the probabilities is under the pre-specified level. If several pairs have the same probability, all of them are added to the area together. It is necessary because the acceptance region must be well-defined and there is no other reasonable rule about which pair should be included in the acceptance region from those having the same probability.

The acceptance region defines a statistical test for H0: (p1 = p1(hypot) , p2 = p2(hypot)). If the observed (k1, k2) pair is not in the area, H0 is rejected. The p-value

http://www.ecology.uni-corvinus.hu ● ISSN 1589 1623

belonging to a certain (k1, k2) pair can be calculated stopping the process when it adds the pair to the acceptance region: then p = 1- sum of the probabilites of pairs in the area.

The algorithm doesn't calculate the probability of each sample point. First it determines a starting point: the sample point having the highest probability. It is ([n1·p1],[n2·p2]) or one of its neighbors, where [x] represents the biggest whole number, which is not greater than x. It means 9 pairs, their probabilities will be calculated and they will be added to the array of neighbors, nei. Then the following general step is repeated: The program looks for the maximum probability in nei, adds the points that have this probability to the acceptance region, deletes them from nei, and adds all their neighbors to nei. This step is repeated until the stop condition will be true: the program reaches either the pre-specified level or the observed (k1, k2) pair.

The two-dimensional binomial distribution is strictly monotonically decreasing in each direction away from its peak, so the above algorithm will really produce the acceptance region, because the biggest probability not in the area must be a neighbor of the area. The acceptance region looks like an ellipse, and nei will contain plots as the outline of the ellipse.

Confidence region

For given n1, n2, k1, k2, pv, ss the program calculates the confidence set, which consist of those (p1, p2) pairs, for which (k1, k2) is in the pv-level acceptance area belonging to (p1, p2) at a step size of ss.

Figure 1 shows the structure of the confidence region for n1=n2=20, k1=k2=1, pv=0.95, stepsize=250. The top left corner of the picture is (p1, p2)=(0, 0) and the bottom right corner is (p1, p2)=(0.292, 0.288). Holes are visible in the figure.

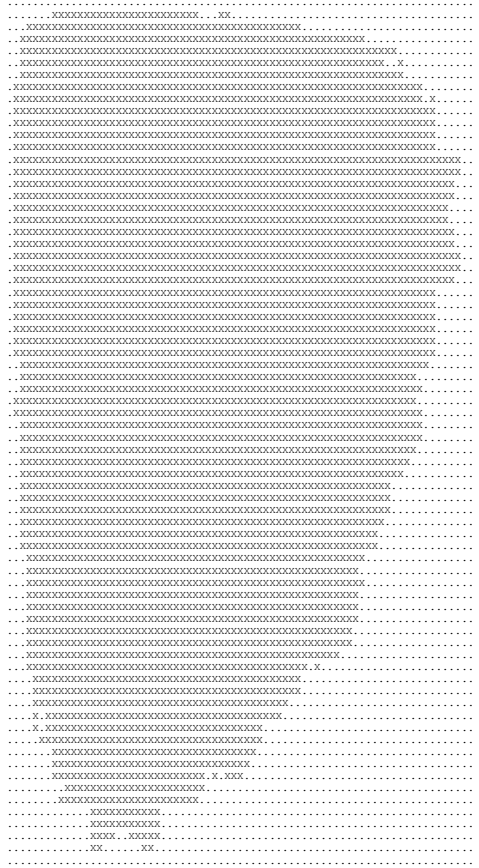

Figure 1. *Shape of the confidence set*

http://www.ecology.uni-corvinus.hu ● ISSN 1589 1623

In the general case the program has to determine the acceptance region for p1 and p2 pairs, where p1=i/ss (i=0,1,…,ss) and p2=j/ss (j=0,1,…,ss), so the previously described process should run (ss+1)2 times. It needs a lot of calculation, and most pairs won't belong to the confidence set. That's why the program first scans one row and one column only, where the area is possibly the widest. The optimal places are appriximately at k1/n1 and k2/n2. Unfortunately, the confidence set is not convex and may have holes and disjoint parts. If ki is close to zero or to ni, it is very hard to estimate, which row and column is best to scan; this part of the algorithm should still be refined.

During those scans the program stores the minimum and maximum value of pi belonging to the confidence region, called pi1 and pi2. If we were sure, these were the most extreme points of the region, it would be enough to check the [p11 , p12]x[p21 , p22] area. Unfortunately it is not true, so the rectangle has been expanded by ss/40 in every direction. This amount is enough to surely discover the whole confidence set, but the program checks a lot of irrelevant pairs as well. This part of the algorithm should be refined too.

During the calculation of the confidence set, it is possible to compute confidence intervals for p1, p2, p1-p2, p1/p2 and odds(p1)/odds(p2). The program stores their minimum and maximum values during the process, and replaces them, if it is necessarily. Finally the variables contain the global minimum and maximum of these functions of the probabilities together with the points of the parameter space where these values were taken.

Application

The method was applied to construct a two-dimensional confidence set for sensitivity and specificity of transrectal ultrasonography for pregnancy testing in ewes on 25 to 30 days of gestation [2]. Samples consisted of 34 pregnant and 50 non-pregnant ewes, in which the number of correct diagnosis was 11 and 46, respectively. This results in the estimates Se = 32.3%, Sp = 92.0%.

Figure 2 shows the structure of the confidence region for n1=34, n2=50, k1=11, k2=46, pv=0.95, stepsize=150. The top left corner of the picture is (p1, p2)=(0.14, 0.76) and the bottom right corner is (p1, p2)=(0.547, 0.987).

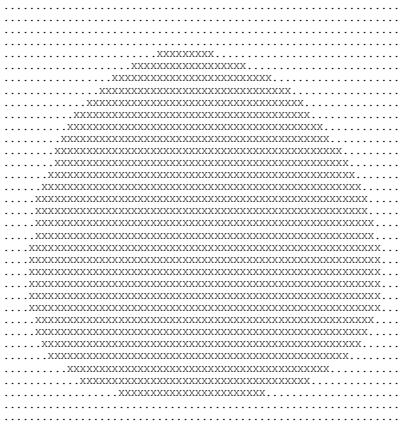

Figure 2. *Shape of the confidence set in this application*

Discussion

As we decribed, we have developed an algorithm and a computer program, which is able to make a simultaneous statistical test for the binomial parameters (probabilities)

http://www.ecology.uni-corvinus.hu ● ISSN 1589 1623

where (H0: p1 = p1(hypot) , p2 = p2(hypot)), and to give a simultaneous confidence set from observed values of two independent samples.

Based on several optimization steps, the program is now fast enough to produce useful results for sample sizes up to 300 and with a precision of 0.00001. The program is available on the first autor's home page (www.univet.hu/users/atzs).

Acknowledgment. The project is sponsored by grant OTKA T049157.

REFERENCES

[1] Agresti A (2003): Dealing with discreteness: making 'exact' confidence intervals for proportions, differences of proportions, and odds ratios more exact – Statistical Methods in Medical Research 12 (1): 3-21.

[2] Karen A, Szabados K, Reiczigel J, Beckers JF, Szenci O (2004): Accuracy of transrectal ultrasonography for determination of pregnancy in sheep: effect of fasting and handling of the animals – Theriogenology 61 (7-8): 1291-1298

[3] Newcombe R.G. (1998): Interval estimation for the difference between independent proportions: Comparison of eleven methods – Statistics in Medicine 17 (8): 873-890.

[4] Reiczigel J. (2003): Confidence intervals for the binomial parameter: some new considerations – Statistics in Medicine 22 (4): 611-621.

[5] Sterne, T. E. (1954): Some remarks on confidence or fiducial limits – Biometrika 41 (1-2): 275-278.

http://www.ecology.uni-corvinus.hu ● ISSN 1589 1623

BIOMETRIC INVESTIGATION OF HUMAN- AND VETERINARY-BIOLOGICAL EFFECTS OF ELECTROMAGNETIC FIELDS

L. BÖRZSÖNYI[1*]-SZABÓ F.[2]-BECKERS J. F.[3]-SULON J.[3]-FODOR J.[1]-SZENCI O.[2]

*e-mail: *Borzsonyi.Laszlo@aotk.szie.hu*

[1]*Department of Biomathematics and Informatics, Faculty of Veterinary Science, Szent István University of Budapest H-1078 Budapest, István u. 2, Hungary (phone: +36-1-478-4212; fax: +36-1-478-4217)*

[2]*Clinic for Large Animals, Faculty of Veterinary Science, Szent István University of Budapest H-2225 Üllő, Hungary (phone: +36-29-521-300; fax: +36-29-521-303)*

[3]*Department of Physiology of Reproduction, Faculty of Veterinary Medicine, University of Liege, Bd de Colonster No20, P71, Bat. B41, B-400 Sart-Tilman, Belgium (phone. +32-43664161; fax: +32-477297018)*

(Received 10th Sep 2005, accepted 10th Oct 2006)

Abstract. In our days attention has been focused on the analysis of the effects of electromagnetic fields both in human and veterinary medicine. The significance of analyses has been underlined by both therapeutic and noxions effects of magnetic field therapies to the living organism. Due to the fact that modern technical devices are widely used, the phenomena and data observed in connection with their use urge exact evaluation and analysis.

The exact effect mechanism of electromagnetic field therapies is not quite clear. The oxygen uptake of cells is supposedly increased by the induced magnetic field [18]. Electromagnetic field therapies in human and veterinary medicine are primarily used for treating soft tissue lesions [8], and bone and joint disorders [9]. There are some new investigations trying to explain the effects of the treatments for positive and negative stress sensibility. In the first part of our study the therapeutic and noxious effects observed in human and veterinary biology are summarised without aiming at completeness. In the second part the effect of magnetic field therapy in horses is thoroughly examined. The local effects of electromagnetic field treatments as well as the biological effects of electromagnetic therapy using magnetic blanket on blood gas and biochemical parameters are tested. Paired t-test was applied in the course of biometric evaluations.

The description of blood gas and acid-base parameters may it possible to apply magnetic field therapies for healing purpose as well as prevent stress-related diseases in race horses. The results of our investigation might lead to the conclusion that they are adaptable in human medicine as well.

Keywords: magnetic protection of the environment magnetic field therapy, electrosmog, blood gas parameters, paired t-test, error of first kind.

Introduction

The investigation of magnetic field effects goes back to a long history. There are records about the use of magnetic bars for therapeutic purposes in the territory of today's Turkey as early as 1000 B.C. [7]. There were written documents about the effects of magnetic field treatments in human medicine as early as the XVth century. The analysis of magnetic field effects and therapy has been in the forefront of

http://www.ecology.uni-corvinus.hu ● ISSN 1589 1623

investigations first in human then in veterinary medicine since the 1990-es [2]. It has been proved unambiguously that certain magnetic field therapies have healing, some others noxious effects on the living organism. When we use modern technical devices today, such questions are naturally raised: Do the single devices have deleterious effects on the environment and the living organism? How should we use these devices adequately? It is also a fact that in several cases it is not easy to demonstrate explicitly the deleterious effect of certain magnetic field on the environment, and we can conclude only from representative statistical figures that the diseases occuring significantly more frequently might be attributed to some magnetic field effect in the background [3].

It is reasonable to examine the electromagnetic protection of the environment from two aspects. We should focus partly on the biological effects, partly on electromagnetic compatibility. Electromagnetic compatibility means the ability of a device to operate adequately in an electromagnetic environment without causing intolerable inconveniences in the operation of another device [22]. In other words, its potential jamming-stability is sufficiently large- its jamming-emission is tolerably small. Concerning electromagnetic field effects, the jamming may originate from external and internal sources. An internal source means that the device jams itself. The external source of jamming may be artificial (e.g.: caused by human) or natural (e.g.: cosmic radiation, lightning). The jamming caused by humans may be directed (e.g.: radiofrequency radiation) or non-directed resulting from the side effect of an operating device (e.g.: neon tube). The time aspects of the jamming may be permanent/continuous or temporary. In case of permanent/continuous jamming the frequency spectrum is given, which may be periodic and non-periodic. With directed permanent/continuous periodic jamming we speak about linear-, with non-periodic jamming permanent/continuous Fourier spectrum. The frequency ranges of electromagnetic radiation are shown in Fig. 1, those of electromagnetic inconveniences in Fig. 2.

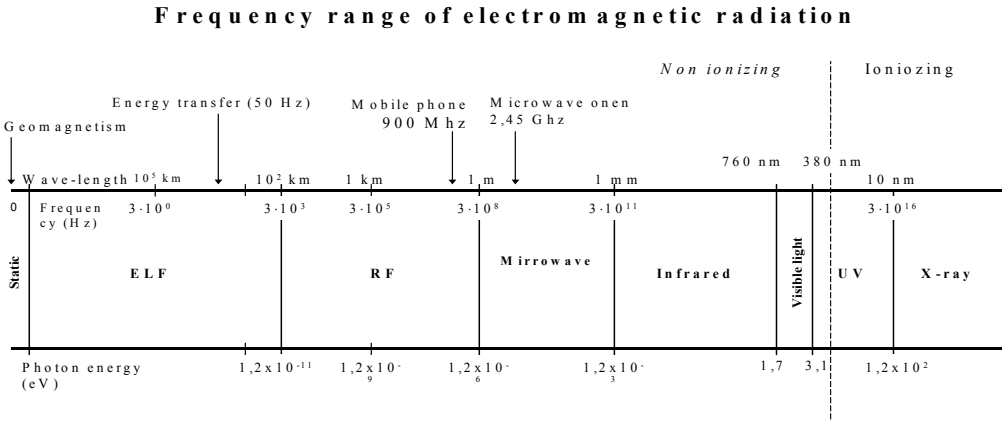

Figure 1. *Frequency range of electromagnetic radiation [22]*

http://www.ecology.uni-corvinus.hu ● ISSN 1589 1623

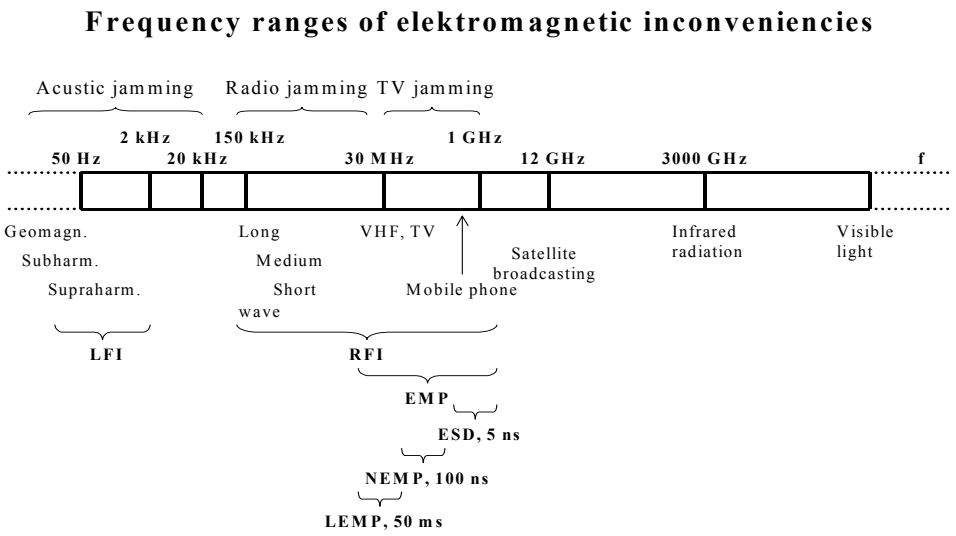

Figure 2. *Frequency range of electromagnetic inconveniences [22]*

Electromagnetic inconveniences may spread via radiation, wires, coupling or other ways. The most significant factor in the defence against the inconvenient electromagnetic effects is the recognition in time of the noxious effect and then the compensation or termination of it.

There are several observations reporting on the noxious and therapeutic effects on the living organism of electromagnetic fields. Thus it is comprehensible that electromagnetic protection of the environment as a new problem has been added to the long-existing, well-known problems of environmental protection.

Human-related noxious effects of electromagnetic fields

The collective name for electromagnetic effects noxious to living human organisms is electrosmog. Electrosmog is a scientifically based, biologically acting environmental factor, which occurs as a secondary product of electromagnetic fields and radiations as soon as it gets connected with living organisms. Human organisms give individual responses to the various electromagnetic effects and electrosmog. There are pronouncedly electrosensible people to electrosmog. Observations confirm that the effects of electromagnetic field are the most noxious with women in the period of menopause due to the change of the hormonal activity, and with children up to the age of approximately 13 due to the higher water content of their bodies. When electrosmog has noxious effects, the general, most frequently occuring disorders, the effects influencing blood circulation and the nervous system may be classified [19].

The most frequently occuring symptoms

General exertion, depression, weariness, headache, tinnitus, rapid asthenopia, temporary diplopia, smarting of the eyes, vertigo, weakening of concentration, forgetfulness, rapid aging, loss of skin flexibility, vibration (permanent electric charge) of one's hair, typical nasty taste in the mouth (metallic fillings, implantations),

http://www.ecology.uni-corvinus.hu ● ISSN 1589 1623

arthralgia, frequent spasms in the hands and feet, gastralgia, faeces irregularity (diarrhea, constipation) [19].

Effects influencing blood circulation

Unsteady blood pressure (fluctuations), rapidly developing high blood pressure, tachycardia, high pulse rate, disorder of the heart rhythm, ECG alterations, and blood picture alterations[20].

Effects influencing the nervous system

Sleep disorders, nervousness, EEG alterations, and disorder of the central nervous system, tinnitus, head-noises, and complete nervous breakdown [19].
Beside this, gradual progress in the impairment of the immune system is observable as a result of electrosmog.

Human-related therapeutic effects of electromagnetic fields

Electromagnetic effects of adequate intensity are widely used in therapeutics. The latest applications: microwave ballon therapy for dilating sclerotic bloodvessels and coronary arteries; microwave thermography for discovering tumors and blood circulation disorders; microwave hyperthermia for destroying cancerous tissues combined with medicinal treatment; rapid warming-up treatment: it is based on the thermis effect of microwave radiation, e.g.: refrigerated blood, warming-up of organs coming from the organ-bank prior to transplantation; etc [10], [12].

Deleterious effects of electromagnetic field in veterinary medicine

It is easy to understand that there are fewer noxious effects of electromagnetic field observed in veterinary science but there, too, are some striking examples. Calves born in the vicinity of a TV transmission tower had frequent physical deformities [20]. Newborn calves: two thoracic legs tilted backwards at the hooves (unability to walk); born with two heads (non-viable); born with six legs (on the back +two legs). The cattle-shed was within a radius of 150 meters in each case [4], [20].

An experiment was conducted with hen's eggs during the embryonic development. A treated and a control group were selected at random from an identical population. The treated group was radiated with electromagnetic field of 1 kHz modulated between 0,9 mW/cm^2 – 1,25 GHz. The hatched chickens showed signs of abnormal deformities. Spastic toes, double beak, typical deformities on the legs and eyes (limited eyesight, inability to walk) [5], [20].

Telstra (an Australian Telephone Company) irradiated 100 mice with a mobile phone in operation 2X30 minutes daily over a period of 18 months and compared them with a control group of 100 untreated mice. The occurence of lymphadenoma was significantly higher (twice as much) in the treated group [17], [20].

Therapeutic effects of electromegnetic field observed in veterinary medicine

The number of applied healing therapy with electromagnetic field is low but increasing in number. In an experiment a control and a treated group of aged male rats were selected at random from a population of the same age. The testis of the rats in the treated group was irradiated with infrared lamp for some time. The rats of the treated group turned out to show significantly higher ($p < 0,001$) sexual activity.

http://www.ecology.uni-corvinus.hu ● ISSN 1589 1623

Hazards of modern technical devices and their appropriate use

Nowadays nearly all households use TVs, microwave ovens, monitors (joined to computers), night current, radio-alarm clocks, magnetic door opener, and mobile phones as means of personal communication. Their use is not without dangers. The use of a device results in the appearance of a so-called „radiating field" [20]. The appearing electrosmog decreases with the distance from the device growing. Thus, adequate environmental protection may lead to the termination or significant decrease in the noxiousness. A few practical instructions to the adequate use of the devices:

- An operating TV should be watched from a distance seven times the length of the screen diameter.
- You should be standing at least one meter away from the operating microwave oven and definitely not look into the oven (it might cause cataract formation in the eye) [5].
- Computer monitors emit electromagnetic and electrostatic radiation noxious to health. The top legible line of the screen should be at eye level so that the lower parts of the body get a lower amount of radiation. When it is used over a long period it is recommended to make 5-10 minute pauses to rest the eyes. Never keep your head too close to the screen. Statistical figures show that three out of ten monitors irradiate over the permissible limit [12], [22].
- The radio-alarm clock should be kept at a distance of at least 1.5 meters from the head.
- The mobile phone should be kept in the bag rather than in the pocket close to the body. It definitely weakens the immune system and might promote the development of thymus cancer and lymphadenoma [1], [20]!
- The magnetic door opener should not be keep next to the mobile phone. The battery of the mobile phone will go flat in a short time.
- The bed should be place far from the halogen lamp converter and the night current receiver [15].

Materials and methods

Effects of electromagnetic field therapy on horses

Testing local effects of electromagnetic therapy in horses

The following experiment was performed with 10 horses. Magnetic wraps were placed on tarsal and metatarsal region of right and left hind limbs of the horses and they were exposed to magnetic field therapy. Blood was withdrawn from each horse five times from v. saphena and a. metatarsalis:

- Sample 1: control (state prior to treatment)
- Sample 2: Thermic T_0 (placement of magnetic wraps for 16 minutes without applying magnetic field treatment)
- Sample 3: Magnetic T_0 (Magnetic wraps were taken off, followed by a 15-minute pause, the magnetic wraps were placed back and magnetic field treatment was applied for 16 minutes and finally blood was with drawn)

http://www.ecology.uni-corvinus.hu ● ISSN 1589 1623

- Sample 4: Magnetic T_1 (Magnetic wraps were taken off, blood was withdrawn 15 minutes later)
- Sample 5: Magnetic T_2 (blood was withdrawn again 30 minutes after the magnetic field treatment)

The body temperature of animals as well as the blood gas and acid-base parameters (pH, pCO2, pO2, HCO3, TCO2, ABE, SBE, SBC, SAT) of the with drawn arterial and venous blood were measured [3]. Paired sample t-test was used to specify the significant deviations between the treated and control groups.

Testing the effects of electromagnetic blanket in horses

Healthy horses of different sexes and ages (n=11) were investigated with regard to the effects of magnetic blanket on the physical and blood gas and acid-base parameters of the horses. Cannula was inserted in the arteria facialis of the horses and blood was withdrawn from each of them at 8 predetermined points of time.

- Sample 1: Control (state prior to treatment).
- Sample 2: 20 minutes later the horses got in a state of stress (excitation, pinching about).
- Sample 3: Right after 5 minutes' trotting blood was withdrawn.
- Sample 4: Following a 15-minute rest blood was withdrawn again
- Sample 5: The magnetic blanket was placed on for 16 minutes but the electric source was not turned on.
- Sample 6: The blanket was taken off and 15 minutes later blood was withdrawn.
- Sample 7: The blanket was placed on again, and was made to operate with full intensity for 16 minutes. Right after this blood was withdrawn.
- Sample 8: The blanket was taken off, the horses had a 15-minute rest, and then blood was withdrawn.

The horses' pulse rate, respiration rate and temperature values as well as the blood gas and acid-base parameters (pH, pCO2, pO2, HCO3, SAT) were determined in each case. The change in the horses'state of stress in relation to the control and certain stress phases was tested using paired t-test. To be exact, the following samples were involved in the comparison:

- I. 1 - 2 control and state of stress
- II. 1 - 3 control and trotting following the stress
- III. 2 – 3 stress and trotting
- IV. 3 – 4 trotting and rest
- V. 4 – 5 rest and magnetic blanket on without electric source
- VI. 5 – 6 magnetic blanket on without electric source turned on and rest
- VII. 6 – 7 before and after turning on the magnetic blanket
- VIII. 7 – 8 magnetic field treatment and rest following it

Effect of electromagnetic blanket on the biochemical parameters

We conducted an experiment on 11 horses for 5 days in order to get data about LDH, AST and CK biochemical parameters by providing 16-minute treatments after putting

http://www.ecology.uni-corvinus.hu ● ISSN 1589 1623

on the magnetic blanket and withdrawn blood right before and after the treatment. Our observations were evaluated by paired sample t-test.

Results and analyses

Local effects of electromagnetic field therapy in horses

The results have been summarised in Table 1. Table 1 demonstrates that the results of arterial and venous tests differ from one another. The state right after the magnetic field therapy (Magnetic T_0) shows significant deviation compared to the control group in almost all the parameters (except for pO2 and SAT). Evaluating arterial and venous tests we can conclude that the test results of arterial blood reflected the effects of the treatment more sensibly. The question is: What can be the explanation of it? In Table 1 it is also observable that ABE, SBE and SBC parameters show significant deviation, as compared to the control, 15 minutes after the magnetic field therapy, and so do pCO2, pO2, HCO3 és TCO2 parameters after another 15 minutes. The probable conclusion from it is that magnetic field therapies have protracted effects and thus the changes of certain parameters get manifested somewhat later.

Table 1. *Results of the local effects of electromagnetic field therapy in horses based on the comparison between the control and treated groups, where ns=non significant and tend=tendency.*

Test	**Arterial (p<)**									
	Temp.	**pH**	**pCO2**	**pO2**	**HCO3**	**TCO2**	**ABE**	**SBE**	**SBC**	**SAT**
Thermic T_0	ns	ns	0,01	ns	tend	0,05	0,05	0,01	tend	ns
Magnetic T_0	tend	ns	0,01	0,01	0,01	0,01	0,05	0,05	0,05	0,05
Magnetic T_1	ns	ns	ns	ns	tend	tend	0,05	0,05	0,05	ns
Magnetic T_2	ns	ns	0,05	0,01	0,05	0,01	0,01	0,01	0,05	0,01
Test	**Venous (p<)**									
	Temp.	**pH**	**pCO2**	**pO2**	**HCO3**	**TCO2**	**ABE**	**SBE**	**SBC**	**SAT**
Thermic T_0	ns	ns	ns	0,05	ns	ns	ns	ns	ns	0,05
Magnetic T_0	tend	ns	0,05	ns	0,01	0,01	0,01	0,01	0,01	ns
Magnetic T_1	ns	0,05	ns	0,05	ns	ns	ns	ns	ns	ns
Magnetic T_2	ns		ns	0,05	ns	ns	ns	ns	ns	ns

Test results of the effects of electromagnetic therapy in horses using magnetic blanket

It is reasonable to raise the question whether significant changes can be detected between two treatments or between the control and the treatment. Which are the temporary changes to which horses respond really sensibly? This is the reason why we applied paired t-test. The results are summed up in Table 2. The results show that no significant changes can be detected with the use of magnetic blanket as far as the tested blood parameters are concerned. Blood and SAT reflect the change of the state of horses under stress. It is worth noting that horses give significant responses in their physical parameters (pulse, SAT) to such events as placing on and taking off the magnetic blanket or drastic stress.

http://www.ecology.uni-corvinus.hu ● ISSN 1589 1623

Table 2. *Test results of the effects of electromagnetic therapy in horses based on comparison between control and treated as well as treated and treated groups, where ns=non significant and tend=tendency.*

	I.	II.	III.	IV.	V.	VI.	VII.	VIII.
Pulse	ns	0,05	ns	0,01	ns	0,05	ns	ns
Resp.	ns	ns	tend	tend	ns	ns	ns	ns
Temp.	ns	ns	ns	ns	ns	ns	ns	ns
pH	0,01	tend	0,01	ns	ns	tend	ns	ns
pO_2	tend	ns	0,05	ns	ns	ns	ns	ns
pCO_2	ns	ns	ns	ns	ns	ns	ns	ns
HCO_3	ns	ns	ns	ns	tend	ns	ns	ns
Saturation	ns	0,05	0,05	ns	ns	0,05	ns	ns

Results of the effects of electromagnetic therapy on the biochemical parameters using magnetic blanket

Table 3 contains the results of paired t-test before and after electromagnetic field treatments. It is obvious from the table that the biochemical parameters show significant deviations on day 1, day 2 and day 5. There is no change on day 4.

Table 3. *Results of the effects of electromagnetic therapy on the biochemical parameters LDH, AST and CK, where ns=non significant and tend=tendency.*

	Day 1	Day 2	Day 3	Day 4	Day 5
LDH	ns	0,01	0,05	ns	ns
AST	0,05	0,001	ns	ns	0,05
CK	0,05	ns	ns	ns	0,05

We might suppose that magnetic therapy affects the immune system of animals. On the first two days of magnetic field therapy the organism gives a natural response to the electromagnetic field therapy and the tested parameters show significant deviations. In the meantime, the organism attempts to compensate the magnetic field effect and on day 4 it protects itself from the inconvenient external effect. From day 5 the inconvenient external effect appears again, which the immune system attempts to compensate periodically or in some other way. Longer period (months) would be required to justify our hypothesis. Namely, that protracted, consequently carried out electromagnetic field therapy would lead to the impairment of the immune system.

We note that when one is applying paired t-test and making several pairwise comparisons, the error of first kind may be increased. We plan a detailed analysis of experiments on representative samples, one- and two-way (repeated measures) analysis of variance models.

Conclusion

Comparing human and veterinary biological results we can state that the effects of electromagnetic field are expressed latently, but have significant biological effects and consequencies. Special attention should be paid to the electromagnetic protection of the

http://www.ecology.uni-corvinus.hu ● ISSN 1589 1623

environment. It is an urgent task to learn about the effect mechanism of electromagnetic radiation having noxious or therapeutic effect in the field of both human and veterinary biology.

Acknowledgement. Authors thank Horst Leopold and Wallner (Med Tech Produktions- und Vetriebs GmbH, Linz, Austria) for providing the MCR Vet electromagnetic field set.

REFERENCES

[1] Adams, J.M., Cary, S. (1991): Transgenic models of tumor development. – Science 254:1161-1167.
[2] Ahlborn, A., Feychting, M. (1993): Magnetic fields and cancer in children residing near Swedish high-voltage power lines. – Am. Jur. Epidemiol. 138:467-481.
[3] Barnothy, M.F. (1964): Biological Effects of Magnetic fields. – Pelnum Press, New York (51 p.)
[4] Börzsönyi, L., Fodor, J., Varga, J., Szenci, O. (2004): Biometrical characterization of blood gas and acid-base parameters in newborn calves in the postpartal period. – 25th Annual Conference The International Society for Clinical Biometrics, Leiden, (145 p.)
[5] Hamrick, P.E., Fox, S.S. (1977): Rat lymphocytes in culture exposed to 2450 MHz (CW) microwave radiation. – J. Microwave Power 12: 125-132.
[6] Hoffsis, G.F., Murdich, P.W., Tharp, V.L., Ault, K. (1970): Plasma concentration of cortisol and corticosterone in the normal horse. – Am. J. Vet. Res. 31: 1379-87.
[7] Maurino, RM. (1991): From Thales to Lauterbut, or from Iodestone to MR imaging: magnetism and medicine. – Radiology; 180: 593-612.
[8] Ieran, M. (1990): Effect of low frequency pulsing electromagnetic fields on skin ulcers of venous origin in humans: A double blind study. – J. Orthop. Res. 8: 276-282.
[9] Kobluk, C.N., Johnston, G.R., Lauper, L. (1994): A scintigraphic investigation of magnetic field therapy on the equine third metacarpus. – Vet. Comp. Orth. Traum. 7: 9-13.
[10] Kósa, L., Börzsönyi, L. (1999): Napjaink allergiái és biostatistika – Allergy Today and Biostatistics. – CD-ROM, AUTOMEX, CYBERTSTONE, TRANS-EUROPE Kft, Budapest, (350 p.)
[11] Lozán, J.L., Kausch, H. (1998): Angewandte Statistik für Naturwissenschaftler. – Parey Buchverlag, Berlin (152 p.)
[12] Mátay, G., Zombory, L. (2003): A rádiófrekvenciás sugárzás élettani hatásai és orvosbiológiai alkalmazásai (Physiological effects and human biological applications of radiofrequency radiation; Book in Hungarian). – Műegyetemi Kiadó, Budapest.
[13] Polk, Ch. Postow, E. (1996): Handbook of Biological Effects of Electromagnetic Field CRC – Press, Boca Raton, New York, London (112 p.)
[14] Ramsey, P.H. (1980): Exact type I error rates for robustness of Student's T test with unequal variances. – Journal of. Educational Stat. 5: 337-49.
[15] Ramey, D.W. (1999): Magnetic and electromagnetic therapy in horses. – Compendium on Continuing Education for the Practicing Veterinarian. 21: 553-560.
[16] Rasch, D., Herrendörfer, G., Bock, J., Victor., Guiard, V. (1996): Verfahransbibliothek Versuchsplanung- und –ausertung. – R. Oldenburg Verlag, München Wien, 433 p., 847 p.)
[17] Repacholi, M.H., Basten, A., Gebski, V., Nooman, D., Finnie, J., Harris A. W. (1997): Lyphomas in Eμ-Pim1 transgenic mice exposed to pulsed 900 Mhz elektromagnetic Filds. – Radiation Research. 147: 631-640.
[18] Steyn, P.F., Ramey, D.W., Kirschvink, J., Uhrig, J. (2000): Effect of a static magnetic field on blood flow to the metacarpus in horses. – J. Am. Vet. Med. Ass. 217: 6, 874-877.
[19] Varga, A. (1999): Elektrosmog. Ein wissenschaftlich begründeter und biologisch wirksamer Umweltfaktor. – The Journal of Natural Science 2: 50-55.

http://www.ecology.uni-corvinus.hu ● ISSN 1589 1623

[20] Varga, A. (2002): Grundlage des Elektrosmogs in Bilder. – Verlag Umweelt + Medizin, Heidelberg (114 p.)
[21] Wilcox, R.R.: (2001): Fundamental of modern statistical methods. – Springer-Verlag, New York, Inc. (84 p.)
[22] Zombory, L. (2005): Electromagnetic protection of the environment (lecture in Hungarian)
[23] Zombory, L., Mátay, G. (2005): Physiological effects and human biological applications of radiofrequency radiation. (Book in Hungarian, in press)

http://www.ecology.uni-corvinus.hu ● ISSN 1589 1623

Jared Diamond
COLLAPSE: HOW SOCIETIES CHOOSE TO FAIL OR SUCCEED

Viking Books, ISBN 0-670-03337-5

reviewed by
R. H. RANDALL
North Idaho College/Coeur d' Alene, Idaho
Washington State University/Pullman, Washington

Mankind has been remarkably successful at surviving and succeeding throughout the world. However, there have been disasters and calamities as well as successful civilizations. Men have often destroyed the very environment which nurtured them, whether through over-hunting, or over-grazing. And now, at a time when hurricanes, floods, and droughts, have increased in intensity, one seeks information and insight as to the possible causes and for consequences for human society, not just for natural events, but regarding human activity as well. Professor Jared Diamond has written a serious book to examine such phenomena concerning their social and environmental impacts. He uses detailed information from diverse sources on many societies which have undergone - indeed often caused - important environmental degradation with the result (often) of total disaster for the humans involved. He also documents how some cultures with an enlightened appreciation and knowledge of their own circumstances have survived by working with the natural world to create sustainable societies, successful for many hundreds of years.

Diamond's criteria for the examination throughout the work are: 1) Inadvertent environmental damage and its possible reversibility, 2) Climate change, 3) Hostile Neighbors, 4) Decreased support by friendly neighbors (e.g., the Greenlanders doom will be hastened by their failure to maintain relations with Europe), 5) Society's responses to its problems. Says the author, "A society's responses depend on it's political, economic and social institutions and on its cultural values. Those institutions and values affect whether the society values (or even tries to solve) its problems." (p.14-15)

Diamond begins with the American state of Montana, a beautiful land, known for its mountains, streams, and prairies, wildlife and rugged individualists. This picture today is deceiving. The environment here has been poisoned by mining operations; salinization is occurring at a rapid rate; and there is a social battle at several levels between residents who wish to retain the old ways and values and others who wish to change the land from predominantly agricultural to residential life depending upon a service economy and tourist trade. Montanans are divided on population growth, governmental regulation and how the land is to be used. It is shocking given the modern changes in economy which proceed apace, that if the state were not part of the United States, it would, according to the author, be a failed state due to the environmental damage, poverty of many of its people, and its dependence on outside assistance in the form of governmental programs.

http://www.ecology.uni-corvinus.hu ● ISSN 1589 1623

Diamond's point is that Montana is an example of a drama being reenacted out throughout the world today. However his methodology in the second part is to first delve into the past to examine societies which have been destroyed primarily due to environmental degradation (caused by the factors listed above) or those societies that made crucial, disciplined decisions, which allowed them to survive to this day.

He discusses with rich detail why many societies failed: Easter, Pitcairn and Henderson Island; the Anasazi and Mayan in North and South America, and the Greenland Norse. While examples of harsh climate change caused some irreparable damage, he maintains that often the elements for disruption and disaster were self-caused. Of the Greenland Norse he says, that in addition to some fluctuations in weather cycles, soil erosion caused by overgrazing, failure to adapt to different conditions from those experienced at another place and time, refusal to learn from a successful indigenous people and an inflexible and incompetent power structure which "created a conflict between the short term interests of those in power, and the long term interests of the society as a whole."(p.276)

Part II ends with successful examples of survival: the New Guinea Highlands, where sustainable agriculture has been practiced for over 6000 years, Tikopia, and Japan under the Tokugawa rulers, and others.

The third part is given to describing some modern societies: Rwanda, the Dominican Republic, and Haiti, The People's Republic of China and Australia. Practices for good and ill are discussed and interesting details emerge constantly. The societies examined are all struggling with the effects of growth, globalization and environmental decline. Diamond's tone here is not condemnatory: it is scholarly, seeking to educate and enlighten. He points out many mistakes of the past and present attempts to slow down destructive practices and heal their damage. Of China he says, "China's leaders have been able to solve problems on a scale scarcely possible for European and American leaders: for instance by mandating a one child policy to reduce population growth and by ending logging…On the other hand, China's leaders have also succeeded in creating messes on a scale scarcely possible for European or American leaders…."(p.374) He cites the destruction of the public education system during the cultural revolution and the growing environmental and social problems now emerging. (Public demonstrations have recently led to armed hostilities between villagers and officials over income distribution, and lack of public services.)

Part four, "Practical Lessons," examines the issues of why some societies make bad decisions. He discusses the failure to anticipate, to perceive problems, and rational bad behaviors, and disastrous values. These had been touched on before but here Diamond recapitulates and addresses in detail these factors, as well as other irrational, destructive choices and actions which lead to environmental and societal collapse. Of values he maintains "Perhaps a crux of success or failure as a society is to know which core values to hold on to, and which ones to discard and replace with new values when times change."(p.433) He had illustrated this clearly with the wool industry in Australia, which has largely been given up, in favor of new technologies and less environmentally damaging practices. He concludes with "Signs of Hope" and points out that some societal leaders do rise to the occasion - leaders who have the courage, and are willing

http://www.ecology.uni-corvinus.hu ● ISSN 1589 1623

to risk criticism and even failure - to propose sacrifice and hard work to address problems in their nascent stage, before they become intractable. He cites John Kennedy and numerous European leaders and peoples (p.440) for their willingness to take dramatic stands to solve problems, thus leading to greater possibilities for survival.

Diamond spends an incisive chapter on big business and the environment discussing the good, the bad, and the truly ugly. He says"…environmental practices of big businesses are shaped by a fundamental fact that for many of us offends our sense of justice. Depending on the circumstances, a business really may maximize its profits, at least in the short term by damaging the environment and hurting people."(p.483) His effort in this chapter is spent showing examples of good business/environmental practice contrasted with poor ones. (It should be noted that there are businesses which do strive to be good neighbors.) However he concludes astonishingly that since businesses are really there to make money for owners and stockholders, and not to mind the environmental practices of the enlightened, the ultimate responsibility for environmental disaster lies with the public. "In the long run, it is the public, either directly or through its politicians, that has the power to make destructive policies unprofitable and illegal, and to make sustainable environmental policies profitable."(p.484)

This position is mistaken at several levels. First of all it implies companies bear no responsibility for bad practices, that they are 'non-moral actors' and have no responsibility for the consequences of their actions or failures to act, and that simply does not work in the moral and real world. It ignores the principle that truly moral leaders look out for the welfare of their people, environmental sustainability, and the consequences of their actions on the sustainability of future generations.

Secondly, there would be no reason to laud the responsible corporations and politicians (which he does) if their actions were not environmentally respectable - especially as he goes to some pains to show that responsible environmental management has costs, as well.

Finally, it seems quite misplaced to say that citizens - where ever they may be - are consulted/and/or allowed to have the moral/technical input he claims it will take to establish justice and sustainability. Responsible and non-responsible corporations hire professionally trained scientists and technicians to help guide work in the extractive and productive industries, to maximize efficiency and productivity, and hopefully safety and environmental soundness, and to minimize environmental degradation. It is their responsibility along with competent governmental agencies to accomplish this. While it is true cynics and lobbyists - and some politicians - serve some businesses that have no intention to do the right thing - it surely doesn't follow that it is the public's fault that they do not wish to do so!

It is hopefully true that given the right information and opportunity to decide such issues the people may make their voices heard and respected. It is not always so, but it is surely a goal of democracy that it be so. But it is not the case that most of the world's people have ever had such an opportunity. While it may be true that it will be informed, conscientious citizens who finally make the moral weight of environmental

http://www.ecology.uni-corvinus.hu ● ISSN 1589 1623

responsibility, sustainability and justice a reality in all such endeavor, it does not follow that the lack of such a state of affairs exonerates malfeasance, degradation, destruction and even murder by those who have been responsible for it.

Diamond concludes with chapter 16, "The World as Polder: What Does It All Mean To Us Today?" He is summing up in an interesting way, and claims that he is a "cautious optimist." (p.521) He cites the Dutch response to disastrous floods in 1953, which killed nearly 2000 citizens. This instigated environmentally, and socially responsible, far-sighted policy for the nation, carried on to this day.

There are he says twelve very critical issues we must face. They are the destruction of natural habitats, including de-forestation; the loss of wild foods, especially fish from increasingly polluted seas, lakes and rivers; loss of biodiversity; enormous loss of soil by natural damage (wind and water) and poor agricultural drainage; the overuse and depletion of major sources of energy; the degradation and loss of fresh water; the loss of available solar energy; the release of toxic chemicals into the total environment; the effects of invasive species on native life; global warming caused by a steady increase of 'greenhouse gasses'; increasing human population with its concomitant requirements for more clean air, water, space etc; and finally the impacts upon the earth and what he sees as the looming conflict between the developed and developing worlds regarding rising expectations.

"Even if the human populations of the Third World did not exist, it would be impossible for the First World alone to maintain its present course, because it is not in a steady state but depleting its own resources as well as those imported from the Third World…. What will happen when it finally dawns on all those people in the Third World that current First World standards are unreachable for them, and that the First World refuses to abandon those standards for itself?"(p.496)

That of course is a major issue and one which many leaders are contemplating: it is also in my opinion why education, discipline and responsible decision making need to come to the fore - not as in my own country, with an over-reliance on market mechanisms to achieve needed reforms and restoration. Notwithstanding any positive use of such market oriented solutions to problems, the market was not designed for this, and these issues are too serious to rely overmuch on such strategies.

I found the middle and final section of this final chapter which Diamond calls "One-liner Objections" and "Reasons for Hope," to be amongst the liveliest and most interesting in the book. Here he examines 'reasons' often advanced to delegitimize environmental concerns.(p.503) Here he seems forthright and at times even adamant. To the claim that we cannot afford good environmental practices, he points out that in the long term it is cheaper and better to avoid illnesses caused by pollution, and asserts "That illustrates why the U.S. Clean Air Act of 1970, although its cleanup measures do cost money, has yielded estimated net health savings (benefits in excess of costs) of about $1 trillion per year, due to saved lives and reduced health costs."(p.504)

He illustrates the shortcomings of views that new technology will solve our problems, that we have inexhaustible resources, that poverty is a thing of the past, etc.,

http://www.ecology.uni-corvinus.hu ● ISSN 1589 1623

with facts, and reasoned responses. To his credit, he states that it is incumbent on the First World citizens to begin making more responsible choices, for environmental responsibility and transgenerational sustainability, and concludes that the "interconnectedness" of the modern world makes it possible for awareness and education regarding these issues, problems, and possible solutions on a scale never before available to man.

Conclusion: I found Collapse to be highly readable, very informative and especially powerful with respect to illustrating the interconnectedness of the problems we face.

Diamond's choice of failed societies, while not exhaustive seems to illustrate his points well and convincingly. While his work might have been stronger had he examined other well-known societal calamities (e.g., Rome), given his emphasis upon environmental issues and factors, one sees clearly a steady and deadly set of consequences which are either addressed or ignored, to the success or diminishment of the society involved. I was disappointed in his attribution of non-responsibility for corporate polluters, and his misguided comments in this regard: I thought his summary discussion of the major problems we face was very well done, and his answers to objections, powerful, engaging and very appropriate. He addressed major environmental and social issues of the day in some complexity and balance. It is because of this that I recommend this work and indeed have assigned it to my students, with the hope that they will give it the serious attention it and the subject matter deserve.

I am very grateful for the suggestions and criticism of Professor Daniel Holbrook and Royce Grubic at Washington State University. Any errors are entirely my own.

http://www.ecology.uni-corvinus.hu ● ISSN 1589 1623